Dissertation
der Fakultät für Biologie
der Ludwig-Maximilians-Universität München
zur Erlangung des Dr. rer. nat.

IRES elements – a new tool for regulation of gene expression of rabies virus

vorgelegt von
Adriane Marschalek
München, 08. Juli 2010

Erstgutachterin: Prof. Dr. Ruth Brack-Werner

Zweitgutachter: Prof. Dr. Benedikt Grothe

Sondergutachter: Prof. Dr. Karl-Klaus Conzelmann

Tag der mündlichen Prüfung: 27. Januar 2011

Part of this work is published:

Marschalek A, Finke S, Schwemmle M, Mayer D, Heimrich B, Stitz L, Conzelmann KK. 2009. Attenuation of rabies virus replication and virulence by picornavirus internal ribosome entry site elements. J Virol. **83**(4):1911-9.

Marschalek A, Drechsel L, Conzelmann KK.
2011. The importance of being short: The role of rabies virus phosphoprotein isoforms assessed by differential IRES translation initiation. European Journal of Cell Biology. In press.

TABLE OF CONTENTS

LIST OF TABLES AND FIGURES

LIST OF ABBREVIATIONS

1. INTRODUCTION 1

1.1. RABIES VIRUS 1

1.1.1. TAXONOMY 2
1.1.2. VIRUS STRUCTURE AND GENOME ORGANIZATION 2
1.1.3. VIRAL GENE EXPRESSION AND RNA SYNTHESIS 3
1.1.4. ORGANIZATION OF RV PHOSPHOPROTEIN 5
1.1.5. VIRAL REPLICATION CYCLE 7
1.1.6. PATHOGENICITY 9
1.1.7. MECHANISMS OF RV TO COUNTERACT INNATE IMMUNITY 9
1.1.7.1. Interferon induction and signaling induced by rhabdoviruses 9
1.1.7.2. Rabies virus countermeasures to prevent IFN induction and IFN signaling 12
1.1.8. USE OF *MONONEGAVIRALES* AS VIRAL VECTORS 13

1.2. INTERNAL RIBOSOME ENTRY SITES (IRES) 15

1.2.1. CAP-DEPENDENT TRANSLATION INITIATION 15
1.2.2. INTERNAL TRANSLATION INITIATION BY INTERNAL RIBOSOME ENTRY SITES (IRES) 16
1.2.2.1. Viral IRES elements: Discovery and classification 18
1.2.2.2. Cellular IRES elements 22
1.2.2.3. IRES transacting factors (ITAFs) 23

1.3. AIM OF THIS STUDY 24

2. MATERIAL AND METHODS 26

2.1. MATERIALS 26

2.1.1. CHEMICALS 26
2.1.2. BUFFERS 26
2.1.3. ENZYMES 28
2.1.4. KITS 29
2.1.5. CONSUMABLES 29
2.1.6. OTHER REAGENTS 29
2.1.7. CELL CULTURE 30
2.1.7.1. Reagents 30
2.1.7.2. Cells 30
2.1.7.3. Cell culture media 31
2.1.8. BACTERIA 32
2.1.9. OLIGONUCLEOTIDES 32
2.1.10. PLASMIDS 35
2.1.11. VIRUSES 42
2.1.12. ANTIBODIES 42

2.2. MOLECULAR BIOLOGY METHODS 43

2.2.1. PREPARATION OF PLASMID DNA 43
2.2.2. POLYMERASE CHAIN REACTION (PCR) 44
2.2.3. ELECTROPHORETIC SEPARATION OF DNA FRAGMENTS 44
2.2.4. ISOLATION OF DNA FRAGMENTS FROM AGAROSE GELS 45
2.2.5. DNA MODIFICATIONS 45
2.2.5.1. Fragmentation of DNA with restriction endonucleases 45
2.2.5.2. Generation of blunt ends by Mung Bean Nuclease and Klenow enzyme 45
2.2.5.3. Dephosphorylation of 5'ends 45
2.2.6. LIGATION 45
2.2.7. SEQUENCING OF DNA 46

2.2.8. CLONING OF CDNAS FOR THE GENERATION OF RECOMBINANT RVS 46
2.2.8.1. Generation of cDNAs for SAD RL-IRES-FL *46*
2.2.8.2. Generation of cDNAs for SAD IRES eCFP *46*
2.2.8.3. Generation of cDNAs for SAD FMDV-P and SAD FMDV-P1x34 ..... *47*
2.2.9. USE OF E.COLI 47
2.2.9.1. Bacterial culture *47*
2.2.9.2. Production of competent E.coli bacteria *48*
2.2.9.3. Transformation of XL-1 competent E.coli *48*
2.2.10. ISOLATION OF RNA FROM CELLS 48
2.2.11. REVERSE TRANSCRIPTION (RT) 49
2.2.12. ELECTROPHORETIC SEPARATION OF RNAS 49
2.2.13. NORTHERN BLOT 49

2.3. CELL CULTURE 50

2.3.1. CULTIVATION OF CELL LINES 50
2.3.2. FREEZING OF CELLS 50
2.3.3. TRANSFECTION OF CELLS 50
2.3.3.1. $CaPO_4$- Transfection by the mammalian transfection kit (Stratagene) *50*
2.3.3.2. Transfection with Lipofectamine2000 ..... *50*
2.3.3.3. Transfection with Polyethylenimin (PEI)25 ..... *51*
2.3.4. IMMUNOFLUORESCENCE 51
2.3.4.1. Acetone fixation *51*
2.3.1.2. Fixation with 3% paraformaldehyde *51*
2.3.1.3. Immunostaining *51*
2.3.5. MICROSCOPY 51
2.3.6. IMMUNOHISTOCHEMISTRY OF BRAIN SLICE CULTURES 52

2.4. VIROLOGICAL METHODS 52

2.4.1. GENERATION OF RECOMBINANT RABIES VIRUS FROM CDNA (VIRUS RESCUE) 52
2.4.2. PREPARATION OF VIRUS STOCKS 53
2.4.3. TITRATION OF VIRUS 54
2.4.4. PURIFICATION OF VIRUS PARTICLES BY IODIXANOL DENSITY GRADIENT CENTRIFUGATION 54
2.4.5. INFECTION OF ORGANOTYPIC BRAIN SLICE CULTURES 54
2.4.5. MOUSE INFECTION EXPERIMENTS 55

2.5. BIOCHEMICAL METHODS 55

2.5.1. PREPARATION OF DENATURED PROTEIN LYSATES 55
2.5.2. ELECTROPHORETIC SEPARATION OF PROTEINS BY SDS-POLYACRYLAMID-GELS (SDS-PAGE) 55
2.5.3. WESTERN BLOTTING 56
2.5.4. LUCIFERASE-ASSAY 57

2.6. STATISTICAL ANALYSIS 57

3. RESULTS 58

3.1. RNA VIRUS-BASED REPORTER SYSTEMS FOR THE CHARACTERIZATION OF IRES ELEMENTS 58

3.1.1. GENERATION OF A NEW RNA VIRUS-BASED DUAL LUCIFERASE REPORTER SYSTEM FOR CHARACTERIZATION OF IRES ELEMENTS 58
3.1.1.1. Sequences predicted to contain IRES elements promote reporter gene expression from plasmids *58*
3.1.1.2. Gene expression of SAD RL-IRES-FL *60*
3.1.1.3. RL expression by SAD RL-IRES-FL reflects viral replication levels *61*
3.1.1.4. Activity of viral IRES elements in different cell lines *63*
3.1.1.5. No effect of viral 3'UTRs on IRES activities within SAD RL-IRES-FL *65*
3.1.1.6. An altered start codon context does not change relative IRES activities *67*
3.1.1.7. IRES activities quantified by the optimized new RV based dual luciferase system *69*

3.1.2. GENERATION OF A VIRUS-BASED REPORTER SYSTEM FOR CHARACTERIZATION OF IRES ELEMENTS ON SINGLE CELL LEVEL USING eCFP AS A REPORTER GENE 71
3.1.2.1. SAD IRES eCFP reporter RVs 71
3.1.2.2. IRES-dependent eCFP expression in different cell lines 73
3.1.2.3. Quantification of eCFP expression by fluorescence microscopy 74
3.1.2.4. 5'UTR of the cellular p27 mRNA displays only marginal activity in translation initiation 77
3.1.2.5. No induction of IFN by IRES elements within the RV genome 78

3.2. USE OF IRES ELEMENTS TO REGULATE RABIES VIRUS REPLICATION 79

3.2.1. ATTENUATION OF RV BY PICORNAVIRAL IRES ELEMENTS 79
3.2.1.1. Generation of recombinant SAD IRES-P viruses 79
3.2.1.2. Attenuated growth kinetics of SAD IRES-P 81
3.2.1.3. Genome stability of SAD IRES-P 82
3.2.1.4. Diminished IFN antagonism of IRES-P RV 82
3.2.1.5. Attenuated replication of IRES-controlled RVs in brain slice cultures 84
3.2.1.6. Severe attenuation of IRES-dependent RVs in vivo 87
3.2.2. CHANGING THE RATIO OF FULL-LENGTH AND TRUNCATED RABIES VIRUS P PRODUCTS BY THE USE OF THE FMDV IRES 88
3.2.2.1. Expression of different RV P forms by SAD FMDV-P 88
3.2.2.2. Different P forms are incorporated into rabies virus particles 91
3.2.2.3. Involvement of RV P products in IFN antagonism of RV 92
3.2.2.4. Influence of changed RV P ratios on virus growth 94

4. DISCUSSION 96

4.1. A RABIES VIRUS-BASED HETEROLOGOUS SYSTEM TO EXPLORE TRANSLATION INITIATION BY IRES ELEMENTS 96

4.1.1. TRADITIONAL SYSTEMS FOR CHARACTERIZATION OF IRES ACTIVITIES 96
4.1.2. ADVANTAGES OF A NEW, RV-BASED REPORTER SYSTEM FOR CHARACTERIZATION OF IRES ACTIVITIES 98
4.1.3. USE OF THE NEW RV-BASED REPORTER SYSTEMS FOR ANALYSIS OF IRES ACTIVITIES 100
4.3.1.1. Potential influences on IRES activities 101
4.3.1.2. Analysis of the p27 5'UTR 103
4.3.1.3. Ribosome landing 104

4.2. USE OF PICORNAVIRAL IRES ELEMENTS AS A TOOL FOR REGULATION OF RABIES VIRUS GENE EXPRESSION 105

4.2.1. USE OF IRES ELEMENTS TO CONTROL RV P EXPRESSION AND THEREBY RV REPLICATION AND IFN ESCAPE 106
4.2.2. ANALYSIS OF RV P FORMS BY IRES-CONTROLLED RVS 110

5. SUMMARY 114

6. ZUSAMMENFASSUNG 116

APPENDIX 118

REFERENCES 124

CURRICULUM VITAE 145

DANKSAGUNG 146

LIST OF TABLES AND FIGURES

Tab. 1: Cell lines used in this work

Tab. 2: Oligonucleotides for cloning

Tab. 3: Oligonucleotides for sequencing

Tab. 4: Expression plasmids

Tab. 5: Fullength cDNAs (pSAD…) and the corresponding recombinant RVs.

Tab. 6: Antibodies

Tab. A1: The order of *Mononegavirales* (2002a)

Tab. A2: Viral IRES elements (Baird et al., 2006)

Tab. A3: Cellular IRES elements (Baird et al., 2006)

Fig. 1: Virus structure.

Fig. 2: RNA synthesis and gene expression by rhabdoviruses.

Fig. 3: Organization of RV phosphoprotein.

Fig. 4: RV life cycle.

Fig. 5: Interferon induction and IFN signaling induced by rhabdoviruses.

Fig. 6: Schematic representation of eukaryotic translation initiation mechanisms.

Fig. 7: Classification of IRES elements.

Fig. 8: 5'cap-independent reporter gene expression from IRES containing plasmids.

Fig. 9: Generation of SAD RL-IRES-FL reporter viruses.

Fig. 10: Growth of SAD RL-IRES-FL.

Fig. 11: Quantification of IRES activities by SAD RL-IRES-FL.

Fig. 12: Influence of different 3'UTRs on IRES activities.

Fig. 13: SAD RL-IRES-FL reporter viruses with changes in the start codon context.

Fig. 14: Quantification of IRES activities measured with SAD RL-IRES-FL_OATG.

Fig. 15: Generation of SAD IRES eCFP reporter viruses.

Fig. 16: IRES-dependent eCFP expression from SAD IRES eCFP.

Fig. 17: Quantification of IRES-dependent eCFP expression from SAD IRES eCFP by measurement of fluorescence intensities.

Fig. 18: Analysis of translation initiation by the 5'UTR of the cellular p27 mRNA.

Fig. 19: Influence of IRES elements on induction of type I IFN.

Fig. 20: IRES-dependent expression of RV P.

Fig. 21: Growth of IRES-controlled RV in cell culture.

LIST OF ABBREVIATIONS

°C	degree celsius
µg	microgramm
µl	microliter
µm	micro meter
µM	micro molar
5'-PPP-	5' triphosphate
aa	amino acid
ABLV	Australian bat lyssavirus
ADP	adenosine di-phosphate
AEV	avian encephalomyelitis virus
AGP	antigenome promoter
amp	ampicillin
AP1	adaptor protein 1
APS	ammoniumpersulfat
ATP	adenosine tri-phosphate
AUG	start codon
βgal	β-galactosidase
Bcl-2	B-cell lymphoma 2
Bip	immunoglobulin heavy-chain binding protein
bp	base pair
BVDV	bovine viral diarrhea virus
CARD	caspase activation and recruitment domain
CAT	chloramphenicol-acetyl transferase
CD	cluster of differentiation
CDK	cyclin dependent kinase
cDNA	complementary desoxy ribonucleic acid
cm	centimeter
CMV	cytomegalovirus
CNS	central nervous system
CrPV	cricket Paralysis virus
CSFV	Classical swine fever virus
CTD	C-terminal domain
C-terminal	carboxy-terminal
CVS	Challenge virus strain
d	days
DAPI	4',6-diamidino-2-phenylindole
DC	dendritic cell
dCTP	desoxycytidintriphosphat
del	deletion
DIH4	Sendai virus defective interfering particle clone 4
DLC	dynein light chain
DMEM	Dulbecco's Modified Eagle Medium
DMSO	Dimethylsulfoxid
DNA	desoxy ribonucleic acid

dNTP	desoxyribonucleosidtriphosphate
DRBP76	double-stranded RNA binding protein 76
dsRNA	double stranded ribonucleic acid
DUVV	duvenhage virus
E.coli	*Escherichia coli*
e.g.	*exempli gratia*, for example
EBLV	European bat lyssavirus
eCFP	enhanced cyan fluorescent protein
eCFP	enhanced cyan fluorescent protein
ECL	enhanced chemiluminescence
EDTA	ethylenediaminetetraacetic acid
eGFP	enhanced green fluorescent protein
eGFP	enhanced green fluorescent protein
eIF	eukaryotic translation initiation factor
EMCV	Encephalomyocarditis virus
ER	endoplasmic reticulum
et al.	et altera
FasL	Fas ligand
ffu	focus forming units
FGF	fibroblast growth factor
Fig	figure
FL	firefly luciferase
FMDV	Foot-and-mouth disease virus
g	gramm
G	glycoprotein
GDP	guanosine di-phosphate
GMEM	Glasgow Minimal Essential Medium
GP	genome promoter
GTP	guanosine tri-phosphate
h	hour
HAV	Hepatitis A virus
HCV	Hepatitis C virus
HIF	hypoxia induced factor
HIV	human immunodeficiency virus
hnRNP	heterogenous ribonucleoprotein
HRP	horseradish peroxidase
hrs	hours
HRV	Human rhinovirus
HSV	Herpes simplex virus
i.c.	intracranially
IF	in frame
IFN	interferon
IFNAR	interferon α receptor
IGR	intergenic region
IKK-i	inhibitor of κB kinase i
IPS-1	interferon-beta promoter stimulator 1

IRES	internal ribosome entry site
IRF	interferon regulatory factor
ISRE	IFN stimulated response element
ITAF	IRES transacting factor
J	Joule
JAK	janus kinase
kan	kanamycin
kb	kilo bases
KSHV	Kaposi's sarcoma-associated herpesvirus
l	liter
L	large protein, polymerase
La	Lupus erythematodes autoantigen
LB	lysogeny broth
LBV	Lagos bat virus
LC8	light chain 8
log_{10}	decadic logarithm
LU	light units
Luc	luciferase
M	molar
M	matrix protein
MDA 5	melanoma differentiation associated gene 5
MEM	Minimal Essential Medium
mg	milligramm
min	minute
ml	milliliter
mM	millimolar
mm	millimeter
MOI	multiplicity of infection
MOKV	Mokola virus
mRNA	messenger ribonucleic acid
N	nucleoprotein
N^0	non-RNA bound nucleoprotein
NaAc	natrium acetate
nAChR	nicotinic acetylcholine receptor
NAP1	NAC-associated protein 1
NC	nucleocapsid
NCAM	neural adhesion molecule
NES	nuclear export signal
NF45	nuclear factor 45
NF-κB	nuclear factor kappa B
ng	nanogramm
NK -cell	natural killer cell
nl	nanoliter
NLS	nuclear localization signal
nm	nanometer
nM	nanomolar

nm	nanometer
NS	non-structural protein
NNSV	non-segmented negative strand RNA viruses
nt	nucleotide
N-terminal	amino-terminal
OATG	original start codon
OF	out of frame
ORF	open reading frame
P	phosphoprotein
p.i.	post infection
P/S	penicillin/streptomycin
p75 NTR	p75 neurotrophin receptor
PAMP	pathogen associated molecular pattern
PBS	phosphate buffered saline
PBS-T	PBS plus TWEEN
PCBP	polyC binding protein
PCR	polymerase chain reaction
pDC	plasmacytoic dendritic cell
PEI	polyethylenimin
PEP	post-exposure prophylaxis
PEV	porcine enterovirus
PFA	paraformaldehyde
Pfu	*Pyrococcus furiosus*
PKC	protein kinase C
pmol	pico Mol
PO	peroxidase
polyIC	polyinosinic:polycytidylic acid
PRR	pathogen recognition receptor
PSIV	*Plautia stali* intestine virus
PTB	polypyrimidine tract binding protein
PTV	porcine teschovirus
PV	poliovirus
PVDF	polyvinyliden-fluorid
py	poly pyrimidine
RD	regulatory domain
rel.	relative
RhPV	*Rhopalosiphum padi* virus
RIG-I	retinoic acid inducible gene I
RL	renilla luciferase
RLR	RIG-I like receptors
RNA	ribonucleic acid
RNP	ribonucleoprotein
rpm	revolutions per minute
RPMI	Roswell Park Memorial Institute
RSV	respiratory syncytial virus
RT	reverse transcriptase
RT	room temperature
RV	rabies virus

RVPK	rabies virus protein kinase
SAD	Street Alabama Dufferin
SAP	shrimp alkaline phosphatase
SDS	sodium dodecylsulfate
SDS-PAGE	sodium dodecylsulfate polyacrylamide gel electrophoresis
SeV	Sendai virus
siRNA	small interfering ribonucleic acid
sld	stem loop domain
SPV	simian picornavirus
SRp20	serine-rich splicing factor 20
ssRNA	single stranded ribonucleic acid
STAT	Signal Transducers and Activators of Transcription
SV	Simian virus
Tab	table
TANK	TRAF family member-associated NFκB activator
Taq	*Thermus aquaticus*
TBK1	TANK binding protein 1
TBKBP	TBK binding protein
TEMED	Tetramethylethylendiamin
TLR	toll-like receptor
TNF	tumor necrosis factor
TRAF	TNF Receptor Associated Factor
tRNA	transfer ribonucleic acid
$tRNA_i$	initiator tRNA
TSV	Taura shrimp virus
TYK	tyrosine kinase
U	units
UNR	upstream of n-ras
UTR	untranslated terminal region
UV	ultra violet
V	volt
VEGF	Vascular Endothelial Growth Factor
vRNA	viral ribonucleic acid
vRNP	viral ribonucleoprotein
VSV	Vesicular stomatitis virus
w/v	weight per volume
wt	wild type

1. INTRODUCTION

1.1. Rabies virus

Rabies virus is the causative agent of rabies, one of the oldest known infectious diseases. Already 2,300 years B.C. first cases were described, which relate an acute, progressive and incurable encephalitis to the contact with a “mad” dog (Rupprecht et al., 2002). Two main forms of rabies are existing. The sylvatic form of rabies is found mainly on the northern hemisphere and is transmitted by wild animals, as e.g. foxes, badgers, martens in Europe and coyotes, racoons, skunks or bats in America. On the southern hemisphere primarily the urban form of rabies occurs, with roaming dogs as the main reservoir (Doerr and Gerlich, 2009).

As a classical zoonosis, rabies is transmitted by bites or scratches of infected animals. After transmission the virus is transported along axons in retrograde direction to the central nervous system (CNS). The incubation period varies between few days to several months. After first unspecific symptoms, like headache or fever, an acute state of infection develops with symptoms like hydrophobia, enhanced salivation, unconsciousness and coma, which finally lead to death (Charlton, 1994).

The first rabies virus vaccine was developed by Louis Pasteur in 1885. He vaccinated Joseph Meister, who was bitten by a rabid dog, with rabbit medulla homogenate and thereby invented the rabies post-exposure prophylaxis (PEP) (Doerr and Gerlich, 2009). Present vaccines against rabies consist of cell culture-derived, inactivated virus particles. The post-exposure prophylaxis comprises passive immunization with neutralizing antibodies against the rabies virus glycoprotein and in addition an active immunization with the dead vaccine (Doerr and Gerlich, 2009).

In Europe the continuous oral vaccination of foxes allows a successful control of rabies. However worldwide 40,000-50,000 lethal human cases of rabies occur per year, particularly in rural regions of India and Africa (Doerr and Gerlich, 2009).

1.1.1. Taxonomy

Together with the families of *Paramyxoviridae*, *Filoviridae* and *Bornaviridae*, the family of *Rhabdoviridae* was classified into the order of *Mononegavirales* (2002a). Members of the *Mononegavirales* have commonalities in their genome organization, gene expression and viral composition. Their genome consists of a non-segmented single stranded RNA of negative polarity, which is tightly enwrapped by the nucleoprotein and forms a stable helical ribonucleoprotein complex (RNP). New virus particles are formed by budding at cellular membranes.

The family of *Rhabdoviridae* contains viruses that can infect a broad range of hosts, like plants, invertebrates and vertebrates (Fu, 2005). This family is further subclassified into six genera (*Lyssavirus, Vesiculovirus, Ephemerovirus, Novirhabdovirus, Cytorhabdovirus, Nucleorhabdovirus*) among which lyssaviruses and vesiculoviruses are the two largest groups. Within the lyssaviruses beside rabies virus (RV, genotype 1) six other genotypes exist. These are Lagos bat virus (LBV, genotype 2), Mokola virus (MOKV, genotype 3), Duvenhage Virus (DUVV, genotyp 4), European bat lyssaviruses (EBLV1, genotype 5 and EBLV2, genotype 6) and the Australian bat lyssavirus (ABLV, genotype 7) (Tab. A1). Although homologous in their sequences, the genotypes show a relatively great diversity in their antigenic structures (Dietzschold et al., 1983). The genus *Vesiculovirus* contains arboviruses, which can infect insects and mammals. The well-known and characterized vesicular stomatitis virus (VSV) is the prototypic member of this genus. This virus is able to cause a disease which is similar to that of foot-and-mouth disease in cattles and pigs (Brown et al., 1967).

1.1.2. Virus structure and genome organization

Rabies virus forms bullet-shaped enveloped particles of approximately 180 nm length and 75 nm width. These contain a non-segmented single strand RNA of negative polarity with a size of approximately 12 kb as a genome.

The viral RNA is tightly enwrapped by approximately 11,000 copies of the nucleoprotein (N) and associated with several copies of the phosphoprotein (P) and the viral polymerase (L). Thereby a stable, helical RNP is formed (Naeve et al., 1980), which protects the RNA from degradation or RNA interference by siRNAs. The inside of the viral membrane is covered by the matrixprotein (M), whereas transmembrane glycoproteins (G) form trimeric spikes which are embedded into the membrane (Fig. 1).

The viral RNA comprises five genes encoding nucleoprotein, phosphoprotein, matrixprotein, glycoprotein and polymerase in the order 3'-N-P-M-G-L-5'. All genes are giving rise to monocistronic, 5'capped mRNAs from which the viral proteins are translated (Fig. 2). All are structural proteins of the virion, being essential for virus replication and spread.

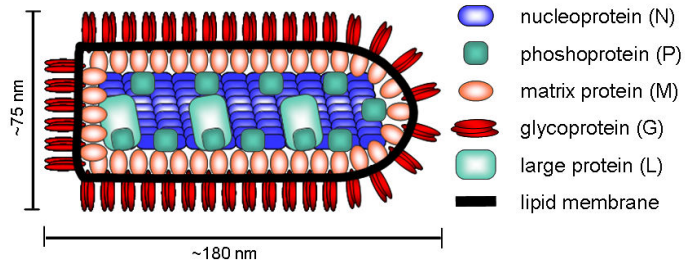

adapted from Doerr/Gerlich: Medizinische Virologie; 2. Auflage; Thieme

Fig. 1: Virus structure.
RV forms enveloped particles with a bullet-shaped form, a length of 180 nm and a width of 75 nm. The viral RNP consists of the genomic RNA tightly encased by the N protein and associated with the viral RNA-dependent RNA polymerase consisting of P and L proteins. The M protein is associated with both RNP and the envelope. The rabies glycoprotein forms approximately 400 trimeric spikes which are tightly arranged on the surface of the virus.

The P gene contains four in frame AUGs, such that four N-terminally truncated P forms are translated by ribosomal leaky scanning. So called "leader" and "trailer" sequences at the 3' and 5' ends of the genome are untranslated terminal regions of 50 to 150 bp, which are partially complementary to each other. These sequences contain the viral promoter and furthermore are templates for short, non-polyadenylated, triphosphate RNAs. All viral genes are separated by gene borders, conserved regulatory regions comprising a gene end (transcription stop and polyadenylation signals) and a gene start (transcription start signal). Between the stop/start sequences short, non-transcribed intergenic regions of 2-24 nt are inserted (Fig. 2).

1.1.3. Viral gene expression and RNA synthesis

The basic mechanisms of *Mononegavirales* RNA synthesis and the functions of proteins involved are highly conserved, in spite of a mostly poor sequence homology (Luo et al., 2007). The RNP is necessary for viral gene expression and RNA synthesis, serving as a template for the viral polymerase, which is composed of a large catalytic subunit L and the polymerase cofactor P (Fig. 2). Except for some plant rhabdoviruses grouped in the genus *Nucleorhabdovirus*, the RNA synthesis, as well as the whole replication cycle, takes place in the cytoplasm within small cytoplasmic inclusion bodies, the so called "Negri bodies".

For transcription, the genomic RNA ("-"strand) is used as a template. RNA synthesis starts at the 3' end of the genomic RNA with the synthesis of a short leader RNA (58 nt long), which is neither capped nor polyadenylated, but is carrying a 5' triphosphate (Abraham and Banerjee, 1976; Colonno and Banerjee, 1976). Afterwards transcription of the rhabdovirus mRNAs takes place in a sequential mode starting at the 3' terminal genome promoter, such that monocistronic, 5'capped and polyadenylated mRNAs for each viral gene are transcribed. Capping is carried out by the viral polymerase (Both et al., 1975; Li et al., 2006; Ogino and Banerjee, 2007). As the viral polymerase dissociates at the gene borders quite often and then can start transcription only at the 3'leader region, mRNAs of the genes most proximal to the 3' end are the most abundant ones, whereas amounts of transcribed mRNAs decrease progressively towards the 5' end (Banerjee, 2008). The steepness of this transcription gradient is regulated by the length of the gene borders. This allows an accurate control of RNP replication and gene expression, which is inalienable for a successful virus infection (Fig. 2).

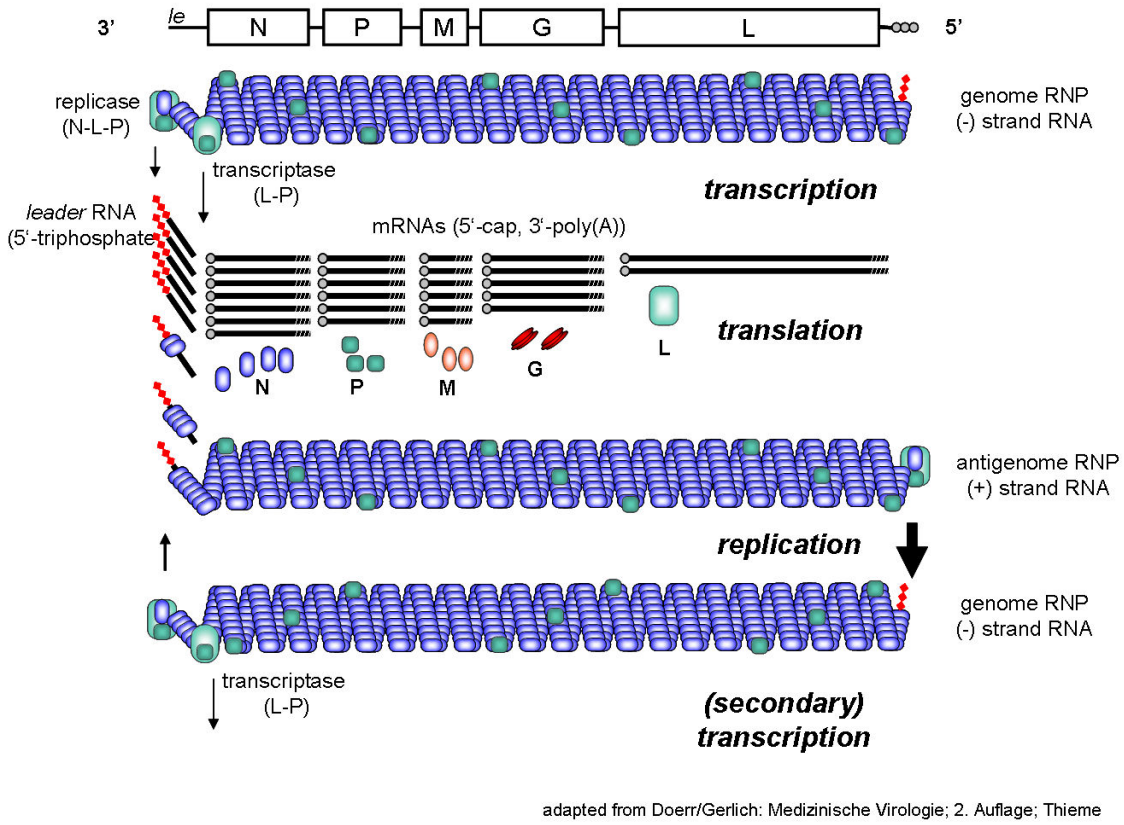

Fig. 2: RNA synthesis and gene expression by rhabdoviruses.
The viral transcriptase (L-P) transcribes monocistronic, 5' capped and polyadenylated mRNAs for each viral gene, using the genomic RNP as template. In addition, leader RNAs are synthesized, carrying a 5' triphosphate. As the transcriptase dissociates at the gene borders, the amount of transcribed mRNAs decreases progressively towards the 5' end. As soon as enough viral proteins are translated the viral replicase (N-L-P) synthesizes a full-length antigenome ("+" strand), which is co-transcriptionally packed by N and P proteins into antigenome RNPs. The antigenome RNP acts as a template for the replication of an excess of genomic RNPs. From these either new mRNAs are transcribed (secondary transcription) or they are packed into new viral particles.

As soon as enough N is synthesized, replication starts (Patton et al., 1984). In this process the P protein takes over two functions. First, it is needed as a chaperone for N, which in the presence of P specifically encapsidates the viral RNA (Curran and Kolakofsky, 2008; Curran et al., 1995; Horikami et al., 1992). Second, it forms together with N and L the replicase complex (N-L-P). The viral replicase generates a fullength antigenome ("+" strand), starting at the 3' end of the antigenome and ignoring the transcription signals within the gene borders. The antigenome is cotranscriptionally packed by N and P proteins into antigenome RNPs with a 5' terminal adenosine (5'-PPP-A…), and afterwards acts as a template for the replication of an excess of genomic RNPs. From these either new mRNAs are transcribed (secondary transcription) or they are packed into new viral particles (Fig. 2).

The balance between RNP replication and mRNA transcription is a tightly regulated process. The regulation involves the structural matrix protein (M) (Finke and Conzelmann, 2003; Finke et al., 2003). RV M downregulates transcriptase activity and concurrently supports RNP replication. An amino acid (aa) at position 58 within RV M has been shown to be critical for this function. The loss of transcription leads to cytopathic effects, pointing out, that transcription regulation by M is essential for suppression of gene expression, in order not to kill the cells (Finke et al., 2003).

Furthermore, the M protein, together with the viral glycoprotein, is essential for virus assembly and budding at the cell surface. During this process M condenses the newly synthesized RNPs (Mebatsion et al., 1999; Buonocore et al., 2002) and provides the contact between the nucleocapsid (NC) and the virus envelope (Fig. 1).

The viral glycoproteins are incorporated as trimeric spikes into the viral membrane. The transmembrane G protein is the major viral antigen and pathogenicity factor of rabies virus (Morimoto et al., 2000; Finke and Conzelmann, 2005a), being responsible for attachment to target cells and membrane fusion. High levels of glycoprotein expression were found to be responsible for induction of apoptosis in infected cells, whereas downregulation of G expression prevents induction of apoptosis and is correlated with virus pathogenicity (Faber et al., 2002; Morimoto et al., 1999; Prehaud et al., 2003; Sarmento et al., 2005).

1.1.4. Organization of RV phosphoprotein

The RV phosphoprotein (P) is an essential structural protein of rabies virus, which takes over different, very important viral functions. Diverse domains, necessary for certain functions, are mapped and characterized (Gerard et al., 2009) (Fig. 3).

The phosphoprotein is a structural protein of 297 aa length. As already described, the P protein serves as a chaperone that associates with nucleoprotein (N) and therefore is essential for virus RNA encapsidation. Two independent N-binding domains were described. One domain, localized between aa 10-52, most likely interacts with newly synthesized non-RNA bound nucleoprotein (N^0), in order to maintain it in a soluble, RNA-free form (Mavrakis et al., 2006; Chen et al., 2007). Another N-binding domain in the C-terminus (aa 185-297) is essential for the P protein's transcriptional activity (N-RNA) (Mavrakis et al., 2003; Chenik et al., 1994; Jacob et al., 2001; Mavrakis et al., 2004). The N-terminus (aa 1-19) of RV P was shown to be crucial for interaction with the C-terminal domain of L protein, providing the basis for its function as the polymerase cofactor (Chenik et al., 1998). Furthermore, RV P contains a structured domain in the central part (aa 52-189), which is responsible for oligomerization (Ding et al., 2006; Gerard et al., 2007; Gigant et al., 2000; Jacob et al., 2001). Four isomers of protein kinase C (PKC) and a until now not characterized cellular rabies virus protein kinase (RVPK) are phosphorylating RV P at different serines (S63, S64, S162, 210, 271) (Gupta et al., 2000) (Fig. 3).

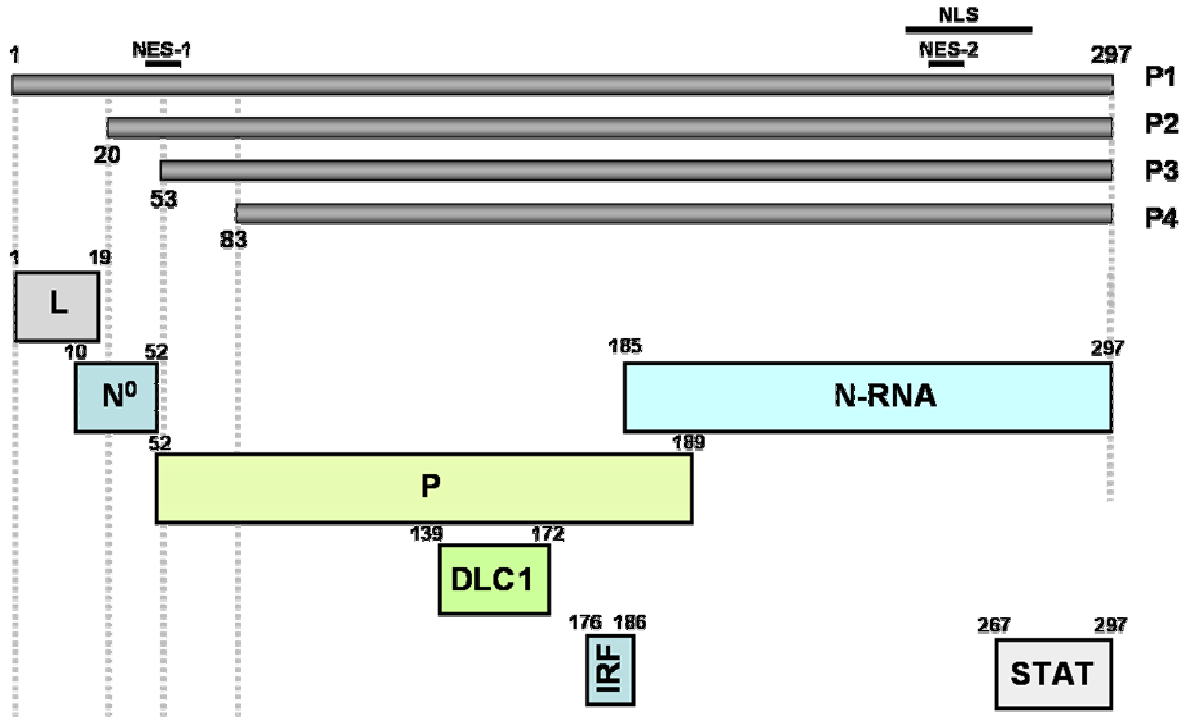

Fig. 3: Organization of RV phosphoprotein.
From the RV P gene in addition to the full-length P protein (**P1**) three N-terminally truncated P forms (**P2, P3, P4**) are expressed. The full-length P protein (297 aa) contains binding domains for interaction with the polymerase (**L**), newly synthezised N ($\mathbf{N^0}$), and dynein light chain (**DLC1**). In addition, an oligomerization domain (**P**) is contained between aa 52 to aa 189 and a domain necessary for binding to nucleocapsids (**N-RNA**) between aa 185 and aa 297. Due to its binding to interferon regulatory factor 3 (**IRF**) and to phosphorylated STATs (**STAT**), it is able to counteract the host innate immune system.

Furthermore it was shown that RV P interacts with the cytoplasmic dynein light chain (DLC1; LC8) (Jacob et al., 2000; Raux et al., 2000) by a domain located between aa 139-172. The initial hypothesis, that the DLC1-P interaction might be responsible for the retrograde axonal transport of RNPs was challenged by the findings that RV transport occurs in axonal transport vesicles (Klingen et al., 2008; Mebatsion, 2001). Thus it is suggested that DLC1-P interaction might be involved in modulating viral transcription in neuronal cells (Tan et al., 2007)

RV phosphoprotein was shown to be a potent inhibitor of IFN induction (Brzozka et al., 2005) and IFN signaling (Brzozka et al., 2006). A domain, which is essential for interference with IRF activation, is located in the central part at aa 176-186. The C-terminal domain (aa 267-297) contains the STAT1 binding site, important for inhibition of IFN signaling by RV P (Brzozka et al., 2006; Vidy et al., 2005) (Fig. 3).

In the SAD strain in addition to full-length P (P1) three N-terminally truncated forms of RV P (P2-P4) are expressed from the RV P mRNA by translation initiation at downstream in frame start codons (aa 20, aa 53, aa 83), due to a ribosomal leaky scanning mechanism (Eriguchi et al., 2002). Fullength P1 and P2 are located in the cytoplasm, whereas a fraction of P3 and P4 was shown to locate to the nucleus, due to the lack of the N-terminal nuclear export signal 1 (NES-1). The subcellular localization of different P forms is determined by NES-1 (aa 49-58) and NES-2, as well as a nuclear localization import signal (NLS), located in the C-terminal domain (CTD) between aa 211 and aa 260 (Pasdeloup et al., 2005; Moseley et al., 2007) (Fig. 3). Previously, it was shown that RV lacking P2-P4 is able to support viral transcription and replication and shows no great differences to wt RV, in terms of growth and IFN escape. This indicates that the presence of truncated P forms is not required for RV replication *in vitro* (Brzozka et al., 2005).

1.1.5. Viral replication cycle

Typically, rabies virus is transmitted by bites or scratches from infected animals or per mucosa directly into motor neurons (Ugolini, 2008). It is transported along axons in retrograde direction towards the central nervous system (CNS), using the cellular, microtubule-dependent and dynein-mediated, retrograde cargo transport system of axons (Greber and Way, 2006). This axonal transport proceeds within transport vesicles in which complete enveloped RV particles are carried as a cargo (Klingen et al., 2008). The following spread of RV within the CNS *in vivo* occurs via trans-synaptic spread, which also depends on RV glycoprotein (Etessami et al., 2000; Wickersham et al., 2007b). Replication of RV takes place in specific regions of the CNS, like hippocampus, amygdala and neocortex. Several

receptors in the CNS facilitate virus entry into neurons and thereby link RV to its neurotropism (Fig. 4A). Common neuron specific receptors proposed for RV entry are the p75 neurotrophin receptor (p75NTR) (Tuffereau et al., 1998; Tuffereau et al., 2001), the neural adhesion molecule (NCAM, CD56) (Thoulouze et al., 1998) and the nicotinic acetylcholine receptor (nAChR) (Lentz et al., 1982). As RV is able to infect also non neuronal cells, it is evident that also ubiquitous receptors with weak affinity can be used for entry (Lafon, 2005b; Reagan and Wunner, 1985). After receptor binding, RV is uptaken by the host cell via endocytosis into clathrin coated vesicles. A subsequent pH-dependent, RV G-mediated membrane fusion leads to the realease of the viral RNP into the cytoplasm (Roche and Gaudin, 2004; Gaudin, 2000) (Fig. 4C,D). Therefore, the RV glycoprotein is responsible for transport, entry and spread within the CNS, which makes it the major determinant for RV neurotropism and pathogenesis (see below).

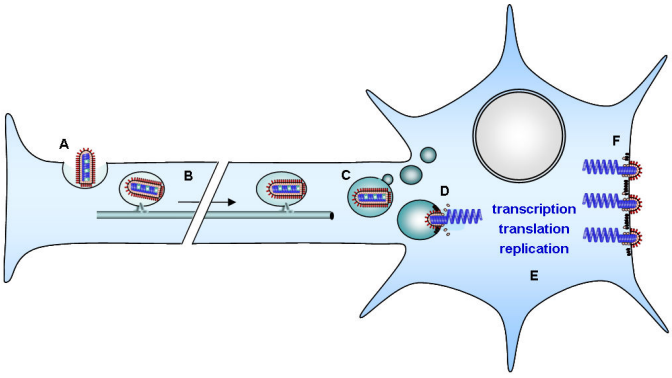

adapted from Doerr/Gerlich: Medizinische Virologie; 2. Auflage; Thieme

Fig. 4: RV life cycle.
(A) RV entry is mediated by receptor mediated endocytosis. (B) Enveloped virus particles are transported within vesicles along axons in retrograde direction, using the microtubule-dependent dynein-mediated cargo system.
(C, D) The viral RNP is released from vesicles into the cytoplasm by pH-dependent, RV G-mediated membrane fusion. (E) RNA synthesis and gene expression occur in the cytoplasm. (F) After accumulation of newly synthesized RNPs, M and G proteins, budding of viral particles occurs at the cell membrane.

Once the virus has entered the host cell cytoplasm, the viral nucleocapsid achieves a relaxed form, which is active for RNA synthesis and gene expression. After accumulation of newly synthesized RNPs, M and G proteins, budding of viral particles occurs at the cell membrane. Also here RV G (together with RV M) plays an important role. RV G is co-translationally inserted into the endoplasmic reticulum (ER), with its C-terminus anchored in the ER membrane. Afterwards it is transported by the secretory pathway within the Golgi apparatus to the cellular membrane. After accumulation of the matrix protein in the cytoplasm, it binds at the cell membrane to newly synthesized vRNPs, leading to their condensation. The condensed and M-bound RNPs interact with the cytoplasmic regions of the glycoproteins, which results in budding of new virus particles from the cell surface. Virus budding is supported by diverse cellular machineries with which the matrix protein is interacting.

1.1.6. Pathogenicity

The glycoprotein is the major determinant of rabies virus neuropathogenicity, as it is responsible for receptor binding and subsequent endocytosis. The correlation between the glycoprotein and rabies virus pathogenesis becomes evident when two RV strains are compared. The vaccine strain Street Alabama Dufferin (SAD) B19 is almost apathogenic after peripheral infection. However the exchange of its glycoprotein by the one of the Challenge Virus Strain (CVS), renders the virus virulent and pathogenic (Morimoto et al., 2000; Morimoto et al., 2000; Finke and Conzelmann, 2005b). RVs containing no glycoprotein are unable to spread *in vitro* and *in vivo* (Etessami et al., 2000; Mebatsion et al., 1996a). Furthermore, RV G is the only viral antigen, which induces the production of neutralizing antibodies.

The host immune system reacts against RV mainly with production of neutralizing antibodies, which depend on B lymphocytes and CD4+ T-cells and which are crucial for clearance of RV from the CNS. After infection with rabies virus chemokines are produced and mononuclear inflammatory cells (NK-cells, T- and B- lymphocytes) can infiltrate the CNS. In contrast to attenuated RV, only a slight activation of innate immune response was observed after infection with pathogenic RVs (Perry and Lodmell, 1991; Hooper et al., 1998; Wang et al., 2005b; Nakamichi et al., 2004).

The general strategy of RV is to bypass the host immune system in order to reach the CNS (Finke and Conzelmann, 2005b; Dietzschold et al., 2005; Lafon, 2005a). Therefore, it avoids destruction of neurons and of the peripheral nervous system, by minimizing induction of the innate immune response and inflammation. For that reason RV has developed mechanisms to counteract the host immune system (see below). Once th virus reached the brain, replication and spread occurs. RV infected neurons retain their integrity but upregulate FasL levels, and thereby induce apoptosis of T-cells, shortly after the T-cells cross the blood-brain barrier (Baloul et al., 2004). Attenuated virus strains may induce apoptosis by accumulation of glycoproteins in the ER of infected cells, which is correlated with reduced neuroinvasiveness.

1.1.7. Mechanisms of RV to counteract innate immunity

1.1.7.1. Interferon induction and signaling induced by rhabdoviruses

Activation of the innate immune response plays a crucial role for the survival of the infected host as it occurs long before adaptive immune responses. Numerous cytokines are involved in innate immune responses. Among them, interferons (IFNs) play a key role in turning on mechanisms of antiviral defense and regulating adaptive immunity. The family of interferons

consists of two main types. The group of mammalian type I interferons comprises a single IFNβ protein and diverse IFNα subtypes, whereas type II interferon consists of one single IFNγ protein. Depending on the cell type various types of interferon are produced at different time points. Although most cell types are able to produce type I interferons, the main source of IFNα in humans are plasmacytoic dendritic cells (pDCs). In contrast, IFNγ is produced only by certain cells like natural killer (NK) cells, macrophages, CD4+ and CD8+ T-lymphocytes and by neurons.

Activation of the innate immune system occurs after recognition of non-self structures or conserved pathogen associated molecular patterns (PAMPs) by pattern recognition receptors (PRRs). In case of virus infections, the viral nucleic acids are the major PAMPs, which are recognized by the immune system and thereby induce production of antiviral type I IFNs and other cytokines (Hornung et al., 2006; Pichlmair and Reis e Sousa, 2007; Uematsu and Akira, 2007; Yoneyama and Fujita, 2007). Viral RNAs can be recognized by extra- or intracellular PRRs.

The main PRRs for viral RNA are represented by RIG-I like receptors (RLRs), including RIG-I (retinoic acid inducible gene I) and MDA 5 (melanoma differentiation associated gene 5). Both are DExD/H box RNA helicases, found to be essential for production of type I IFNs (Childs et al., 2007; Yoneyama et al., 2004; Yoneyama et al., 2005) and type III IFN (IFNλ) (Onoguchi et al., 2007) in response to RNA virus infection. Both RLRs share a conserved architecture. They consist of two N-terminal CARD domains, mediating downstream signaling, a central DECH box helicase domain and a specific short C-terminal domain (CTD) or regulatory domain (RD) (Saito et al., 2007). Although both helicases are closely related and both are activated by dsRNA or the dsRNA analogue polyIC (Yoneyama et al., 2004; Gitlin et al., 2006), they respond to different RNA viruses. RIG-I recognizes various positive and negative strand RNA viruses, whereas MDA5 is activated only by a few positive strand RNA viruses (Gitlin et al., 2006; Kato et al., 2006; Kato et al., 2005). RIG-I activation occurs upon binding of specific ligands, like e.g. 5’ triphosphate containing RNA (Hornung et al., 2006; Pichlmair et al., 2006), to the RD of RIG-I. In case of rhabdoviruses viral RNAs with 5’ triphosphates include the leader RNA, the genome, and the antigenome RNA. As full-length RNAs are present only in a tightly packed form within nucleocapsids, most likely the leader RNA of rhabdoviruses represents the main RIG-I ligand. Binding results in an ATPase dependent conformational change. This stimulates self-association and leads to an “open” state, in which the CARD domains are accessible for several interaction partners, inducing a signaling cascade that involves diverse regulatory proteins

(Rieder and Conzelmann, 2009). This pathway leads to the activation of the kinases TBK1 and IKK-i, which in turn activate IRF3 by phosphorylation. Phosphorylated IRF3 dimerizes and translocates into the nucleus, where it activates the IFNβ promoter, together with the transcription factors NF-κB and AP1 (Fig. 5).

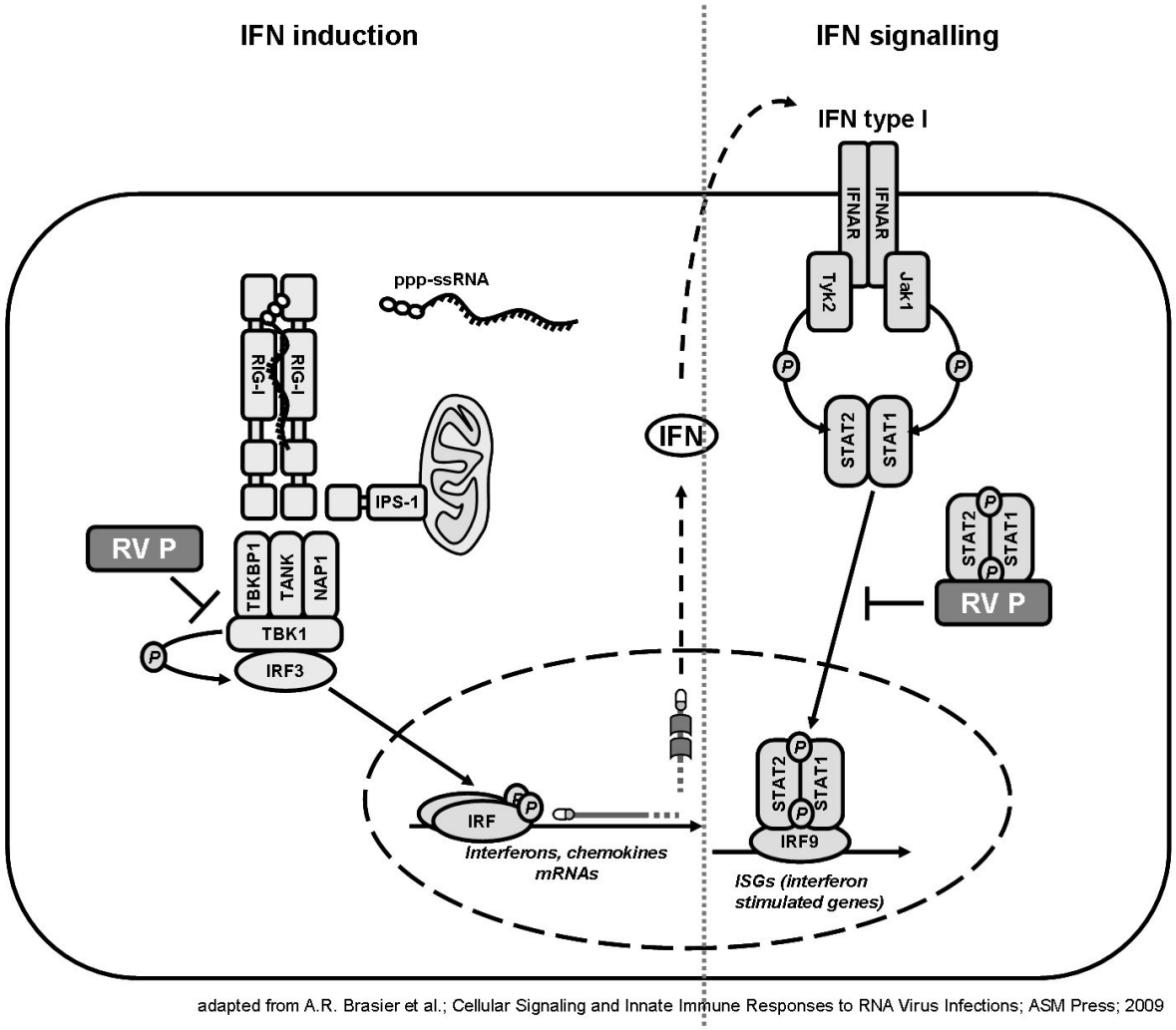

Fig. 5: Interferon induction and IFN signaling induced by rhabdoviruses.
Recognition of RV triphosphate RNAs by RIG-I results in association of CARD domains of RIG-I and IPS-1. This induces the recruitment of a complex in which TBK1 phosphorylates IRF3, resulting in IRF3 dimerization, import into the nucleus, and transcriptional activation of the IFNβ gene. IRF3 phosphorylation is blocked in the presence of RV P. Secreted IFN binds to the IFNAR, leading to phosphorylation of STATs by JAK1 and TYK2. Phosphorylated STATs dimerize, are imported into the nucleus, where they induce together with IRF9, expression of interferon stimulated genes (ISGs). RV P binds to phosphorylated STATs and thereby prevents their translocation in the nucleus.

Toll-like receptors (TLRs) correspond to the group of transmembrane PRRs. In contrast to RLRs, which are expressed ubiquitously, TLRs are located as single-span transmembrane glycoproteins at the surface or at endosomal membranes of specialized immune cells. Out of twelve members of TLRs in mammals, TLR3/4 and TLR7/8/9 are able to induce IFN induction after virus infection, by recruitment and activation of intracellular adaptor molecules and kinases (for review see (Uematsu and Akira, 2007). In case of rhabdoviruses it was shown that TLRs 3,4 and 7 play a role in IFN induction (Lee et al., 2007; Georgel et al., 2007).

Secreted IFN is acting in an auto- or paracrine way by binding to the ubiquitous IFNα receptors (IFNARs). Binding results in activation of the canonical Janus-kinase/signal transducer and activator of transcription (JAK/STAT) pathway. Upon IFN α/β binding the IFNAR associated kinases TYK2 and JAK1 phosphorylate and activate STAT1 and STAT2, resulting in the formation of a heterodimeric complex, consisting of STAT1 or STAT2 and IRF9. This leads to the expression of several interferon-stimulated genes (ISGs) with antiviral or immune stimulatory activity, which feed back in a positive feedback loop (Platanias, 2005) (Fig. 5).

1.1.7.2. Rabies virus countermeasures to prevent IFN induction and IFN signaling

The general strategy of RV for survival is to avoid the host immune system until the virus reaches the CNS. Therefore RV has evolved strategies to interfere with the IFN system, which allows to preserve the integrity of the host cells, in order to reach the CNS, where it replicates best (Finke and Conzelmann, 2005b; Lafon, 2005a).

The multifunctional RV phosphoprotein, which is involved in several essential functions of viral RNA synthesis, is the main viral factor, which counteracts the innate immune system. Expression of RV P specifically prevents phosphorylation and activation of IRF3 and IRF7 (Brzozka et al., 2005), most likely by interfering with the formation of the IPS-1-linked NAP1/TBKBP/TANK complex. Thus, IFN induction by RIG-I is completely blocked (Fig. 5).

Beside inhibition of IFN induction it is furthermore important for viruses to develop means to target also IFN signaling, for counteracting IFN-induced antiviral effects and preventing positive feedback and stimulation of the IFN system (Brzozka et al., 2007; Haller et al., 2007; Randall and Goodbourn, 2008). Also here, the RV phosphoprotein takes over the major role. RV P binds specifically to activated, phosphorylated STAT and thereby prevents its import into the nucleus, such that IFN induced activation of ISGs is prevented (Brzozka et al., 2006;

Vidy et al., 2005; Vidy et al., 2007) (Fig. 5). Whereas the C-terminal 10 aa of P are crucial for counteracting IFN signaling, an internal stretch of 10 aa (residues 176-186) is required for efficient inhibition of IFNβ production (Fig. 3). This demonstrates that P combines two genetically independent functions in antagonizing the IFN system.

1.1.8. Use of *Mononegavirales* as viral vectors

The establishment of a reverse genetics system to recover rhabdoviruses from cDNA, makes it possible to genetically engineer recombinant viruses (Schnell et al., 1994). This allows first to study different aspects of the viral life cycle by mutational experiments (Mavrakis et al., 2004; Albertini et al., 2006; Albertini et al., 2008) as well as the identification of cellular interaction partners. And second, to make use of rhabdoviruses for biomedical application, like e.g. vaccination, gene therapy or oncolytic virotherapy.

Besides their ability to infect a broad range of host cells, rhabdoviruses offer other attractive features for their use as gene expression vectors. Due to the helical structure of rhabdovirus RNPs, no restrictions in regard of the viral coding capacity are imposed. Thus, insertions of up to 4.5 kb are described in case of VSV (Haglund et al., 2000). Since rhabdovirus replication occurs completely in the cytoplasm, it is unlikelly that viral genes or inserted foreign genes are incorporated into the host genome. In addition, rhabdoviruses have, due to the protection of their RNA in the RNP complex, a poor recombination rate. This results in the maintenance of even dispensable sequences over 25 passages of recombinant RVs (Mebatsion et al., 1996b). However, after manipulations affecting virus fitness, revertants can be selected (Wertz et al., 2002; Mebatsion et al., 1996b).

An important task in the approach to use RV and other *Mononegavirales* as safe vectors, is to attenuate their pathogenicity. Therefore, strategies for virus attenuation were subject of intensive examinations. The prime candidate for RV attenuation is the phosphoprotein as a multifunctional virus protein. Particularly its function as the IFN antagonist makes this protein suitable for attenuation of the virus in IFN competent cells. So, recombinant RVs expressing low amounts of RV P, like SAD GFP-P (Finke et al., 2004) or SAD ΔPLP (Brzozka et al., 2005), are severely attenuated in IFN competent cells and therefore are interesting for the development of safe vectors or vaccines. Another strategy for virus attenuation is the establishment of so called single cycle gene deletion vectors. In these one or more essential virus genes are deleted, like e.g. M- or G-deficient viruses (Metbatsion et al.,1999; Etessami et al., 2000; Wickersham et al., 2007a), which cannot spread. This allows virus replication in cells, which are complemented in trans by the lacking proteins.

As rhabdovirus gene expression is regulated on transcriptional level by a transcription gradient, it is possible to determine the expression level of foreign genes by the position of insertion within the genome. Thus, foreign genes, inserted at the end of the RV genome are expressed only to marginal levels (Brzozka et al., 2005; Finke et al., 2000; Finke and Conzelmann, 2003), whereas gene insertions in closer proximity to the 3'end are expressed more abundantly (McGettigan et al., 2003). One should be aware that all insertions can change the transcriptional gradient and thereby also gene expression of downstream genes like e.g. the polymerase. However a particularly favorable position for extra genes is between the genes for the glycoprotein and the polymerase, within the G/L gene border, as insertions within this position do not greatly affect viral replication (Mebatsion et al., 1996b). Ambisense gene expression is another possibility to insert extra genes into rhabdoviruses. For this purpose, the promoter of the RV antigenome (AGP) has to be exchanged by the genome promoter (GP), such that not only replication but also transcription is carried out. This enables expression of multiple foreign genes from the antigenome without influencing the transcriptional gradient of the viral mRNAs (Finke and Conzelmann, 1997).

Using these diverse methods, a great number of foreign genes have been incorporated into recombinant RVs. Among them were e.g. genes for the non-structural proteins (NS1/NS2) of the respiratory syncytial virus (RSV) (Schlender et al., 2005), Hepatitis C virus (HCV) glycoproteins (Buonocore et al., 2002; Siler et al., 2002), the chloramphenicol-acetyl-transferase (CAT) (Finke and Conzelmann, 1997; Mebatsion et al., 1996b), the enhanced green fluorescent protein (eGFP) or other fluorescent proteins (Klingen et al., 2008; Finke et al., 2004; Wickersham et al., 2007b). Especially the possibility of stable incorporation of fluorescent proteins into recombinant and attenuated RVs is being exploited to generate tools for synaptic tracing (Wickersham et al., 2007b; Wickersham et al., 2007a) or live imaging of axonal transport, entry and release of virus particles (Finke et al., 2004; Klingen et al., 2008).

1.2. Internal ribosome entry sites (IRES)

1.2.1. Cap-dependent translation initiation

The majority of mRNAs is translated by initiation depending on a 7-methyl guanosine cap structure at their 5' end (Shatkin and Manley, 2000). The cap nucleotide m^7GTP is linked by a 5'-5'-triphosphate to the first transcribed nucleotide. This cap structure is generated by host-based transcription and post-transcriptional modifications. Viruses use either the cellular capping machinery for their mRNAs or contain polymerases with their own capping activity (Ogino and Banerjee, 2008; Ogino and Banerjee, 2007; Wang et al., 2007). It has been well described that this cap structure is important for recognition of mRNAs by ribosomes and the following translation initiation (Sonenberg et al., 1979) (for recent review see (Sonenberg and Hinnebusch, 2009). The cap structure binds the cap binding protein, eukaryotic translation initiation factor (eIF) 4E (eIF4E), which in turn forms the heterotrimeric complex eIF4F, consisting of the factors eIF4E, eIF4G and eIF4A. After interaction with eIF3 (Lamphear et al., 1995), the cap-bound eIF4F complex facilitates binding of a preassembled pre-initiation complex, in which the 40S ribosomal subunit associates with the ternary complex of eIF2, GTP and Met-tRNA$_i$. The pre-initiation complex than scans downstream until it reaches an AUG in a favorable "Kozak" sequence context (A/GxxAUGG/A) (Kozak, 1987). This scanning process is facilitated by the ATP-dependent RNA helicase eIF4A within the eIF4F complex. Stimulated by the cofactors eIF4B or eIF4H, it can unwind secondary structures in the mRNA that might impair the way of scanning towards the start codon (Marintchev et al., 2009). Once the pre-initiation complex arrives at the matching start codon, the scanning process is stopped and GTP within the eIF2-GTP-Met-tRNAi ternary complex is hydrolysed. eIF2-GDP and other eIFs are released, such that the 60S ribosomal subunit can join and an 80S initiation complex is formed, leading to subsequent translation elongation (Fig. 6A).

In addition to the basic factors essential for translation initiation, a multitude of other eIFs plays important roles in the initiation process. Among them eIF1 and eIF1A are involved in start codon selection. The C-terminal region of eIF1A together with eIF1 promotes scanning when non-AUGs are occupying the P-site within the pre-initiation complex, whereas the N-terminus of eIF1A arrests scanning and induces eIF1 release at AUG codons (Fekete et al., 2007; Passmore et al., 2007). The multisubunit factor eIF3 interacts with all other components and with the 40S ribosomal subunit. Thereby it plays not only a role in assembly of the pre-initiation complex, but is also important for recruiting it to the mRNA by binding to eIF4G (Pisarev et al., 2008; Pestova et al., 2007; Hinnebusch et al., 2007). Another factor stimulating translation initiation is the polyA binding protein (PABP). It covers the

polyA tail of the mRNA and interacts with eIF4G (Tarun, Jr. et al., 1997), leading to the circularization of the mRNA, by linking the cap and the polyA tail in a “closed loop”. This could stimulate translation initiation by recycling of post-termination ribosomes.

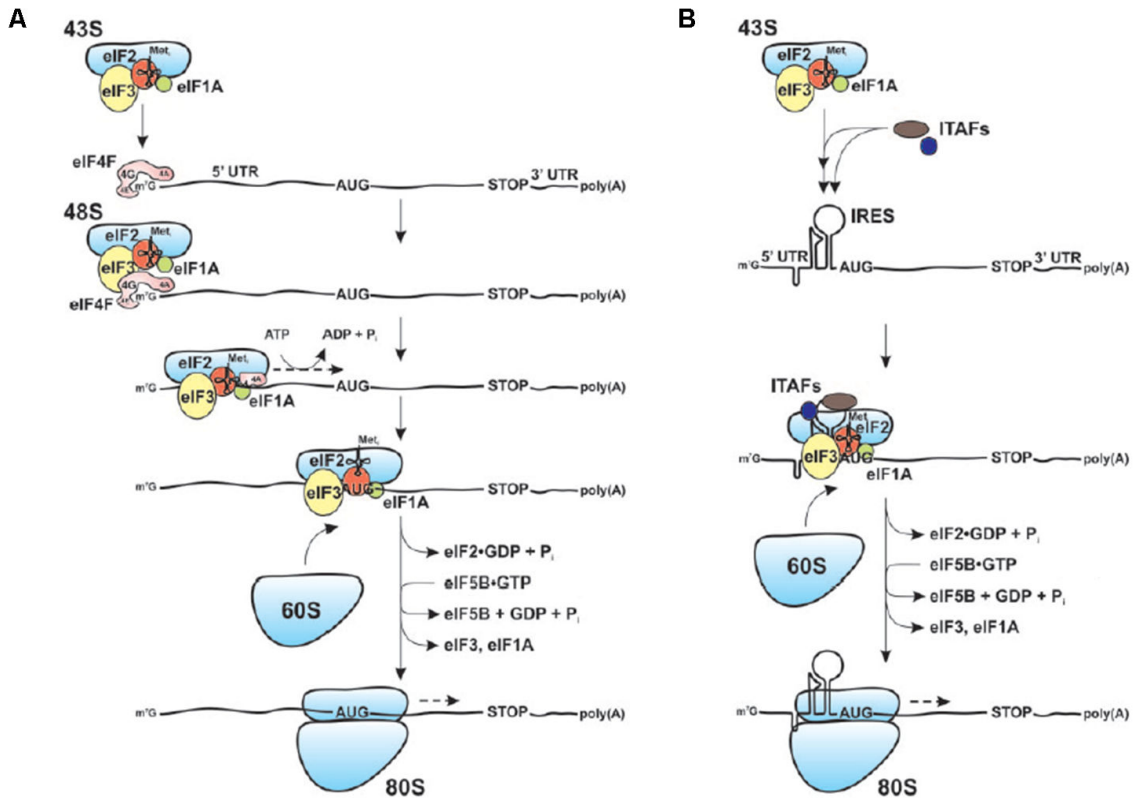

adapted from A. A. Komar & M. Hatzoglou; Internal Ribosome Entry Sites in Cellular mRNAs: Mystery of Their Existence; JBC; 2005

Fig. 6: Schematic representation of eukaryotic translation initiation mechanisms.
(A) 5’cap dependent translation. 5’cap-dependent translation initiation can be summarized in three steps. First the 43S initiation complex, consisting of the 40S subunit, eIF2/GTP/Met-tRNA$_i$, and eIF3, binds to the 5’cap structure, promoted by eIF4F. In this step eIF1A facilitates the Met-tRNAi binding to the 40S ribosome. Second, the 48S complex scans downstream along the mRNA until it reaches the initiation codon. In the third step, initiation factors are released; the 60S subunit joins and forms the 80S ribosome, a process which is furthermore catalyzed by eIF5B. (B) Internal translation initiation by IRESs. This way of translation initiation comprises only two steps. First, the 43S ribosome complex is directly recruited to the IRES on the mRNA, in close proximity to the start codon, which is facilitated by different ITAFs. The second step resembles that of 5’cap dependent translation initiation, in which initiation factors are released, the 60S subunit joins and the 80S ribosome is formed.

1.2.2. Internal translation initiation by internal ribosome entry sites (IRES)

Internal ribosome entry sites (IRES) are long sequences within the 5’UTR of viral and cellular RNAs. These sequences form stable secondary structures, which are capable to directly recruit ribosomes to the initiation region at the RNA, without scanning along the mRNA. Thereby they allow an alternative, 5’cap-independent, internal translation initiation and bypass a subset of eIFs. Instead they are often stimulated by IRES transacting factors (ITAFs) (Belsham and Sonenberg, 2000).

In contrast to the cap-dependent translation initiation mechanism, IRES-dependent translation initiation is a rather slow process (Ochs et al., 1999; Andreev et al., 2007) (Fig. 6B). While in case of initiation by 5'cap structures many eIFs are necessary for the subsequent steps, in case of IRES-dependent initiation these are undertaken by different domains within the IRES structure, which undergo conformational changes by the help of special ITAFs (Kolupaeva et al., 2003). Translation initiation via picornaviral IRES elements starts with the recruitment of the translation machinery, which occurs rather fast (Ochs et al., 1999). Certain domains of the IRES interact with canonical initiation factors. eIF4G, eIF4A and its stimulating cofactor eIF4B interact with the IRES. (Kolupaeva et al., 2003; Lomakin et al., 2000; Ochs et al., 1999; Pestova et al., 1996a; Pestova et al., 1996b). The following steps resemble those of cap-dependent translation initiation. Binding of eIF4G to eIF3 leads to the recruitment of the ribosome, bringing the viral RNA into the proximity of the binding cleft of the 40S subunit. The second step of IRES-dependent translation initiation results in the right positioning of the viral RNA in the decoding center of the ribosome (Jang et al., 1990; Pestova et al., 2007; Doudna and Sarnow, 2007). The exact progression and which factors or IRES domains are involved in this process are still under examination. As this step, in comparison to the preceding capture of the translation machinery, is a very time consuming process, it seems that important changes must occur. Moreover, the large central domain of picornaviral IRESs has to interact with the 40S subunit. Although it was shown that this domain is essential for the initiation process, the complete procedure is unknown (Martinez-Salas et al., 2008; Martinez-Salas et al., 2001). The whole progress of the capture of the ribosome and its exact positioning on the viral RNA is stimulated by additional cellular proteins, so called IRES transacting factors (ITAFs). Each type of IRES element has evolved own structures within different domains, which interact with these ITAFs and thereby regulate their IRES initiation activity (Jang, 2006). Remarkably, IRES elements of the Hepatitis C virus (HCV) and Cricket Paralysis Virus (CrPV) are able to accomplish the whole translation initiation process with a minimum or even without canonical initiation factors (Niepmann, 2009) (Fig. 6B).

The fact that IRES containing viruses are able to initiate translation independently of a 5'cap structure, allows them to interfere with the host translation machinery, without affecting their own gene expression. In regard to this point, many picornaviruses have evolved strategies to interfere selectively with the cellular protein synthesis and concurrently utilize the host's translational resources for viral protein synthesis, which contributes to the fast replication phenotype of picornaviruses. Members of the *Picornaviridae*, like e.g. Poliovirus (PV), human rhinovirus (HRV) or foot- and-mouth disease virus (FMDV) encode

eIF4G-cleaving proteases ($2A^{pro}$ in case of PV and HRV and L in case of FMDV) (Krausslich et al., 1987; Lamphear et al., 1993; Lamphear et al., 1995; Devaney et al., 1988). Proteolytic cleavage results in separation of the N-terminal from the C-terminal domain of eIF4G. As the N-terminal part contains the binding site for eIF4A, cap-dependent translation initiation is impaired, whereas the C-terminal part supports IRES-dependent translation initiation (Pestova et al., 1996b). Another example of interference with the host translation machinery is given by the encephalomyocarditis virus (EMCV). In addition to expression of EMCV 2A protein, which binds to the 40S ribosomal subunit and impairs its binding to the cap structures (Groppo and Palmenberg, 2007), EMCV infection results in dephosphorylation of the eIF4E-binding protein 1 (4E-BP1). 4E-BP1 binds to eIF4E and thereby prevents its interaction with the cap structure (Gingras et al., 1996), which does not influence the virus protein synthesis.

1.2.2.1. Viral IRES elements: Discovery and classification

The structures, now known as "internal ribosome entry site" (IRES) were first discovered within the RNA genomes of picornaviruses. In this first study, Pelletier and Sonenberg could show that the 5' untranslated terminal region (UTR) of poliovirus, belonging to the genus *Enterovirus*, was able to direct protein synthesis within a synthetic dicistronic mRNA (Pelletier and Sonenberg, 1988). Analogous studies identified similar structures in other picornaviruses, like EMCV (Jang et al., 1988), FMDV (Belsham and Brangwyn, 1990), HRV (Borman and Jackson, 1992), representing *Cardiovirus, Aphtovirus* and *Rhinovirus*, respectively. In the following years other viruses were described to initiate their translation via IRES elements, like e.g. hepaci- (Tsukiyama-Kohara et al., 1992) and pestiviruses (Rijnbrand et al., 1997) (order of *Flaviviridae*) or Cricket paralysis virus (CrPV) (Jan and Sarnow, 2002) (order of *Dicistroviridae*) (Tab. A2).

Depending on their structure, mechanism of translation initiation and their recruitment of canonical factors, viral IRES elements can be divided into the groups of *Picornaviridae*, *Flaviviridae* and *Dicistroviridae* (Fig. 7). The group of IRES elements from *Picornaviridae* is furthermore subclassified into type I-IV. IRES elements of PV and HRV2 belong to the type I IRESs of the *Enterovirus* group. The type II comprises IRESs of *Cardio*- and *Aphtoviruses* with EMCV and FMDV as prototypes, whereas the Hepatitis A virus (HAV) IRES belongs to type III. Type IV IRES elements, like the recently discovered Porcine teschovirus (PTV) IRES (Kaku et al., 2002), show a high similarity to the IRES of Hepatitis C virus (HCV) (Belsham and Jackson, 2000; Belsham and Jackson, 2000; Doudna and Sarnow, 2007).

IRES elements of *Picornaviridae*

The structures of IRESs from type I, type II and type III share a high similarity (Jackson et al., 1994; Pilipenko et al., 1989a) (Fig.7). Invariantly, the large central domain consists of a four way junction with stable base-pairs (Brown et al., 1991) and resembles the characteristic four way junction of tRNAs (Sprinzl et al., 1989). Upstream of the central domain additional structures are present, which are able to interact with auxiliary ITAFs. Structures located downstream of the central domain were shown to bind canonical initiation factors, especially eIF4G (Kolupaeva et al., 2003). As regions of eIF4G are bound which differ from those which interact with the 5'cap structure, viruses including an IRES element of type I-III can afford to cleave eIF4G, resulting in the inhibition of the host's protein synthesis without affecting their own translation (Krausslich et al., 1987; Lamphear et al., 1993; Lamphear et al., 1995; Devaney et al., 1988). Downstream of the eIF4G binding domain a conserved oligopyrimidine tract (py) and an AUG codon, placed 15 to 20 nucleotides downstream of the py tract, are located (Jang et al., 1990). These two cis-elements together with the eIF4G binding domain are thought to be responsible for the correct placement of the 40S ribosomal subunit at this so called entry point, which then either directly starts translation or scans to find the next start codon of the viral RNA (Pilipenko et al., 1994; Kaminski et al., 1994).

In this last step of translation initiation IRES types I and II differ between each other. The type II IRES elements from EMCV and FMDV can directly start translation from the AUG within the starting point, although the FMDV IRES prefers a second AUG, located 84 nt downstream, reached by an unconventional way of "scanning" (Lopez and Martinez-Salas, 1999). In contrast in IRESs belonging to type I, like the PV or HRV2 IRES, the AUG within the entry point is essential for the right positioning of the ribosome, while it is silent for translation. Only a second AUG, located 156 nts downstream, which is reached by scanning, serves for start of translation. However, up to now it is not known whether scanning occurs in a processive or discontinuous way (Andreev et al., 2007; Belsham, 1992).

Although the HAV IRES, belonging to type III IRES elements, has a similar structure, its activity in translation initiation is much lower compared to IRES elements from type I or II (Glass et al., 1993; Brown et al., 1991; Brown et al., 1994). Another characteristic of this type of IRES is the necessity of an intact form of eIF4F (comprising eIF4E, eIG4G, eIF4A) (Ali et al., 2001), although the basis of this requirement is not entirely clear (Fig. 7).

As the Porcine Teschovirus (PTV) belongs to the *Picornaviridae* due to its genome organization and sequence, its IRES is included into the group of picornaviral IRES elements of type IV (Kaku et al., 2002). However the PTV IRES itself is very similar to the IRES

elements of *Flaviviridae* in view of its structure and functionality (see below). Other members of type IV IRES elements are IRESs from simian virus 2 (SV2), porcine enterovirus-8 (PEV-8) (Krumbholz et al., 2002), simian picornavirus type 9 (SPV9) (de Breyne et al., 2008) and the avian encephalomyelitis virus (AEV) (Bakhshesh et al., 2008).

IRES elements of *Flaviviridae*

IRES elements from to the Flavirus group compile IRESs from Hepatitis C Virus (HCV) (Tsukiyama-Kohara et al., 1992), as the prototype, but also pestivirus IRESs, like the one of Bovine viral diarrhea virus (BVDV) or of Classical swine fever virus (CSFV) (Rijnbrand et al., 1997; Poole et al., 1995). These IRES elements differ completely in both structure, which has been solved recently, and functionality, from the picornaviral IRESs (Fraser and Doudna, 2007) (Fig. 7). While stem loop domains (sld) I and II of the 340 nt long HCV 5'UTR are involved in genome replication, sld II to IV represent the IRES, which also includes some nucleotides of the protein coding region. Also in this IRES group the four way junction forms the central domain (sld III), consisting of stem loops IIIe, stem loop IIIf and the pseudoknot. The central domain can directly bind the ribosome and position it at the initiator codon, without the involvement of any initiation factors or ITAFs and initiate translation even in the absence of the ternary complex, consisting of eIF2, GTP and Met-tRNA$_i$, which is needed just for the right positioning of the ribosome at the entry point (Pestova et al., 1998b). Upper domains of sld III can bind eIF3 with a low affinity and thereby support initial 40S binding to the IRES, while its binding is essential for 60S ribosomal subunit joining to the 48S complex (Otto and Puglisi, 2004).

IRES elements of *Dicistroviridae*

The IRES of Cricket paralysis virus (CrPV) (Wilson et al., 2000b) belongs to the group of Dicistrovirus IRES elements and is located within the intergenic regions (IGR) between the two open reading frames of the virus. This group has absolutely minimized its needs for canonical factors and auxiliary proteins and thereby has optimized its binding to the ribosome (Fig. 7). Similar to the HCV IRES the CrPV IRES folds into a complex tRNA-like structure and binds to the P-site within the ribosome, resulting in translation initiation completely independent of the initiator tRNA directly from the A-site (Wilson et al., 2000a). Similar IRES elements are contained in the 5'UTRs of *Plautia stali* intestine virus (PSIV), *Rhopalosiphum padi* virus (RhPV) and Taura shrimp virus (TSV) (Sasaki and Nakashima, 2000).

Picornaviridae		scanning	use of AUG1 and AUG2		factors
type I Enteroviruses e.g. PV, HRV2	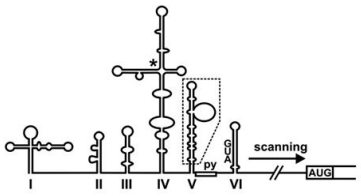	+	-	++++	eIF4G eIF4A eIF4B eIF3 eIF2 ITAFs 40S+
type II Cardio-/Aphtoviruses e.g. EMCV, FMDV	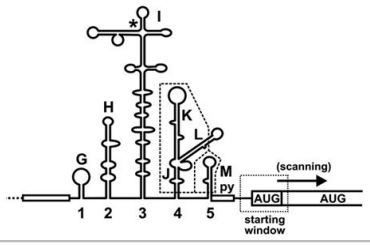	- (EMCV) + (FMDV)	++++ +	- +++	eIF4G eIF4A eIF4B eIF3 eIF2 ITAFs 40S+
type III Hepatoviruses e.g. HAV	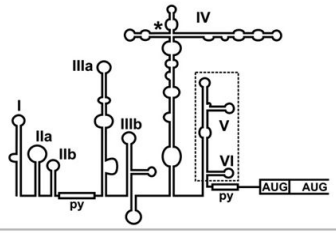	-	-	++++	eIF4G eIF4A eIF4B eIF3 eIF2 ITAFs 40S+
type IV Teschovirus e.g. PTV	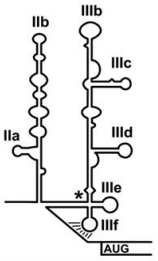	-	++++	-	eIF3 eIF2 40S+
Flaviviridae Hepacivirus: HCV Pestiviruses: BVDV, CSFV	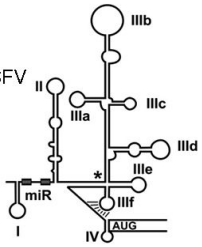	-	++++	-	eIF3 eIF2 40S+
Dicistroviridae e.g. CrPV	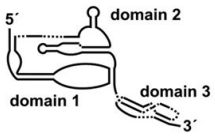	-	++++	-	40S

*: central domain, **py**: oligopyrimidine tract, **punctuated boxes**: initiation factor binding domains; **40S+:** 40S ribosomal subunit with Met-tRNA$_i$

modified from (Niepmann, 2009; Filbin and Kieft, 2009; Belsham, 2009)

Fig. 7: Classification of diverse IRES elements.
IRES elements can be classified into three groups of IRESs from *Picornaviridae*, *Flaviviridae* and *Dicistroviridae*. Types I-III of picornavirus IRESs are similar in structure and functionality, whereas type IV resembles those of the group of Flavivirus IRESs. Possible scanning processes and the use of the first and/or second AUG are indicated by (-) and (+). Dependent on the IRES elements, different cellular proteins are necessary for internal translation initiation.

1.2.2.2. Cellular IRES elements

In addition to their 5'cap structure, also some cellular mRNAs were described to contain IRES elements (Tab. A3). Under different types of stress, like e.g. apoptosis, hypoxia, ER-stress, and during mitosis cap-dependent translation is impaired, due to a reduced amount of the available ternary complex (eIF2–GTP–Met-tRNAi) and other factors essential for translation. The presence of an IRES allows ongoing synthesis of essential proteins and moreover a favored synthesis of some additional proteins, which are required for the stress response or to aid recovery from the stress stimulus (Spriggs et al., 2008). The activity of all cellular IRESs depends on ITAFs, whose expression levels and localization are changed under specific stress conditions and thereby become available for certain IRESs. Among these, PTB acts as a general ITAF (Sawicka et al., 2008). Additional more specific ITAFs are e.g. PCBP (Evans et al., 2003), hnRNP A1 (Bonnal et al., 2005; Lewis et al., 2007), La protein and UNR. Similar to viral IRES elements (Tab. A2) these proteins are thought to act as RNA chaperones which remodel the structure of the IRES into an active configuration (Mitchell et al., 2003).

The secondary structure has been derived for several cellular IRESs with enzymatic and chemical probing. A common Y structure (Le and Maizel, Jr., 1997) had been predicted for cellular IRESs based on the computational comparison of several orthologs of the UTRs from mRNA for the immunoglobulin heavy-chain binding protein (Bip) and fibroblast growth factor 2 (FGF2). In all these studies on cellular IRES, only some show a preference for structure preservation to retain full activity, suggesting that there is no need for an overall structure as seen in some viral IRESs.

A major difference between IRES elements of RNA viruses and cellular IRESs is their site of synthesis. Picornavirus RNAs are synthesized in the cytoplasm, whereas the site of production of cellular RNAs is in the nucleus. Thus, viral RNAs encounter factors necessary for translation initiation only in the cytoplasm and therefore can form a translation competent RNP complex only with proteins present in the cytoplasm. In contrast cellular mRNAs have the possibility to interact with several proteins and complexes within the nucleus and are exported to the cytoplasm most likely within an RNP complex, which also could harbor ITAFs, used for IRES activity (Semler and Waterman, 2008).

From this point of view IRES elements from DNA viruses, whose transcription takes place in the nucleus by RNA Pol II, could have ITAF compositions which resemble those of cellular IRESs (Semler and Waterman, 2008). The first DNA virus, described to contain an IRES element within its mRNA was Kaposi's sarcoma-associated herpesvirus (KSHV)

(Bieleski and Talbot, 2001). Further IRES elements were described in Herpes simplex virus (HSV) (Griffiths and Coen, 2005), rous sarcoma virus (RSV) (Deffaud and Darlix, 2000) and in the human immunodeficiency virus type 1 and 2 (HIV-1, HIV-2) (Buck et al., 2001; Herbreteau et al., 2005) (Tab. A2).

1.2.2.3. IRES transacting factors (ITAFs)

In addition to some canonical initiation factors, IRES elements require auxiliary cellular proteins, which modulate their activities and either stimulate or repress IRES activity. These ITAFs contain several RNA binding motifs, which allow interaction with multiple sites within the IRES, resulting in stabilization of the tertiary structure (Niepmann, 2009; Belsham and Sonenberg, 2000; Belsham, 2009).

In general, picornavirus type I IRESs bind more ITAFs than type II IRESs. Among them are UNR (upstream of n-ras) (Triqueneaux et al., 1999), PTB (polypyrimidine tract binding protein) (Auweter and Allain, 2008), La protein (Lupus erythematodes autoantigen) (Maraia and Bayfield, 2006), PCBP2 (polyC binding protein 2) (Bedard et al., 2004), SRp20 (serine rich splicing factor) (Bedard et al., 2007) and DRBP76 (double-stranded RNA binding protein 76) (Merrill and Gromeier, 2006; Merrill et al., 2006). In contrast, the major ITAF binding to type II IRESs is PTB (Sawicka et al., 2008). In addition, ITAF45 was described to have a stimulatory effect on the FMDV IRES in proliferating cells (Monie et al., 2007). The fact that ITAF45 is not present in resting cells, lead to a possible explanation why FMDV is not able to replicate in resting neuronal cells. Even for the HCV IRES, which is known to bind to the small ribosomal subunit in the absence of initiation factors, some ITAFs were reported. HCV IRES activity is stimulated e.g. by the La protein (Ali et al., 2000; Izumi et al., 2004), the heterogeneous nuclear ribonucleoprotein (hnRNP) Q (Kim et al., 2004) and hnRNP L (Hahm et al., 1998), which furthermore interacts with hnRNP D.

The full molecular mechanism of the action of theses proteins on IRES elements is not completely solved, as all proteins can have different ways of action. So they can act as RNA chaperones, like e.g. PTB and UNR, to stabilize the RNA or to introduce conformational changes. Moreover they can also interact with other cellular proteins, like e.g. PTB with hnRNP L or PCBP2 with SRp20.

Some of these ITAFs were suggested to influence the viral cell tropism. Beside ITAF45 (see above) DRBP76 was described, which is expressed to higher amounts in neuronal cells. It was shown that the presence of DRBP76 represses translation initiation by the HRV2 IRES, whereas it has no effect on the PV IRES. This led the authors hypothezise that repression of

HRV2 IRES by DRBP76 excludes efficient propagation of HRV2 in neuronal cells. As it has no effect on the PV IRES, PV can replicate efficiently in neurons, resulting in its neuropathogenicity (Merrill and Gromeier, 2006; Merrill et al., 2006).

1.3. Aim of this study

Rabies virus (RV), belonging to the family of *Rhabdoviridae*, is a prototype of *Mononegavirales* and therefore can serve as a model for all members of this order. Gene expression of *Mononegavirales* is regulated almost completely at the transcriptional level and relies on the canonical 5'end-dependent translation of capped monocistronic viral mRNAs. Previous attempts to control gene expression of RV focused mainly on modifications on transcriptional level (Brzozka et al., 2005); (Finke and Conzelmann, 2005a); (Finke et al., 2000). The main aim of this study, however, was the development of an alternative strategy to control expression of essential gene products of rabies virus (RV) on the translational level by the use of IRES elements.

In order to use IRES elements to control RV gene expression, I first had to screen for suitable IRES elements. Common plasmid-based reporter systems for the characterization of IRES activities are error-prone due to several side effects and therefore are severely criticized (Kozak, 2003; Kozak, 2007; Kozak, 2005). Therefore, I decided to establish two new RV-based systems, using eCFP or luciferase as reporter genes, which do not suffer from drawbacks appearing on plasmid level. In the following, the use of these systems allowed characterization of a variety of IRESs. Specifically, I compared the activities of diverse IRES elements and analyzed potential cell specific features of IRESs. Furthermore, I wanted to address questions about influences of picornaviral 3'UTRs on IRES activities and about start codon usage by different IRES elements.

The identified and characterized IRES elements were then used to control expression levels of the essential and multifunctional RV phosphoprotein (P). As RV P is critically required for both viral replication and escape from the host interferon response, regulation of P expression by IRES elements should result in regulation of virus replication as well as in altered countermeasures against the host IFN response. Replication and IFN escape of the

IRES-controlled RVs were examined not only in cell culture, but also in murine brain slice cultures, resembling a primary neuron network, as well as in mouse experiments.

Moreover, I exploited specific features of the FMDV IRES, which preferentially initiates translation at a second, downstream initiation codon (Lopez and Martinez-Salas, 1999). Thereby, I aimed to change the relative ratios of N-terminally truncated P proteins, expressed from the P gene, by leaky scanning, within FMDV IRES-controlled RVs. These viruses were in the following used to dissect roles of the N-terminally truncated P proteins in the virus life cycle.

2. MATERIAL AND METHODS

2.1. Materials

2.1.1. Chemicals

Chemicals were purchased from INC Biochemicals Inc., Invitrogen, Merck, New England Biolabs, Riedel-de-Häen, Roth, SIGMA-Aldrich, Gibco, Roche. The radiochemical ^{32}P-αCTP was provided by Amersham Pharmacia and Hartmann Analytic.

2.1.2. Buffers

Jagow anode buffer: 200 mM Tris-HCl, pH 8.9

Jagow kathode buffer: 100 mM Tris-HCl, pH 8.25
100 mM Tricin
0.1 % (w/v) SDS

Jagow gel buffer: 3 M Tris-HCl, pH 8.45

Lysis buffer: 62.5 mM Tris-HCl, pH 6.8
2 % SDS
10 % Glycin
6 M Urea
5 % β-mercaptoethanol
0.01 % bromphenolblue
0.01 % phenolred

50x TAE: 400 mM Tris-HCl, pH 7.8
5 mM NaAc
5 mM EDTA

TEN buffer: 50 mM Tris-HCl, pH 7.4
1 mM EDTA
150 mM NaCl

TE buffer : 10 mM Tris-HCl, pH 7.5
5 mM EDTA

Loading solutions:

DNA agarose gels: 0.125 % Orange G
15 % Ficoll 400
10x TAE

RNA agarose gels: 0.125 % Bromphenolblue
0.125 % Xylencyanol
0.125 % Orange G
15 % Ficoll 400
10x TAE

Protein gels: 62.5 mM Tris-HCl, pH 6.8
2 % SDS
10 % Glycerol
6 M Urea
5 % β-Mercaptoethanol
0.01 % Bromphenolblue
0.01 % Phenolred

Phosphate buffered saline (PBS): 8 g NaCl
0.2 g KCl
0.13 g $CaCl_2 \cdot 2H_20$
0.2 g KH_2PO_4
1.15 g $Na_2HPO_4 \cdot 2H_20$
0.1 g $MgCl_2 \cdot 6H_20$

Flexi Prep Solutions: Flexi I: 100 mM Tris-HCl, pH 7.5
10 mM EDTA
200 µg/ml RNase
Flexi II: 0.2 M NaOH
1 % SDS
Flexi III: 300 mM KAc, pH 5.75

50x Phosphate buffer: 250 mM $Na_2HPO_4 \cdot 2H_2O$
250 mM $NaH_2PO_4 \cdot H_2O$

Zeta-Hybridization-Mix: 1 mM EDTA
7 % SDS
0.25 M Na_2HPO_4
0.25 M NaH_2PO_4

Zeta Wash: 5 %/1 % SDS
1 mM EDTA
4 x 50x Phosphate buffer

Transfer buffers: Western Blot: 10x Semi-Dry: 480 mM Tris-HCl
20 mM EDTA
80 mM $MgCl_2$

Northern Blot: 20x SSC: 3 M NaCl
0.3 M Na Citrate$\cdot 2H_2O$

2.1.3. Enzymes

Restriction endonucleases	New England Biolabs (NEB)
T4-DNA-Ligase	New England Biolabs (NEB)
Klenow-Polymerase	New England Biolabs (NEB)
Mung Bean Nuclease	New England Biolabs (NEB)
Shrimp alkaline Phosphatase (SAP)	Roche
Taq DNA-Polymerase	Biomaster
BioPfu DNA-Polymerase	Biomaster
Herculase II Fusion DNA polymerase	Stratagene

Stratascript Reverse Transcriptase	Stratagene
Transcriptor Reverse Transcriptase	Roche
DNase	Fermentas
RNase	Roche

2.1.4. Kits

ECL detection kit	Perkin-Elmer
RNeasy kit	QIAGEN
QIAquick PCR purification/Gel extraction/Nucleotide removal	QIAGEN
Mammalian Transfection Kit	Stratagene
Lipofectamine 2000	Invitrogen
Nucleobond AX100	Macherey & Nagel
Dual Luciferase Kit	Promega
QuantiTect SYBR Creen PCR	QIAGEN

2.1.5. Consumables

Hyperfilm	GE Healthcare
Reactiontubes	Eppendorf
Polypropylen-tubes	BD Falcon
Cryo tubes	Nunc
Cell culture dishes/ flasks	Nunc
Sterile filters	Millipore
Immobilon-FL transfer membrane	Millipore
Whatman	Schleicher&Schuell
Nitrocellulose membrane	Schleicher&Schuell

2.1.6. Other reagents

ampicillin (amp)	Gibco BRL
kanamycin (kan)	Gibco BRL
G418	PAN
DNA 1 kb ladder	Gibco BRL
dNTPs	NEB
IFN-α A/D	PBL
poly IC	SIGMA

PEI	SIGMA
Lipofectamine2000	Invitrogen
FuGene6	Roche
prestained protein ladder	Bio-Rad
RNase Inhibitor	Roche
Skim milk powder	Merck

2.1.7. Cell culture

2.1.7.1. Reagents

All cell culture reagents were purchased from Invitrogen.

Dulbecco´s Modified Eagle medium (DMEM)
Glasgow Minimal Essential Medium (GMEM)
Roswell Park Memorial Institute Medium (RPMI)
Newborn Calf Serum (NCS)
Fetal Calf Serum (FCS)
Tryptosephosphat *broth* 50x
MEM-Aminoacids, 50x
L-Glutamin (200mM), 100x
Penicillin/Streptomycin (P/S)
Trypsin-EDTA (0,25% Trypsin, 1mM Na-EDTA)
Dulbeccos PBS (without Ca^{2+} and Mg^{2+})

2.1.7.2. Cells

Tab. 1: Cell lines used in this work

cell line	origin	description	medium
HEK 293T	human	embryonic kidney cells expressing the SV40 large T antigen	DMEM 3+
HEp-2	human	laryngeal epidermoid carcinoma cells	DMEM 3+
HepG2	human	hepatocellular carcinoma cells	DMEM 3+
Huh7	human	hepatocellular carcinoma cells	DMEM 3+

Vero	simian	kidney cells	DMEM 3+
NIH 3T3	murine	fibroblasts	DMEM 3+
NS20Y	murine	neuroblastoma cells	DMEM 3+
MDBK	bovine	kidney cells	DMEM 3+
MHH-NB11	human	neuroblastoma cells	RPMI 3+
DK-MG	human	glioblastoma cells	RPMI 3+
BHK-21	hamster	kidney cells	GMEM 4+
BSR T7/5	hamster	kidney cells expressing bacteriophage T7 RNA polymerase	GMEM 4+

2.1.7.3. Cell culture media

DMEM 3+: DMEM
10 % fetal calf serum
1 % L-glutamine
0.4 % Penicillin/Streptomycin

GMEM 4+: GMEM
10 % newborn calf serum
2 % Tryptose phosphate broth
2 % MEM Amino acids
0.4 % Penicillin/Streptomycin

RPMI 3+: RPMI
10 % fetal calf serum
1 % L-glutamine
0.4 % penicillin/streptomycin

2.1.8. Bacteria

For DNA plasmid preparation *E.coli* XL-1 blue (Stratagene) were grown in LB supplemented with the required antibiotics (ampicillin or kanamycin).

LB: 5 g NaCl
5 g yeast extract
10 g Bactotryptone
1 mM $MgSO_4$

LB++: 5 g NaCl
5 g yeast extract
10 g Bactotryptone
21 mM $MgSO_4$
10 mM KCl

2.1.9. Oligonucleotides

Oligonucleotides were purchased from Metabion.

Tab. 2: Oligonucleotides for cloning

#	primer	sequence (5'…3')
5	NP f.	GAA TTC GCT AGC GAA GTT GAA TAA CAA AAT GCC GG
6	NP r.	GTG GAT CCC GGG GCA TGT TTG GGA TGG TTC G
7	HRV f.	GAA TTC GCT AGC ATC GTT AAC TTA GAA GTT TTT C
8	HRV r.	GTG GAT CCC GGG GCA TGG TGC CAA TAT ATA TAT TGT ATA TAT TGT AAC C
9	PV f.	GAA TTC GCT AGC ATC AGA CGC ACA AAA CCA AG
10	PV r.	GTG GAT CCC GGG GCA TGG ATA ACA ATC TGT GAT TGT CAC C
11	hu p27 forw	GAA TTC GCT AGC CCA CCT TAA GGC CGC GCT C
12	hu p27_356 for	GAA TTC GCT AGC CCG ACG CCG GCA AGG TTT GG
17	hu p27 revStu2	GTG GAT AGG CCT CAT CTT CTC CCCGGG TCT GC
18	RL-forw	GAA TTC TCT AGA ATA ACT AGT ATG ACT TCG AAA GTT TA
19	RL_rev	GTG GAT GCT AGC TTA TTG TTC ATT TTT GAG AAC
20	FF_forw	GAA TTC CCC GGG ATG GAA GAC GCC AAA AAC ATA
21	FF_rev	GTG GAT GCG GCC GCT TAC AAT TTG GAC TTT CC
22	b-Act+	GGC ATC GTG ATG GAC TCC

24	b-Act2- (528)	CCG CCA GAC AGC ACT GTG TTG GCG TA
25	BVDV forw	GAA TTC GCT AGC GTA TAC GAG AAT TAG AAA AGG
26	BVDVrev	GTG GAG CCC GGG GCA TTT GTG ATC AAC TCC ATG G
27	CSFVforw	GAA TTC ACT AGT GTA TAC GAG GTT AGC TCT TTC
28	CSFV rev	GTG GAT CCC GGG GCA TGG GCC ATG TAC AGC AGA GA
29	HCVforwSpe	ATC TAA ACT AGT GAC ACT CCA CCA TAG ATC ACT
31	HCVrevEcoRV2	GTG GAT GAT ATC TTT GAG GTT TAG GAT TCG TGC TCA T
32	FMDVforw	ATC TAA GCT AGC AGC AGG TTT CCC CAA TGA CA
33	FMDVrev	GTG GAT CCC GGG GCA TAG GGT CAG TAA TTG CAA AGG A
51	FMDV-Pforw	ATA GAA TTC GTT AAC AGC AGG TTT CCC CAA TGA
52	FMDV-Prev	ATA AGA TCT TGC TCA TAG GGT CAG TAA TTG CAA A
56	HpaI N rev	ATA GTT AAC TTA TGA GTC ACT CGA ATA
58	HCV2 rev EcoRV neu	GTG GAT GAT ATC TCT TTG AGG TTT AGG ATT CGT
59	HCV3revEcoRV	GTG GAT GAT ATC CAT GGT GCA CGG TCT ACG ACA
61	HRV UTR sense	ATA GCG GCC GCA GAT ATA GAA ATA GTA AAC TGA TAG TTT ATT AGT TTT ATC CGC GGA TA
62	HRV UTR antisense	TAT CCG CGG ATA AAA CTA ATA AAC TAT CAG TTT ACT ATT TCT ATA TCT GCG GCC GCT AT
63	Polio UTR forw	ATA GC GG CC GC AAC CCT ACC TCA GTC G
64	Polio UTR rev	ATA CCG CGG CTC CGA ATT AAA GAA
67	RLforw Sonde	TTC GTG GAA ACC ATG
72	FF forw_sonde	TGA ATT GGA ATC GAT
75	EcoRV-N forw	ATA GAT ATC ATG GAT GCC GAC AAG
78	RL Sonde forw	GGG TGC TTG TTT GGC ATT
79	RL Sonde rev	TTT CCC ATT TCA TCA GGT GC
80	FF Sonde forw	AGG CTA TGA AGA GAT ACG C
81	FF Sonde rev	GGG AGG TAG ATG AGA TGT G
82	IRES-P_C_rev1 XhoI	ATA CTC GAG TTT GGG ACA TCT CGG ATT TTA TTG TCT AGA GGG ACT GAG GGG AGA GGT TCG GTT AGC AAG ATG TAT A
83	IRES-P_C_rev2	ATA ATC TTA CGT AGG AGG TTC ATT TTA TCA GTG GTG TTG CCT GTT TTT TTC ATG TTG ACT TTG GGA CAT CTC GG
86	DraIII HpaI FMDV-Pforw	ATA CAC CAC GTG GTT AAC AGC AGG TTT CCC CAA TGA
88	RL PV FF_IF rev	GTG CAT CCC GGG CAT GGA TAA CAA TCT GTG AT

89	RL HRV FF_IF rev	GTG CAT CCC GGG CAT GGT GCC AAT ATA TAT ATT GTA T
90	RL FMDV FF_IF rev	GTG CAT CCC GGG CAT AGG GTC AGT AAT TGC AAA GGA
91	RL-PV-FF_OATG rev	GTG CGC CGG GCC TTT CTT TAT GTT TTT GGC GTC TTC CAT GAT AAC AAT CTG GTG
92	RL-HRV-FF_OATG rev	GTG CGC CGG GCC TTT CTT TAT GTT TTT GGC GTC TTC CAT GGT GCC AAT ATA TAT GTG
93	RL-FMDV-FF_OATG rev	GTG CGC CGG GCC TTT CTT TAT GTT TTT GGC GTC TTC CAT AGG GTC AGT AAT TGC GTG
101	RL PV FF_IF rev_neu	GTG CAT CCC GGG CAT GA TAA CAA TCT GTG AT
103	Mut FMDV-PATG1_fwd	GCAATTACTGACCCTATAAGCAAGATCTTTGT
104	Mut FMDV-PATG1_rev	ACAAAGATCTTGCTTATAGGGTCAGTAATTGC
K1	RV P M53I	AATCTCCCTGAGGATATCGGCCGACTTCACC
K2	RV P M53I rev	ATCCTCAGGGAGATTGTCCACCTCT

Tab. 3: Oligonucleotides for sequencing

#	primer	sequence (5'…3')
	1330+	AGATCTCACATACGGAG
	NS3M	TCCACTGATAGATCATCC
	L4M	CAAAGGAGAGTTGAGATTGTAGTC
	G7P	TGAGACCAGACTGTAAGG
S1	GFPrev	GGGCACCACCCCGGTGAACAGCTCCT
S2	RL 3' forw	ATCGTTCGTTGAGCGAGTTCTC
S3	FF 5' rev	TATGTTTTTG GCGTCTTCCA T
S8	FFforw_seq	GGA TGG CTA CAT TCT
S9	RLrev_seq	ACC AAT AAG GTC TGG

2.1.10. Plasmids

Plasmids were purified from *E.coli* XL-1 using the "Nucleobond AX100"-Kit.

Tab. 4: Expression plasmids

name	description	reference
p125-Luc	firefly luciferase expressed by promoter containing binding site for IFNβ	(Yoneyama et al., 1996)
pEGFP-N3	CMV promoter expressing eGFP (enhanced green fluorescent protein)	Clontech Laboratories
pBSK II	pBluescriptII(-) vector, allowing protein expression under control of the T7 promoter	Clontech Laboratories
pTIT	pBSKII(-) expression vector including an additional EMCV IRES and the T7 terminator	(Finke and Conzelmann, 1999)
pTIT-GFP	pTIT expressing eGFP	(Finke and Conzelmann, 1999)
pTIT-N	pTIT expressing RV N	(Finke and Conzelmann, 1999)
pTIT-L	pTIT expressing RV L	(Finke and Conzelmann, 1999)
pTIT-P	pTIT expressing RV P	(Finke and Conzelmann, 1999)
pCR3-IgP	pCR3 expressing RV P, including a N-terminal Ig tag	K. Brzozka
pSK-PVI	pBSKII(-) expressing PV IRES	E. Wimmer
pSK-HRVI	pBSKII(-) expressing HRV2 IRES	E. Wimmer
pECFP-N1	CMV promoter expressing eCFP (enhanced cyan fluorescent protein)	Clontech Laboratories
p253 (p27_575)	expression plasmid for a bicistronic mRNA R-N/P-FF under control of a SV40 promoter; between the coding sequences for renilla and firefly luciferase the long form of the p27 5'UTR is inserted	(Kullmann et al., 2002)

p259 (p27_356)	expression plasmid for a bicistronic mRNA R-N/P-FF under control of a SV40 promoter; between the coding sequences for renilla and firefly luciferase the short form of the p27 5'UTR is inserted	(Kullmann et al., 2002)
pCMV-RL-FF	expression vector for a bicistronic mRNA RL-FF under control of a CMV promoter; between the coding sequences for renilla and firefly luciferase a MCS is inserted	this work
pCMV-RL-FF-N/P	expression plasmid for a bicistronic mRNA R-N/P-FF under control of a CMV promoter; between the coding sequences for renilla and firefly luciferase the N/P gene border is inserted	this work
pCMV-RL-FF-PV_OF	expression plasmid for a bicistronic mRNA R-N/P-FF under control of a CMV promoter; between the coding sequences for renilla and firefly luciferase the PV IRES is inserted, the firefly coding sequence starts with two out of frame ATGs separated by 7 nts	this work
pCMV-RL-FF-HRV2-OF	expression plasmid for a bicistronic mRNA R-N/P-FF under control of a CMV promoter; between the coding sequences for renilla and firefly luciferase the HRV2 IRES is inserted, the firefly coding sequence starts with two out of frame ATGs separated by 7 nts	this work
pCMV-RL-FF-p27_356	expression plasmid for a bicistronic mRNA R-N/P-FF under control of a CMV promoter; between the coding sequences for renilla and firefly luciferase the short form of the p27 5'UTR is inserted	this work
pCMV-RL-FF-p27_574	expression plasmid for a bicistronic mRNA R-N/P-FF under control of a CMV promoter; between the coding sequences for renilla and firefly luciferase the long form of the p27 5'UTR is inserted	this work
pCMV-RL-FF-BVDV	expression plasmid for a bicistronic mRNA R-N/P-FF under control of a CMV promoter; between the coding sequences for renilla and firefly luciferase the BVDV IRES is inserted	this work
pCMV-RL-FF-CSFV	expression plasmid for a bicistronic mRNA R-N/P-FF under control of a CMV promoter; between the coding sequences for renilla and firefly luciferase the CSFV IRES is inserted	this work
pCMV-RL-FF-HCV 1	expression plasmid for a bicistronic mRNA R-N/P-FF under control of a CMV promoter; between the coding sequences for renilla and firefly luciferase a deletion mutant of the HCV IRES is inserted	this work
pCMV-RL-FF-HCV 2	expression plasmid for a bicistronic mRNA R-N/P-FF under control of a CMV promoter; between the coding sequences for renilla and firefly luciferase the HCV IRES is inserted	this work

pCMV-RL-FF-FMDV_OF	expression plasmid for a bicistronic mRNA R-N/P-FF under control of a CMV promoter; between the coding sequences for renilla and firefly luciferase the FMDV IRES is inserted, the firefly coding sequence starts with two out of frame ATGs separated by 7 nts	this work
pCAGGs	expression vector, allowing protein expression under control of the chicken β actin promoter	F. Weber
pCR3	expression vector, allowing protein expression under control of the T7 promoter	Invitrogen
pCR3-PV_I	pCR3 expressing the PV IRES	this work
pCR3-$HRV2_I$	pCR3 expressing the HRV2 IRES	this work
pCMV RL-FF_PV_IF	expression plasmid for a bicistronic mRNA R-N/P-FF under control of a CMV promoter; between the coding sequences for renilla and firefly luciferase the PV IRES is inserted; the firefly coding sequence starts with two in frame ATGs separated by 6 nts	this work
pCMV RL-FF_HRV2_IF	expression plasmid for a bicistronic mRNA R-N/P-FF under control of a CMV promoter; between the coding sequences for renilla and firefly luciferase the HRV2 IRES is inserted the firefly coding sequence starts with two in frame ATGs separated by 6 nts	this work
pCMV RL-FF_FMDV_IF	expression plasmid for a bicistronic mRNA R-N/P-FF under control of a CMV promoter; between the coding sequences for renilla and firefly luciferase the FMDV IRES is inserted the firefly coding sequence starts with two in frame ATGs separated by 6 nts	this work
pCMV RL-FF_PV_OATG	expression plasmid for a bicistronic mRNA R-N/P-FF under control of a CMV promoter; between the coding sequences for renilla and firefly luciferase the PV IRES is inserted	this work
pCMV RL-FF_HRV_OATG	expression plasmid for a bicistronic mRNA R-N/P-FF under control of a CMV promoter; between the coding sequences for renilla and firefly luciferase the HRV2 IRES is inserted	this work
pCMV RL-FF_FMDV_OATG	expression plasmid for a bicistronic mRNA R-N/P-FF under control of a CMV promoter; between the coding sequences for renilla and firefly luciferase the FMDV IRES is inserted	this work

Tab. 5: Fullength cDNAs (pSAD…) and the corresponding recombinant RVs (SAD…).

name	description	reference
pSAD L16	plasmid containing full-length cDNA, carrying nucleotide sequence of RV Street Alabama Dufferin B19	(Conzelmann and Schnell, 1994)
pSAD G DsRed NP	pSAD L16 with DsRed insertion in front of the coding sequence of the L mRNA; between the G and the DsRed coding sequences the N/P gene border is inserted	(Klingen et al., 2008)
pSAD G TIMER-NP	pSAD L16 with DsRed(TIMER) insertion in front of the coding sequence of the L mRNA; between the G and the DsRed(TIMER) coding sequences the N/P gene border is inserted	S. Finke
pSAD G TIMER-PV	pSAD L16 including a bicistronic mRNA (G - PV-IRES - DsRed (Timer))	S. Finke
pSAD G TIMER-HRV	pSAD L16 including a bicistronic mRNA (G - HRV-IRES - DsRed (Timer))	S. Finke
pSAD-N/P-eCFP	pSAD L16 with eCFP insertion in front of the coding sequence of the L mRNA; between the G and the eCFP coding sequences the N/P gene border is inserted	this work
pSAD-PV-eCFP	pSAD L16 including the bicistronic mRNA (G – PV IRES - eCFP)	this work
pSAD-HRV-eCFP	pSAD L16 including the bicistronic mRNA (G – HRV2 IRES - eCFP)	this work
pSAD G eCFP-FMDV	pSAD L16 including the bicistronic mRNA (G – FMDV IRES - eCFP)	this work
pSAD G eCFP-BVDV	pSAD L16 including the bicistronic mRNA (G – BCDV IRES - eCFP)	this work
pSAD G eCFP-CSFV	pSAD L16 including the bicistronic mRNA (G – CSFV IRES - eCFP)	this work
pSAD- eCFP-p27_356	pSAD L16 including the bicistronic mRNA (G – p27 IRES_356 - eCFP); p27_356 is a shorter form of p27	this work
pSAD- eCFP-p27_574	pSAD L16 including the bicistronic mRNA (G – p27 IRES_574 - eCFP); p27_356 is the fulllength p27	this work
pSAD G eCFP-HCV3	pSAD L16 including the bicistronic mRNA (G – HCVdel IRES- eCFP); HCV3 is a C-term. deletion mutant of the HCV IRES	this work
pSAD G eCFP-HCV2	pSAD L16 including the bicistronic mRNA (G – HCV IRES- eCFP)	this work

pSAD RL-N/P-FL	pSAD L16 with the insertion of the coding sequence of Renilla and firefly luciferase in front of the coding sequence of the L mRNA; between the Renilla and Firefly coding sequences the N/P gene border is inserted (bicistronic mRNA R-N/P-FF)	this work
pSAD RL-PV-FL_IF	pSAD L16 with the insertion of the coding sequence of Renilla and firefly luciferase in front of the coding sequence of the L mRNA; between the Renilla and Firefly coding sequences the PV IRES is inserted (bicistronic mRNA R-PV-FF), the firefly coding sequence starts with two in frame ATGs separated by 6 nts	this work
SAD RL-PV-FL_OF	pSAD L16 with the insertion of the coding sequence of Renilla and firefly luciferase in front of the coding sequence of the L mRNA; between the Renilla and Firefly coding sequences the PV IRES is inserted (bicistronic mRNA R-PV-FF), the firefly coding sequence starts with two out of frame ATGs separated by 7 nts	this work
pSAD RL-PV-FL_OATG	pSAD L16 with the insertion of the coding sequence of Renilla and firefly luciferase in front of the coding sequence of the L mRNA; between the Renilla and Firefly coding sequences the PV IRES is inserted (bicistronic mRNA R-PV-FF)	this work
pSAD RL-HRV-FL_IF	pSAD L16 with the insertion of the coding sequence of Renilla and firefly luciferase in front of the coding sequence of the L mRNA; between the Renilla and Firefly coding sequences the HRV IRES is inserted (bicistronic mRNA R-HRV-FF), the firefly coding sequence starts with two in frame ATGs separated by 6 nts	this work
pSAD RL-HRV-FL_OF	pSAD L16 with the insertion of the coding sequence of Renilla and firefly luciferase in front of the coding sequence of the L mRNA; between the Renilla and Firefly coding sequences the HRV IRES is inserted (bicistronic mRNA R-HRV-FF), the firefly coding sequence starts with two out of frame ATGs separated by 7 nts	this work
pSAD RL-HRV-FL_OATG	pSAD L16 with the insertion of the coding sequence of Renilla and firefly luciferase in front of the coding sequence of the L mRNA; between the Renilla and Firefly coding sequences the HRV IRES is inserted (bicistronic mRNA R-HRV-FF)	this work

pSAD RL-FMDV-FL_IF	pSAD L16 with the insertion of the coding sequence of Renilla and firefly luciferase in front of the coding sequence of the L mRNA; between the Renilla and Firefly coding sequences the FMDV IRES is inserted (bicistronic mRNA R-FMDV-FF), the firefly coding sequence starts with two in frame ATGs separated by 6 nts	this work
pSAD RL-FMDV-FL_OF	pSAD L16 with the insertion of the coding sequence of Renilla and firefly luciferase in front of the coding sequence of the L mRNA; between the Renilla and Firefly coding sequences the FMDV IRES is inserted (bicistronic mRNA R-FMDV-FF), the firefly coding sequence starts with two out of frame ATGs separated by 7 nts	this work
pSAD RL-FMDV-FL_OATG	pSAD L16 with the insertion of the coding sequence of Renilla and firefly luciferase in front of the coding sequence of the L mRNA; between the Renilla and Firefly coding sequences the FMDV IRES is inserted (bicistronic mRNA R-FMDV-FF)	this work
pSAD RL-BVDV-FL	pSAD L16 with the insertion of the coding sequence of Renilla and firefly luciferase in front of the coding sequence of the L mRNA; between the Renilla and Firefly coding sequences the BVDV IRES is inserted (bicistronic mRNA R-BVDV-FF)	this work
pSAD RL-CSFV-FL	pSAD L16 with the insertion of the coding sequence of Renilla and firefly luciferase in front of the coding sequence of the L mRNA; between the Renilla and Firefly coding sequences the CSFV IRES is inserted (bicistronic mRNA R-CSFV-FF)	this work
pSAD RL-HCV-FL	pSAD L16 with the insertion of the coding sequence of Renilla and firefly luciferase in front of the coding sequence of the L mRNA; between the Renilla and Firefly coding sequences the fulllength HCV IRES is inserted (bicistronic mRNA R-HCV-FF)	this work
pSAD RL-HCVdel-FL	pSAD L16 with the insertion of the coding sequence of Renilla and firefly luciferase in front of the coding sequence of the L mRNA; between the Renilla and Firefly coding sequences a C-term deletion mutant of the HCV IRES is inserted (bicistronic mRNA R-HCVdel-FF)	this work

pSAD RL-p27-FL	pSAD L16 with the insertion of the coding sequence of Renilla and firefly luciferase in front of the coding sequence of the L mRNA; between the Renilla and Firefly coding sequences the p27 IRES is inserted (bicistronic mRNA R-p27-FF)	this work
pSAD RL-HRV-FL-PV3'	pSAD L16 with the insertion of the coding sequence of Renilla and firefly luciferase in front of the coding sequence of the L mRNA; between the Renilla and Firefly coding sequences the HRV IRES is inserted (bicistronic mRNA R-HRV-FF), the bicistronic mRNA ends with the original PV 3' end	this work
pSAD RL-HRV-FL-HRV3'	pSAD L16 with the insertion of the coding sequence of Renilla and firefly luciferase in front of the coding sequence of the L mRNA; between the Renilla and Firefly coding sequences the HRV IRES is inserted (bicistronic mRNA R-HRV-FF), the bicistronic mRNA ends with the original HRV 3' end	this work
pSAD RL-PV-FL-PV3'	pSAD L16 with the insertion of the coding sequence of Renilla and firefly luciferase in front of the coding sequence of the L mRNA; between the Renilla and Firefly coding sequences the PV IRES is inserted (bicistronic mRNA R-PV-FF), the bicistronic mRNA ends with the original PV 3' end	this work
pSAD RL-PV-FL-HRV3'	pSAD L16 with the insertion of the coding sequence of Renilla and firefly luciferase in front of the coding sequence of the L mRNA; between the Renilla and Firefly coding sequences the PV IRES is inserted (bicistronic mRNA R-PV-FF), the bicistronic mRNA ends with the original HRV 3' end	this work
pSAD PV-P	pSAD L16 in which the N/P gene border was replaced by the PV IRES	S. Finke
pSAD HRV2-P	pSAD L16 in which the N/P gene border was replaced by the HRV2 IRES	S. Finke
pSAD FMDV-P	pSAD L16 in which the N/P gene border was replaced by the FMDV IRES	this work
pSAD FMDV-P_1x34	pSAD FMDV-P; G→A mutation in second AUG of the P gene	this work
pSAD ΔPLP	pSAD L16 with a displacement of the P ORF behind the L ORF	(Brzozka et al., 2005)
pSAD G GFP	pSAD L16, containing eGFP as an additional gene between the G and L ORFs	S. Finke

2.1.11. Viruses

Recombinant rabies viruses (listed in Tab. 5) used in this study are derived from SAD L16, a recombinant rabies virus, carrying the nucleotide sequence of Street Alabama Dufferin (SAD) B19, an attenuated rabies virus strain used for oral immunization with entire nucleotide sequence determined (gene bank accession number M31046.1).

Furthermore, a Sendai virus defective interfering particle stock (DIH4) was used (Strahle et al., 2006).

2.1.12. Antibodies

Tab. 6: Antibodies

Antibody	species	description	reference
primary antibodies			
Centocor™	mouse	FITC-conjugated, monoclonal IgG against RV N	Fa. Centocor, Malevin, PA, USA
S50	rabbit	polyclonal serum against RV RNPs	J. Cox, BFAV Tübingen
S86	rabbit	polyclonal serum against RV N	J. Cox, BFAV Tübingen
P160-5	rabbit	polyclonal serum against RV P	S.Finke; FLI Insel Riems
HCA05/1	rabbit	polyclonal serum against RV G	Fa. Metabion, Planegg-Martinsried
E559	mouse	monoclonal serum against RV G from a mouse-hybridoma cell line	J. Cox, BFAV Tübingen
FCA05/1	rabbit	polyclonal serum against the N term of RV P	Fa. Metabion, Planegg-Martinsried
GCA05/1	rabbit	polyclonal serum against the C term of RV P	Fa. Metabion, Planegg-Martinsried
M1B3	rabbit	polyclonal serum against RV M	J. Cox, BFAV Tübingen
anti-actin	rabbit	IgG fraction of antiserum against actin	SIGMA
anti-GFP	rabbit	polyclonal serum against GFP	Invitrogen
anti-DRBP76	mouse	monoclonal IgG against DRBP76	BD Biosciences
anti-FLAG	rabbit	monoclonal IgG against FLAG peptide	SIGMA
anti-FLAG	mouse	monoclonal IgG against FLAG peptide	SIGMA

anti-GFAP	rabbit	polyclonal serum against GFAP	abcam
secondary antibodies			
anti-rabbit-PO	goat	peroxidase (PO)-conjugated anti-rabbit IgG	Dianova
anti-mouse-PO	goat	peroxidase (PO)-conjugated anti-mouse IgG	Dianova
anti-rabbit-alexa488	goat	alexa488-conjugated anti-rabbit IgG	Molecular Probes
anti-rabbit-alexa633	goat	alexa633-conjugated anti-rabbit IgG	Molecular Probes
anti-mouse-alexa488	goat	alexa488-conjugated anti-mouse IgG	Molecular Probes
anti-mouse-alexa633	goat	Alexa633-conjugated anti-mouse IgG	Molecular Probes
anti-rabbit-Cy3	goat	Cy3-conjugated anti-rabbit IgG	Jackson ImmunoResearch

2.2. Molecular biology methods

2.2.1. Preparation of plasmid DNA

Small amounts of plasmid DNA from *E.coli* were obtained by mini preparation after Sambrook *et al.* (1989).

Buffers for mini preparation

buffer Flexi I	**buffer Flexi II**	**buffer Flexi III**
100 mM Tris-HCl, pH 7.5	200 mM NaOH	300 mM KAc, pH 5.75
10 mM EDTA, pH 8	1 % (w/v) SDS	
400 µg/ml RNaseI		

1 ml of an overnight culture of transformed *E.coli* was pelleted by centrifugation (5,000 rpm, RT, 5'). The pellet was resuspended in 200 µl of Flexi I and lysed with additional 200 µl of Flexi II by inverting and 5' incubation at room temperature. For the neutralisation 200 µl Flexi III were added, inverted and incubated for 5' on ice. The supernatant was separated by centrifugation (14,000 rpm; 4°C; 5') and mixed with 400 µl of isopropanol to precipitate the

DNA. The precipitated DNA was pelleted by centrifugation (14,000 rpm; 4°C; 10'), air dried and dissolved in 50 µl H_20.

Higher amounts of plasmid DNA were isolated from 50 ml overnight culture of transformed *E.coli* by using the Nucleobond AX100-Kit from Macherey & Nagel following the manual.

2.2.2. Polymerase chain reaction (PCR)

For analytic PCRs the *Taq* DNA-Polymerase was used. For amplification of DNA fragments, used for further cloning the *Pfu*-DNA-Polymerase was used instead. A typical PCR reaction was performed in 100 µl:

PCR-reaction:
- 100 ng template DNA (or 2 µl of the RT product)
- 2.5 µl forward Primer (25 pmol)
- 2.5 µl reverse Primer (25 pmol)
- 10 µl DMSO
- 10 µl 10x Polymerase reaction buffer incl. $MgSO_4$
- 1 µl dNTPs (25µmol)
- 5 U polymerase (*Taq*- or *Pfu*-)
- add 100 µl H_2O

The reaction was denatured for 30'' at 95°C. The following 35 cycles consist of a denaturation step at 95°C for 1', primer annealing at 43°C-47°C for 1' and the elongation step at 72°C for 1-4' (depending on length of the PCR fragment). At the end the reaction was once heated up at 72°C for additional 10'. The PCR products were checked by electrophoresis on a 1% agarose gel and purified by the QiaQuick PCR purification Kit (QIAGEN) following the manual instructions.

2.2.3. Electrophoretic separation of DNA fragments

DNA-loading buffer:

15 % (w/v)	Ficoll 400
0.125 % (w/v)	OrangeG+
5 x	TAE buffer

For the electrophoresis of DNA fragments 1% agarose gels in TAE buffer were used. As running buffer 1xTAE with 0.02% ethidiumbromide was utilized. The DNA was 1:6 mixed with the DNA loading buffer and separated by 4-8 V/cm. The size of the DNA fragments was detected with help of a 1 kb ladder (Invitrogen) by UV at λ=254 nm.

2.2.4. Isolation of DNA fragments from agarose gels

DNA fragments were isolated from agarose gels using the QiaQuick Gel Extraction Kit.

2.2.5. DNA modifications

2.2.5.1. Fragmentation of DNA with restriction endonucleases

For fragmentation of plasmid DNA or PCR products restriction endonucleases and their appropriate buffers from New England Biolabs (NEB) were used. A typical restriction reaction contained DNA, restriction buffer with BSA and the restriction enzymes in H_2O. The restriction was performed at the enzyme specific temperatures for 2 h or overnight.

2.2.5.2. Generation of blunt ends by Mung Bean Nuclease and Klenow enzyme

To generate blunt ends *Mung Bean* Nuclease (cuts off overhang single stranded DNA) or the Klenow polymerase (fills 5'ends and degrades 3'overhangs) from NEB were used after instructor manuals.

2.2.5.3. Dephosphorylation of 5'ends

To avoid religation events in fragmented plasmid DNA, the DNA was 5' dephosphorylated by the *shrimp alkaline phosphatase* (SAP) after manufacturer's instructions right after the digestion reaction.

2.2.6. Ligation

For ligation of DNA fragments the purified DNA from the backbone and the inserts were mixed with 1 µl T4-DNA-ligase, 2 µl 10x T4-DNA ligase reaction buffer (incl. ATP). H_2O was added to a final volume of 20 µl. The ligation was incubated overnight at 16°C.

2.2.7. Sequencing of DNA

Sequencing of constructed plasmids or DNA fragments was performed in the lab of Dr. Blum at the Gene Center (LAFUGA) or Eurofins (Martinsried) (now MWG, Ebersberg). For sequencing reactions at the lab of Dr. Blum 500 ng DNA were dissolved in 5 µl H_2O and mixed with 3 pmol/µl of the sequencing primers. For sequencing reactions at Eurofins/MWG 100-200 ng/µl of DNA were premixed with 15 pmol/µl sequencing primers in an end volume of 15 µl.

2.2.8. Cloning of cDNAs for the generation of recombinant RVs

All recombinant cDNAs were constructed on the basis of the full-length RV cDNA (SAD L16).

2.2.8.1. Generation of cDNAs for SAD RL-IRES-FL

a) Cloning strategy for pCMV RL-IRES-FL

For construction of pCMV RL-IRES-FL first a pCMV RL-FL plasmid was generated. To this end, RL was PCR amplified from pCMV-RL (Invitrogen) using oligonucleotides #18/#19 and inserted into pECFP-N1 (Clontech) after XbaI/NheI digestion. In a second step, FL was PCR amplified using oligonucleotides #20/#21and inserted into the intermediate plasmid (pECFP-RL) after SmaI/NotI digestion. Into the resulting pCMV RL-FL plasmid, IRES elements or the RV N/P gene border were inserted after PCR amplification by appropriate oligonucleotides (Tab. 2), including SmaI or EcoRV and NheI as restriction sites.

b) Cloning strategy for pSAD RL-IRES-FL

For construction of pSAD RL-IRES-FL, pSAD G DsRed-NP (Klingen et al., 2008) was used as a backbone. The bicistronic RL-IRES-FL reporter constructs were inserted from the appropriate pCMV RL-IRES-FL plasmids into pSAD G DsRed-NP (NheI/NotI) after SpeI/NotI digestion, resulting in pSAD RL-IRES-FL cDNAs.

3'UTRs were inserted into pSAD RL-IRES-FL after PCR amplification of the PV 3'UTR and HRV2 3'UTR, respectively, and following NheI/NotI digestion.

2.2.8.2. Generation of cDNAs for SAD IRES eCFP

For construction of pSAD N/P eCFP, pSAD PV eCFP and pSAD HRV2 eCFP, pSAD G TIMER-NP, -PV, -HRV were used as a backbone. The eCFP ORF was inserted from pECFP-N1 (Clontech) by SmaI/NotI restriction and following ligation into pSAD G TIMER-IRES plasmids.

Generation of pSAD IRES eCFP cDNAs, including IRES elements from FMDV, CSFV, HCV and the 5'UTR of the p27 mRNA, was performed using pSAD HRV2 eCFP as a backbone. By NheI/SmaI restriction the HRV2 IRES was replaced by the other IRES elements, which were PCR amplified with appropriate oligonucleotides before.

2.2.8.3. Generation of cDNAs for SAD FMDV-P and SAD FMDV-P1x34

Generation of SAD FMDV-P was performed in three steps. First the FMDV IRES was PCR amplified from pCMV RL-FMDV-FL using oligonucleotides #51/52 and digested by EcoRI/BglII. The resulting fragment was afterwards inserted into pCR3-IgP (EcoRI/BglII), resulting in pIG FMDV-P. In a second step, RV N was PCR amplified from pTIT-N using oligonucleotides #75/#56 and EcoRV/HpaI digested. The resulting fragment was then inserted into pIG FMDV-P (SnaBI/HpaI), resulting in pIG N-IRES-P. In the last step a first PCR (PCR#1) was performed using pIG N-IRES-P as a template and oligonucleotides #75/#82. The resulting PCR product of ~2.5 kB was then used as a template for a second PCR (PCR#2) with oligonucleotides #57/#83. The resulting PCR#2 product was then inserted into pSAD L16 after AvrII/SnaBI digestion, leading to pSAD FMDV-P.

pSAD FMDV-P1x34 was generated by mutagenesis PCR of pSAD FMDV-P using mutagenesis oligonucleotides #K1/#K2.

2.2.9. Use of E.coli

2.2.9.1. Bacterial culture

LB medium:

1% (w/v) Bacto-Trypton
0.5 % (w/v) yeast extract
0.5 % (w/v) NaCl
1 mM $MgSO_4$

LB agar plates:

1% (w/v) Bacto-Trypton
0.5 % (w/v) yeast extract
0.5 % (w/v) NaCl
1 mM $MgSO_4$
1.5 % (w/v) agar

Depending on the selection marker in the used plasmids, LB media and LB agar plates were mixed with the antibiotics ampicillin (100 mg/ml) or kanamycin (25 mg/ml). *E.coli* cultures were incubated overnight at 37°C on a shaker.

2.2.9.2. Production of competent E.coli bacteria

Media:

LB^{++} medium	**$CaCl_2$ buffer**
LB medium	60 mM $CaCl_2$
20 mM $MgSO_4$	10 mM Pipes, pH 7.1
10 mM KCl	15 % (v/v) glycin

100 ml LB^{++}-Medium were mixed with 1 ml of a fresh overnight culture of *E.coli* XL1-Blue bacteria and incubated at 37°C on a shaker. After reaching an optical density $(OD)_{660}$ of 0.6, the bacteria were pelleted by centrifugation (4,000 rpm, 4°C, 10'). The pellet was resuspended in 1/4 volume of ice cold $CaCl_2$ buffer and incubated for 40' on ice. The bacteria were once more pelleted by centrifugation (4,000 rpm, 4°C, 10') and resuspended in 1/20 volume of $CaCl_2$ buffer. After 1-3 h of incubation on ice, the competent XL1-Blue bacteria were aliquoted and stored at -80°C.

2.2.9.3. Transformation of XL-1 competent E.coli

For transformation 50 µl competent XL-1 *E.coli* were thawed on ice, mixed with 10 µl of the ligation reaction or 100 ng of plasmid DNA and incubated on ice for 20'. After a heat shock (2', 42°C) the bacteria were cooled down for 2' on ice. The bacteria were then mixed with 200 µl of LB++ and incubated for 30-45' at 37°C on a shaker. The transformed bacteria were afterwards either plated on LB agar plates containing the appropriate antibiotics or were grown in LB media (plus antibiotics).

2.2.10. Isolation of RNA from cells

RNA was isolated from cells using the RNeasy Kit from QIAGEN. 1 x 10^6 cells were lysed in 700 µl RLT buffer incl. mercaptoethanol, mixed with 700 µl 70% EtOH and loaded onto a column. After centrifugation (14,000 rpm, 1 min) the column was washed once with 750 µl RW1 buffer and twice with 500 µl RPE buffer. After drying the column by centrifugation for an additional minute, the RNA was eluted in 40 µl RNase free H_2O. The concentration was measured with the Nanodrop (Peqlab).

2.2.11. Reverse transcription (RT)

Standard RT PCR was performed using the Roche Transcriptor RT (Roche). Therefore 1-6 µg RNA were mixed with 3 µl primer (specific reverse primer, oligo dT, Random Hexamer primers) in a final volume of 13 µl. After incubation at 65°C for 10 min 4 µl RT buffer, 0.5 µl RNase inhibitor, 2 µl dNTPs and 0.5 µl Transcriptor RT were added and incubated at 55°C for 30 min. To inactivate the enzyme the reaction was heated for 5 min at 85°C.

2.2.12. Electrophoretic separation of RNAs

For the electrophoresis of RNAs, denaturing 2% agarose gels were used. One gel consists of 2 g agarose dissolved in 172.5 ml phosphate buffer and 27.5 ml Formaldehyde (37%). As running buffer 1x phosphate buffer was used. 2.7 µg of the RNAs were solved in 7.2 µl RNase free H_2O and mixed with 3 µl 5 x phosphate buffer and 1.8 µl glyoxal. To denature the RNAs, the mix was incubated at 56°C for 45 min. The RNA solution was mixed with 3 µl Blue Juice and separated at 25 V overnight. The separated RNA was stained with acridinorange and detected by UV at λ=254 nm.

2.2.13. Northern Blot

RNAs were transferred on a nylon membrane by vacuum blotting. The agarose gel containing the separated RNAs was layed on a nylon membrane. As blotting buffer 3x SSC was used. To transfer the RNAs the vacuum was applied at -100 bar for 2 h. After blotting the membrane was air dried and the RNA was fixed by UV cross-linking at 0.125 J.

To label the probes with ^{32}P the nick end translation kit from Amersham was used. 100 ng of DNA were mixed with 4.2 µl dNTPs without cytosin, 2 µl ^{32}P-dCTP and 3 µl of the polymerase were mixed in a final volume of 20 µl. After incubating the reaction for 90 min at RT the probe was purified using the nucleotide removal kit (QIAGEN) and denatured for 5 min at 95°C. Hybridization was performed in 8 ml of Zeta-Hybridization-Mix containing the ^{32}P- labeled probe at 68°C overnight in an incubator. After hybridization the membrane was washed once with 5% Zeta-Wash and twice with 1% Zeta-Wash and air dried. The radioactively labeled RNAs were detected by exposing the membrane to a photosensitive screen or a ^{32}P sensitive film (GE Healthcare) for at least 2 h. The screen was analyzed using a storm scanner (Molecular Dynamics; GE Healthcare).

2.3. Cell culture

2.3.1. Cultivation of cell lines

All cell lines (2.1.7.2) were cultivated at standard conditions at 37°C, 5% CO_2 and 100% humidity. Twice a week adherent cells were detached by trypsinization, 1/6 to 1/10 of them were mixed with appropriate, fresh media plus needed antibiotics (2.1.7.3) and seeded into new cell culture flasks.

2.3.2. Freezing of cells

To store cell lines for several month or years, cell lines were freezed and stored in liquid nitrogen. For freezing 3 x 10^6 cells were trypsinized, resuspended in 5 ml of their appropriate medium and incubated on ice. After adding 8% (v/v) DMSO by pivoting the cells on ice, 1 ml aliquots of the cells were at first slowly freezed at -80°C and stored in liquid nitrogen 24 h later.

2.3.3. Transfection of cells

Cells were transfected by $CaPO_4$ using the mammalian transfection kit from Stratagene, by Lipofectamine2000 or PEI25.

2.3.3.1. $CaPO_4$- Transfection by the mammalian transfection kit (Stratagene)

3 x 10^5 cells were seeded into 6 well dishes and incubated overnight. 1 h before transfection cells were washed with DMEM without serum. DNA in a final volume of 90 µl was mixed with 10 µl of solution #1 of the kit on ice. After addition of 100 µl of solution #2 and incubation at room temperature for 10-20 min the transfection mix was dripped onto the cells. 3- 5 h post transfection the cells were washed with their appropriate media and incubated at standard conditions.

2.3.3.2. Transfection with Lipofectamine2000

2.5 x 10^5 cells were seeded into 24 well dishes and incubated overnight. 2.5 µl Lipofectamine2000 per 1 µg DNA in 100 µl DMEM without serum were incubated for 5 min at RT, afterwards the DNA (in 100 µl DMEM without serum) was added. The DNA/Lipofectamine2000 mix was incubated further 20 min at RT and dripped onto the cells. Cells were incubated at standard conditions.

2.3.3.3. Transfection with Polyethylenimin (PEI)25

2.5 x 10^5 cells were seeded into 24-well dishes and incubated overnight. 2 µl PEI25 per 1 µg DNA was dissolved in 200 µl DMEM without serum. After adding the DNA, the tube was gently flicked and incubated for 20 min at RT. After dropping the transfection mix onto the cells, they were incubated at standard conditions

2.3.4. Immunofluorescence

2.3.4.1. Acetone fixation

Cells were washed once with 1x PBS, once with cold 80% acetone, fixed with cold 80% acetone for 20 min at 4°C and air dried.

2.3.1.2. Fixation with 3% paraformaldehyde

Cells were washed once with 1x PBS, once with 3% paraformaldehyde and fixed with 3% paraformaldehyde. After 20 min of incubation at room temperature the cells were washed three times with 1x PBS. For permeabilization the fixed cells were incubated in 0.5% Triton-X100 for 10 min and afterwards again washed with 1x PBS.

2.3.1.3. Immunostaining

For immunostaining the fixed cells were stained with primary antibodies for 1.5 h at 37°C. After three washing steps with 1x PBS, cells were incubated with the secondary antibodies also for 1.5 h at 37°C and then washed three times with 1x PBS.

For confocal microscopy stained cells on coverslips were embedded with hard mounting medium (Vectashield®) on microscope slides.

2.3.5. Microscopy

For fluorescence microscopy of cells a fluorescence microscope (Olympus IX 71) was used, using UV- or transmission light.

For confocal microscopy the confocal laser scanning microscope Zeiss Axiovert 200/LSM510 Metasystem was used. For detection of eCFP, a laser with a wave length of 458 nm and the filter BP 475-525 was used, whereas alexa-633 fluorescence was detected with a laser at the wave length 543 nm and the filter BP 560-615. Measurements were carried out, using optimal settings for the detection of fluorescence intensities from cells infected with SAD HRV2 eCFP.

2.3.6. Immunohistochemistry of brain slice cultures

Immunohistochemistry experiments of brain slice cultures were performed by Prof. M. Schwemmle at the Department of Virology of the Institute for Medical Microbiology and Hygiene in Freiburg.

Cultures selected for immunofluorescence analysis and DAPI nuclear staining were fixed with 4% paraformaldehyde in 0.1 M phosphate buffer (PB), pH 7.4 for 3 h. After several rinses with PB for 1 h the Millipore membrane with the cultures on top was cut off, mounted on an agar block and resliced into 50 µm sections using a vibratome. Free floating sections were then incubated in PB containing 5% normal goat serum (NGS) and permeabilized with 0.1% Triton-X100 in PB for 30 min and further incubated with primary antibodies (anti-calbindin, a marker for dentate granule cells, dilution 1:10,000 and SWANT; S50, recognizing RV RNP at 1:50) in PB containing 1% NGS overnight at 4°C. After five-times washing for 15 min each with PB, sections were incubated with secondary antibodies (Cy3-conjugated goat anti-rabbit IgG, diluted 1:800 and Alexa 488-conjugated goat anti-mouse IgG, diluted 1:200, respectively) for 2 h at room temperature in the dark. Sections were extensively washed with PB, followed by DAPI stain for 2 min (dilution 1: 10^6), washed again in PB and mounted onto gelatin-coated slides, embedded with immunomount (Shandon). Sections were digitally photographed (Zeiss ApoTome).

2.4. Virological methods

2.4.1. Generation of recombinant rabies virus from cDNA (Virus rescue)

For the generation of recombinant rabies virus out of cDNA, 80-90% confluent BSR T7/5 cells in 3.5 cm^2-cell culture dishes were transfected using the mammalian transfection kit (Stratagene) (2.6.1.4). Per reaction 5 µg pTIT-N, 2.5 µg pTIT-P, 2.5 µg pTIT-L and 10 µg of the full length rabies virus cDNA (pSAD …) were mixed with H_2O to a final volume of 40 µl and stored on ice. Afterwards 10 µl of solution #1 were added to the DNA samples on ice and mixed by gently pipetting up and down 3-4 times on ice. In a second step 100 µl of solution #2 were added and mixed again by gently pipetting up and down 3-4 times. After 10-20 min incubation at room temperature the 200 µl DNA-transfection-mix were added dropwise onto the cells without removing the 1 ml DMEM without any supplements. To reach an adequate distribution dishes were finally slowly pivoted in an 8-shape. After incubation for 3-5 h at

37°C the transfected cells were washed once with GMEM4+ medium and then incubated in 2 ml GMEM4+ medium for 72 h at 37°C.

To amplify the newly generated viruses from the supernatant two supernatant passages were following. Therefore 3 x 10^5 fresh BSR T7/5 cells were seeded into 3.5 cm^2-cell culture dishes in a final volume of 1 ml and were mixed in suspension with the whole supernatant from the transfected cells (passage #1A). 2 ml of fresh GMEM4+ medium were put onto the transfected cells which were then incubated together with the passage #1A for further 72 h at 37 °C. The supernatant passage was repeated using the supernatant from passage #1A after 72 h (passage #1B). To ensure if generation of recombinant rabies virus was successful, cells from passage #1A were fixed 72 h after transfer of the supernatant with 80 % acetone and stained against the RV N protein (Centocor®) by direct immunofluorescence (see 2.6.1.5.), while the supernatant from passage #1A was transferred into tubes and stored at 4°C or on ice. If foci were detectable, the supernatant from passage #1A could be titrated and used to prepare virus stocks (see 2.4.2.).

Cells from passage #1B were also fixed 72 h after transfer of the supernatant with 80 % acetone and stained against the RV N protein (Centocor®) by direct immunofluorescence (see 2.6.1.5.), while the supernatant from passage #1B was transferred into tubes and stored at 4°C or on ice. If foci were detectable, the supernatant from passage #1B could again be titrated and used to prepare virus stocks (see 2.4.2.).

If no foci could be detected on cells from passage #1A or #1B, the transfected cells were detached from the 3.5 cm^2-cell culture dishes and mixed with fresh GMEM4+. 1/8 of the transfected cells were transferred into a new 3.5 cm^2-cell culture dish and mixed with GMEM4+ to a final volume of 2 ml. The remaining 7/8 of the transfected cells were seeded into a 25 cm^2-cell culture flask and mixed with GMEM4+ to a final volume of 8 ml. All transfected cells were incubated for further 72 h at 37 °C.

The split transfected cells from the 3.5 cm^2-cell culture dish were fixed with 80 % acetone and stained against the RV N protein (Centocor®) by direct immunofluorescence (see 2.6.1.5.) after 72 h. If foci were detectable, the 8 ml supernatant from the split transfected cells from the cell culture flask were titrated and used to prepare virus stocks (see 2.4.2.).

2.4.2. Preparation of virus stocks

For the preparation of virus stocks 7.5 x 10^5 BSR T7/5 cells are infected with virus at a MOI between 0.01 and 0.1 in a final volume of 8 ml and incubated for 48 h at 37°C. For the first harvest (48 h p.i.) the supernatant is centrifuged at 1800 rpm at 4°C for 10 min to remove

cellular material, aliquoted and stored at -80 °C. The infected cells were incubated for a further 48 h at 37°C in 8 ml of fresh GMEM4+ .The second harvest was performed identically 96 h p.i.

2.4.3. Titration of virus

For virus titration 1.2 x 10^4 BSR T7/5 cells were seeded into all concavities of a 96-well plate in a final volume of 100 µl and incubated at 37°C for 2 h, leading to an attached cell layer. For every virus supernatant seven serial 10fold dilutions (10^{-1} to 10^{-7}) in GMEM without any supplements were prepared. 100 µl of every dilution were transferred onto the seeded BSR T7/5 cells in the 96-well plate to a final volume of 200 µl. After incubation at 37°C for 48 h, the cells were fixed with 80% acetone and stained against the RV N protein (Centocor®) by direct immunofluorescence.

Virus titers were determined by counting foci in the well of the dilution where the fewest foci were detectable and in the next lower dilution, each in duplicates. The virus titer was then the mean of foci from four wells multiplied by the dilution.

2.4.4. Purification of virus particles by Iodixanol density gradient centrifugation

For purification of virus particles Iodixanol-density gradients (Optiprep™, Axis-Shield) were used. Therefore, 3 x 10^6 BSR T7/5 cells were infected at a MOI of 1. 48 h p.i. 8 ml of supernatants were harvested. In a first centrifugation step (5 min, 1800 rpm, 4°C) cell debris was removed. 10% to 40%- density gradients were prepared by layering 6 ml of each 10%- and 40%- solution of Iodixanol into centrifugation tubes. Supernatants were put onto the gradients. After centrifugation for 18 h at 27,000 rpm and 4°C in an ultracentrifuge (Beckman SW28), the upper 8 ml of the gradients were discarded. The lower 12 ml were collected in 12 x 1 ml fractions. For Western Blot analysis (2.5.3) of the purified virus particles, fractions were mixed with the same amount of lysis buffer.

2.4.5. Infection of organotypic brain slice cultures

Brain slice culture experiments were performed by Prof. M. Schwemmle at the Department of Virology of the Institute for Medical Microbiology and Hygiene in Freiburg.

Hippocampi were dissected from neonate mouse pups (P0-P1) and cut into 400 µm horizontal sections with a tissue chopper. The sections were placed into petri dishes filled with cold minimum essential medium (MEM) supplemented with 2mM glutamine at pH 7.3. Obviously intact slices were placed onto humidified porous membranes of cell culture inserts

(CM30, Millipore Corporation) and transferred sterile into six-well plates containing 1.2 ml of medium (for details, see (Brinks et al., 2004)). Slices were cultivated for 4-8 d at 37°C with 5% CO_2 in humidified atmosphere and the medium was changed every third day. Slice cultures were infected immediately after preparation with 1.5 µl of virus stock, corresponding to ca. 2.4 x 10^4 ffu.

2.4.5. Mouse infection experiments

Mouse infection experiments were performed by Prof. L. Stitz at the Institute of Immunology at the Friedrich-Loeffler-Institut in Tübingen.

Wildtype (wt) and transgenic IFNAR$^{-/-}$ mice were originally obtained from M. Aguet, Zurich, and kept in the SPF-facility at the Institute of Immunology, Friedrich-Loeffler-Institute, Tübingen. Age and sex-matched adult wt or IFNAR$^{-/-}$ mice (Muller et al., 1994) were infected i.c. into the left hemisphere with up to 10^5 ffu in 20 µl and newborn mice with 10 µl. The animals were observed daily three times and scored for the appearance of neurological signs on an arbitrary scale of 1-3 (level 1 for slight neurological signs such as beginning ataxia and slightly reduced motility; level 2 for increased neurological signs such as trembling and/or disorientation after tail spinning; level 3 for severe signs of disease such as ruffled fur, hunched position and inability to move). Animals scored twice at level 3 or at level 2 at noon and level 3 in the afternoon were immediately sacrificed according to the German Animal Protection law and serum and organs were preserved.

2.5. Biochemical methods

2.5.1. Preparation of denatured protein lysates

1 x 10^6 cells were lysed in 500 µl lysis buffer and boiled for 5 min at 95°C.

2.5.2. Electrophoretic separation of proteins by SDS-Polyacrylamid-Gels (SDS-PAGE)

For the separation of proteins Jagow gels of middle (16 x 14 cm) or of big (20 x 20 cm) size were used.

At first the separation gel was prepared, filled between two glas plates, fixed in a filling aperture (peqlab) and overlaid with isopropanol. After polymerization of the separation gel the isopropanol was discarded. The stacking gel was prepared, mounted onto the polymerized separation gel and the comb was inserted. The polymerization took further 1-2 h.

Gels were loaded with 30-100 µl of protein lysates and run at 40-80 V overnight in running apertures from peqlab filled with Jagow anode and cathode buffer.

Separation gels:
12 ml Jagow gel buffer
8-14 % acrylamid
2 ml glycerol
17 µl TEMED
175 µl APS
add H_2O to a final volume of 36 ml per middle sized gel
or 54 ml per big sized gel.

Stacking gels:
3.5 ml Jagow gel buffer
4 % acrylamid
18 µl TEMED
116 µl APS
add H_2O to a final volume of 14 ml per middle sized gel
or 21 ml per big sized gel.

2.5.3. Western Blotting

For the immunological detection of proteins, separated by gel electrophoresis, they were blotted onto a Polyvinyliden-Fluorid (PVDF)-Membrane (MILLIPORE). Prior to the semi-dry blotting the membrane had to be activated in methanol and washed in ice-cold 1x semidry buffer, like the gel itself. For the protein transfer from the gel onto the membrane the gel was laid onto the membrane and both were put between two whatman papers, soaked with 1x semidry buffer. The protein transfer occurred in a blotting chamber (BIORAD) at 400 mA for 2 h for middle sized gels or for 3 h for big sized gels.

After the transfer the membrane was blocked for at least 1 h in 5 % milk in PBS.

For the immunological detection of the proteins the membrane was incubated for 1-2 h with the primary antibody, diluted in PBS. After three times washing with PBS-T (PBS + 0.5 % TWEEN) the membrane was incubated further 1-2 h with the secondary antibody, diluted in PBS-T and washed afterwards once more for three times with PBS-T. Depending which secondary antibody was used Detection of proteins occured by ECL (PERKIN-ELMER) on a light sensitive film, when a HRP-(horseradish peroxidase)-coupled secondary antibody was used. When a fluorescently labeled secondary antibody was used, proteins were imaged by the

Typhoon9400-Variable Mode Imager (Amersham Biosciences) at 300-600 V, the intensity of bands was then quantified using the software ImageQuant 5.0.

2.5.4. Luciferase-Assay

For detection of Luciferase activity in cell lysates the „Dual Luciferase Reporter Assay System“ (PROMEGA) was used, according to the supplier's instructions. Therefore 2.5 x 10^5 cells were lysed in 250 µl of passive lysis buffer. Depending on the luciferase activity 20 or 2 µl of the lysates were subjected to the dual luciferase assay (Promega) in a luminometer (Berthold) according to the supplier's and manufacturer's instructions.

2.6. Statistical Analysis

As a statistical method for characterization of significant differences between the means of two independent samples the t-test was used. As a tool "Open Source Epidemiologic Statistics for Public Health Version 2.3" was utilized.

3. RESULTS

3.1. RNA virus-based reporter systems for the characterization of IRES elements

3.1.1. Generation of a new RNA virus-based dual luciferase reporter system for characterization of IRES elements

3.1.1.1. Sequences predicted to contain IRES elements promote reporter gene expression from plasmids

The use of bicistronic reporter gene plasmids is the classical method to prove that RNA sequences are able to promote 5'cap-independent, "internal" translation initiation. These reporter plasmids usually include a bicistronic mRNA, which contains ORFs for two reporter genes, e.g. renilla and firefly luciferase, separated by the sequence of interest. From such reporter plasmids the first reporter is translated 5'cap-dependently. There are only two mechanisms known, how translation initiation occurs. Either enabled by a 5' cap structure or an internal translation initiation, mediated by an IRES. Thus, translation of the second reporter gene within this construct should take place if the inserted sequence is able to initiate translation independent of a 5'cap-structure. We used this classical method, based on reporter plasmids to test whether sequences within 5'UTRs from different RNAs can mediate expression of a downstream reporter gene. For this purpose, bicistronic pCMV RL-IRES-FL reporter plasmids were generated, containing 5'UTRs of viral RNAs, including picornaviruses (poliovirus (PV), human rhinovirus type 2 (HRV2), foot-and mouth disease virus (FMDV)), pestiviruses (bovine viral diarrhea virus (BVDV), classical swine fever virus (CSFV)) and hepatitis C virus (HCV) belonging to the family hepacivirus. In addition, the 5'UTR from a cellular mRNA coding for the cell cycle regulator p27 and which has been proposed to contain an IRES element was included. The reporter plasmids contain the ORFs for renilla-(RL) and firefly-(FL) luciferase and are driven by the promoter of the cytomegalovirus (CMV). Within the plasmids the 5'UTR sequences are inserted between the luciferase ORFs. Accordingly, these pCMV RL-IRES-FL reporter plasmids give rise to 5'capped and polyadenylated bicistronic mRNAs. They should serve for 5'cap-dependent translation of RL, whereas translation of the downstream firefly luciferase is mediated by the IRES elements

(Fig. 8A). For quantification of reporter gene expression by the inserted sequences, the reporter plasmids were transfected into BSR T7/5 cells. Cells were lysed 48 h post transfection and subjected to a dual luciferase assay to measure RL and FL activity. FL expression was normalized to RL expression and compared to the relative reporter gene expression from pCMV RL-PV-FL, containing the PV IRES, which served as a standard (100%).

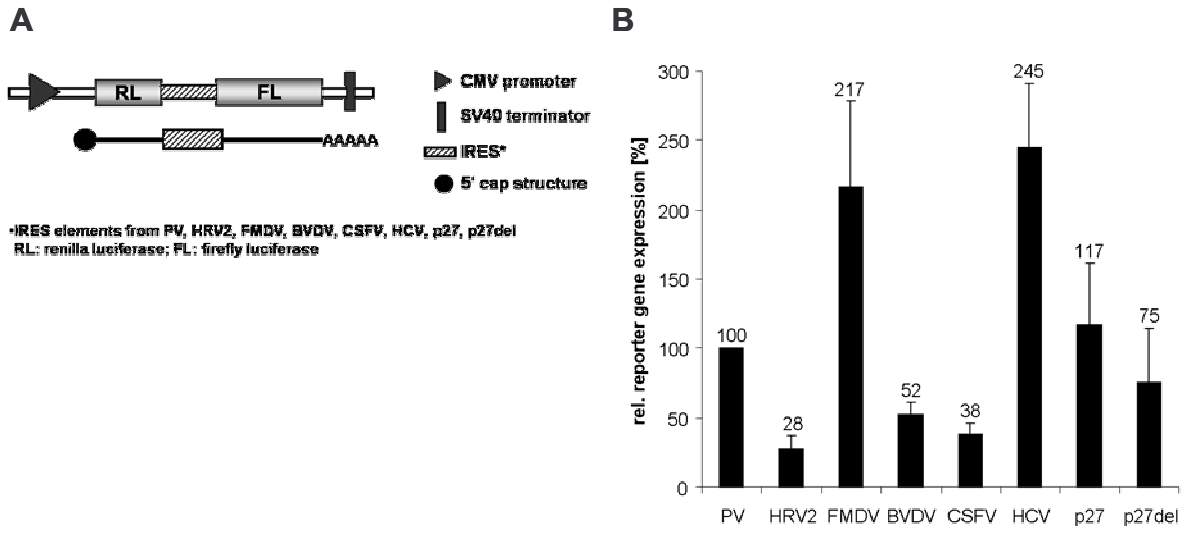

Fig. 8: 5'cap-independent reporter gene expression from IRES containing plasmids.
(A) Organization of RL/FL reporter plasmids. IRES elements of PV, HRV2, FMDV, BVDV, CSFV, HCV, p27 and a deletion mutant of p27 (p27del) were inserted between the ORFs for renilla- (RL) and firefly- (FL) luciferase. The CMV promoter provides the transcription of a bicistronic RL/FL mRNA from which RL is expressed 5'cap-dependently whereas FL is translated in dependence of the inserted IRES elements. (B) BSR T7/5 cells transfected with the indicated reporter plasmids were lysed at 48 h post transfection and subjected to the dual luciferase reporter assay. The activity of FL in relation to RL determined for pCMV RL-PV-FL was set to 100%. Error bars indicate standard deviation from three parallel experiments.

All plasmids, which contain either viral IRES sequences or two forms of the predicted cellular p27 IRES, mediated expression of the downstream reporter gene FL, though to different extents. Compared to pCMV RL-PV-FL, plasmids containing IRES elements of HRV2, BVDV and CSFV expressed reduced levels of firefly luciferase (28%, 52% and 38%), whereas plasmids containing IRES elements from FMDV and HCV led to a higher FL expression (217% and 245%, respectively). Transfection of plasmids comprising two variants of the p27 UTR showed intermediate FL expression (117% and 75%) (Fig. 8B).

A plasmid, serving as a negative control, expressing 0% FL compared to the PV IRES, could not be included in these experiments, as no sequence is known which certainly lacks cryptic promoters as well as potential splice sites, leading to the transcription of two monocistronic, 5' capped mRNAs for RL and FL.

Thus, all used 5'UTR sequences predicted to contain viral or cellular IRES elements, mediated expression of the downstream FL from a bicistronic RL/FL DNA reporter construct, though to different extents.

3.1.1.2. Gene expression of SAD RL-IRES-FL

The use of reporter plasmids to analyze IRES activities has severe disadvantages, which are extensively discussed (Kozak, 2003; Kozak, 2007). The possible presence of cryptic promoter sequences in the DNA and additional splice acceptor sites in RNA, could lead to the transcription or generation of additional monocistronic mRNAs, from which the downstream reporter gene is translated in a 5'cap-dependent manner. Reporter gene expression from these additional mRNAs cannot be distinguished from reporter gene expression by internal translation initiation and therefore would cause false positive results.

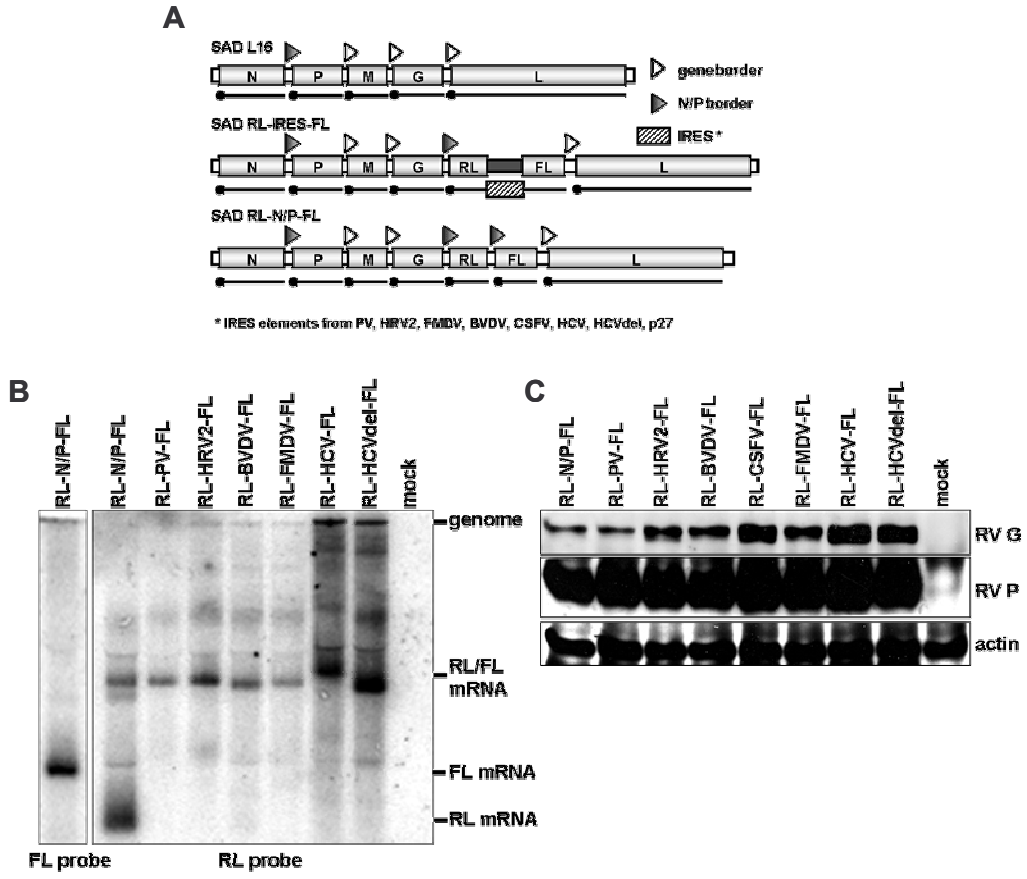

Fig. 9: Generation of SAD RL-IRES-FL reporter viruses.
(A) Organization of dual luciferase reporter RVs. A bicistronic cDNA comprising the IRES elements of PV, HRV2, FMDV, BVDV, CSFV, p27, HCV and a deletion mutant of HCV (HCV del) between the r*enilla* (RL) and firefly luciferase ORF (FL) was inserted as an additional gene between the coding regions of the RV glycoprotein (G) and the polymerase (L). In the control virus SAD RL-N/P-FL the IRES was replaced by the N/P gene border such that two monocistronic 5'capped mRNAs (RL mRNA, FL mRNA) are transcribed. (B) Transcription of bicistronic RL/FL mRNAs (SAD RL-IRES-FL) and individual monocistronic mRNAs (SAD RL-N/P-FL) analyzed by Northern blot experiments with RNA isolated from virus-infected BSR T7/5 cells. (C) Expression of RV P and G from different SAD RL-IRES-FL reporter viruses analyzed by Western Blot with lysates from BSR T7/5 cells, infected with an MOI of 3 at 48 h p.i. .

To reveal and to circumvent these problems occurring on plasmid level, we generated a new system to characterize IRES elements in the context of rabies virus (RV) and thereby obviated problems which appear on DNA level or by cryptic splice sequences. In addition, since RV transcription occurs exclusively in the cytoplasm, splicing events can be excluded.

To this end, we generated recombinant reporter RVs, with an additional bicistronic gene comprising the above described RL-IRES-FL sequences, located between the RV glycoprotein (G) and the polymerase (L) genes. In addition to the five original 5'capped, monocistronic mRNAs for each viral gene, these reporter viruses (SAD RL-IRES-FL) should express one bicistronic mRNA. From this bicistronic mRNA RL should be expressed 5'cap-dependently, whereas translation of FL depends on the respective IRES element. In addition, we constructed a control virus (SAD RL-N/P-FL), in which the IRES was replaced by the N/P gene border, leading to the transcription of two individual monocistronic 5'capped reporter mRNAs (Fig. 9A). Northern Blots with RNA extracted from infected BSR T7/5 cells were hybridized with ^{32}P-labelled probes against RL and FL, respectively. These Northern Blots proved the transcription of an additional bicistronic RL/FL mRNA and excluded the presence of individual monocistronic mRNAs for RL and FL as it was the case in the SAD RL-N/P-FL control virus. In addition, a band appeared in the lane of the control virus with the same mobility as the bicistronic RL/FL mRNA. This band should likely correspond to a G/RL readthrough mRNA, which has a similar predicted size to the RL/FL mRNA (Fig. 9B). To show that these reporter RVs are able to express essential viral proteins, I performed Western blot analysis, showing expression of two essential proteins, the RV phosphoprotein (P) and of RV glycoprotein (G) from SAD RL-IRES-FL reporter RVs as well as from the SAD RL-N/P-FL control virus (Fig. 9C).

Hence, I was able to generate recombinant SAD RL-IRES-FL RVs, which transcribe an additional bicistronic RL/FL mRNA in dependence of IRESs and which still are able to express viral proteins, being essential for vial replication.

3.1.1.3. RL expression by SAD RL-IRES-FL reflects viral replication levels

The presence of IRES elements or an additional bicistronic mRNA might have an influence on the replication of the virus. To exclude this possibility I performed multi-step growth curves on BSR T7/5 cells. All reporter viruses grew to titers of 1 x 10^7 to 1 x 10^8 ffu/ml at 48 h p.i., which indicates that in spite of the insertion of IRES elements and a bicistronic mRNA into the viral genome all reporter viruses are replication competent (Fig. 10A).

To quantify IRES activities with the help of the reporter viruses, expression of RL was used for normalization. As RL is translated from the bicistronic mRNAs in a 5'cap-dependent way, expression levels should change only in dependence of viral replication. To prove this, BSR T7/5 cells were infected with the indicated viruses and RL expression was measured 24 h, 48 h and 72 h p.i. (Fig. 10B). Like viral titers obtained from the growth curve experiments (Fig. 10A), also RL-LU (renilla luciferase light units) values usually differed by one $\log_{10}$ 48 h p.i. between the different reporter viruses in BSR T7/5 cells. This demonstrates first that RL expression from reporter RVs can be used as a marker for virus replication in a similar manner as viral titers. Second, these results confirm data from growth curves (Fig.10A), which showed that viral replication is still possible after insertion of IRES elements or a bicistronic mRNA into the viral genome.

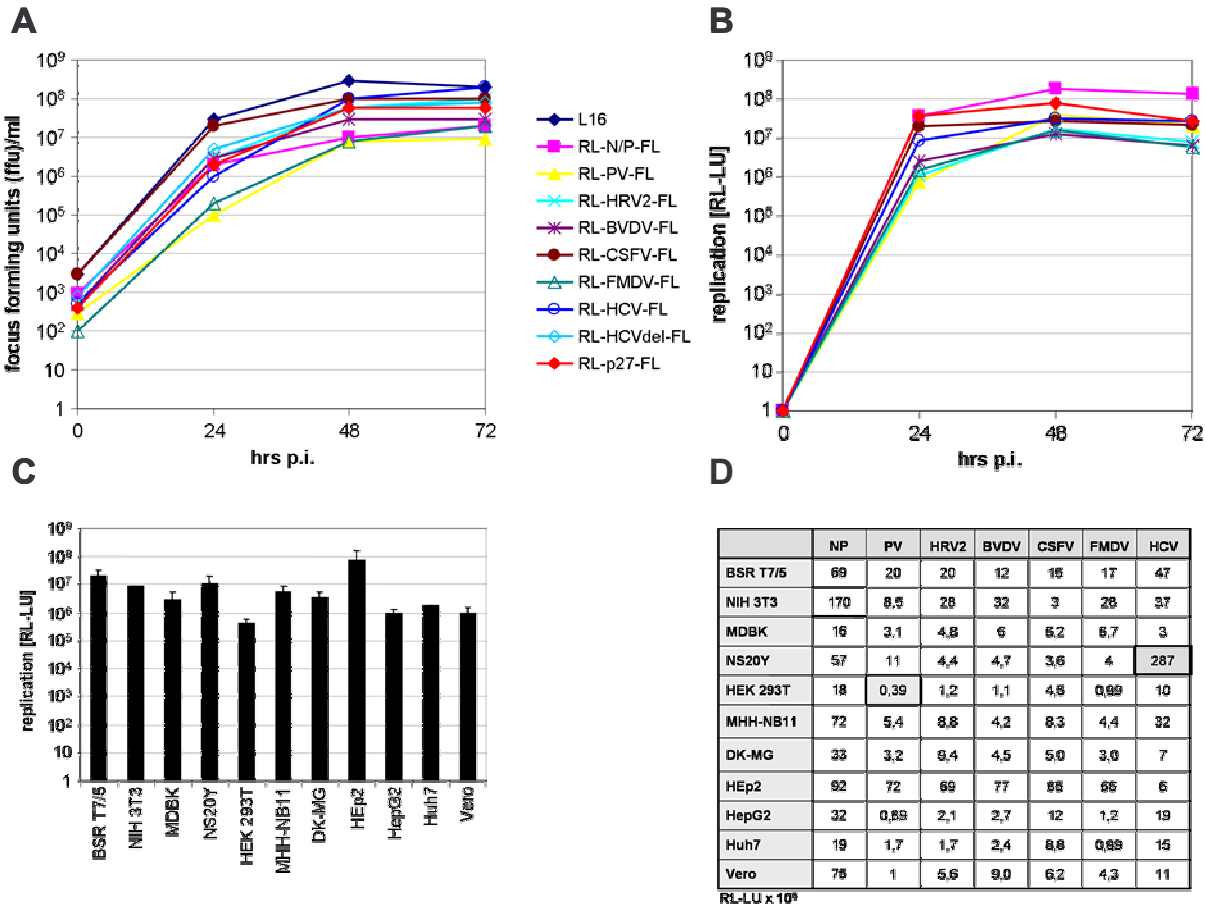

	NP	PV	HRV2	BVDV	CSFV	FMDV	HCV
BSR T7/5	69	20	20	12	16	17	47
NIH 3T3	170	8,5	28	32	3	28	37
MDBK	16	3,1	4,8	6	5,2	5,7	3
NS20Y	57	11	4,4	4,7	3,6	4	287
HEK 293T	18	0,39	1,2	1,1	4,8	0,69	10
MHH-NB11	72	5,4	8,8	4,2	8,3	4,4	32
DK-MG	33	3,2	9,4	4,5	5,0	3,0	7
HEp2	92	72	69	77	88	66	6
HepG2	32	0,88	2,1	2,7	12	1,2	19
Huh7	19	1,7	1,7	2,4	8,8	0,69	15
Vero	76	1	5,6	9,0	6,2	4,3	11

RL-LU x 10^9

Fig. 10: Growth of SAD RL-IRES-FL.
Replication of SAD RL-IRES-FL on BSR T7/5 cells. BSR T7/5 cells were infected with the indicated viruses at a MOI of 0.1 (A) or a MOI of 3 (B). Infectious virus titers in the supernatants (A) or absolute light units of renilla luciferase (RL-LU) (B) were determined at the indicated time points. (C, D) Replication of reporter viruses in different cell lines. Indicated cell lines were infected with SAD RL-PV-FL (C) and other SAD RL-IRES-FL viruses (D) at a MOI of 3, 48 h p.i. Absolute values of renilla light-units (RL-LU) were measured. Error bars indicate standard deviation. Highlighted boxes indicate the lowest and the highest values.

This alternative method to check viral replication, namely by RL expression from reporter viruses, was in addition used to analyze replication of the reporter viruses in different cell lines. To this end, diverse cell lines from different origin were infected with SAD RL-IRES-FL and RL expression was measured 48 h p.i. (Fig.10C,D). The replication of different reporter viruses varied by two $\log_{10}$ RL-LU in NIH 3T3 and NS20Y cells (Fig. 10D). Also the comparison of RL expression by the same reporter virus between different cell lines (Fig. 10C, D) showed differences of max. 2.5 $\log_{10}$. These data confirm that RV is able to infect and replicate in different cell types. Furthermore these results demonstrate the applicability of the new RV-based dual luciferase system on different cells.

These experiments demonstrate first, that RL expression by the reporter viruses reflects their replication in different cell lines. Furthermore they allow us to use RL expression as a marker for virus replication in diverse cell lines. Second, we could confirm that the recombinant reporter viruses are capable to infect and to replicate different cells, which can be measured either by viral titers or by reporter gene expession. By these findings we are able to use RL expression for normalization of IRES-dependent FL translation, to make sure that differences occurring in FL expression are not based on changes in viral replication. Due to the fact that SAD RL-PV-FL replication (RL expression) shows the lowest variability among diverse cell lines (Fig. 10C), in the following experiments all IRES activities are related to SAD RL-PV-FL (set as 100%).

3.1.1.4. Activity of viral IRES elements in different cell lines

Depending on their structure, the mechanisms to initiate translation and the dependence on additional factors, IRES elements are grouped into different groups and types. It is known that there are differences in the activity of diverse IRESs. Until now, IRES activities were determined by plasmid based reporter assays, whose drawbacks were discussed above. Also another method, which makes use of chimeric picornaviruses with exchanged IRES elements, harbors disadvantages. 5'UTRs of positive strand RNA viruses are known to be essential not only for virus gene expression but also for virus replication. Therefore, results obtained for IRES activities by those systems might be influenced by effects on virus replication rather than translation initiation, possibly compromising the results, achieved by systems, using chimeric picornaviruses. None of these systems is capable to reveal the exact activity of IRESs in terms of translation initiation. In order to circumvent shortcomings of common reporter systems, we used the newly generated RV based dual luciferase system to quantify IRES activities. Analyses included quantification of activities of picornaviral IRES elements

belonging to type I (PV, HRV2), type II (FMDV), and flaviviral IRESs (BVDV, CSFV, HCV), as well as the elucidation of possible cell specific features.

In order to measure the ability of IRES elements to initiate translation, expression of firefly luciferase was determined in cell lines from non-primate (Fig. 11A) and primate (Fig. 11B) origin, infected with SAD RL-IRES-FL reporter viruses. IRES activities were quantified by normalizing IRES-dependent FL activity to 5'cap-dependent RL activity. As before, the FL/RL ratio was related to SAD RL-PV-FL (set as 100%). Of the picornaviral IRES elements (PV, HRV2 and FMDV) the PV IRES showed the highest activity in all cell lines tested, followed by the HRV2 IRES. The lowest value for picornaviral IRES dependent translation initiation was obtained by the FMDV IRES. This relative activity of picornaviral IRESs stayed similar in all tested cell lines, indicating a gradient of IRES activities of PV>HRV2>FMDV.

A comparable pattern was also visible in activities of flaviviral IRESs (BVDV, CSFV, HCV). Here, the HCV IRES initiated internal translation the best, whereas CSFV IRES activity was lower in all cell lines and BVDV IRES activity was often at detection limits. Like in case of picornaviral IRESs, the activities of flaviviral IRES elements showed high variations from one cell type to the other (e.g. HCV IRES, presenting 21% of the PV IRES activity in Vero and 505% in HEp2 cells). Although we observed variations in IRES activities according to the cell lines, no cell or species specificity was apparent.

These experiments confirm the functionality of the newly established RV-based dual luciferase system for the quantification of activities from three types of viral IRES elements. With this system we could show that all tested IRES elements are active in various cell types of different origins. None of the IRESs is restricted to a special cell type. Irrespective of the cell type a general activity gradient was observed, being: PV>HRV2>FMDV and HCV>CSFV>BVDV, respectively. For further investigations, we decided to take a closer look at the picornaviral IRES elements.

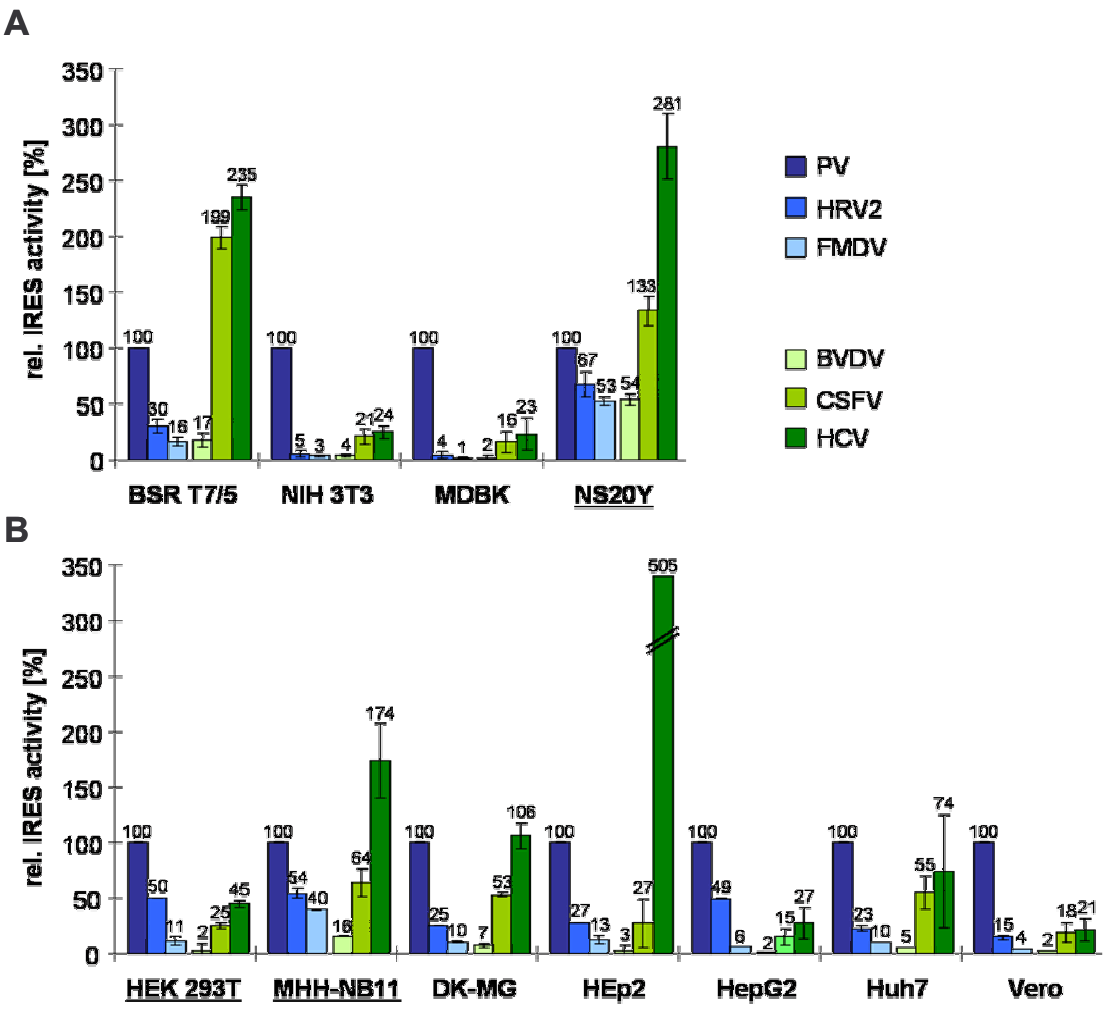

Fig. 11: Quantification of IRES activities by SAD RL-IRES-FL.
Cell lines from non-primate (A) and primate species (B), including cells of neuronal origin (underlined) were infected with the recombinant SAD RL-IRES-FL reporter viruses containing the IRES of PV, HRV2, FMDV, BVDV, CSFV and HCV. At 48 h p.i. cells were lysed and subjected to the dual luciferase reporter system. The activity of FL to RL of SAD RL-PV-FL was set to 100%. One representative experiment including data for every cell line from three parallel infections is shown. Error bars indicate standard deviation.

3.1.1.5. No effect of viral 3'UTRs on IRES activities within SAD RL-IRES-FL

In the original viral context IRES elements are situated close to the 5'end of the viral genome. For members of the family of *Picornaviridae* it is known that sequences in the 3'end are associated with the 5'UTR, forming a quasi-circular structure, which is essential for efficient viral replication (Pelletier et al., 1988). We investigated if these sequences within the 3'UTR of the viral genome are also necessary for a full functionality in internal translation initiation of IRES elements and whether they have an influence on cell specificity. Specifically, we tested the influence of the 3'UTRs from PV and HRV2 on PV and HRV2 IRES activities within SAD RL-IRES-FL. Recombinant SAD RL-IRES-FL-3'UTR RVs were generated by insertion of the 3'UTR of PV or HRV2 downstream of the FL ORF in the SAD RL-IRES-FL background (Fig. 12A).

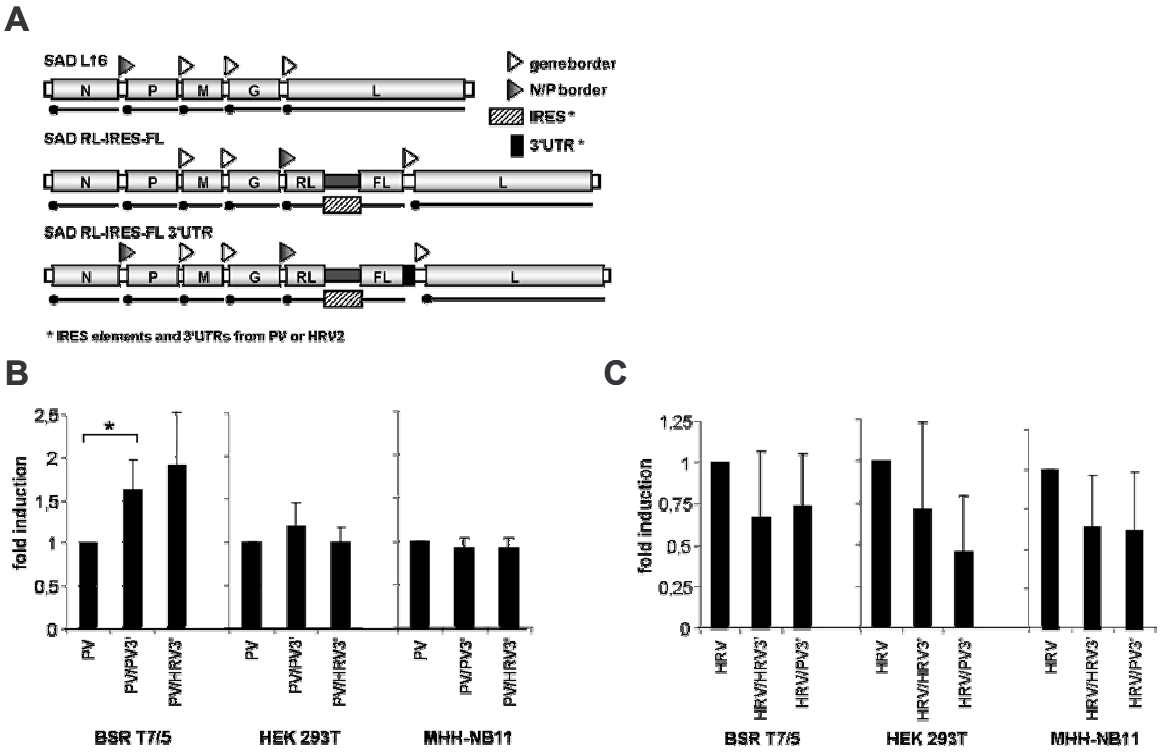

Fig. 12: Influence of different 3'UTRs on IRES activities.
(A) cDNA organization. The original 3'UTRs of PV and HRV2 were inserted downstream of the coding region for FL. Influence of 3'UTRs on PV IRES (B) and HRV2 IRES (C) activity. BSR T7/5, HEK 293T and MHH-NB11 cells were infected with the indicated viruses at a MOI of 3. 48 h p.i. cells were lysed and subjected to the dual luciferase assay. The ratio of FL/RL of SAD RL-PV-FL (B) or SAD RL-HRV2-FL (C) was set as 1 in every cell line. One representative experiment out of at least three independent experiments is shown, including data for every cell line from three parallel infections. Error bars indicate standard deviation.
* $p<0.05$ (t-test).

BSR T7/5, HEK 293T and MHH-NB11 cells were infected with the recombinant reporter viruses and IRES activities were measured by the dual luciferase assay 48 h p.i. Relative IRES activities were quantified by normalizing FL to RL expression and setting the FL/RL ratio of SAD RL-PV-FL (Fig. 12B) or SAD RL-HRV2-FL (Fig. 12C) respectively, as 1.

In general no significant influence of the 3'UTRs on the PV IRES activity (Fig. 12B) and on the HRV2 IRES activity (Fig. 12C) could be observed in any of the cell lines tested ($p\geq0.05$). Only PV IRES activity in BSR T7/5 cells was slightly elevated (1.5 fold) in presence of the PV 3'UTR ($p<0.05$) (Fig. 12B).

These data indicate that the PV IRES activity can be enhanced by the PV 3'UTR only to minimal extent. Exept of this minor effect, no significant differences in PV and HRV2 IRES activities could be observed depending on a 3'UTR. Moreover, the presence of a 3'UTR has no influence on the cell specificity of IRES elements, as none of the effects was apparent only in one certain cell type. As there is no general, significant effect of 3'UTRs on picornaviral IRESs 3'UTRs were not included in the SAD RL-IRES-FL system in further experiments.

3.1.1.6. An altered start codon context does not change relative IRES activities

The exact mechanism, how IRES elements place ribosomes onto the right start codon, is not fully understood. Two possibilities are discussed. First, ribosomes could be positioned directly onto the start codon at the RNA by a defined secondary structure of the IRES element. Second, ribosomes could be "caught" by the IRES elements, which then "scan" the RNA until they reach the start codon, similar as in 5'cap-dependent translation initiation. Depending on which of both possibilities applies, the surrounding of the start codon would have an impact on the efficiency of translation initiation. To investigate how changes in the start codon context of our system influence IRES activities, recombinant SAD RL-IRES-FL reporter viruses were generated, which contained a single AUG (SAD RL-IRES-FL_OATG) or two AUGs. The two AUGs were either separated by six nucleotides, such that they were in frame (SAD RL-IRES-FL_IF), or by seven nucleotides, to cause an out of frame context (SAD RL-IRES-FL_OF) (Fig. 13A).

Growth characteristics of SAD RL-IRES-FL_OATG on BSR T7/5 cells at 48 h p.i. were similar to those of the parental RV SAD L16, and to a virus transcribing an extra monocistronic gene downstream of G (SAD G eGFP). Maximal infectious titers of 1-2 x 10^8 ffu/ml at 48 h p.i. were obtained (Fig. 13B). Next we quantified activities of PV, HRV2 and FMDV IRES elements in the three different start codon contexts. Hence, different cell types were infected with the SAD RL-IRES-FL reporter viruses and relative IRES activities were measured by normalizing FL to RL expression and relating the FL/RL ratio to SAD RL-PV-FL_OATG (set as 100%) (Fig. 13C).

In all cell lines tested (except of HepG2 cells), PV IRES activities were highest in a reporter construct, which contains only one start codon (SAD RL-PV-FL_OATG). In constructs, which contain two AUGs in-frame (SAD RL-PV-FL_IF) or out of frame (SAD RL-PV-FL_OF), PV IRES activities were reduced. An out of frame context led to lowest PV IRES activities in all cells, being 48% to 15% compared to PV IRES activities in OATG context. This effect was observed in all cell lines, such that a cell specific influence on start codon selection seems not to exist.

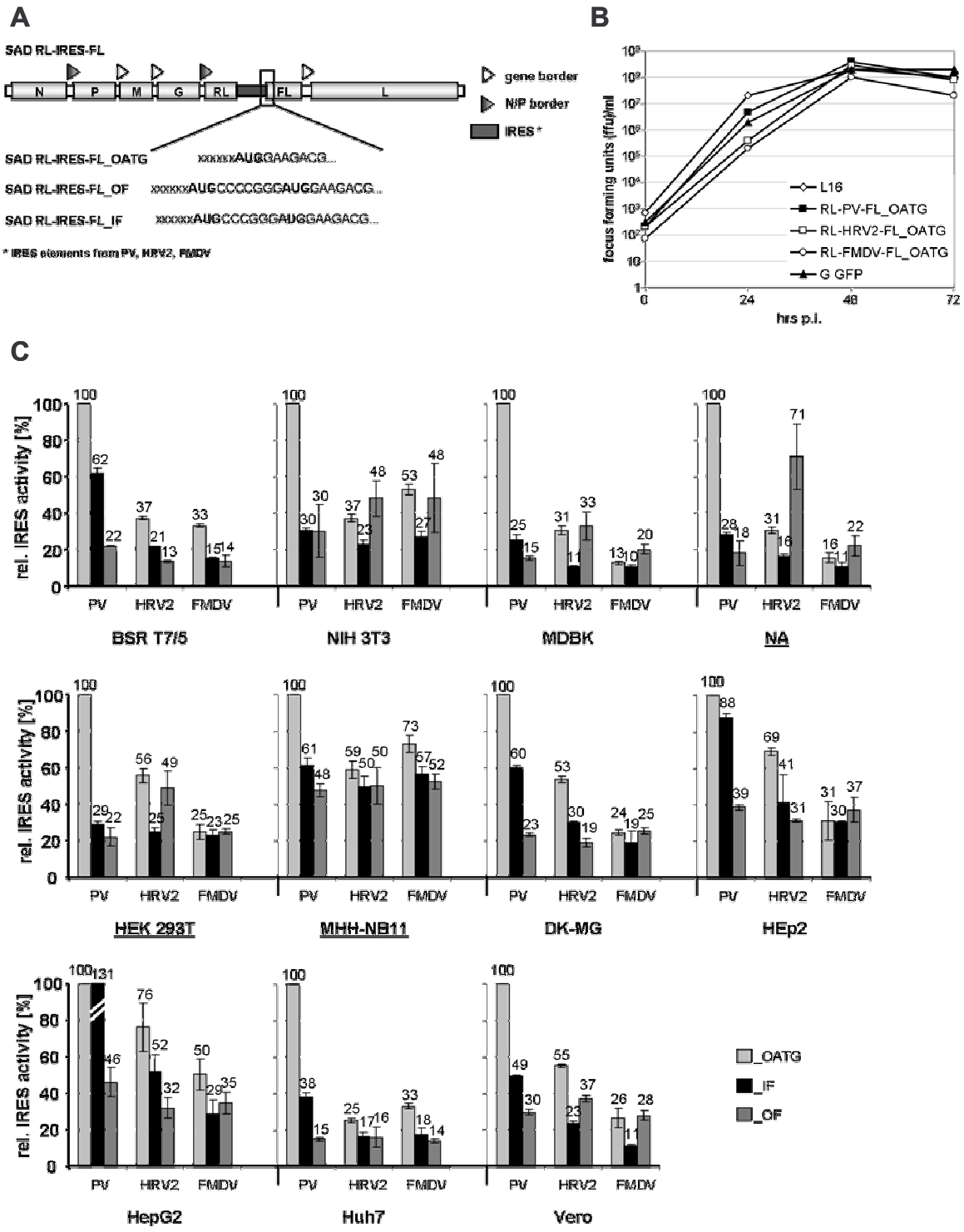

Fig. 13: SAD RL-IRES-FL reporter viruses with changes in the start codon context.
(A) SAD RL-IRES-FL viruses were generated, which contain only the AUG of the FL downstream of the IRES elements of PV, HRV2 or FMDV (SAD RL-IRES-FL_OATG). The other viruses contain two AUGs, which were either separated by seven nucleotides, such that the AUGs were out of frame (SAD RL-IRES-FL_OF) or separated by six nucleotides, leading to an in frame-context of the AUGs (SAD RL-IRES-FL_IF). (B) Growth of SAD RL-IRES-FL_OATG. BSR T7/5 cells were infected with the indicated viruses at a MOI of 0.1 and infectious virus titers were determined at the indicated time points. As a control, a virus, containing GFP as an additional gene between G and L (SAD G GFP) was used. (C) IRES activities in virus infected cells. Indicated cell lines were infected with SAD RL-IRES-FL-OATG (light grey), _IF (black), _OF (dark grey) at a MOI of 3. 48 h p.i. cells were lysed and subjected to the dual luciferase assay. The activity of FL to RL of SAD RL-PV-FL_OATG in every cell line was set to 100%. One representative out of at least three independent experiments is shown, including data for every cell line from three parallel infections. Error bars indicate standard deviation.

Results with reporter viruses, containing the HRV2 IRES were not as clear as with the PV IRES reporter viruses. Only in four of the eleven cell lines tested, HRV2 IRES activities were highest in reporter viruses with only one AUG (SAD RL-HRV2-FL_OATG). In the other cells, reporter viruses, which contain two AUGs in out of frame context (SAD RL-HRV2-FL_OF) showed comparable or even better firefly expression than reporter viruses containing only one AUG (SAD RL-HRV2-FL_OATG). Firefly expression from SAD RL-HRV2-FL_IF was never higher than in SAD RL-HRV2-FL_OATG. Compared to the PV IRES the HRV2 IRES performed worse in all cell lines (exept HepG2) in recombinant reporter RVs, which contain only one AUG or two in frame AUGs. Reporter gene expression from SAD RL-HRV2-FL_OF was similar or better than SAD RL-PV-FL_OF.

A different picture was apparent in case of the FMDV IRES. It is known that FMDV IRES efficiently initiates translation from a second, downstream AUG (Lopez and Martinez-Salas, 1999). Major differences were not evident for the IRES activities in the OATG-, IF- and the OF-viruses. Indeed, in most cell types, FL activity in OF-context was greater or equal to that in OATG-context. In addition, IRES activities in OF-context were greater than in IF-context.

Taken together, all three picornaviral IRES elements show stable activity when translation initiation is limited to just one start codon (OATG). The presence of a second AUG impedes translation initiation of the PV IRES, which is not the case for the HRV2 and the FMDV IRES in most cells. When the two AUGs are out of frame, the FL expression is even lower in case of the PV IRESs, since a functional FL can be translated only from the second start codon. In contrast, translation initiation by the FMDV IRES is similar in both IF- and OF-context, in most cell lines. Thus a general mechanism of start codon selection by different picornaviral IRES elements could not be elucidated by the reporter viruses, used here. However, we could demonstrate that levels of firefly expressed from all constructs depended on the used IRES element and did not appear to be cell-type dependent.

3.1.1.7. IRES activities quantified by the optimized new RV based dual luciferase system

From the previous experiments, including several variations and optimizations, it is obvious that the newly established RV based dual luciferase system is suitable for the quantification of various IRES elements. This optimized system (OATG) was used to once more compare different IRES activities in various cell types from different origin and in order to investigate possible cell specific phenotypes (Fig. 14).

A

	PV	HRV	FMDV
BSR T7/5	116	820	135
BHK21	43	110	37
NIH 3T3	4	11	6
MDBK	15	3	2
NS20Y	14	38	13
HEK 293T	16	29	22
MHH-NB11	17	26	18
DK-MG	15	29	26
HEp2	32	82	38
HepG2	133	2150	170
NA	24	37	26
Vero	27	46	30

RL-LU x 10^6

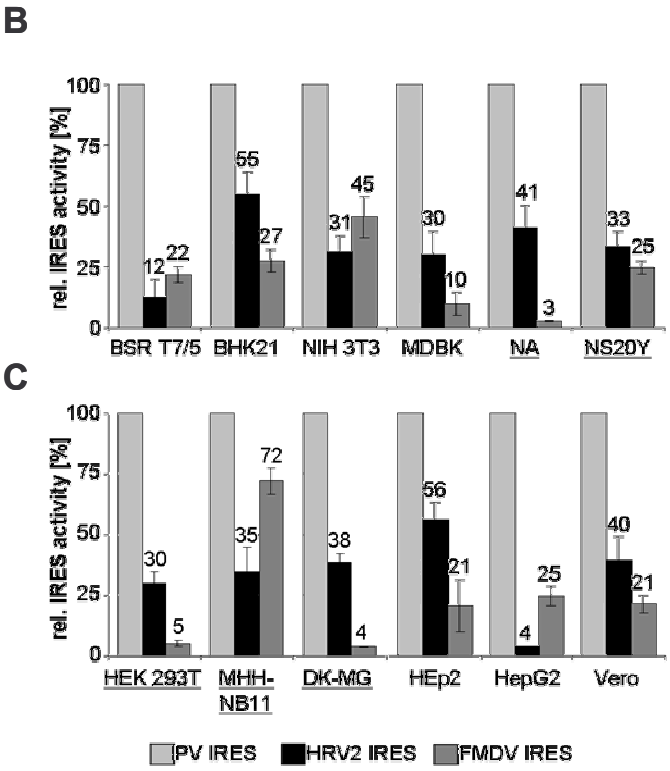

Fig. 14: Quantification of IRES activities measured with SAD RL-IRES-FL_OATG.
(A) Replication of reporter viruses in different cell lines. Indicated cell lines were infected with SAD RL-IRES-FL viruses at a MOI of 3 and 48 h p.i. RL-LU were measured. Highlighted boxes indicate the highest or lowest RL-LU values, respectively. Cell lines from non-primate species (B) and of primates (C), including cells of neuronal origin (underlined) were infected with the recombinant SAD RL-IRES-FL_OATG reporter viruses containing the IRES of PV (light grey), HRV2 (black), or FMDV (dark grey). At 48 h p.i. RL and FL activities were measured using the dual luciferase reporter system. The activity of FL to RL determined for SAD RL-PV-FL was set to 100%. Data for every cell line are from at least two independent experiments each including three parallel infections. Error bars indicate standard deviation.

Diverse cell lines were infected with the SAD RL-IRES-FL_OATG reporter viruses and subjected to the dual luciferase assay. Relative IRES activities were quantified by normalizing FL to RL expression and relating the FL/RL ratio to SAD RL-PV-FL (set as 100%) in every cell line. As described before, RL activities reflect the overall virus replication. RL expression between cell lines ranged from 2 x 10^6 RL-LU in bovine MDBK cells to 2 x 10^9 RL-LU in the human hepatoma cell line (HepG2). This range of 3 $\log_{10}$ is likely to be due to the capacity of RV to replicate in the diverse cell lines and to minor extent to differences in the amount of measured cell extracts, because of different size and confluency of diverse cell types. The highest variation between viruses within one cell line was only one $\log_{10}$, observed in human HepG2 cells. This reflects a relative stable replication of different viruses within a given cell line. Replication of RV is supported especially well in BSR T7/5, HEp-2 and HepG2 cells, whereas it is impaired in NIH 3T3 and MDBK cells (Fig. 14A).

The characterization of the HRV2 IRES was of particular interest, because of its proposed neuronal cell specific restrictions (Gromeier et al., 1996; Merrill and Gromeier, 2006; Merrill et al., 2006). While the HRV2 IRES was less active than the PV IRES in all cells tested, specific defects in neuronal cells were not confirmed. Rather, the HRV2 IRES was noticeably active in cells of neuronal origin, such as the the mouse NA cells (41% of PV IRES activity, respectively) (Fig. 14B). In human MHH-NB11 and murine NS20Y cells both IRES elements performed poorly in absolute values, but in comparison to PV, the HRV2 IRES still showed 35% and 33% activity, respectively (Fig. 14B). Also in human HEK 293T cells, which were claimed to be of neuronal origin (Shaw et al., 2002), the HRV2 IRES showed activity of 30% compared to PV IRES. In non-neuronal cells HRV2 IRES activity showed a broad range of 4% to 56% of the PV IRES, with no species- or organ specific influence detectable.
Thus, these data do not support the reported specific restriction of HRV2 IRES translation initiation activity in neuronal cell types. Rather they indicate an intrinsic low activity of the HRV2 IRES compared to the PV IRES, irrespective of the cell line.
In most cell lines tested, the FMDV IRES showed the least activity with the construct used here.

3.1.2. Generation of a virus-based reporter system for characterization of IRES elements on single cell level using eCFP as a reporter gene

3.1.2.1. SAD IRES eCFP reporter RVs

The use of different reporter genes for IRES activity was previously reported to yield diverse outcomes (Hennecke et al., 2001). To ensure that the results we obtained with our newly established dual luciferase reporter system do not depend on the identity of the firefly reporter gene, additional reporter RVs were constructed. The use of a fluorescent protein as a reporter should furthermore allow the proof of the obtained results on single cell level. A RV-based reporter system was generated, using eCFP (enhanced cyan-fluorescent protein) as a reporter gene for the characterization of IRES elements. For generation of recombinant SAD IRES eCFP RVs, viral or cellular IRES elements and the downstream eCFP reporter gene were inserted into the 3’ non-coding region of RV G. Specifically, IRESs from PV, HRV2, FMDV, CSFV, HCV and HCV del (a HCV IRES deletion mutant) were used. As a potential candidate for a cellular IRES element we tested two forms of the 5’UTR of the cellular p27 mRNA, predicted to contain an IRES. In addition, a control virus was generated comprising eCFP as

an additional gene between the coding regions of RV G and L under control of an additional copy of the N/P gene border (SAD N/P eCFP) (Fig. 15A).

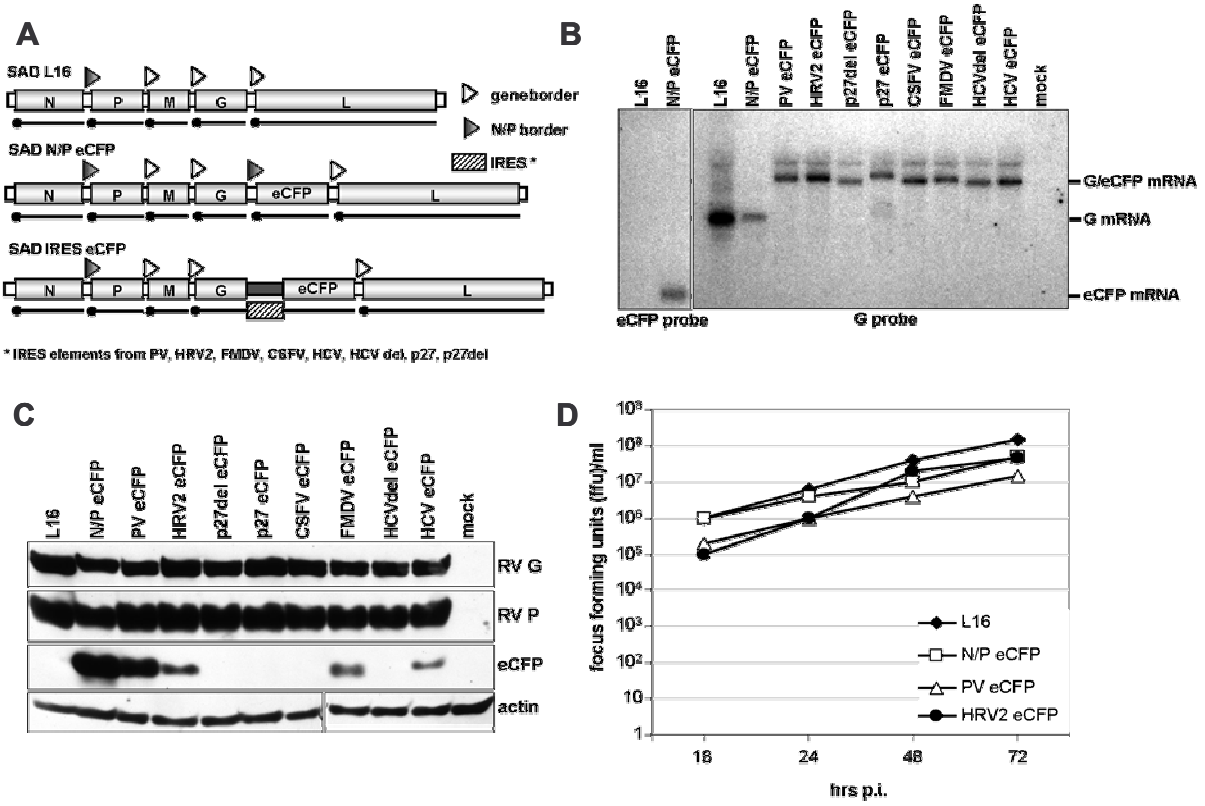

Fig. 15: Generation of SAD IRES eCFP reporter viruses.
(A) Organization of SAD IRES eCFP. SAD IRES eCFP reporter viruses were generated by inserting IRES elements of PV, HRV2, FMDV, CSFV, HCV, a deletion mutant of HCV (HCV del) and two forms of the predicted p27 IRES and the downstream eCFP reporter gene into the 3‘ non-coding region of the G mRNA. The control virus SAD eCFP (N/P) contains an additional N/P geneborder upstream of eCFP. (B) Transcription of bicistronic G/eCFP mRNAs (SAD IRES eCFP) instead of two individual monocistronic mRNAs (SAD N/P eCFP) analyzed by Northern Blot experiments with RNA isolated from virus-infected BSR T7/5 cells. (C) 5’cap-dependent translation of RV G and P compared to IRES-dependent expression of eCFP investigated by Western Blots with lysates from BSR T7/5 cells, infected with a MOI of 3 at 48 h p.i. (D) Growth of SAD IRES eCFP. BSR T7/5 cells were infected with the indicated viruses at a MOI of 0.1 and infectious supernatant virus titers were determined at the indicated time points.

Northern Blot experiments with RNA from infected BSR T7/5 cells were performed and probed against sequences of RV G and eCFP (Fig. 15B). Instead of two monocistronic mRNAs for RV G and eCFP, as it was the case in the control virus (SAD N/P eCFP), SAD IRES eCFP viruses transcribe only one bicistronic G/eCFP mRNA. From wt SAD L16 solely the G mRNA is transcribed. In addition to the band for G/eCFP mRNA, a slightly larger band appeared, most likely representing an M-G/eCFP readthrough mRNA. Western Blot experiments demonstrated that from the bicistronic mRNA in SAD IRES eCFP infected BSR T7/5 cells both RV G and eCFP were expressed (Fig. 15C). The expression of the glycoprotein, which is translated 5’cap-dependently, from all viruses, including SAD L16,

depends only on the replication status of RV. In contrast, expression levels of eCFP differed relative to the activity of the used IRES element. No or little eCFP could be detected in cells infected with reporter viruses containing the IRES elements of CSFV and HCVdel. Also the 5'UTR of the cellular p27 mRNA did not support expression of eCFP, indicating no or only very little activity in translation initiation (Fig. 15C).

The expression of a bicistronic mRNA, the presence of IRES elements, or expression of eCFP might have an influence on the virus replication in general. In order to exclude this, multi-step growth curves were performed on BSR T7/5 cells with some of the SAD IRES eCFP viruses in comparison to SAD L16 and the control virus SAD N/P eCFP (Fig. 15D). All tested viruses were able to replicate, indicating that IRES elements or the additional bicistronic mRNA in the reporter viruses have no great attenuating effect on the overall virus replication.

Thus, we were able to generate a second eCFP reporter system based on rabies virus. These recombinant IRES eCFP reporter viruses transcribe a bicistronic mRNA from which the RV glycoprotein is expressed 5'cap-dependently to similar levels. In contrast expression of the eCFP reporter depends on the activity of the inserted IRES element.

3.1.2.2. IRES-dependent eCFP expression in different cell lines

With the SAD IRES eCFP reporter RVs we aimed to exclude the possibility that the identity of the used reporter gene causes artificial results and to verify the data, obtained with the RV-based dual luciferase reporter system on single cell level. Thus, eCFP expressing RVs were used to analyze the IRES activities in BSR T7/5, NA, MHH-NB11 and DK-MG cells. Western Blot analyses from cells infected with SAD IRES eCFP were performed and stained against RV P and the IRES-dependently expressed eCFP (Fig. 16).

In all four cell lines RV P was expressed to levels, which depended on the replication of the recombinant viruses. In contrast, levels of eCFP, which is translated in an IRES-dependent manner, differed dependent on the IRES element used. Differential activity of the picornaviral IRES elements was particular well visible in the hamster kidney cells (BSR T7/5) and in human glioblastoma cells (DK-MG), revealing the best activity for the PV IRES and the lowest for the IRES of FMDV (Fig. 16, see also Fig. 15C). eCFP expression mediated by the HRV2 IRES was intermediate in these cell lines. In MHH-NB11 cells eCFP expression by all IRESs was low, such that reporter gene expression by the HRV2 and the FMDV IRES was hardly detectable. Also in NA cells, eCFP expression by the PV IRES was detectable. However, in contrast to data obtained by the dual luciferase system (Fig. 14) reporter gene expression by FMDV IRES appeared to be better than the one of HRV2 IRES.

Although quantification of IRES activities after Western Blotting is not as straightforward as with the RL/FL system, approximate relative IRES activities can be observed. Thus, we could demonstrate that the RV-based eCFP reporter system is capable to visualize IRES activities in different cell lines by reporter gene expression. As for the dual luciferase reporter viruses, the relative IRES activities remained unchanged, being PV>HRV2 in all cells, irrespective of their origins.

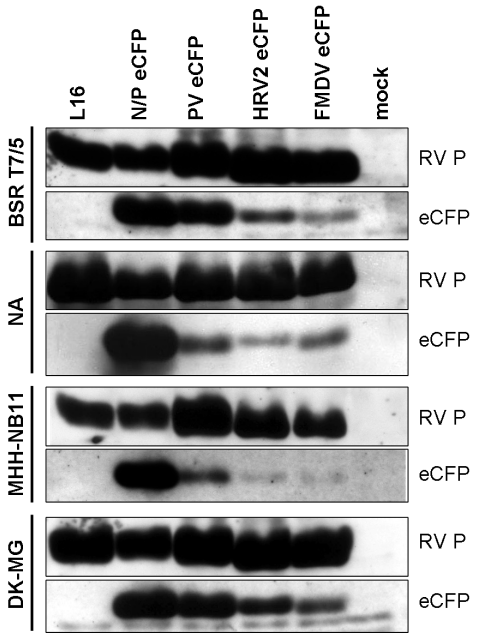

Fig. 16: IRES-dependent eCFP expression from SAD IRES eCFP.
Comparison of RV P and IRES-dependently translated eCFP analyzed by Western Blots with lysates from BSR T7/5, NA, MHH-NB11 and DK-MG cells infected with a MOI of 3 at 48 h p.i.

3.1.2.3. Quantification of eCFP expression by fluorescence microscopy

An alternative method to quantify IRES activities in the RV-based eCFP system (SAD IRES eCFP) is the measurement of eCFP fluorescence intensities. This was performed in a variety of infected cells using the confocal laser scanning microscope (LSM) Axiovert 200 including the LSM510 Metasystem (Zeiss) and the appropriate software.

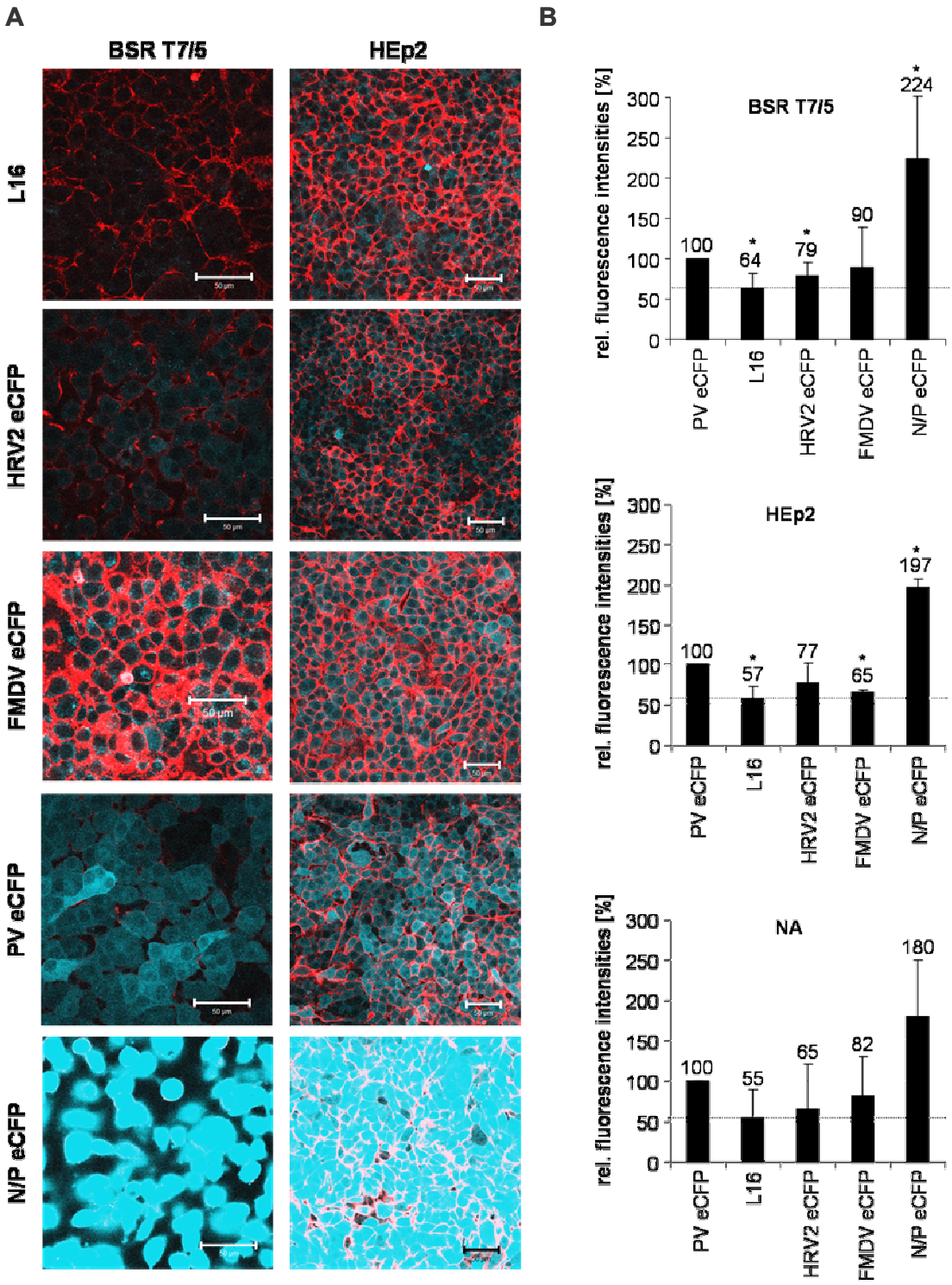

Fig. 17: Quantification of IRES-dependent eCFP expression from SAD IRES eCFP by measurement of fluorescence intensities.

(A) BSR T7/5 and HEp-2 cells were infected with the indicated viruses at a MOI of 1. 48 h p.i. cells were fixed with 3% PFA and stained against the viral glycoprotein (alexa-633, in red; eCFP shown in blue) and analyzed by confocal laser scanning microscopy. Scale bars: 50µm. (B) Calculation of relative fluorescence intensities in infected BSR T7/5, HEp2 and NA cells. Fluorescence intensities were measured using the Zeiss LSM510 Metasystem software. Measurements were carried out using optimal settings for the detection of eCFP expression in cells infected with SAD HRV2 eCFP. The fluorescence intensity of eCFP to RV G of SAD PV eCFP for every cell line was set to 100%. One representative experiment including data for every cell line from three parallel infections is shown. Error bars indicate standard deviation. Dotted lines indicate background blue fluorescent signal of SAD L16.

* $p<0.05$ (t-test).

BSR T7/5, HEp2 (Fig. 17A,B) and NA cells (Fig. 17B) were infected with SAD IRES eCFP containing the IRESs of PV, HRV2 and FMDV and with the control virus (SAD N/P eCFP). Cells were fixed, stained against the RV glycoprotein and analyzed by laser scanning microscopy (Fig. 17A). In SAD IRES eCFP infected cells, RV G appeared predominantly at the cell surface, whereas eCFP expression showed a cytoplasmic distribution (Fig. 17A). Although RV G is expressed from the same mRNA as eCFP, its expression depends solely on the viral transcription and replication. Therefore, RV G can be used for normalization of IRES-dependent translation of eCFP. For the quantification of eCFP expression, settings were adjusted, such that eCFP and RV G fluorescence were detectable in SAD HRV2 eCFP infected cells. IRES activities were calculated by normalizing fluorescence intensities of eCFP to RV G and setting the ratio eCFP/RV G of SAD PV eCFP as 100% (Fig. 17B). In spite of parallel infection at identical MOI, the replication status in the cells, represented by RV G expression, varied remarkably. Different levels of IRES-dependent eCFP expression were visible already in the microscopic images (Fig. 17A). In BSR T7/5 cells, highest eCFP fluorescence was obtained by the PV IRES and eCFP fluorescence by the HRV2 IRES was lower (79% of PV IRES), whereas the FMDV IRES showed no significant differences in eCFP expression, relative to the PV IRES. In contrast, in HEp2 cells the FMDV IRES showed 65% of eCFP expression in comparison with the PV IRES and no significant difference in reporter gene expression was apparent in case of the HRV2 IRES. In NA cells no significant differences were measurable with this method (Fig. 17B). Obvious cell specific differences, however, were not observed.

The main disadvantage of this new RV-based eCFP reporter system results from highly sensitive microscopy settings. Settings had to be adjusted in a way that detection of the low eCFP levels, expressed by the HRV2 IRES, were detectable. However these sensitive settings led to a high background in cells infected with the negative control virus SAD L16 (55-64% compared to PV IRES-dependent eCFP expression) on the one hand. On the other hand, thereby eCFP levels from the positive control virus (SAD N/P eCFP) are far beyond the linear scale and therefore are not reliable.

Taken together, the RV based eCFP reporter system for quantification of IRES activities in general confirms the results obtained by the SAD RL-IRES-FL reporter viruses on single cell level. Also with this reporter system activities are highest for the PV IRES, whereas the IRESs of HRV2 and FMDV show a lower activity. Thus, we can exclude that IRES activities, which were measured by the dual luciferase system, depend on the use of FL as a reporter gene. Nevertheless, the system is not as feasible as the RL-IRES-FL system.

3.1.2.4. 5'UTR of the cellular p27 mRNA displays only marginal activity in translation initiation

RNA elements in the 5'UTR region of several cellular mRNAs have been described to initiate translation under stress conditions when the 5'cap-dependent translation initiation is inhibited. The validity of such observations is an extensively discussed topic. One of the cellular mRNAs containing a predicted IRES element is the mRNA of the cell cycle regulator p27. Intriguingly, in the DNA-based reporter plasmid system, described above, the presence of the p27 UTR sequences led to considerable expression of the reporter gene (Fig. 8). We therefore investigated the capability of its 5'UTR region to initiate translation initiation using our two reporter systems, SAD IRES eCFP (Fig. 18A) and SAD RL-IRES-FL (Fig. 18B).

A

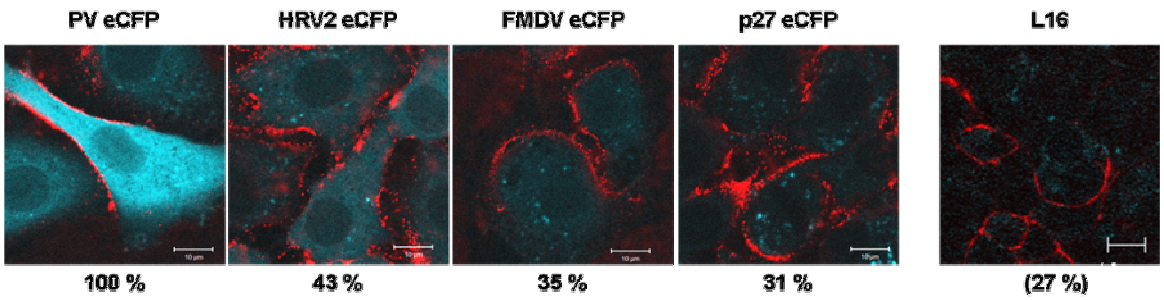

B

cell lines	BSR T7/5	Vero	HEp2
relative p27 5'UTR-dependent FL activity compared to PV IRES (100%)	3%	2%	6%

Fig. 18: Analysis of translation initiation by the 5'UTR of the cellular p27 mRNA.
(A) Analysis of internal translation initiation by the p27 5'UTR using SAD IRES eCFP reporter viruses. BSR T7/5 cells were infected with the indicated viruses at a MOI of 1. 48 h p.i. cells were fixed with 3% PFA, stained against the viral glycoprotein and analyzed by confocal laser scanning microscopy. As a comparison a picture of SAD L16-infected BSR T7/5 cells, from another experiment is included. Numbers below the pictures indicate relative eCFP fluorescence intensities (in blue), calculated by ImageJ and compared to fluorescence intensities of SAD PV eCFP (100%). (B) Quantification of internal translation initiation by the p27 5'UTR using SAD RL-IRES-FL reporter viruses. BSR T7/5, Vero and HEp2 cells were infected at a MOI of 3. 48 h p.i. cells were lysed and subjected to a dual luciferase assay. The activity of FL/RL determined for SAD RL-PV-FL for every cell line was set to 100%. Mean data from one representative out of at least three independent experiments are shown, including data for every cell line from three parallel infections.

BSR T7/5 (Fig. 18A,B), Vero and HEp2 (Fig. 18B) cells were infected with SAD p27 eCFP (Fig. 18A) or SAD RL-p27-FL (Fig. 18B) reporter viruses and IRES activities were compared to the PV IRES (set as 100%) (Fig. 18B). In both systems reporter gene expression by the 5'UTR of the cellular p27 mRNA was only at the detection limit, in case of SAD RL-p27-FL it is 2-6% of SAD RL-PV-FL in different cell lines (Fig. 18B). As in both reporter systems, values obtained were not distinguishable from background levels, the p27 5'UTR cannot be considered to act as an IRES element in this system. High values of reporter gene expression,

obtained by the plasmid-based reporter system (Fig. 8) therefore might be due to a cryptic promoter or an additional splice site within the sequence of the p27 5'UTR, rather than due to an internal translation initiation activity. However it also might be that the p27 5'UTR requires interaction with specific RNA binding proteins in the nucleus to act as an IRES, which is not given with our RV-based systems.

3.1.2.5. No induction of IFN by IRES elements within the RV genome

IRES elements form stable secondary structures including regions of dsRNA, which are recognized by the innate immune system, e.g. by the RNA helicases RIG-I or MDA5, or by toll-like receptor (TLR) 3 (Rieder and Conzelmann, 2009), leading to the induction of IFN. As in further experiments IRES elements were used to attenuate RV replication and virulence and to change the virus' ability to counteract the innate immune system, it was necessary to rule out the possibility that the insertion of IRES elements into the RV genome induces IFN. For that reason, IFN induction by different recombinant rabies viruses was compared in an IFN induction reporter gene assay.

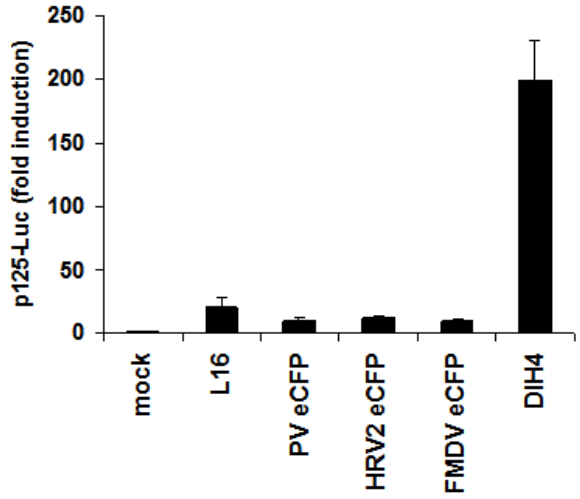

Fig. 19: Influence of IRES elements on induction of type I IFN.
HEK 293T cells were transfected with an IFNβ promoter-controlled reporter plasmid (p125-Luc) and infected at a MOI of 1 with the indicated viruses. 24 h p.i. cells were lysed and subjected to the dual luciferase reporter assay. The ratio of FL-LU and RL-LU,expressed from a co-transfected pCMV-RL plasmid, was compared to the mock infected control, set as one. As a control, DIH4, a Sendai virus defective interfering particle preparation, shown to be a potent IFN inducer, was used. One representative experiment out of at least three independent experiments is shown, including data from three parallel experiments. Error bars indicate standard deviation.

HEK 293T cells were transfected with a reporter gene plasmid from which FL is expressed under control of the IFNβ promoter (p125-Luc), infected with different recombinant rabies viruses and subjected to the dual luciferase assay. IFNβ promoter-driven firefly luciferase activity was quantified by normalizing FL expression to RL, which was constitutively expressed from a co-transfected pCMV-RL plasmid, and relating the FL/RL ratio to mock infected cells. Compared to the positive control DIH4, a Sendai virus defective interfering particle preparation, shown to be a potent IFN inducer (Strahle et al., 2006), FL activity by wt RV SAD L16 was very low, due to the expression of the viral phosphoprotein as an IFN

antagonist. Like wt RV SAD L16, the recombinant reporter viruses (SAD IRES eCFP) containing different IRESs did not activate the IFNβ promoter (Fig. 19).
These data indicate that type I IFN is not induced by the insertion of IRES elements into the RV genome, when expression levels of viral P are not affected.

3.2. Use of IRES elements to regulate rabies virus replication

3.2.1. Attenuation of RV by picornaviral IRES elements

3.2.1.1. Generation of recombinant SAD IRES-P viruses

In order to control expression of RV genes and to render replication of RV dependent on the specific translation activity of IRES elements, we used the IRES elements of PV and HRV2. The RV phosphoprotein was considered as the most promising target. It is necessary for replication in two ways. First, it is the essential co-factor of the viral polymerase (L). Second, it acts as a chaperone for encapsidation of viral RNA (Curran and Kolakofsky, 2008; Curran et al., 1995; Horikami et al., 1992). Furthermore, RV P potently counteracts type I IFN induction by targeting IRF3 and IRF7 phosphorylation (Brzozka et al., 2005) and JAK/STAT signaling of type I and type II IFN by preventing translocation of phosphorylated STATs to the nucleus (Brzozka et al., 2006). Thereby, RV P strongly interferes with the establishment of an antiviral state. Thus, attenuation of P expression should not only attenuate viral mRNA synthesis and virus replication, but also increasing the degree of the host IFN response in IFN-competent systems and diminish the resistance of RV to IFN.
Recombinant SAD IRES-P viruses were generated in which the authentic N/P gene border comprising the transcriptional stop/restart signal sequences was replaced by the IRES elements of PV and HRV2 (Fig. 20). In order to obtain viable virus, P must be translated from the bicistronic mRNA in an IRES-dependent manner, whereas RV N is expressed 5'cap-dependently. Recombinant viable viruses SAD PV-P and SAD HRV2-P were rescued by standard procedures (Schnell et al., 1994) indicating that P was synthesized at levels sufficient to support autonomous virus replication. Transcription of bicistronic N-P mRNAs from the recombinant RVs was confirmed by Northern Blot experiments with RNA from infected BSR T7/5 cells. In both cases, an RNA species of 3 kb comprising N and P sequences was present in infected cells, whereas the typical monocistronic N and P mRNAs of wt RV (SAD L16) were not detectable (Fig. 20B). Western Blot experiments from

SAD IRES-P infected BSR T7/5 cells, revealed that P protein is expressed in virus infected cell cultures (Fig. 20C). As determined by fluorescence imaging and compared to wt SAD L16, which expresses P from a monocistronic, capped mRNA (100%), P accumulated to 56% in SAD PV-P infected cells, and to 34 % in SAD HRV2-P infected cells at 48 h p.i. (Fig. 20C). This confirmed the previously observed lower activity of the HRV2 IRES, in reporter gene experiments. Notably, the reduced levels of P did not greatly affect expression of other virus proteins, as indicated by a less pronounced reduction of N protein levels (Fig. 20C).

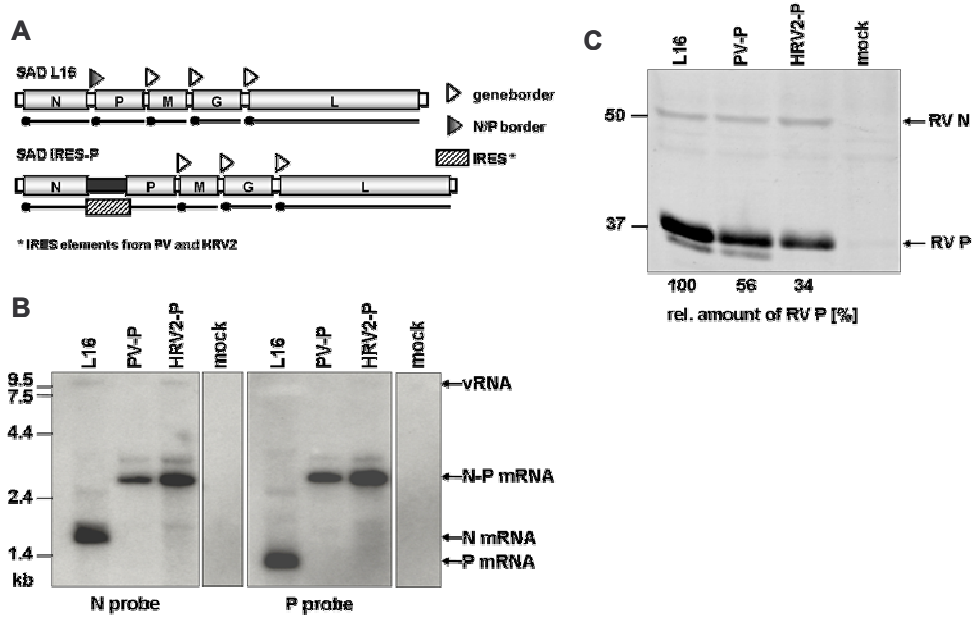

Fig. 20: IRES-dependent expression of RV P.
(A) Organization of SAD IRES-P. For generation of SAD IRES-P, the transcription signal sequences of the N/P gene border were substituted by the IRES elements of PV and HRV2 such that a bicistronic N-P mRNA is transcribed and P protein expression depends on internal translation initiation by the IRES elements. BSR T7/5 cells infected with the indicated RV were analyzed 48 h p.i. by Northern (B) and Western Blotting (C). Amounts of P protein relative to RV N were quantified and related to P protein levels of SAD L16 (100%) (C).

Thus, we could generate recombinant rabies viruses (SAD IRES-P) expressing the phosphoprotein from a bicistronic N-P mRNA in an IRES-dependent manner. Consistent with the results for PV and HRV2 IRES activities obtained by the reporter systems, P levels translated by IRES elements from PV and HRV2 are reduced to 56% and 34%, respectively, compared to wt RV (SAD L16). Thereby, we were able to demonstrate for the first time that it is possible to control expression of an essential protein from a negative strand RNA virus on translational level by the use of picornaviral IRES elements.

3.2.1.2. Attenuated growth kinetics of SAD IRES-P

As mentioned before, RV P plays an important role in virus replication, as an essential polymerase cofactor and being involved in the encapsidation of newly synthesized RNA. To investigate the impact of reduced P translation by SAD IRES-P on the overall replication of the viruses *in vitro*, multi-step growth curves were performed in BSR T7/5 cells, which do not produce type I IFN in response to virus infection, as well as in IFN-competent NA cells (Fig. 21).

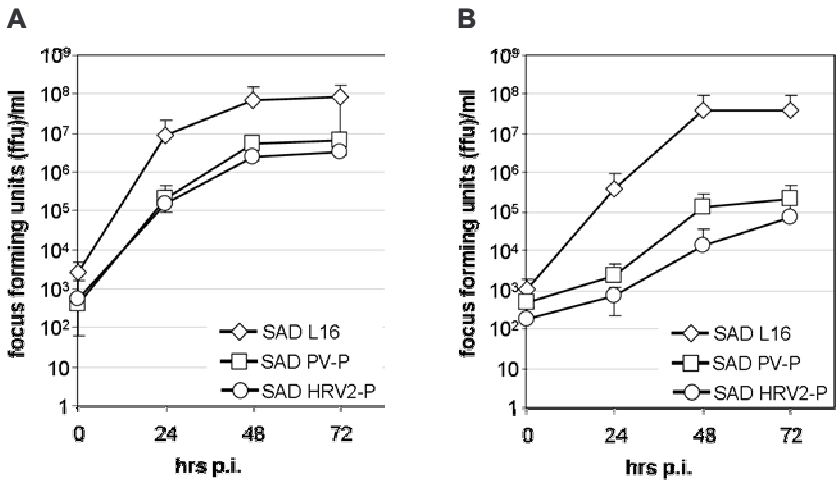

Fig. 21: Growth of IRES-controlled RV in cell culture.
IFN-incompetent BSR T7/5 cells (A) and IFN-competent NA cells (B) were infected with the indicated viruses at a MOI of 0.1 and infectious supernatant virus titers were determined at the indicated time points. Titers for every time point are from at least three independent experiments. Error bars indicate standard deviation.

Growth kinetics on BSR T7/5 cells revealed a ten- and twenty-fold reduction of peak infectious virus titers for SAD PV-P and SAD HRV2-P, respectively (Fig. 21A). These results corroborate the correlation of specific IRES translational activity, levels of P protein, and virus RNA synthesis in an IFN-deficient system. In the IFN-competent cell line, mouse NA cells (Fig. 21B), a further reduction of greater than one $\log_{10}$ for both SAD PV-P and SAD HRV2-P was observed. This indicates a further attenuation of virus growth by the IFN system of the host cells, due to reduced levels of the IFN antagonist RV P.

These data indicate that reducing translation initiation of RV P by picornaviral elements leads to attenuation of viral growth kinetics in IFN-incompetent BSR T7/5 cells due to diminished expression of the polymerase cofactor and encapsidation chaperone RV P. The function of the phosphoprotein as the main IFN antagonist of rabies virus becomes clear by growth curves in IFN-competent NA cells, where viral growth of SAD IRES-P is further reduced. Thus, translational control of RV P by picornaviral IRES elements leads to attenuation of viral replication at multiple steps of the viral life cycle.

3.2.1.3. Genome stability of SAD IRES-P

For rhabdoviruses it was shown that dispensable and neutral sequences, which were introduced into the viral genome, are stable for over 25 virus passages (Mebatsion et al., 1996b). This phenomenon can be explained in part by the poor recombination rate of rhabdoviruses, most likely due to the tight RNP complex, protecting the RNA. However, after manipulations interfering with the virus amplification revertants can occur (Wertz et al., 2002; Mebatsion et al., 1996b). As recombinant SAD IRES-P viruses are impaired in virus replication, genome stability had to be investigated. Therefore, virus containing supernatants from BSR T7/5 cells, infected with SAD PV-P or SAD HRV2-P were passaged every two to three days onto fresh BSR T7/5 cells.

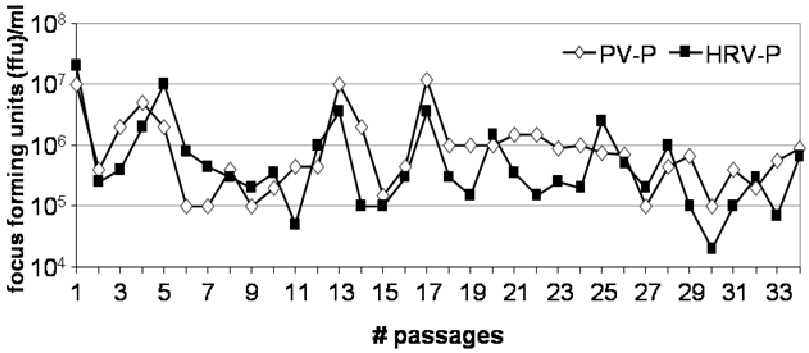

Fig. 22: Long term passages of SAD IRES-P.
BSR T7/5 cells were infected with SAD PV-P or SAD HRV2-P at a MOI of 1. Every two to three days viral supernatant was passaged onto fresh BSR T7/5 cells and virus titers were determined.

Infectious supernatant titers (Fig. 22) and nucleotide sequences of the IRES elements were determined after every passage. Neither replication capacity, nor IRES sequences of both SAD IRES-P viruses changed up to passage 34.

Thus we could show that the genomic organization of both SAD IRES-P viruses is stable over 34 passages and no revertants appeared. This furthermore confirms the genomic stability of rhabdoviruses, which also applies to our SAD IRES-P viruses.

3.2.1.4. Diminished IFN antagonism of IRES-P RV

Previously it was shown that P is the major IFN antagonist of rabies virus. On the one hand, it counteracts type I IFN induction by targeting IRF3 and IRF7 phosphorylation (Brzozka et al., 2005). On the other hand JAK/STAT signaling is prevented by inhibiting translocation of phosphorylated STATs to the nucleus (Brzozka et al., 2006). Reduced P levels therefore should not only limit the capacity of RV to counteract transcriptional induction of IFN but

should also increase the sensitivity of RV to exogenous IFN. Hence, reporter gene experiments in which IFN induction and IFN signaling can be analyzed were performed in HEK 293T cells.

IFN induction assays revealed an increased expression of FL from the IFNβ dependent reporter plasmid p125-Luc in cells infected with SAD IRES-P viruses compared to wt RV (L16) infected cells (Fig. 23A). However, compared to the previously described SAD ΔPLP (Brzozka et al., 2005), which expresses only trace amounts of P and which therefore is a potent IFN inducer, FL activity remained moderate. This indicates a P dose-dependent deficiency in the capacity of the recombinant SAD IRES-P to prevent activation of the IFNβ promoter.

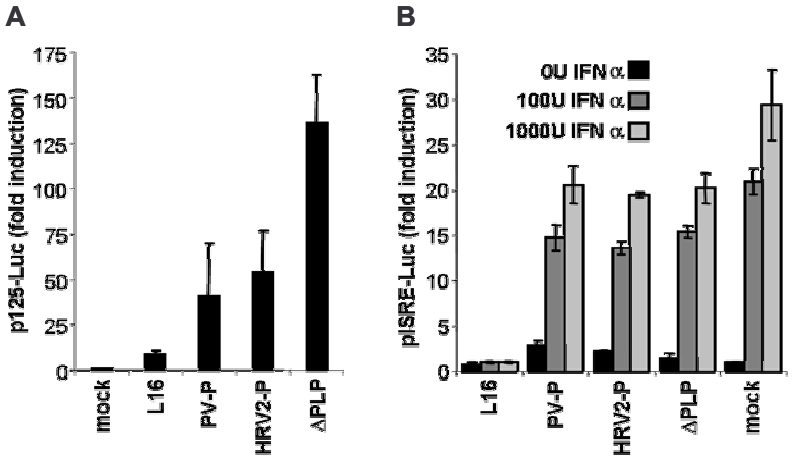

Fig. 23: Viral defects in counteracting IFNβ induction and JAK/STAT signaling.
(A) Activation of the IFNβ promoter by SAD IRES-P. HEK 293T cells were transfected with an IFNβ promoter-controlled reporter plasmid (p125-Luc) and infected at a MOI of 3 with the indicated viruses. 24 h p.i. cells were lysed and subjected to the dual luciferase reporter assay. The ratio of FL-LU and RL-LU (expressed from a constitutive active, co-transfected pCMV-RL) was compared to the mock infected control, set as one. One representative out of at least three independent experiments is shown, including data from three parallel experiments. Error bars indicate standard deviation. (B) Inhibition of IFN-stimulated gene expression by the indicated RV was analyzed in IFN-negative BSR T7/5 cells. Cells were infected at a MOI of 1. Six hours later infected cells were transfected with the ISRE (IFN stimulated response element) promoter-controlled reporter plasmid (pISRE-Luc) and pCMV-RL for normalization. 24 h p.i. cells were treated with the indicated doses of IFNα A/D. FL and RL activities were determined 48 h p.i.. Error bars indicate standard deviation from at least three parallel experiments.

Furthermore, the ability to counteract JAK/STAT signaling was examined in the IFN-incompetent BSR T7/5 cells to exclude effects of feed-back by endogenous IFN. In cells treated with recombinant IFNα A/D, wt RV SAD L16 almost completely prevents FL expression from transfected pISRE (IFN stimulated response element)-Luc whereas both SAD HRV2-P and SAD PV-P could restrain FL expression only to some extent (Fig. 23B).

Thus, IRES-mediated translational attenuation of P also limits the virus' ability to counteract the cellular IFN response.

These data confirm the role of RV P as the major antagonist of the host IFN system. SAD IRES-P viruses, which express low levels of RV P, show a clear defect in their ability to interfere with IFN induction and signaling, in addition to their attenuated replication.

3.2.1.5. Attenuated replication of IRES-controlled RVs in brain slice cultures

The previous experiments demonstrated reduction of the expression of the essential rabies virus P protein by IRES-dependent translation initiation. As RV P is necessary not only for the replication of rabies virus but also plays a major role in counteracting the host's innate immune system, SAD IRES-P viruses are attenuated in growth and are furthermore more susceptible to the IFN response of the host, leading to a highly attenuated phenotype in cell culture.

Hippocampal brain slice cultures provide a potent system to analyze virus growth and tropism in a relevant primary neuronal cell networks. To confirm the results obtained from *in vitro* studies, IRES-controlled RVs were characterized in organotypic hippocampal slice cultures from newborn C57 BL/6 mice (Mayer et al., 2005). These experiments were performed by M. Schwemmle in Freiburg. Cultured hippocampal slices were exposed to preparations of SAD L16, SAD PV-P, or SAD HRV2-P immediately after explantation from mice. Compared to uninfected brain slices, hippocampal cytoarchitecture was not significantly changed in slices, which were infected with SAD PV-P and SAD HRV2-P for 8 days (Fig. 24A, left panels). Analysis of vitality of slice cultures revealed an intense tissue damage of a significant part of the SAD PV-P and a majority of the SAD L16 infected cultures, 8 days p.i. (Fig. 24A, right graph). At earlier time points (5 d p.i.) the extent of tissue damage in SAD L16 infected cultures was similar compared to 8 days p.i., whereas most cultures infected with SAD PV-P or SAD HRV2-P showed no or only mild tissue damage (Fig. 24A).

Differences between replication of SAD PV-P, SAD HRV2-P and SAD L16, observed in cell culture experiments, were confimed also in hippocampal brain slices from wt mice (Fig. 24B). In those only sparse viral antigen signals were detectable in cultures from wt mice infected with SAD HRV2-P at 3 to 4 d p.i.. A slightly increased staining against the RV nucleoprotein could be observed in SAD PV-P infected wt slices (Fig. 24B, upper panel). In contrast, RV N immunolabeling was prominent in SAD L16 infected cultured hippocampi (Fig. 24B, upper panel). This led us suggest that the observed tissue damage (Fig. 24A) at later time points of infection correlates with the growth efficiency of these RVs.

Moreover, the role of RV P as the major IFN antagonist of the virus could also be addressed in brain slice experiments. Cultured hippocampal slices from mice lacking a functional IFNα receptor ($IFNAR^{-/-}$) were infected with SAD L16, SAD PV-P, or SAD HRV2-P and stained against RV N at 8 d p.i. (Fig. 24B, lower panel). In comparison to wildtype mice, viral antigen signals in infected brain slices from $IFNAR^{-/-}$ mice were much more prominent. In comparison to organotypic brain slices from wt mice, infection of slices from mice, lacking a functional IFNα receptor ($IFNAR^{-/-}$) with SAD L16, SAD PV-P and SAD HRV2-P revealed much more prominent signals for RV N, reflecting an unrestricted growth of RV in tissues which are impaired in innate immunity. The facilitated replication became visible particularly well in $IFNAR^{-/-}$ cultures infected with SAD IRES-P (Fig. 24B, lower panel). While in wt brain slice cultures only some viral antigen signals were detectable in $IFNAR^{-/-}$ cultures, SAD IRES-P viruses were distributed throughout the whole culture.

Previously it was reported that the HRV2 IRES is inhibited in neuronal cells, in contrast to the PV IRES (Gromeier et al., 1996; Merrill and Gromeier, 2006). This would implicate that SAD HRV2-P is not able to replicate in neuronal cells, whereas replication of SAD PV-P should not be impaired. To address this, the cellular distribution of SAD HRV2-P and SAD PV-P in the hippocampal slices was further analyzed. No obvious differences were observed at 8 d p.i. (Fig. 24C). Independent of the virus used, labeling of viral antigen often displayed a punctuated staining, indicating virus-containing axonal elements (Fig. 24C, arrowheads). Virus antigen was verifiable in some granule cell somata, being also positive for the neuronal marker calbindin as a neuronal marker (Fig. 24C). Specific translational defects of the HRV2 IRES in neurons were thus not apparent and therefore a limited tropism for neurons did not contribute to the observed attenuation of SAD HRV2-P relative to SAD PV-P. Rather, a generally lower translational activity of the HRV2 IRES is the basis of attenuation.

These data demonstrate the attenuation of the recombinant IRES-controlled rabies viruses due to reduced levels of P also in organotypic hippocampal slice cultures of wt mice, which display a relevant primary neuronal tissue. Furthermore, predicted translational defects of the HRV2 IRES in neuronal cells (Gromeier et al., 1996; Merrill and Gromeier, 2006) could be excluded, as all examined recombinant rabies viruses replicated in neuronal cells. This indicates that the observed attenuation phenotype of the HRV2 IRES-controlled viruses in murine brain slices does not rely on a neuron specific defect of the HRV2 IRES.

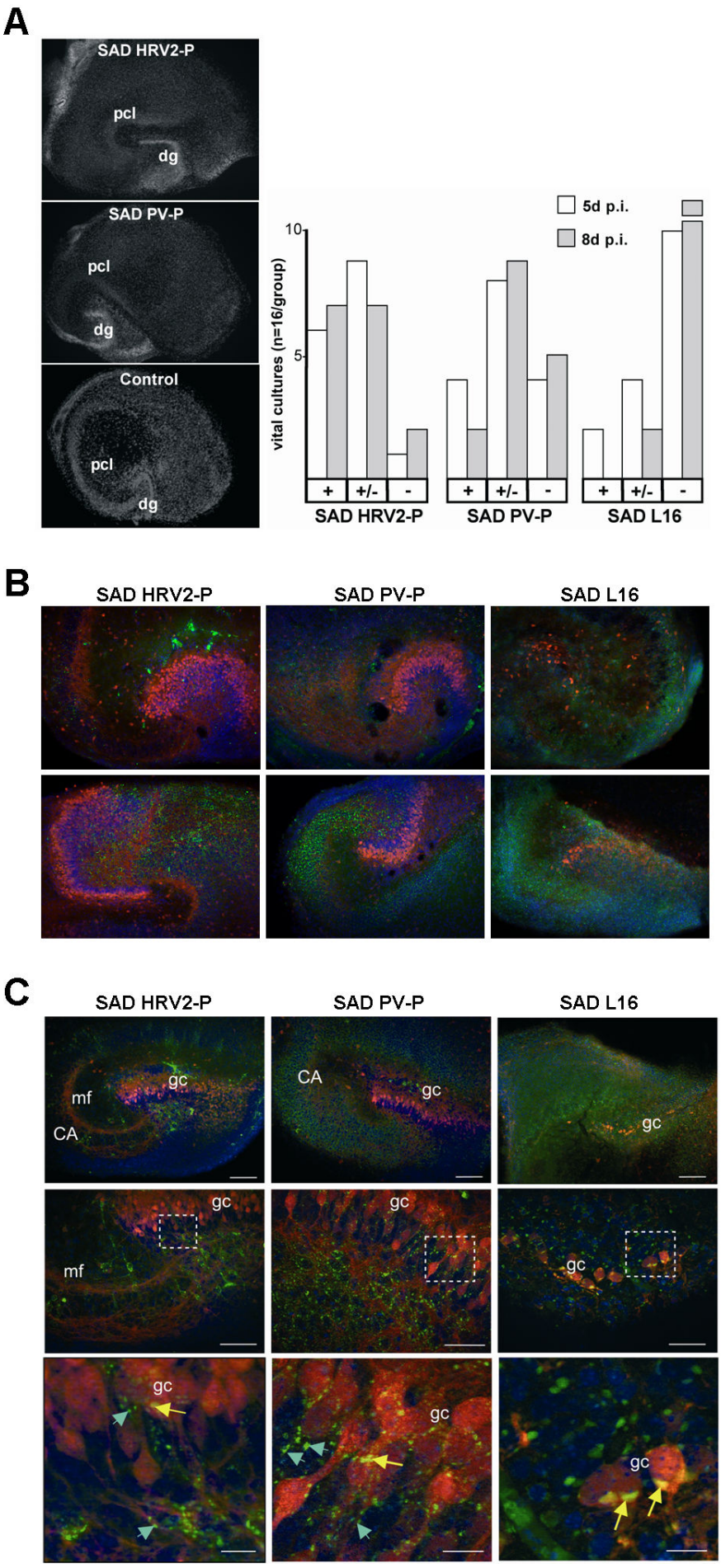

Fig. 24: Replication of IRES-controlled RVs in organotypic hippocampal slice cultures. Hippocampal slice cultures from newborn mice (C57/BL6) were infected with 2 x 10^4 ffu of SAD HRV2-P, SAD PV-P or SAD L16. After the indicated time periods, slices were fixed and 50 µm sections were prepared and immunostained against RV N (green), calbindin (red) and counterstained with DAPI (blue). (A) Impact of RV infection on the hippocampus damage. Left panels: Survey of a DAPI-stained hippocampal culture infected with SAD HRV2-P and SAD PV-P for 8 d. Right graph: extent of tissue damage induced by the different virus strains 8 d p.i. based on DAPI staining. (+) no; (+/-) partial and (-) severe loss of hippocampal organization. n=16/group refers to the number of organotypic slice cultures investigated for each virus. (B) Virus spread of SAD HRV2-P, SAD PV-P or SAD L16 in hippocampal slice cultures of wt (upper panel) and IFNAR$^{-/-}$ (lower panel) mice; 8 d p.i. (C) Distribution of RV N antigen in hippocampal cultures infected with SAD HRV2-P (left panel), SAD PV-P (middle panel) and SAD L16 (right panel). Axonal profiles (arrowheads) and calbindin-labeled granule cell somata (arrow) are indicated. CA: cornu ammonis, dg: dentate gyrus, gc: granule cells, mf: mossy fiber projection, pcl: pyramidal cell layer. Scale bars: upper panels 200 µm, middle panel (SAD HRV2-P, SAD PV-P) 100 µm, middle panel (SAD L16) 50 µm, lower panels 15 µm.

3.2.1.6. Severe attenuation of IRES-dependent RVs *in vivo*

The results obtained from cell culture and brain slice culture experiments demonstrated attenuation of recombinant SAD IRES-P by reduced expression levels of P. To explore how these effects observed *in vitro* affect virus pathogenicity, *in vivo* experiments were performed by L. Stitz at the FLI, Tübingen. Three week-old (Fig. 25A,C) or newborn (Fig. 25B,D) wt (Fig. 25 A,B) and IFNAR$^{-/-}$ (Fig. 25C,D) mice were inoculated intracranially (i.c.) with the recombinant RVs with doses ranging from 1 x 10^2 to 1 x 10^5 ffu/mouse.

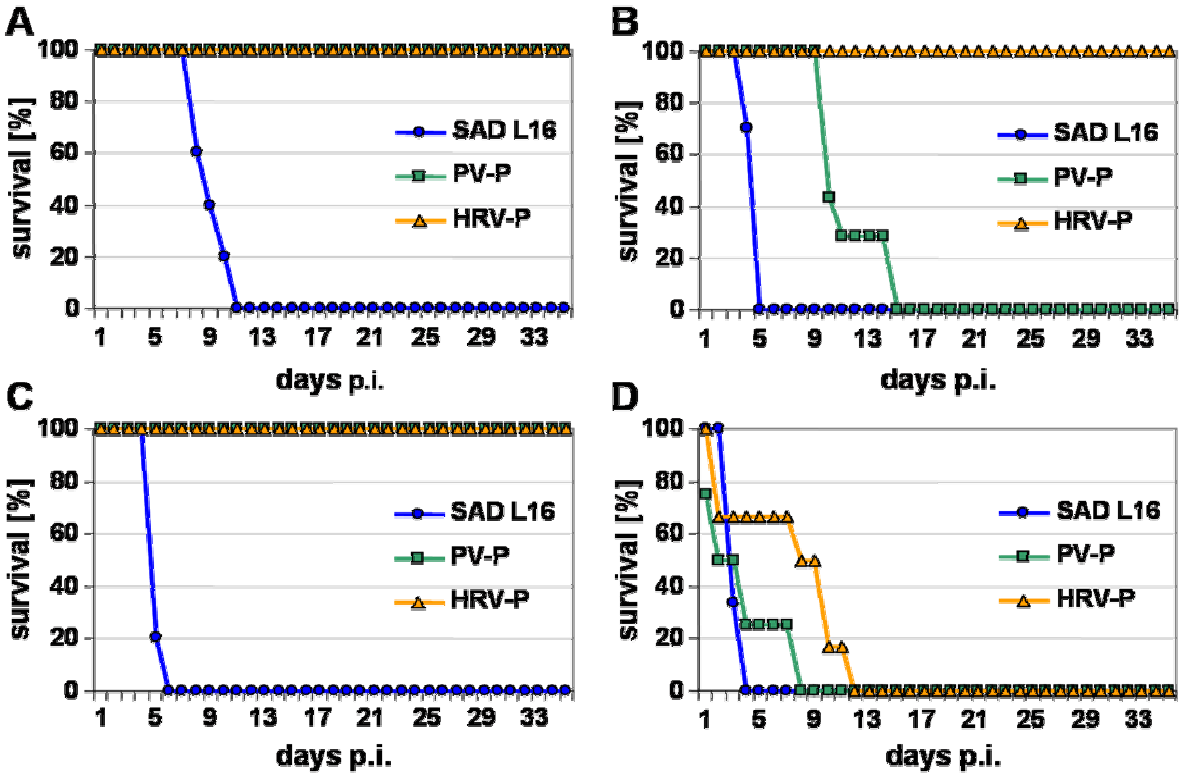

Fig. 25: Survival of mice after i.c. infection with recombinant RVs.
Three week-old wt (A) or IFNAR$^{-/-}$ mice (C) were infected i.c. with 1 x 10^5 ffu/mouse and newborn wt (B) or IFNAR$^{-/-}$ (D) mice with 100 ffu/mouse of SAD L16 (black circles), SAD PV-P (white squares) and SAD HRV2-P (black triangles). Percentage of survived mice of each group is indicated.

Wt SAD L16 virus was lethal at all doses within 11 days of incubation. All animals showed similar symptoms of pathogenicity with ruffled fur and haunched back. In striking contrast, both SAD HRV2-P and SAD PV-P were completely apathogenic in adult mice (Fig. 25A). Even increasing the virus dose to 3 x 10^5 ffu/mouse brain did not result in any death or symptoms by SAD HRV2-P (not shown). Surprisingly, even mice lacking the IFNα receptor (IFNAR$^{-/-}$) did not succumb to rabies after i.c. injection of either SAD PV-P or SAD HRV2-P (Fig. 25C). Only in newborn mice the recombinant IRES-dependent viruses were able to cause disease. SAD PV-P was lethal within 15 days, whereas all mice survived after i.c.

injection of SAD HRV2-P, indicating a more profound attenuation of the latter (Fig. 25B). The attenuated phenotype of SAD HRV2-P was even evident in newborn IFNAR$^{-/-}$ mice. Although all three viruses were able to kill newborn IFNAR$^{-/-}$ mice, differences in the time course of disease were apparent. SAD L16 killed mice within 4 days, while mice infected with SAD PV-P succumbed to rabies 8 d p.i. and SAD HRV2-P-infected mice died as late as 12 d p.i. (Fig. 25D). Thus, as observed for virus replication *in vitro* and in brain slice experiments, attenuation of IRES-controlled RV *in vivo* was dependent on the degree of IRES translation initiation. This leads to a highly attenuated phenotype of SAD PV-P, which is even more pronounced in case of SAD HRV2-P.

In summary, IRES-dependent translation initiation of the essential rabies virus P protein, leads to reduced expression levels. First, this results in attenuated viral mRNA synthesis and virus replication in cell culture and in murine brain slices, as RV P serves as an essential co-factor of the viral polymerase and acts as a chaperone for encapsidation of viral RNA (Curran and Kolakofsky, 2008; Curran et al., 1995; Horikami et al., 1992). Second, SAD IRES-P viruses show a severe defect in counteracting the innate immune response and the establishment of an antiviral state, due to reduced amounts of RV P. Both effects, attenuated growth and improved innate immune response, enable a faster clearance of the virus by the host. Mouse experiments demonstrated an extremely attenuated phenotype of both SAD IRES-P viruses *in vivo*, even after intercerebral injection.

3.2.2. Changing the ratio of full-length and truncated rabies virus P products by the use of the FMDV IRES

3.2.2.1. Expression of different RV P forms by SAD FMDV-P

The RV P ORF harbors four in-frame AUGs. In addition to the full-length P (P1), three N-terminally truncated P products (P2-P4) are generated in RV-infected cells by ribosomal leaky scanning. Although it was shown that full-length P alone is sufficient for all described functions of the phosphoprotein (Brzozka et al., 2005), it is still not clear if the additional P products have specific functions in the virus context.

A specific feature of the FMDV IRES is preferential translation initiation (80%) from an AUG(2) located 84 nt downstream of AUG(1) (Andreev et al., 2007). In contrast, translation

initiation by the PV IRES preferentially takes place at the first AUG, whereas the second, downstream AUG is recognized to a lower extent.

To address the role of truncated P proteins in the context of virus infection, we have made use of the FMDV IRES. Recombinant SAD FMDV-P viruses were generated by replacing the authentic N/P gene border with its transcriptional stop/restart signal sequences by the IRES element of FMDV. In addition, a SAD FMDV-P mutant was constructed, with a G→A mutation in the second AUG of the RV P mRNA (SAD FMDV-P_1x34). This mutation prevents expression of P2 (Fig. 26).

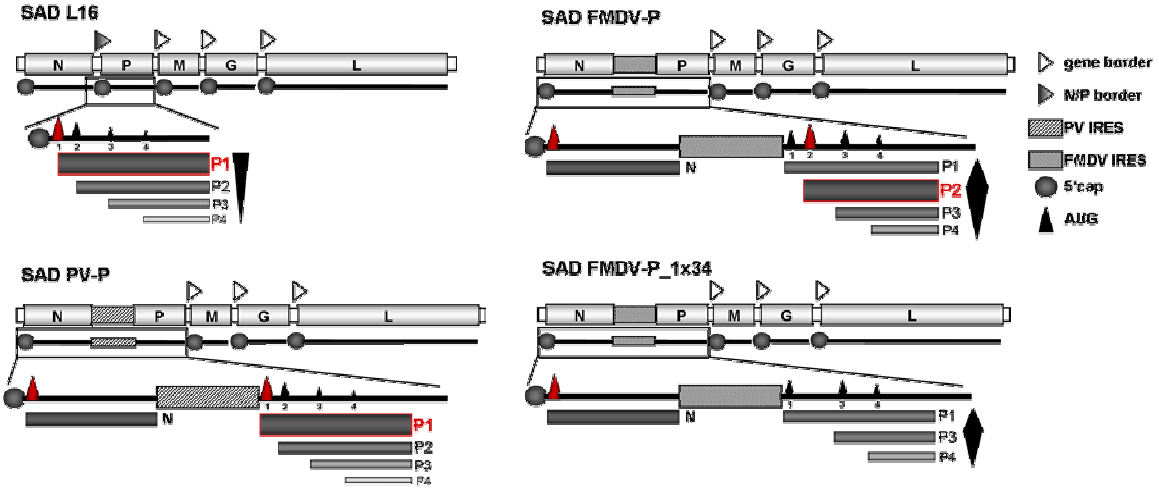

Fig. 26: Generation of recombinant RVs expressing RV P forms in different ratios
Wt RV (SAD L16) transcribes one monocistronic 5'capped mRNA for P, containing four in frame AUGs, from which four P products (P1-P4) are translated by ribosomal leaky scanning. In SAD PV-P and SAD FMDV-P the original N/P gene border was replaced by IRES elements of PV and FMDV. This leads to the transcription of a bicistronic N-P mRNA from which N is translated 5'cap-dependently, whereas expression of P1-P4 depends on specific features of the used IRES element. In case of the PV IRES the first AUG is preferentially used for translation initiation. In contrast, the FMDV IRES prefers the second, downstream AUG for initiation of translation, leading to an inverted P1:P2 ratio compared to SAD PV-P. SAD FMDV-P_1x34 contains a G→A mutation in the second AUG, destroying the second initiation codon. Therefore SAD FMDV-P_1x34 is defective in expression of P2.

Northern Blot experiments with RNA from infected BSR T7/5 cells confirmed the transcription of bicistronic N-P mRNAs from the recombinant RVs. From all SAD IRES-P viruses, a bicistronic mRNA of 3 kb, containing N and P sequences was expressed in infected cells. The monocistronic N and P mRNAs of wt RV were not detectable in cells infected with SAD IRES-P (Fig. 27A). To dissect expression of different P products from different IRES containing viruses, infected BSR T7/5 cells were furthermore analyzed by Western Blot experiments and following quantification by fluorescence imaging (Fig. 27B). Compared to wt SAD L16, expression of RV N and RV P in total (P1+P2+P3), was reduced in cells infected with SAD PV-P, SAD FMDV-P or SAD FMDV-P_1x34. As predicted, however the

ratio between P1 and P2 expression varied between the different viruses. As in SAD L16, also in SAD PV-P infected cells predominantly P1 was presented (64%), whereas P2 accumulated to lower levels (35,5%), leading to a P1:P2 ratio of 1.8:1. P3 expression was under the detection limit. In case of SAD FMDV-P infected cells, more P2 (67%) was expressed than P1 (31%), such that the P1:P2 ratio was inverted to 1:2.1 (Fig. 27B). Furthermore, the shift towards a downstream AUG was continued also in direction of P3, such that P3 was expressed to 2% in case of SAD FMDV-P. After deletion of the second AUG in SAD FMDV-P_1x34, no P2 could be detected. However, levels of P1 and P3 changed in cells infected with SAD FMDV-P_1x34, such that P1 was expressed to 73%. As no second AUG is present, translation initiation was shifted towards AUG3, leading to a high expression of P3 (26.6%), being even elevated compared to wt RV.

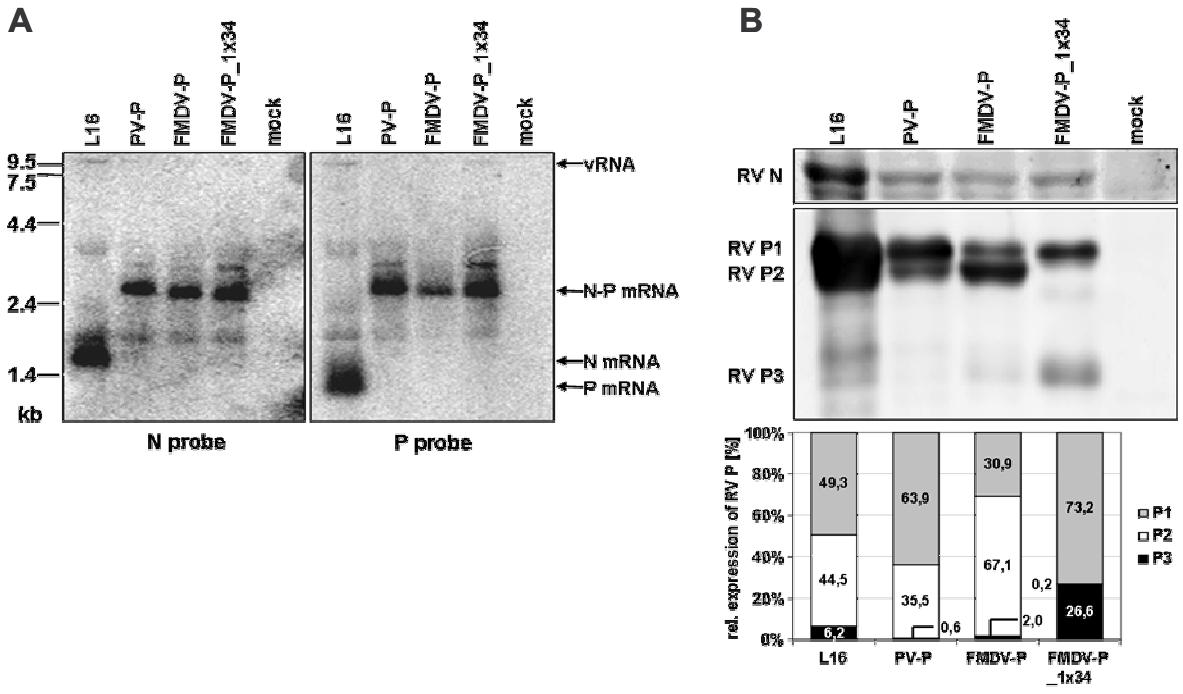

Fig. 27: Expression of different RV P forms by SAD FMDV-P in infected cells.
(A) Northern Blot experiment with RNA from infected BSR T7/5 cells. (B) Quantification of P protein levels by fluorescence imaging. Western Blot experiments showing expression of N and P protein in extracts from BSR T7/5 cells infected for 48 h with the indicated viruses. Graphs below the lanes indicate relative levels of RV P1, P2, P3 after normalization with RV N in comparison to total P (P1+P2+P3) (100%).

Thus, also the FMDV IRES can be used to direct RV P expression in recombinant RVs. A characteristic of the FMDV IRES is the preferential translation initiation at a downstream AUG. Accordingly the use of this IRES element in recombinant RVs leads to the change of ratios of P products translated from the bicistronic N-P mRNA. These recombinant viruses provide the opportunity to analyze different ratios of P products from the virus, without

deleting certain forms. While SAD PV-P shows a gradient of P products similar to wt RV, being P1>P2>P3, the gradient is changed to P2>P1>P3 in SAD FMDV-P. SAD FMDV-P_1x34 expresses high levels of P1 and P3, being even higher than in wt RV infected cells.

3.2.2.2. Different P forms are incorporated into rabies virus particles

Until now it is not completely clear how packaging of viral RNPs into new viral particles occurs and which proteins are involved in this process. We first wanted to address the question, which of the four P forms is incorporated into rabies virus particles and whether a changed ratio of cellular P products in infected cells is reflected in virus particles. Supernatants from virus infected BSR T7/5 cells were collected and virus particles were purified by sucrose density gradient ultracentrifugation. All twelve gradient fractions were analyzed by Western Blotting and stained against RV RNPs (Fig. 27A). Signals for viral RNPs accumulated in fractions 2-9, with a peak in fractions 3 and 4 for most viruses analyzed. Except for SAD FMDV-P_1x34, all virus particles contained RV P1, P2 and P3 to different extent, indicating that at least P1-P3 are incorporated into virus particles. SAD FMDV-P_1x34 particles did not contain P2, such that only P1 and P3 were present.

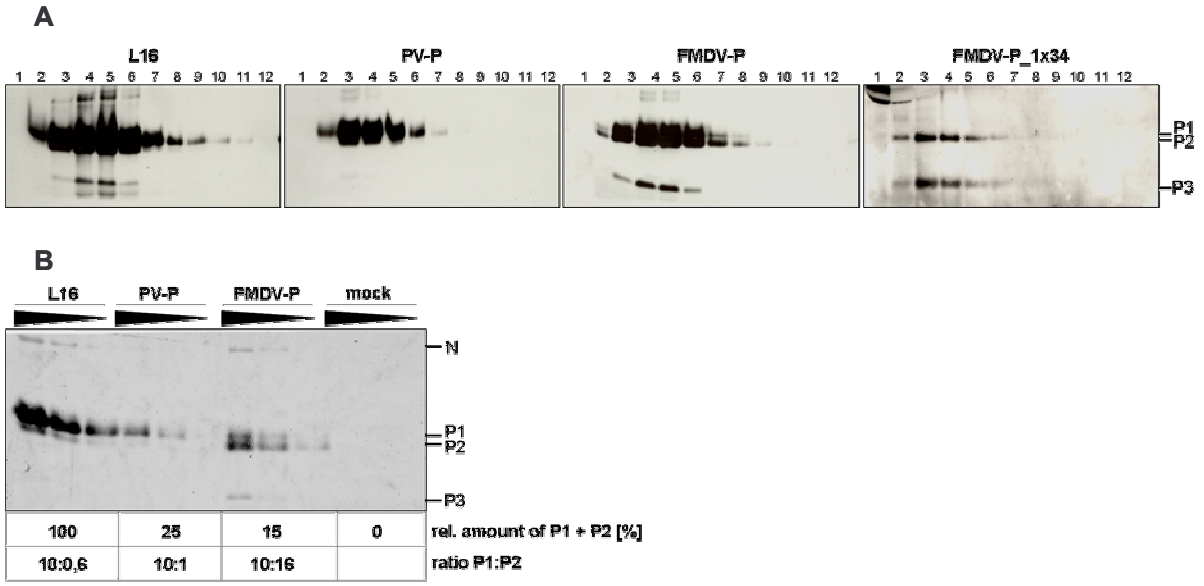

Fig. 28: Incorporation of different RV P forms into virus particles.
BSR T7/5 cells were infected with the indicated viruses at a MOI of 1. At 48 h p.i. virus supernatants were harvested, separated by density gradient centrifugation and analyzed by Western Blotting against RV P of all gradient fractions (A). Dilutions of the peak fraction #4 were analyzed by Western Blotting. Numbers below the lanes indicate relative levels of RV P after normalization with RV N and in comparison with P levels of SAD L16 (100%) and the ratio between P1 and P2 (B).

To investigate the relative amounts of P1 and P2 in different virus particles, peak fractions of SAD L16, SAD PV-P and SAD FMDV-P were diluted and analyzed by Western Blot. Expression levels of total P (P1+P2) were quantified by fluorescence imaging. Relative amounts were calculated by relating P expression levels to levels of RV N (P/N) and comparing those to the P/N ratio of SAD L16 particles (100%) (Fig. 28B). Relative amounts of total P in SAD FMDV-P were low (15%) compared to total P levels in SAD PV-P particles (25%) and SAD L16 particles (100%), indicating reduced growth kinetics of SAD PV-P in BSR T7/5 cells compared to SAD FMDV-P. As in infected cells (Fig. 27B), the ratio of P1 to P2 was similar in SAD PV-P (10:1) and SAD L16 (10:0.6), however inverted in SAD FMDV-P (10:16) (Fig. 28B). The shift of translation initiation from the first to a downstream AUG in case of SAD FMDV-P resulted in higher levels of P3 in SAD FMDV-P particles (Fig. 28A,B), which appear to be even above P3 amounts in wt RV particles.

Taken together, these data confirm the properties of translation initiation by the FMDV IRES, with respect to the use of a second, downstream AUG. This is, in contrast to the IRES element of PV, which preferentially initiates at the first AUG, though from the second AUG also products are translated to a small degree (Lopez and Martinez-Salas, 1999). By the use of the FMDV IRES element we were able to change the relative expression of RV P products in virus infected cells from P1>P2 in wt RV and SAD PV-P to P2>P1 in SAD FMDV-P infected cells. The shifted ratio towards P2 was also observed in virus particles, giving rise to changed relative amounts of incorporated P forms into virus particles from P1>P2>P3>P4 in case of SAD L16 and SAD PV-P particles, compared to P2>P1/P3 in SAD FMDV-P particles.

3.2.2.3. Involvement of RV P products in IFN antagonism of RV

RV P is the major IFN antagonist of rabies virus. First, it inhibits induction of type I IFN by preventing phosphorylation of IRF3 (Brzozka et al., 2005). Second, it binds to phosphorylated STAT and thereby interferes with JAK/STAT signaling (Brzozka et al., 2006). It was shown that full-length P (P1) is able to realize both functions (Brzozka et al., 2005). However it was not further examined if other P products are helpful in counteracting the innate immune system. By the use of recombinant RVs expressing different ratios of P forms (SAD PV-P, SAD FMDV-P and SAD FMDV-P_1x34), we intended to address the role of additional P forms in IFN antagonism.

The roles of P products in interference with IFN induction in the virus context were examined, using a reporter gene assay in which FL is expressed under the control of the IFNβ promoter from transfected p125-Luc in HEK 293T cells (Fig. 29A). Compared to SAD L16,

activation of the IFNβ promoter by SAD PV-P and SAD FMDV-P was increased. However compared to SeV DIH4, a Sendai virus defective interfering particle preparation, described to be a potent IFN inducer (Strahle et al., 2006), induction remained moderate. Although expressing different ratios of P1 vs. P2, no significant difference in IFNβ promoter induction could be observed between SAD PV-P and SAD FMDV-P. Expression of total P by SAD FMDV-P_1x34 was very low in this experiment. Therefore, the poor induction of type I IFN by SAD FMDV-P_1x34, is presumably due to a reduced amount of virus, instead of a enhanced ability to counteract IFN induction.

These data suggest that both P1 and P2 are able to inhibit IFN induction after virus infection, as changing relative amounts of P1 vs.P2 did not significantly change the extent of inhibition (Fig. 29A).

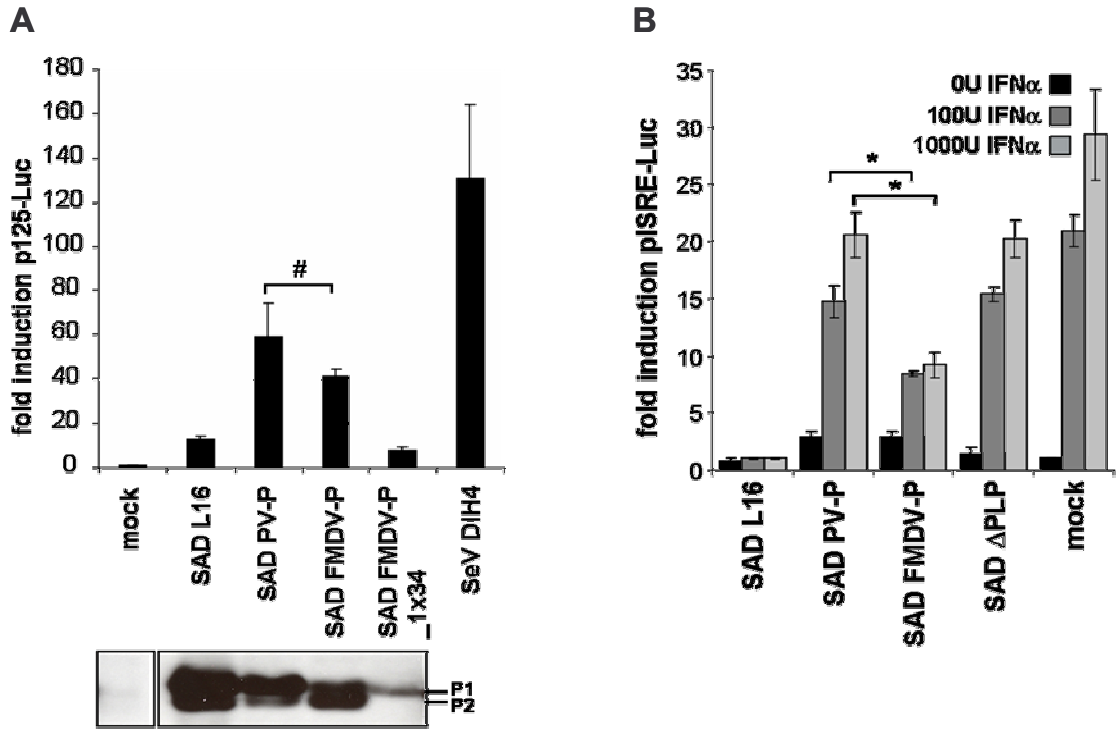

Fig. 29: Role of RV P products in counteracting IFNβ induction and JAK/STAT signaling.
(A) IFNβ promoter activation by SAD IRES-P. HEK 293T cells were transfected with an IFNβ promoter-controlled reporter plasmid (p125-Luc) and infected at a MOI of 3 with the indicated viruses. 24 h p.i. cells were lysed and subjected to the dual luciferase reporter assay. The FL/RL ratio was compared to the mock infected control, set as one. One representative experiment out of at least three independent experiments is shown, including data from three parallel experiments. Error bars indicate standard deviation. #: p>0,05 (t-test). P expression, detected by Western Blot, is indicated below. (B) Inhibition of IFN-stimulated gene expression by the indicated RV was analyzed in IFN-negative BSR T7/5 cells. Cells were infected at a MOI of 1. Six hours later, infected cells were transfected with the ISRE (IFN stimulated response element) promoter-controlled reporter plasmid (pISRE-Luc) and pCMV-RL for normalization. 24 h p.i. cells were treated with the indicated doses of IFNα A/D. FL and RL activities were determined 48 h p.i.. Error bars indicate standard deviation from at least three parallel experiments. For comparison SADΔPLP was included, which was previously decribed (Brzozka, et al. 2005) to be a potent IFN inducer, expressing only trace amounts of P. * p<0,05 (t-test).

Moreover, the influence of changed RV P expression levels on JAK/STAT signaling was examined in IFN-incompetent BSR T7/5 cells (Fig. 29B). In cells treated with recombinant IFN α A/D, wt RV SAD L16 almost completely prevented JAK/STAT signaling, as measured by FL activity, expressed from pISRE (IFN stimulated response element)-Luc, whereas SAD PV-P could restrain FL expression only to some extent (Fig. 29B). SAD FMDV-P which expresses more P2 and P3 and less P1 than SAD PV-P, however was more potent in inhibition of the JAK/STAT pathway. Thus, it seems that although changed relative amounts of RV P1, P2, and P3 are not influencing the virus' ability to inhibit IFN induction (Fig. 29A), a significant difference in inhibition of JAK/STAT signaling (Fig. 29B) was observed.
Therefore, recombinant RVs, in which relative ratios of P1-P4 are changed, behave differently, suggesting a regulatory role of certain P forms in IFN signaling.

3.2.2.4. Influence of changed RV P ratios on virus growth

As described before, RV P plays an essential role in virus RNA replication, as a polymerase cofactor and a chaperone for encapsidation of viral RNA (Curran and Kolakofsky, 2008; Curran et al., 1995; Horikami et al., 1992). Nevertheless, it is not clarified yet which of the truncated P products can take part in these functions. In order to explore the roles of individual P forms in virus growth, multi-step growth curves in IFN-incompetent BSR T7/5 cells and IFN-competent NA cells were performed with different SAD IRES-P in comparison to wt RV (SAD L16) and a RV mutant, lacking P2 (SAD FMDV-P_1x34) (Fig. 30).

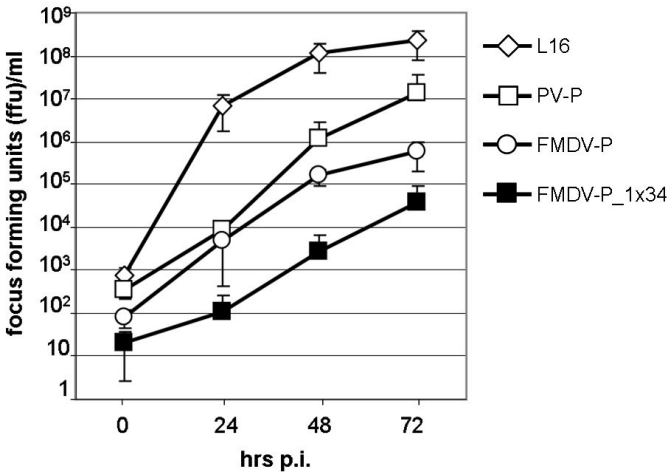

Fig. 30: Influence of changed ratios of full-length and truncated P forms on viral replication.
IFN-incompetent BSR T7/5 cells were infected with the indicated viruses at a MOI of 0.1 and infectious supernatant virus titers were determined at the indicated time points. Titers for every time point are from at least three independent experiments. Error bars indicate standard deviation.

In IFN-incompetent BSR T7/5 cells growth kinetics of SAD PV-P, SAD FMDV-P and SAD FMDV-P_1x34 were reduced in comparison to SAD L16 (Fig. 30). Titers of SAD PV-P were 1-2 log_{10} beyond wt RV SAD L16, as observed before, and replication of SAD FMDV-P was attenuated even more strongly, growing 3 log_{10} beyond wt RV. The replication of a SAD FMDV-P mutant virus lacking P2 (SAD FMDV-P_1x34) was even more attenuated in BSR T7/5 cells, such that titers were 4 log_{10} under titers of SAD L16.

These data demonstate that replication of recombinant RVs, expressing low levels of P1 (SAD FMDV-P) are hindered in virus replication. This replication defect cannot be rescued by higher levels of P2. This indicates that P1 plays the major role in the phosphoprotein's function in viral genome replication. P2 is not able to fulfill this task, as the L-binding domain is located within the first 20 aa of RV P, which are not present in P2. However, P2 could still be active as a chaperone of encapsidation of the RNA by the nucleoprotein, which is a prerequisite for viral replication. Thus, a virus expressing low levels of P1 and in addition lacking P2 completely (SAD FMDV-P_1x34) is attenuated even more strongly in virus growth. However, the exchange of methionine to alanine at amino acid position 20 ($M_{20}A$) within this mutant affects also the sequence of full-length P1 and P3, such that an additional influence of this exchange on virus replication cannot be excluded.

In summary, the FMDV IRES can be used to change relative levels of expression of P1 and P2. This allowed the generation of RVs expressing different ratios of the four P forms (P1-P4) from a bicistronic N-P mRNA (Fig. 27). Using these viruses, we could show, that P1, P2, and P3 are expressed in infected cells and are also incorporated into virions (Fig. 28). Furthermore, we were able to confirm in the virus context, that P1 plays the major role in the phosphoprotein's function in viral genome replication. In addition, P2 counteracts the IFN induction and signaling at least as efficiently as P1 (Fig. 29). Therefore, SAD FMDV-P, expressing low levels of P1 and higher levels of P2 is impaired in growth, but counteracts IFN signaling even more efficiently than SAD PV-P does. Growth curves of SAD FMDV-P_1x34, which expresses low amounts of P1 and no P2 at all, could eventually suggest an additional, potential role of P2 as a chaperone for encapsidation of the viral RNA by RV N, which is essential for RNA replication. Although P1 levels are similar to SAD FMDV-P in BSR T7/5 cells (Fig. 27) this virus is heavily attenuated in replication, leading to the hypothesis that either the lack of P2 or increased levels of P3 are influencing the virus' ability to encapsidate the RNA for a proper RNA replication. However this potential explanation should be proved by further data for RNA encapsidaion.

4. DISCUSSION

Rabies virus belongs to the family of *Rhabdoviridae* and serves as a prototype for all *Mononegavirales*. Its genome consists of five genes coding for the five viral proteins N, P, M, G and L. Gene expression of all members of *Mononegavirales* is regulated almost exclusively on the transcriptional level by the steepness of the transcriptional gradient (Whelan et al., 2004; Conzelmann, 2004). In this work a new strategy was employed to make the expression of an essential viral protein dependent on translation, rather than transcription. This was achieved by the use of internal ribosome entry sites (IRESs). These are known to be utilized by several positive strand RNA viruses for virus protein translation and replication. This approach should be applicable to other members of the *Mononegavirales* as well.

4.1. A Rabies virus-based heterologous system to explore translation initiation by IRES elements

4.1.1. Traditional systems for characterization of IRES activities

The reliability of diverse reporter systems for the characterization of IRES elements is a widely discussed topic. Although known to be highly error-prone (Kozak, 2007), the current method to test putative viral or cellular IRESs, is a mammalian transfection assay using bicistronic reporter plasmids. The popular pRF vector is a SV40 promoter plasmid in which IRES sequences are flanked by upstream renilla luciferase and downstream firefly luciferase ORFs (Macejak and Sarnow, 1991). Expression of the downstream luciferase reporter gene is thought to depend on the activity of the potential IRES to initiate translation internally. The bicistronic reporter plasmids are directly transfected into cells or used to transcribe RNA *in vitro*. In both cases RNAs are generated from which renilla and firefly luciferases are translated. However, the use of the plasmid based reporter system, as well as the transfection of *in vitro* transcribed reporter RNAs, is extremely error-prone. A first hint on this stems from experiments in which the arrangement of the reporter genes within the DNA vector yielded different outcome (Hennecke et al., 2001). Indeed, an accurate re-examination of sequences, predicted to contain IRESs, especially those of cellular mRNAs, like e.g. mRNAs for HIF-1α, p27, Bcl-2, VEGF, revealed the presence of cryptic promoters or splice sites, leading to

5’ end-dependent reporter gene expression from a monocistronic FL mRNA (Bert et al., 2006; Wang et al., 2005a; Kozak, 2005). It was described that the exchange of renilla and firefly luciferase ORFs within pRF by the genes for β-galactosidase (βgal) and chloramphenicol transferase (CAT) alters the activity for the predicted c-myc IRES completely (Nevins et al., 2003). Van Eden demonstrated that the 5’ reporter gene coding for renilla luciferase contains a splice donor site (Van Eden et al., 2004a). The insertion of a sequence, with potential internal translation initiation activity, into this vector might provide a splice acceptor site, leading to splicing events and consequently to reporter gene expression from a monocistronic FL mRNA. Furthermore, the discovery of splicing factors, described to be necessary for efficient “IRES activities” (Bedard et al., 2007; Bushell et al., 2006; Lin et al., 2007), supported the view, that some purported “IRES activities” are due to RNA splicing rather than internal translation initiation.

A possible solution to solve the problem of transfected plasmids would be the use of transfection of *in vitro* transcribed RNAs. However, transfected RNAs might not enter the cell in a stable or functional way (Barreau et al., 2006) and only 10% of RNAs, introduced into the cell by transfection (mainly lipo-fection) is used by the translation machinery, resulting in poor performance. In addition, the use of polymerases *in vitro* does not exclude transcription of shorter RNAs.

Another critical point is the presentation of results for IRES activities by reporter plasmids. In general, in all reporter systems a standard should be included to which results are compared. In DNA-based reporter systems for investigation of IRES activities this is in most cases a bicistronic RNA which contains instead of an IRES element a spacer sequence, predicted not to initiate translation internally. This approach is doubtful, as it is almost impossible to exclude a possible presence of cryptic promoter, additional splice acceptor sites or other influencing regions within a sequence, leading to background activity (Gallie et al., 2000; Van Eden et al., 2004b). Others use already described IRES elements, like the IRES from CrPV (Cevallos and Sarnow, 2005), shown to be very weak in its activity to initiate translation (Humphreys et al., 2005). The low activity of the control is in some studies obscured, by setting it as 1.0. As reporter gene expression by the IRES is further related to questionable preconditions, mentioned before, relative results for translation initiation are imprecise.

In order to exclude problems, occurring on DNA level, in some cases positive strand RNA viruses, like picornaviruses or alphaviruses, were used to analyze IRES activities. In such approaches chimeric picornaviruses were generated, by replacing the original IRES elements by other viral IRESs (Campbell et al., 2005; Gromeier et al., 1996; Merrill and Gromeier,

2006; Merrill et al., 2006; Kamrud et al., 2007). However, IRES elements are an integral part of the terminal UTR structures and are involved in picornavirus RNA replication and packaging (Brown et al., 2004; Bedard and Semler, 2004; Hunziker et al., 2007; Johansen and Morrow, 2000). Therefore, these systems are not specific for translation initiation and the observed effects, particularly the role of ITAFs specifying picornavirus host range, may be caused by mechanisms beyond translation initiation (Sarnow et al., 2005; Martinez-Salas et al., 2008). Influences on replication of positive strand RNA virus therefore might also affect the outcome of analyses of IRES activities, which is compromising the reliability of results, obtained by such systems. Other approaches used positive strand RNA viruses, containing bicistronic reporter constructs within their genome, for examination of activities in internal translation initiation (Kamrud et al., 2007).

4.1.2. Advantages of a new, RV-based reporter system for characterization of IRES activities

In this study a new system was established, in order to obviate deficiencies of DNA-based reporter systems or of systems depending on positive strand RNA viruses. Such a system should allow an easy and accurate characterization of IRES elements in terms of translation initiation, only. Thereby, IRES elements, which are suitable for regulation of RV gene expression, should be identified.

It turned out that RV is a particularly suitable heterologous viral system to explore translation initiation of IRES elements, without suffering from problems discussed before. First, it is known that the RV polymerase recognizes only the viral promoter at the 3'end of the viral RNA and highly conserved and well described special stop/start sequences (GTAAAAAA (N_{2-2x})AACAYYNCT) within the viral gene borders for transcription. Transcription and polyadenylation of upstream genes at the stop sequence, and release of the mRNAs is required for re-initiation at the start sequence of the downstream gene. Internal initiation of the polymerase is therefore not possible. Thus, transcription of two monocistronic RL- and FL mRNAs, by cryptic promoters within the IRES sequence, which is often the case in plasmid reporter systems, can be obviated. Moreover, RV replicates solely in the cytoplasm, such that the reporter RNA is produced in the cytoplasm, without a detour through the nucleus. Consequently, splicing events, due to potential splice sites within the IRESs or the reporter genes can also be excluded. Furthermore, RV is able to replicate *in vitro* in a broad range of cells with almost no restrictions, regarding cell species or types. After infection of diverse cells with reporter RVs, the reporter RNAs are expressed to high amounts directly in the

cytoplasm, excluding modifications of the RNAs, which might appear during the transfection process.

In this study, two RV-based reporter systems were established, using either luciferase or the enhanced cyan fluorescent protein (eCFP) as reporter genes. The first approach makes use of dual luciferase reporter RVs (SAD RL-IRES-FL) to analyze IRES activities. These recombinant reporter RVs contain an extra reporter gene construct, consisting of two ORFs, coding for renilla- (RL) and firefly luciferase (FL), which are separated by diverse IRES elements. Within the virus this bicistronic reporter construct is located between the genes for the viral glycoprotein (G) and the polymerase (L). Consequently, the polymerase of these reporter viruses transcribes in addition to the five viral monocistronic mRNAs, an extra bicistronic RL/FL mRNA.

In a second approach we used eCFP as a reporter. As for the dual luciferase RV, the reporter mRNA is expressed from an additional gene between RV G and L. However, in this case only one reporter gene is inserted, which is translated IRES-dependently from a bicistronic G/eCFP mRNA. From these reporter viruses (SAD IRES eCFP) only five mRNAs are expressed, including one bicistronic G/eCFP reporter mRNA.

In contrast to picornaviruses and other positive strand RNA viruses (Orlinger et al., 2007; Volkova et al., 2008; Kamrud et al., 2007), the IRES elements in the RV replication template are cotranscriptionally encapsidated in a tight RNP (Albertini et al., 2006). This prevents the formation of secondary structures, which might influence the replication. Only in non-encapsidated mRNAs, the IRES is able to form the active secondary structure. Thus, dissection of which IRES interactions and functions are important specifically for translation initiation is therefore straightforward in the RV context.

Some characteristics of RV replication, which could have lead to problems in the usage of the RV-based reporter systems, have been ruled out for the reporter viruses, used in this study. First, expression of an additional bicistronic RL/FL mRNA from a 5’ proximal position in the RV genome does not at all change the transcriptional gradient of the upstream genes N, P, M and G. Only the expression of the catalytic subunit of the viral polymerase (L) may be reduced, but not significantly. Second, IRES elements form highly stable secondary structures within the RNA, which might impair proper encapsidation and replication of the viral RNA. However, all reporter viruses grew to titers which are at the most 10fold below titers of wild type, what is most likely due to the expression of two additional genes. Thus, it seems that neither the slight change in the transcriptional gradient, nor the insertion of a secondary structure, lead to considerably reduced replication and growth of the reporter viruses.

4.1.3. Use of the new RV-based reporter systems for analysis of IRES activities

In order to use the newly established RV-based dual luciferase system (SAD RL-IRES-FL) for investigation of activities of IRES elements from different positive strand RNA viruses, standards and controls had to be included. Although RV is able to replicate in all kind of cells, its efficiency is certainly influenced by several properties of the used cell type. Thus e.g. the presence of an intact IFN system or other antiviral proteins can have an impact on the virus replication. As the RV-based reporter system should be useable in diverse cell types from different origin, changes in reporter gene expression that originate from impaired virus replication, have to be compensated for. Accordingly, expression of renilla luciferase (RL) was used as a standard for quantification of translation initiation activities by the IRES elements. As RL is expressed from the bicistronic reporter mRNA in a 5'cap-dependent manner, its expression depends only on the replication of the virus in the used cells. Thus, RL expression by the recombinant SAD RL-IRES-FL mirrors the virus ability to replicate in a certain cell type and can be equalized with virus replication displayed by viral titers. Accordingly, we could show that RL expression by SAD RL-PV-FL in different cells lies in a range of 2.5 $\log_{10}$, being lowest in IFN-competent HEK 293T cells and higher in IFN-incompetent BSR T7/5 cells.

As discussed before, a proper standard, to which IRES activities can be compared, or a negative control should be included in all analyses. Although the RV-based system rules out influences by cryptic promoters or splicing events, other possible sites that might have an impact on translation initiation cannot be excluded. Indeed, it is possible to put transcription of both reporter genes under control of additional copies of the N/P gene border (SAD RL-N/P-FL), such that RL and FL are translated 5'cap-dependently from monocistronic mRNAs. However, the use of this virus as a control to which other data are related is problematic. First, FL and RL are expressed from separate mRNAs, such that standardization to RL expression is not possible. Second, the steepness of the transcriptional gradient could change in different cell lines, such that reporter gene expression by SAD RL-N/P-FL is not comparable between different cells. In this respect, also this system lacks a proper negative control. Thus, to be able to compare IRES dependent translation initiation, we used relative FL expression by the PV IRES as a standard (100%), in each cell line tested. Reporter viruses containing the PV IRES were chosen, as the PV IRES, which has been studied extensively by several groups and is described to be a "real" IRES element, shows an universally high and stable activity in all cell lines tested within this work, also in the RV-based systems. Indeed,

reporter viruses containing the PV IRES showed the lowest variability among different cells during our examinations.

Using this newly established system, translation initiation activities of IRES elements from different positive strand RNA viruses were analyzed on different cell lines. Specifically, picornaviral IRES elements of type I (PV and HRV2) and type II (FMDV), as well as IRES elements from HCV and from two pestiviruses (BVDV and CSFV), belonging to the group of flaviviral IRESs, were selected. The characterization of these IRES elements appeared particularly promising. One the one hand, these are well known IRESs, which have been well-characterized by biochemical, phylogenetic and structural predictions (Skinner et al., 1989; Pilipenko et al., 1989b; Stewart and Semler, 1998). On the other hand, a lot of studies exist, which suggest their differential use of non-canonical translation factors and ITAFs, and their potential contribution to cell type and species specificity. The analysis of these viral IRESs within the RV-based dual luciferase system revealed that of both picorna- and flaviviral IRES groups behaved similarly, showing activities being PV>HRV2>FMDV and HCV>CSFV>BVDV in cells of primate and non-primate origin.

4.3.1.1. Potential influences on IRES activities

The analysis of picornaviral IRES elements in this approach appeared furthermore promising in view of their relative high efficiency of internal translation initiation, and possible cell-type specific restrictions, which are attributed to differential use of IRES transacting factors (ITAFs) (Holcik and Pestova, 2007; Merrill and Gromeier, 2006; Merrill et al., 2006). Especially for picornavirus type I IRES elements (PV, HRV2) but also type II IRESs (FMDV) a potential celltype specific activity is widely discussed. With respect to this, Merrill et al. claimed that the double-stranded RNA-binding protein 76 (DRBP76), which is mainly expressed in neuronal cells, represses HRV2 IRES activity. This has been suggested to be the reason why efficient HRV2 propagation cannot take place in neurons, compared to poliovirus, which replicates well in neurons, due to its IRES activity, being independent from DRBP76 (Merrill and Gromeier, 2006; Merrill et al., 2006). Also the cell tropism of FMDV, which is not able to replicate in neurons, is related to the stimulatory effect of a certain ITAF (ITAF45) on its IRES. As ITAF45 is ubiquitously expressed in proliferating cells, but not in resting cells, as e.g. neuronal tissue, this is supposed to be the reason of FMDV restriction in the brain. Considering this, we investigated these IRESs more closely. By the use of the RV-based dual luciferase system, cell-type specific restrictions or advantages were neither evident for picornaviral type I IRESs nor for the FMDV IRES, as a member of the picornaviral type II

IRES elements. A universally high activity of the PV IRES element, a lower activity of the HRV2 IRES and the lowest activity of the FMDV IRES were detectable in all cell types. A neuron-specific restriction of HRV2 IRES activity could not be observed by our analyses. Particularly, in HEK 293 cells, which are of neuronal origin (Shaw et al., 2002), and in which chimeric PV containing the HRV2 IRES are severely attenuated (Campbell et al., 2005), we observed a quite high translational activity of the HRV2 IRES. Although one might suspect a specifically lower activity of the FMDV IRES in murine neuronal cells (NA) this could not be confirmed in other murine neuronal cells (NS20Y). Thus, general organ or species specific preferences were not observed for either IRES in this work, which is consistent with other studies (Kauder et al., 2006; Kauder and Racaniello, 2004).

During all analyses of picornaviral IRES activities, using the RV-based dual luciferase system, only a stimulation of the downstream reporter gene expression could be observed. An influence of picornaviral IRESs on the upstream reporter gene within the bicistronic reporter RNA, as proposed by Junemann et al., was never evident (Junemann et al., 2007). Therefore, the hypothesis of Junemann et al., that a picornavirus IRES in a bicistronic RNA system can capture translation initiation factors and hand them over to the translation initiation site of the upstream gene, leading to a stimulation of expression of the upstream gene by the IRES (Junemann et al., 2007), was not supported by the present findings. All reporter systems (rabbit reticulocyte lysates, HeLa extracts or transfection of *in vitro* transcribed mRNAs) used by Junemann et al. are known to be error-prone, harboring disadvantages described for commonly used reporter systems.

In the original context, viral IRES elements are surrounded by the viral genomic sequence, including elements shown to be important for virus replication, like for example cloverleafs at the 5'UTR or secondary structures within the 3'UTR (Andino et al., 1990; Parsley et al., 1997). It was proposed that these elements might also have an impact on translation initiation (Dobrikova et al., 2003a; Dobrikova et al., 2003b; Dobrikova et al., 2006). However, in the present work the insertion of original picornaviral 3'UTRs into the RV-based reporter constructs did not greatly alter the IRES activities effects. Therefore, it seems that the proposed dependence of IRES activities on elements within the 3'UTR are most likely due to effects on the replication of the positive strand RNA viruses, used in those studies. Thus, dissection of which IRES interactions and functions are important specifically for translation initiation is therefore more uncomplicated in the RV context.

4.3.1.2. Analysis of the p27 5'UTR

In addition to viral RNAs, also cellular mRNAs were hypothesized to contain IRES elements. Those are responsible to guarantee ongoing translation of essential proteins, when 5'cap-dependent translation is impaired, such as during cell-stress, hypoxia or apoptosis. In many cases the existence of such cellular IRESs was either not demonstrated in a reliable way or their existence has been disproven by finding of cryptic promoters or splice sites within these sequences. All these discrepancies arose mostly from the lack of exact systems to define and characterize IRESs, leading to contradictory results. Thereby, a whole list of putative cellular IRES elements emerged, among them the 5'UTR of the p27 mRNA. The p27 protein inhibits the cyclin-dependent kinase (CDK) activity, causing cell-cycle arrest within the G_1 phase (Millard et al., 1997). Expression of p27 appears to be regulated on the level of translation, although the mechanism remains unclear (Liu et al., 2005). One postulated, possibility is the presence of an IRES elements within the 5'UTR of its mRNA (Kullmann et al., 2002). However, it appeared that these findings are not reliable, because of the presence of a cryptic promoter within the p27 5'UTR (Liu et al., 2005). Also experiments using transfection of *in vitro* transcribed RNAs were not convincing (Cho et al., 2005). As our new RV-based reporter systems can rule out the most prominent disadvantages of other assays for characterization of IRES elements, this is an alternative approach to test the p27 5'UTR for translation initiation activity. Indeed, downstream reporter gene expression from a transfected plasmid containing the 5'UTR of the p27 mRNA, was high (75-117%), compared to a plasmid containing the PV IRES. However, in both RV-based reporter systems (luciferase and eCFP as reporter genes) the p27 5'UTR shows only marginal expression of the 3' reporter gene. Due to the lack of a definite negative control, we could not clarify if this extremely weak reporter gene expression activity is real activity in internal translation initiation or just background expression. Nevertheless, this finding supports results from several other groups, demonstrating that putative cellular IRES elements are acting very weakly in internal translation initiation, if they exist at all (Nevins et al., 2003; Tinton et al., 2005; Kozak, 2005). Considering this, it is certainly questionable why such weak "IRES" elements should be responsible for the sustaining expression of essential cellular proteins under stress conditions. Additionally it has to be taken into account that 5'cap-dependent translation mechanisms are reduced only to 30%, compared to translation under normal conditions (Fan and Penman, 1970). Anyhow, potential internal translation initiation by the p27 5'UTR cannot be excluded using either of the two RV-based reporter systems. All cellular mRNAs

are synthesized in the nucleus, where they could interact with diverse factors, among them possible ITAFs. In contrast viral RNAs, which are exclusively located in the cytoplasm, are not able to contact these specific nuclear factors (Semler and Waterman, 2008). Therefore, transfection of *in vitro* transcribed reporter RNAs, as well as expression of reporter RNAs from RV, lack this "nuclear experience", which might be the reason why these systems are not able to identify the proposed activity of cellular IRES elements.

4.3.1.3. Ribosome landing

Although the mechanisms of internal translation initiation by IRES elements have been studied for years, it is still not completely understood how the ribosome reaches the initiation codon after binding by IRESs. Two ways of start codon recognition are possible. One hypothesis describes a mechanism in which the ribosome is captured by the IRES element and then scans along the mRNA until it attains an AUG in a favorable Kozak context (Poyry et al., 2001). This continuous scanning process is comparable to the one of 5'cap-dependent translation initiation and requires the two cellular factors eIF1 and eIF1A, being responsible for successful ribosome scanning to the initiation codon (Majumdar and Maitra, 2005; Mitchell and Lorsch, 2008). However, it was shown that eIF1 and eIF1A are not necessary for every IRES element (Pestova et al., 1998a), leading to a second hypothesis. This suggests, catching of the ribosome by certain IRES domains, whereas other domains of the IRES are responsible for a direct positioning of the ribosome onto the initiation codon (Belsham, 1992). Within this process the factors eIF1 and eIF1A are dispensable, as the start codon is reached in a discontinuous way (Pestova et al., 1998a).

However, selection of initiation codons is different between certain types of IRES elements. Picornaviral type I IRESs prefer the most proximal AUG, whereas the FMDV IRES, belonging to type II favors a second, downstream AUG (Belsham, 2009). In order to take a closer look at the process of start codon recognition by those two types of picornaviral IRES elements, reporter RVs containing one or two start codons in "in frame" (IF) or "out of frame" (OF) context were used in this study. Analyses with reporter RVs containing a picornavirus type I IRES (PV or HRV2), revealed a drop of reporter gene expression, when two AUGs where in OF context, compared to two AUGs in IF context. This drop was most likely due to the expression of a non-luciferase protein from the first AUG, when the two AUGs are out of frame. In contrast, reporter gene expression from dual-luciferase reporter RVs, containing the FMDV IRES did not change between IF- or OF- context as drastically as it was the case in reporter RVs containing type I IRESs. As the two AUGs were separated by just

6/7 nucleotides, it might be that this short distance was not recognized as a real spacer, such that scanning could not take place in the common way. The results obtained within this study confirmed general differences between picornaviral type I and type II IRES elements. For identification of a general strategy how ribosomes reach the initiator codon in the individual IRES elements, additional experiments with more sophisticated constructs are needed.
While the dual luciferase system is able to quantify IRES activities within a population of cells, a second RV-based reporter system which uses eCFP as a reporter gene, allowed examination of IRES activities on single cell level. Inspite of its impreciseness and difficulties in its usage, we were able to confirm observations made for picornaviral IRES activities by the dual luciferase system, regarding IRES activities and cell specificity.

Taken together, the new RV-based reporter systems, established in this work are particularly useful for the analysis of IRES elements from RNAs located in the cytoplasm. Compared to other systems it excludes the main critical points, which are present in other approaches. Specifically, the presence of cryptic promoters or additional splice sites within the IRES sequence, which could lead to false positive results, is ruled out. As RV replicates in all cell types to high titers, the reporter RNAs are delivered directly to the cytoplasm of all kind of cells to extremely high amounts, which cannot be achieved by any transfection method. Additional points of criticism on the "common" reporter systems, like dependence on a certain kind of reporter (Hennecke et al., 2001) or alterations in the virus replication, which might influence internal translation initiation were also shown not to apply to the RV-based systems.

4.2. Use of picornaviral IRES elements as a tool for regulation of rabies virus gene expression

A characteristic of *Mononegavirales* is sequential transcription of monocistronic genes from a single 3' terminal promoter (Abraham and Banerjee, 1976; Ball and White, 1976) and attenuation of transcription at gene borders thus giving rise to a transcript gradient (Iverson and Rose, 1981). Accordingly, the gene order and the steepness of the transcript gradient predetermine the level of individual mRNAs and of viral protein production (Ball and White, 1976). The establishment of a reverse genetics system to recover rhabdoviruses from cDNA,

makes it possible to genetically engineer recombinant viruses. This allows first to study different aspects of the viral life cycle, as well as the identification of cellular interaction partners by mutational analysis (Finke and Conzelmann, 2005b) and second to make use of rhabdoviruses for biomedical application, like e.g. vaccination, gene therapy or oncolytic virotherapy (Finke and Conzelmann, 2005a). Approaches to manipulate gene expression of *Mononegavirales* have included shifting genes to other positions in recombinant VSV (Flanagan et al., 2000; Novella et al., 2004) and RV (Brzozka et al., 2005) or engineering gene border sequences to alter the abundance of downstream gene transcripts (Finke et al., 2000; Finke and Conzelmann, 2005a; Finke and Conzelmann, 2005b). In addition, terminal promoters have been engineered to generate ambisense RVs, expressing extra genes from the antigenome (Finke and Conzelmann, 1999; Finke and Conzelmann, 1997).

In the present work we describe a completely new strategy, to modify expression of essential viral proteins. The new approach uses IRES elements to control translation of viral genes and thereby presents a possibility to manipulate viral gene expression on translational level, instead of transcriptional level.

To this end, in this study the group of picornaviral IRES elements (PV, HRV2, FMDV), as well as the group of flaviviral IRESs (BVDV, CSFV, HCV), was analyzed by a RV-based dual luciferase reporter system, as described above. It turned out, that activities of members from both groups were comparable. Picornaviral IRES activities are described to be influenced by diverse factors and/or certain conditions, which appears to be not as important in the case of flaviviral IRES elements. On this account, we have analyzed members of picornaviral IRESs more closely in the RV reporter systems. In the following, we made use of those findings to control RV replication.

4.2.1. Use of IRES elements to control RV P expression and thereby RV replication and IFN escape

In order to control RV replication on translational level by IRES elements, the RV phosphoprotein is the only candidate to target both RV gene expression and the virus' ability to counteract host innate immunity. RV P is acting as the essential polymerase cofactor, necessary for virus replication. Furthermore, it is known to inhibit IFN induction and signaling, which makes it a potent antagonist of the host innate immune system. Notably, translation of the P gene does not only result in expression of a full-length P protein of 297 aa length (P1). In addition, three N-terminally truncated forms of RV P (P2-P4) are expressed by translation initiation at downstream in frame start codons (aa 20, aa 53, aa 83), due to a

ribosomal leaky scanning mechanism (Eriguchi et al., 2002; Chenik et al., 1994). As full-length P1 contains all domains necessary for interaction with different proteins, it is sufficient to support all viral functions. Certainly, functions of the different P forms can be explored in non-viral context by transfection of plasmids, expressing the single P forms. By such approaches cellular localization of the diverse P forms, their binding to other viral or cellular proteins, as well as mapping of different domains within the P protein were analyzed by several groups (Blondel et al., 2002; Gerard et al., 2009; Gigant et al., 2000; Mavrakis et al., 2006; Chenik et al., 1994; Chenik et al., 1998). Such studies lead to a widespread knowledge of the RV P protein and its diverse functions.

IRES-dependent control of P expression was achieved by replacement of the cis-active sequences of the N/P gene border by IRES elements of PV and HRV2. Thereby, a bicistronic N-IRES-P mRNA was transcribed and translation of P was directed by the IRESs. The rescue of viable viruses producing a bicistronic N/P mRNA instead of two monocistronic mRNAs demonstrated the function of both IRESs in this context and the validity of the approach. In reporter gene assays we could show that IRES-dependent translation initiation was reduced compared to 5'cap-dependent translation initiation, originating from the viral gene border. Moreover, translation by the HRV2 IRES was further impaired compared to PV IRES. These findings were confirmed in cells infected with the IRES-controlled RVs. As compared to 5'cap-dependent translation from the standard RV monocistronic P mRNA, IRES-dependent accumulation of P was reduced in infected cells to 56% (PV IRES) and 34% (HRV2 IRES), respectively.

Replication of IRES-controlled RVs in IFN-incompetent cells confirmed the role of RV P as an essential polymerase cofactor. Here growth of the PV IRES-controlled virus (SAD PV-P) was attenuated in comparison with wt RV by one $\log_{10}$, and that of the HRV2 IRES-controlled virus (SAD HRV2-P) even more (1.5 $\log_{10}$). As replication of RV is not affected by the presence of the IRES elements in the viral genome per se, as evidenced by the lack of attenuation of the reporter gene viruses, reduced levels of P must be responsible for the attenuation of both IRES-controlled RVs.

Moreover, growth of RV in IFN-competent cells corroborated the predicted deficits of viruses with reduced P levels in counteracting the host IFN system. Compared to wt RV, which seems to be not affected considerably in growth in the presence of an intact IFN system, the IRES-controlled viruses were further attenuated. Hence, SAD PV-P replicated to titers 2 $\log_{10}$ below wt RV titers and SAD HRV2-P was further attenuated by half a $\log_{10}$. The role of RV P as the IFN antagonist was additionally pointed out in IFN reporter assays. Compared to wt RV,

SAD PV-P and SAD HRV2-P induced conspicuously more luciferase from the IFNβ-promoter, but less than a RV expressing only minute amounts of P from the most 3'distal gene position (SAD ΔPLP) (Brzozka et al., 2005). Inhibition of IFN signaling by the IRES-controlled viruses occurred to negligible levels, similar to SAD ΔPLP. Whereas inhibition of IFN induction appears to depend on the dose of RV P, it seems that for inhibition of IFN signaling a critical threshold of P is required, which was not reached in the IRES-controlled RVs. Thus, IRES-mediated reduced expression of P limits virus growth and the capacity to counteract transcriptional induction of the IFNβ-promoter and to inhibit interferon-dependent JAK/STAT signaling.

In order to assess cell specificity of the IRES-dependent recombinant viruses in relevant primary neuronal networks, we further evaluated virus replication in slice cultures from mouse brains. Similar to cell culture experiments, both viruses were severely attenuated in comparison to the wt RV in murine brain slice cultures. Production of detectable virus antigen and damage of the architecture of the hippocampus cultures was less pronounced after infection by SAD HRV2-P, than by SAD PV-P. Therefore, differences in the replication kinetics between SAD HRV2-P and SAD PV-P were apparent also in a primary neuronal tissues. Notably, however no differences in the distribution of viruses in the cultures could be recognized. Antigen of both IRES-controlled viruses and of wt RV was detected in axon-like structures of hippocampal neurons, confirming the lack of neuron-specific translational defects of HRV2 IRES-mediated P expression in primary cells. This validates the findings from the reporter systems and confirms recently published data (Kauder and Racaniello, 2004; Semler, 2004).

A recent publication shows attenuation of recombinant HSV-1, in which the HRV2 IRES was used to control translation of γ34.5. This protein encoded by HSV-1 counteracts the innate immune system by blocking PKR (Campbell et al., 2007). The authors explained this attenuated phenotype, as a result of neuroattenuation due to a neuron specific inhibition of the HRV2 IRES by the two cellular proteins DRBP76 and NF45, forming a heterodimer exclusively in neuronal cells (Merrill and Gromeier, 2006; Merrill et al., 2006). In contrast, data obtained in our study support the observation, that IRES-mediated translation occurs in all cell types (Kauder and Racaniello, 2004), as observed for other IRES elements like the one from EMCV (Creancier et al., 2000) or Theiler's murine virus (Shaw-Jackson and Michiels, 1999). Thus, our findings do not support the explanation of Campbell et al., that neuroattenuation is the consequence of a cell-specific defect of certain IRES elements. More likely, the attenuated phenotype of the recombinant HSV-1 results from effects on the innate

immune system and from a general poor virus propagation in all tissues leading to viral clearance (Racaniello, 2006), as it is also the case in the present IRES-controlled RVs.

The ideal conception of neuron specific translational attenuation of RV gene expression by the HRV2 IRES was apparently not achievable with the present IRES elements. Anyway, a severe attenuation *in vivo* was expected, due to the observed reduced capacities in replication and in IFN escape. Indeed, reduced growth kinetics and in particular, the impaired IFN countermeasures, due to translational control of P protein synthesis resulted in an astonishing high degree of attenuation *in vivo*, as was obvious from complete loss of mortality in 3-week-old mice after intracerebral infection. Though a major contribution for *in vivo* attenuation was attributed to altered virus growth, IFN mechanisms are supposed to play a crucial role in the elimination of the i.c. injected recombinant rabies viruses from the CNS.

As the RV P protein was identified as an interferon antagonist (Brzozka et al., 2005), a lower P protein synthesis by IRES-controlled RVs, compared to wt RV, could be responsible for the highly effective IFNβ induction and the survival of i.c. infected mice. Both IRES-controlled viruses were highly attenuated leading to 100% survival of infected 3-week-old mice. In 3-day-old suckling IFNAR knock out mice, lacking an intact immune system, a different picture was observed. After inoculation of these mice with SAD PV-P and SAD HRV2-P both viruses were lethal, however with a clearly delayed time course of 4 and 8 days, respectively, in comparison with wt RV infected mice. The residual pathogenicity of IFN-inducing viruses in 3-day-old mice is most probably related to not fully matured immune mechanisms such as IFNα secretion, which has been found to be low for preDCs from 1-day-old mice (Dakic et al., 2004). In addition the HRV2 IRES-dependent translational activity is suggested to be highly age dependent (Kauder et al., 2006), such that newborn mice infected with SAD HRV2-P still died, although with a clear delay in the time point of death.

Indeed, in previous studies it was shown that deletion of the P gene leads to replication-incompetent single round viruses (Finke et al., 2004), which are thus also apathogenic for mice (Morimoto et al., 2005; Cenna et al., 2008). However, attenuated replication-competent RVs could be generated previously only by modification of the G protein, which is responsible for the neuroinvasiveness of RV (Klingen et al., 2008; Faber et al., 2004; Morimoto et al., 2000) and is required for the spread between neurons (Etessami et al., 2000; Wickersham et al., 2007b; Wickersham et al., 2007a). In particular, an arginine residue (R333) of the glycoprotein has been shown to be responsible for RV virulence in adult mice (Dietzschold et al., 1983; Seif et al., 1985; Tuffereau et al., 1989). Thus, attenuating R333 mutations are often incorporated into “second generation” live RV vectors considered as

heterologous vaccines, particularly against HIV-1 (McGettigan et al., 2003). In addition, combinations of R333 variants with other mutations, such as a deletion of an 11 aa stretch representing the dynein light chain binding site of the P protein have been used to further attenuate the viruses (Mebatsion, 2001). The latter modification may reduce RV transcription in brain cells (Tan et al., 2007) while it does not affect the ability of P to counteract IFN. While these RVs are avirulent for adult mice, they still kill suckling or newborn mice after i.c. inoculation (Mebatsion, 2001; McGettigan et al., 2003). With the exception of these glycoprotein mutants (Morimoto et al., 2000) the IRES-controlled RVs described in this work are the first examples of fully replication-competent recombinant RVs that have lost their pathogenic potential even after intracranial injection, by a modification on gene expression level. Neither mutations in the P protein nor the insertion of an extra gene between the N and P genes in a "second-generation RV vector" (McGettigan et al., 2003) were able to provide this clear-cut effect.

The results provided here demonstrate a direct positive correlation of IRES translation activity, accumulation of P protein, RV replication, and the capability of recombinant RV to prevent IFN-mediated antiviral host responses. The present HRV2 IRES-controlled RV is the first example of a fully replication competent recombinant RV that has lost its pathogenic potential even after i.c. injection in newborn mice, illustrating that the IFN antagonistic function of P is a major virulence factor. This new strategy of reducing expression of virulence genes by the use of IRES elements is particularly promising for development of safe live RV vaccines and vectors.

4.2.2. Analysis of RV P forms by IRES-controlled RVs

This and other studies illustrated that RV P is essential for important viral functions like replication and countermeasures against the host innate immune system. Nevertheless, dissection of special functions of the three, additional N-terminally truncated P forms within the virus context was still not feasible. A recombinant RV lacking expression of P2-P4 was not severely attenuated in growth compared to wt RV (Brzozka et al., 2005). As only P1 contains the L-binding domain, which is necessary for its function as the polymerase cofactor, it is essential for virus replication and cannot be deleted from the viral genome. Accordingly, the generation of recombinant viruses, which could help to dissect special roles of the four P forms is challenging. As P1 can take over possible functions of other P forms, their importance is concealed. The deletion of other P forms by mutations within the downstream start codon sequence will not become visible in the presence of P1. Furthermore, these

mutations also change the sequence of full-length P1 from methionine to another amino acid. Therefore differences in the virus phenotype cannot be attributed clearly to the deleted P protein, as also the amino acid exchange might have an effect on the function of full-length P.

In this work this problem was approached by exploiting specific features of the IRES element of FMDV. One characteristic of the FMDV IRES is its mode of start codon selection. As it is for the PV genome, the FMDV genome contains two in frame AUGs downstream of the IRES element. In both cases the ribosome is initially recruited to the first AUG in closest proximity to the IRES (Belsham and Jackson, 2000; Belsham, 1992; Belsham, 2009). But whereas translation initiation by the PV IRES starts directly from this first AUG(1) (Ohlmann and Jackson, 1999), FMDV IRES dependent translation initiation occurs preferentially (80%) from the second AUG(2), located 84 nt downstream of AUG(1) (Andreev et al., 2007; Lopez and Martinez-Salas, 1999). Although we addressed the mechanism of start codon selection by picornaviral IRES elements within the RV-based reporter system, we could not clarify the exact mechanism.

Irrespective of this lack of clarity, the use of the FMDV IRES within recombinant IRES-controlled RVs provides a possibility to change the relative amounts of P1 and P2 within the virus context without changing the sequence of the P gene. Therefore, equivalent to SAD PV-P, recombinant RVs were generated in which P expression from a bicistronic mRNA occurs FMDV IRES-dependently (SAD FMDV-P). SAD PV-P expresses more P1 than P2, thus reflecting the wildtype RV situation. Expression levels of P1 and P2 from SAD FMDV-P are inverted, such that this virus expresses only low amounts of P1, but higher levels of P2. The closer analysis of FMDV IRES-dependent P expression revealed furthermore that the tendency of translation initiation towards a downstream AUG is continued to the third AUG, such that also P3 is expressed to higher amounts, compared to SAD PV-P. This approach is therefore the first one, which allows the generation of recombinant RVs expressing diverse relative amounts of P proteins without deletion of one special P form and without changes in the sequence of the P gene.

By the use of the FMDV IRES-controlled RVs, we could confirm several predicted roles of the four P proteins in the virus context. First, growth curve analyses in IFN-incompetent cells confirmed the essential role of P1 in RNA replication (Mavrakis et al., 2004; Chenik et al., 1998). As only P1 contains the L-binding domain, recombinant RVs, which express low levels of P1 (SAD FMDV-P and SAD FMDV-P_1x34) are attenuated in their growth. This insufficiency cannot be rescued by higher amounts of P2, which is lacking the L-binding domain.

Both domains were shown to be responsible for binding of IRF3 and STAT1, which are necessary for the phosphoprotein's function to interfere with the host immune system (Brzozka et al., 2005; Brzozka et al., 2006; Vidy et al., 2005; Vidy et al., 2007) are located in the C-terminal part of the protein and therefore are contained in all four P forms. As already described, recombinant RVs, which express low amounts of total P (SAD PV-P or SAD ΔPLP (Brzozka et al., 2005)), are hindered in their ability to interfere with IFN induction and signaling. Notably, although amounts of total P, expressed from SAD FMDV-P are similar to those of SAD PV-P, the former virus shows improved IFN antagonism, most likely due to an enhanced expression of P2 and P3 (although P3 levels may be neglectable). This led us suggest that P2 and P3 are sufficient for the function of the P protein as the IFN antagonist, and that both proteins are instrumental in the virus context. As these P forms are not able to take over functions in RNA replication, the whole amount of P2 and P3 is available to counteract the IFN system.

Another feature of RV P is its activity as a chaperone for RNA encapsidation by RV N. As only encapsidated RNA can serve as a template for transcription and replication (Jacob et al., 2001; Gerard et al., 2009), this is another essential function of P, necessary for virus gene expression and RNA replication. Two domains within the P protein were identified to interact with RV N. One domain, located in the N-terminal part between aa 10 and 52, is responsible for binding of newly synthesized nucleoproteins, thereby keeping them in a soluble form (Mavrakis et al., 2006; Chen et al., 2007). In contrast, the second, C-terminal domain allows the binding to already encapsidated RNA, resulting in RNP complex formation (Chenik et al., 1994; Jacob et al., 2001). The importance of the N-terminal domain, involved in RNA encapsidation, is suggested by a recombinant RV expressing P under control of the FMDV IRES, but lacking P2 (SAD FMDV-P_1x34). Although this virus expresses similar amounts of P1 compared to SAD FMDV-P, growth kinetics are reduced by one $\log_{10}$. Although the first 10 aa of the suggested N-binding domain are not included in P2, it seems that P2 is sufficient for the interaction with soluble N, such that a proper RNA encapsidation is assured.

Accordingly, the use of the FMDV IRES for expression of RV P within recombinant RVs (SAD FMDV-P), provides the first possibility to express different amounts or ratios of the four P forms from the same mRNA, without changing its sequence. Further biochemical analyses with these viruses confirmed the importance of diverse binding domains within RV P. Hence, P1 serves as the polymerase cofactor. P2 is lacking this function, but is still able to keep RV N in solution, such that RNA encapsidation is guaranteed. Although P3 cannot take over these two functions, it is still active as IFN antagonist, interfering with IFN induction and

IFN signaling. Taken together, findings demonstrate the teamwork of diverse P forms within the virus, such that all viral functions can be fulfilled properly.

In summary, the present work provides new approaches to study IRES elements in a highly suitable RNA virus system, and to regulate and to modify NNSV protein expression. The novelty of the present approach is the regulation of gene expression of RV, as a model for all other *Mononegavirales*, by IRES-dependent translation initiation of essential gene products. Though there is a big gap in understanding the mechanisms of internal translation initiation (Kozak, 2003; Kozak, 2007) the highly attenuated phenotypes of the IRES-controlled RVs *in vivo*, as well as the combination with IFN-induction phenotypes is encouraging to proceed in this new strategy of Negative Strand RNA virus attenuation. Furthermore, the use of special features of IRES elements, like e.g. the special start codon usage of the FMDV IRES, allows alteration of gene expression, without changing sequences. With increasing knowledge about specific conditions influencing IRES activities, this strategy might be useful in the development of safe life virus vaccines as well as a general mean for the generation of safe NNSV vectors.

5. SUMMARY

Rabies virus (RV; *Rhabdoviridae* family) is a prototype virus of nonsegmented negative strand RNA viruses (*Mononegavirales order).* Its gene expression is regulated almost entirely at the transcriptional level. Efforts to control viral gene expression focused mainly on modifications on transcriptional level. In this work, for the first time an alternative strategy was successfully employed, namely to control expression of essential RV gene products on the translational level, by the use of internal ribosome entry sites (IRES).

At first, a RV-based dual luciferase system, which allows proper characterization of IRES translation initiation activities, was established. Since RV replicates its RNA exclusively in the cytoplasm, this new system does not suffer from drawbacks of conventional DNA plasmid-based reporter systems, including the presence of cryptic DNA promoters and RNA splice sites. The activities of diverse IRES elements from picornaviruses and flaviviruses were determined in a variety of cell lines from different species. While IRESs greatly differed in their capacities to direct of translation initiation (PV>HRV2≥FMDV for picornavirus IRESs and HCV>CSFV≥BVDV for flaviviruses), proposed cell type specific restrictions were not detectable. Moreover, effects of virus-specific 3'UTR sequences on the activities of picornavirus IRES elements could also be excluded, suggesting that these do not affect translation initiation but rather replication functions of the respective IRES elements in the parental virus context. Comparison of picornavirus IRES elements further suggested that start codon selection is determined by the individual IRES. While all IRES elements from RNA viruses exhibited marked activity, a proposed cellular IRES, the 5'UTR of the p27 mRNA, failed to initiate translation in the new RV-based RNA system.

IRES elements of poliovirus (PV) and rhinovirus type 2 (HRV2) were then used to direct the expression of the essential RV phosphoprotein (P) from a bicistronic N-P mRNA. The P protein is critically required for both viral replication and escape from the host interferon response. The IRES elements reduced expression of P to approximately 60% and 30% of wt RV levels, respectively, resulting in specific attenuation of virus replication in cell culture and in neurons of organotypic brain slice cultures. In addition, infection with the recombinant viruses caused an increased activation of the IFNβ promoter, and increased sensitivity to IFN, according to the level of P expression. Intracerebral infection of mice revealed a complete loss of virulence both for wt mice and for transgenic animals lacking a functional IFNα receptor.

The preferential initiation of translation at a downstream AUG by the IRES of FMDV was further utilized to dissect the roles of N-terminally truncated P proteins in the RV life cycle.

Recombinant RVs expressing RV P via the FMDV IRES confirmed the essential, non-redundant role of full-length P (P1) as a polymerase cofactor while truncated P proteins (P2) were still able to support IFN escape.

Taken together, the present work provides a novel approach to study IRESs in the context of RV, and to control RV gene expression by IRES elements. Translational control as described here is a promising strategy to attenuate replication, host immune escape, and virulence of recombinant members of the *Mononegavirales*.

6. ZUSAMMENFASSUNG

Viren deren Genom aus einer einzelnen, nicht-segmentierten RNA negativer Polarität besteht, werden in der Ordnung der *Mononegavirales* zusammengefasst. Prototyp dieser Ordnung ist das Tollwutvirus (rabies virus, RV). Da alle Mitglieder der *Mononegavirales* ihre Genexpression ausschließlich auf transkriptioneller Ebene regulieren, wurden in den bisherigen Arbeiten, Modifikationen, die sich auf die Transkription auswirken, dazu verwendet die Genexpression dieser Viren zu beeinflussen. In dieser Arbeit wurde eine neue Strategie erfolgreich angewandt, die es durch den Einsatz von IRES Elementen (interne ribosomale Eintrittsstelle, engl. internal ribosomal entry site) ermöglicht die Expression der Genprodukte des Tollwutvirus auf Translationsebene zu kontrollieren.

Hierfür wurde zunächst ein RV-basiertes, duales Luziferase-System etabliert, welches ermöglicht die Aktivität von verschiedenen IRES Elementen bei der Translationsinitiation zu bestimmen. Da die Replikation des Tollwutvirus ausschließlich im Zytoplasma stattfindet, unterliegt dieses RV-basierte, duale Luziferase-System nicht den Nachteilen (wie z.B. dem Vorkommen von verborgenen Promotoren oder RNA Spleißstellen) der konventionellen, bisher verwendeten DNA Plasmid-basierten Reportersystemen. Mit Hilfe dieses Systems wurden Aktivitäten verschiedener IRES Elemente der Picorna- und Flaviviren in unterschiedlichen Zelllinien verschiedenen Ursprungs bestimmt. Es stellte sich heraus, dass sich die IRESs im Grad ihrer Aktivität unterscheiden (PV>HRV2≥FMDV für picornavirus IRESs und HCV>CSFV≥BVDV für flavivirus IRESs). Eventuelle zelltyp-spezifische Unterschiede wurden jedoch nicht beobachtet. Des Gleichen zeigten auch virus-spezifische Sequenzen der 3'NTR (nicht translatierte Region) keinerlei Einfluss auf die Aktivität der picornavirus IRESs, so dass angenommen wird, dass diese Sequenzen eher die Funktion der IRES bei der Virusreplikation beeinflussen, als die Translationsinitiation. Ferner konnte durch den Vergleich verschiedener picornavirus IRES Elemente gezeigt werden, dass die Wahl des Startkodons individuell durch die IRES bestimmt werden kann. Im Gegensatz zu den untersuchten viralen IRESs, die alle sehr gute Aktivität aufwiesen, zeigte das 5'NTR der p27 mRNA, das möglicherweise eine IRES enthalten könnte, keinerlei Aktivität in dem neu etablierten RV-basierten, dualen Luziferase-System.

Auch wurden die IRES Elemente des Poliovirus (PV) und des Humanen Rhinovirus Typ 2 (HRV2) dazu verwendet, um die Expression des essentiellen Tollwutvirus Phosphoproteins (RV P) von einer bicistronischen N-P mRNA gezielt zu beeinflussen. Die Einführung der IRESs führt zu einer reduzierten P Expression von 60% im Falle der PV IRES bzw. 30% im

Falle der HRV2 IRES, im Vergleich zur wildtyp RV P Expression. Da RV P sowohl essentiell für Virusreplikation ist, als auch als wesentlicher Antagonist des IFN Systems dient, bewirkt die verminderte P Expression durch die IRESs einerseits eine spezifische herabgesetzte RV Replikation in Zellkultur und in Neuronen organotypischer Hirnschnitte. Andererseits wird nach Infektion mit den rekombinanten Tollwutviren, je nach Grad der P Expression, der IFNβ Promotor verstärkt aktiviert und die Sensitivität gegenüber IFN erhöht. Ferner konnte in Mausexperimenten ein kompletter Virulenzverlust nach intracerebraler Infektion sowohl von wildtyp Mäusen als auch von Mäusen, denen ein funktionaler IFNα Rezeptor fehlt, beobachtet werden.

Außerdem wurde die besondere Eigenschaft der FMDV IRES, bevorzugt das zweite AUG als Startkodon zu nutzen, angewendet, um die einzelnen Rollen N-terminal verkürzter P Proteine im Replikationszyklus des Tollwutvirus zu analysieren. Anhand rekombinanter RVs, die P unter Kontrolle der FMDV IRES exprimieren, konnte die essentielle, einmalige Rolle des vollelänge P Proteins (P1) als Polymerase-Cofaktor bestätigt werden. Dennoch können auch N-terminal verkürzte P Proteine (P2) unterstützend wirken, indem sie z.B. dem Virus dabei helfen dem IFN System zu entgehen.

Zusammenfassend zeigt diese Arbeit einen neuen Ansatz, um einerseits IRES Elemente im Tollwutviruskontext zu untersuchen und andererseits anhand der IRES die RV Genexpression zu kontrollieren. Die in dieser Arbeit beschriebene Translationskontrolle durch IRES Elemente stellt eine viel versprechende Strategie dar, Replikation, Immuneescape und Virulenz aller rekombinanter Vertreter der *Mononegavirales* zu attenuieren.

APPENDIX

family	subfamily	genus	members
Rhabdoviridae		*Vesiculovirus*	Vesicular stomatitis virus (VSV) Chandipuravirus (CHPV)
			rabies virus (RV)
		Lyssavirus	Lagos bat virus (LBV) Mokola virus (MOKV) Duvenhage virus (DUVV) European Bat Lyssavirus 1 (EBLV-1) European Bat Lyssavirus 2 (EBLV-2) Australian Bat Lyssavirus (ABLV)
		Ephemerovirus	bovine ephemeral fever virus (BEFV)
		Novirhabdovirus	Infectious hematopoietic necrosis virus (IHNV)
		Cytorhabdovirus	Lettuce necrotic yellows virus (LNYV)
		Nucleorhabdovirus	Potato yellow dwarf virus (PYDV)
Paramyxoviridae	*Paramyxovirinae*	*Respirovirus*	Sendai virus (SeV)
		Morbillivirus	Measels virus (MeV) Rinderpest virus (RPV)
	Pneumovirinae	*Rubulavirus*	Parainfluenza virus 2 and 4 Mumps virus (MuV)
		Henipavirus	Nipah virus (NiV) Hendra virus (HeV)
		Avulavirus	Newcastle disease virus (NDV)
		Pneumovirus	Avian paramyxovirus 2-9 (APMV 2-9) Respiratory syncytial virus (RSV)
		Metapneumovirus	Avian Metapneumovirus
Bornaviridae		*Bornavirus*	*Borna disease virus* (BDV)
Filoviridae		*Marburgvirus* *Ebolavirus*	Marburgvirus (MARV) Ebola virus (EBOV)

Tab. A1: The order of *Mononegavirales* (2002a)
The order of *Mononegavirales*, includes non-segmented negative-strand RNA viruses, containing the families of Rhabdo-, Paramyxo-, Borna- and Filoviridae (2002b).

Virus	Viral name–product	Viral host	GI (IRES seq. pos.)	Reference
Dicistroviridae; Cripavirus				
CrPV	Cricket paralysis virus ORF1–nonstructural proteins	Insect	8895506 (1–711)	Wilson et al. 2000b
CrPV	ORF2–structural proteins	Insect	8895506 (6025–6216) contains ccu start codon needed for pseudoknot	Wilson et al. 2000b
DCV	*Drosophila* C virus IRES1	Insect	2388672 (1–801)	Johnson and Christian 1998
DCV	*Drosophila* C virus IRES2	Insect	2388672 (6080–6266) contains ccu start codon needed for pseudoknot	Johnson and Christian 1998; Kanamori and Nakashima 2001
PSIV	Plautia stali intestine virus – capsid protein	Insect	2344756 (5949–6195)	Sasaki and Nakashima 1999
RhPV	*Rhopalosiphum padi* ORF2	Insect	2911298 (6327–7112) gca start codon	Domier et al. 2000
TRV	Triatoma virus–5′-UTR	Insect	6003484 (1–551)	Czibener et al. 2005
TRV-IGR	Triatoma virus–intergenic region	Insect	6003484 (5934–6111)	Czibener et al. 2005
TSV	Taura syndrome virus–capsid protein	Shrimp	Contains ccu start codon needed for pseudoknot	Hatakeyama et al. 2004
Flaviviridae; Hepacivirus				
HCV	Hepatitis C virus	Human	12831192 (1–344)	Tsukiyama-Kohara et al. 1992
Flaviviridae; Pestivirus				
BVDV	Bovine viral diarrhea virus	Cow	9836967 (1–385)	Poole et al. 1995
CSFV/ HoCV	Classical swine fever virus/hog cholera virus	Pig	12584212 (1–376)	Rijnbrand et al. 1997
Flaviviridae; Unclassified				
GBV-B	Hepatitis virus insolated B from patient GB	Primates	13162187 (23–448)	Grace et al. 1999
Herpesviridae; Rhadinovirusds (dsDNA)				
KSHV	Karposi-sarcoma-associated herpesvirus v-flip	Human	2065526 (123206–122709)	Bieleski and Talbot 2001; Grundhoff and Ganem 2001; Low et al. 2001
Retroviridae				
F-MuLV	Friend murine leukemia virus glygag and gag polyprotein	Mouse	61544 (1–357) 61544 (1–621)	Berlioz and Darlix 1995
F-MuLV	Friend murine leukemia virus – envelope gene	Mouse	61544 (5492–5780)	Deffaud and Darlix 2000a
HaMSV	Harvey murine sarcoma virus –VL30	Rat	207672 (25–543)	Berlioz et al. 1995
HTLV-1	Human T-cell Lymphotropic virus 1–R and partial U5 region	Human	221866 (354–621) No start codon	Attal et al. 1996
MoMuLV	Moloney murine leukemia virus	Mouse	331973 (912–1040)	Vagner et al. 1995b
RSV	Rous sarcoma virus–gag	Chicken	2801459 (230–382)	Deffaud and Darlix 2000b
RSV-src	Rous sarcoma virus–src	Chicken	2801459 (7066–7131) No proof that full spliced UTR exists	Deffaud and Darlix 2000b
SIV	Simian immunodeficiency virus	Primate	334657 (507–1043)	Ohlmann et al. 2000
Picornaviridae; Aphthovirus				
FMDV	Foot and mouth disease virus	Mammals	61076 (252–716)	Kuhn et al. 1990
Picornaviridae; Cardiovirus				
EMCV	Encephalomyocarditis virus	Human	9626692 (260–836)	Jang et al. 1988
TMEV	Theiler's murine encephalomyelitis virus	Mouse	62039 (31–1070)	Pilipenko et al. 1994

(*continued*)

Virus	Viral name–product	Viral host	GI (IRES seq. pos.)	Reference
Picornaviridae; Enterovirus				
CVB3	Coxsackievirus B3	Human	54399970 (1–745)	Yang et al. 1997
EV71	Enterovirus 71 strain BrCr	Human	1171120 (1–746)	Thompson and Sarnow 2003
PV	Poliovirus	Human	61127 (34–750)	Pelletier and Sonenberg 1988
Picornaviridae; Hepatovirus				
HAV	Hepatitis A virus	Human	329585 (150–720)	Brown et al. 1994
Picornaviridae; Rhinovirus				
HRV	Human rhinovirus	Human	221708 (20–625)	Borman and Jackson 1992
Picornaviridae; Teschovirus				
PTV-1	Porcine teschovirus serotype 1 strain Talfan	Pig	13111645 (146–434)	Pisarev et al. 2004
Lentivirus; primate lentivirus group				
HIV	Human immunodeficiency virus type 1 gag	Human	4558520 (335–808) Note: resides in CDS	Buck et al. 2001
Luteoviridae; Polerovirus				
PLRV	Potato leafroll virus	Plant (potato)	222301 (1513–1728) Includes 211 bases of CDS	Jaag et al. 2003
Potyviridae; Potyvirus				
CPMV	Cowpea mosaic virus	Plant	58910 (161–514)	Thomas et al. 1991
PVY	Potato virus Y	Plant	61450 (1–187)	Levis and Astier-Manifacier 1993
TEV	Tobacco etch virus	Plant	335201 (2–147)	Carrington and Freed 1990
Poxviridae; Avipoxvirus (dsDNA)				
REV	Avian reticuloendotheliosis virus type A	Bird	28927668 (400–974)	Lopez-Lastra et al. 1997
Tobamovirus				
crTMV	Tobacco mosaic virus (Crucifer)–cpgene	Plant	488713 (5456–5606)	Ivanov et al. 1997
Totiviridae; Giardiavirus (dsRNA virus)				
GLV	*Glardia lamblia* virus	*Glardia lamblia*	1352866 (1–369)	Garlapati and Wang 2005

Sequences are either the minimal sequence of the fully functioning IRES or the beginning of the known 5′-UTR. The sequences' 3′-end includes the start codon, position +3. Some errors in the published positions have been corrected upon communications with the authors where possible.

Tab A2: Viral IRES elements (Baird et al., 2006)

Gene name	Function	Organism	GI (IRES seq. pos.)	Reference
α-CaM kinase II	α subunit of Ca-calmodulin-dependent kinase II	Rat	203208 (280–431)	Pinkstaff et al. 2001
ABETA	Amyloid β A4 precursor protein	Human	341201 (899–1049)	Qin and Sarnow 2004
AML1/RUNX1	Transcription factor	Human	2944212 (8498–10040)	Pozner et al. 2000
Antp	Antennapedia–homeotic gene	*Drosophila*	16648361 (1–1709)	Oh et al. 1992
Apaf-1	Pro-apoptotic factor	Human	2330014 (1–580)	Coldwell et al. 2000
APC	Adenomatosis polyposis coli gene	Human	182396 (487–570)	Heppner Goss et al. 2002
ARC	Cytoskeleton association protein	Rat	854413 (1–200)	Pinkstaff et al. 2001
AT1R	Angiotensin II type 1 receptor–G-protein-coupled receptor	Human	18490885 (1–275)	Martin et al. 2003
BAG-1 p36	Anti-apoptotic factor	Human	1143475 (1–413)	Coldwell et al. 2001
Bcl-2	Anti-apoptotic factor	Human	179366 (313–1461)	Sherrill et al. 2004
BiP	ER protein chaperone	Human	1143491 (1–225)	Macejak and Sarnow 1991
βPix-b_L	Pak-interacting exchange factor isoform b	Mouse	37788384 (1–375)	Rhee et al. 2004
Cat-1	Cationic amino acid transporter	Rat	18542255 (1–273)	Fernandez et al. 2001
c-Jun	Transcription factor	Chicken	212221 (500–815)	Sehgal et al. 2000
c-Myb	Transcription factor	Human	45502012 (1–202)	Mitchell et al. 2005
c-Myc	Transcription factor	Human	11493193 (2501–2881, 4506–4523)	Stoneley et al. 1998
Connexin26	Gap junction protein	Human	1762120 (1472–1631, 4780–4804)	Lahlou et al. 2005
Connexin32	Gap junction protein	Human	974140 (404–529, 884–903)	Hudder and Werner 2000
Connexin43	Gap junction protein	Rat	45593193 (1–232)	Schiavi et al. 1999
CCND1	Cyclin D1	Human	22788696 (1380–1591)	Shi et al. 2005
Cyr61	Intracellular signaling	Human	2791897 (1–226)	Johannes et al. 1999
DAP5	Translation initiation factor	Human	1903413 (1–357)	Henis-Korenblit et al. 2000
Dendrin	Putative modulator of the post-synaptic cytoskeleton	Rat	1752674 (1–151)	Pinkstaff et al. 2001
eIF4G	Translation initiation factor	Human	21655145 (341–538)	Johannes and Sarnow 1998
ERα	Estrogen receptor α	Human	182192 (293–814)	Barraille et al. 1999
FMR1	RNA binding protein	Human	1668818 (13698–13964)	Chiang et al. 2001
FGF1a	Fibroblast growth factor 1 A – angiogenic factor	Human	178226 (1–360)	Martineau et al. 2004
FGF1a	Fibroblast growth factor 1 A angiogenic factor	Mouse	4321971 (865–1238)	Martineau et al. 2004
FGF1b	Fibroblast growth factor 1 B angiogenic factor	Human	9125828 (35–185)	Martineau et al. 2004
FGF1c	Fibroblast growth factor 1 C angiogenic factor	Human	Poorly defined	Martineau et al. 2004
FGF1d	Fibroblast growth factor 1 D angiogenic factor	Human	21595686 (10–93)	Martineau et al. 2004
FGF2	Fibroblast growth factor	Human	31361 (486–809)	Vagner et al. 1995a; Bonnal et al. 2003b
HAP4	Transcriptional activator	Yeast	3762 (228–503)	Iizuka et al. 1994
Hairless	Transcription repressor	Fly	157621 (686–1072)	Maier et al. 2002
Hiap2	Anti-apoptotic protein	Human	34367137 (1313–1465)	Warnakulasuriyarachchi et al. 2004
HIF-1α	Transcription factor	Mouse	12857319 (1–287)	Lang et al. 2002
HnRNPA/B	Heterogeneous nuclear riboprotein A/B	Human	33872877 (1–227)	Qin and Sarnow 2004
Hsp70	Heat shock protein	Human	184416 (274–491)	Rubtsova et al. 2003 contradicts Yueh and Schneider 2000
Hsp70	Heat shock protein	Fly (Dm)	157720 (1514–1757)	Hernandez et al. 2004
Hsp101	Heat shock protein	Plant	4584956 (290–438)	Dinkova et al. 2005
IGF-II leader 1	Insulin-like growth factor II–UTR leader 1	Human	26190552 (130580–130698, 139619–139838, 141156–141399, 153434–153443)	Teerink et al. 1995

(*continued*)

Gene name	Function	Organism	GI (IRES seq. pos.)	Reference
IGF-II leader 2	Insulin-like growth factor II–UTR leader 2	Human	6453816 (125–755)	Pedersen et al. 2002
IGF-IR	Growth factor receptor	Rat	204774 (413–1358)	Giraud et al. 2001
Kv1.4	Voltage-gated potassium channel	Mouse	26331157 (1–1201)	Negulescu et al. 1998
La1	RNA binding protein—more abundant transcript	Human	511006 (240–345, 2329–2340)	Carter and Sarnow 2000
La1′	RNA binding protein—less abundant transcript	Human	511006 (698–886, 2329–2340)	Carter and Sarnow 2000
LEF-1	Lymphoid enhancer factor	Human	22858703 (1523–2703)	Jimenez et al. 2005
L-myc	Lung myc	Human	188906 (224–431, 796–807)	Jopling et al. 2004
MAP2	Cytoskeleton-associated protein	Rat	987493 (1–370)	Pinkstaff et al. 2001
Mnt	MAX binding protein–transcriptional repressor	Human	1841919 (35–215)	Stoneley et al. 2001
MS	Methionine synthase	Human	1763268 (126–397)	Oltean and Banerjee 2005
MTG8a (RUNX1T1)	Transcription factor	Human	940399 (1–411)	Mitchell et al. 2005
MYCHEX1	Upstream open reading frame on c-Myc transcript	Human	11493193 (2223–2306)	Nanbru et al. 2001
Myt2	Myelin transcription factor 2	Rat	2246660 (997–1158)	Kim et al. 1998
Nap1L1	Nucleosome assembly protein 1–like 1	Human	461207 (16–142)	Qin and Sarnow 2004
NBS1	Nijmegen breakage syndrome allele	Human	Undefined	Maser et al. 2001
Neurogranin (RC3)	Neural-specific regulator of CaMKII activity	Rat	924645 (4217–4478)	Pinkstaff et al. 2001
Nkx6.1	Homeodomain transcription factor	Mouse	11118686 (2988–3959)	Watada et al. 2000
N-myc	Neuronal myc–transcription factor	Human	11692795 (1–324)	Jopling and Willis 2001
Notch2	Intercellular signaling receptor	Fly	1622786 (1–238)	Lauring and Overbaugh 2000
NPM1	Nucleophosmin	Human	2745708 (1222–1320)	Qin and Sarnow 2004
NRF	NF-κB repressing factor–transcription factor	Human	7406601 (1–656)	Oumard et al. 2000
ODC	Ornithine decarboxylase	Rat	205803 (1–426)	Pyronnet et al. 2000
P150(TIF4631)	Translation initiation factor homolog of eIF4G	Yeast	1323279 (14130–14641)	Zhou et al. 2001
P27(Kip1)	Cyclin-dependent kinase inhibitor	Mouse	532771 (1–221)	Miskimins et al. 2001
PKCδ	Protein kinase C delta	Rat	206180 (7–365)	Morrish and Rumsby 2002
PITSLRE	Cyclin-dependent kinase	Human	507159 (946–1128)	Cornelis et al. 2000; Tinton et al. 2005
PP2Cβ	Protein phosphatase 2Cβ	Rat	12666526 (1–400)	Seroussi et al. 2001
Reaper	Pro-apoptotic protein	Fly (Dm)	476009 (1–174)	Hernandez et al. 2004
Runx2 Type I	Runt-related transcription factor 2–UTR2	Mouse	391766 (1–1018)	Xiao et al. 2003
Runx2 Type II	Runt-related transcription factor 2–UTR1	Mouse	3901257 (1–207)	Xiao et al. 2003
Scamper	Calcium channel	Dog	21553346 (268–368)	De Pietri Tonelli et al. 2003
Smad5	Mediator of bone morphogenetic protein signaling	Human	4433529 (259–360)	Shiroki et al. 2002
SNM1	Homolog of yeast "sensitivity to nitrogen mustard" gene	Human	577302 (1–921)	Zhang et al. 2002
TIE2	Tyrosine kinase with immunoglobulin-like and EGF-like domains 1	Human	28411198 (28326–27857)	Park et al. 2005
TFIID	Transcriptional activator	Yeast	172898 (86–275)	Iizuka et al. 1994
TRKB	Neurotrophin receptor–tropomyosin-related tyrosine kinase	Human	18369868 (3761–4040)	Dobson et al. 2005
Ubx	Ultrabithorax–homeotic gene	Fly	8794 (3518–4115)	Hart and Bienz 1996
Unr	Upstream of N-*ras*	Human	52220548 (1–468)	Cornelis et al. 2005
Utr	Utrophin	Mouse	74144053 (195–704)	Miura et al. 2005
V1br	Vasopressin V1b receptor	Rat	945040 (35–544)	Rabadan-Diehl et al. 2003
VEGF-A*iresA*	Vascular endothelial growth factor–A	Human(mouse)	4154290 (2864–3403), 1134964 (1218–2234)	Stein et al. 1998; Huez et al. 2001

(*continued*)

Gene name	Function	Organism	GI (IRES seq. pos.)	Reference
IGF-II leader 2	Insulin-like growth factor II–UTR leader 2	Human	6453816 (125–755)	Pedersen et al. 2002
IGF-IR	Growth factor receptor	Rat	204774 (413–1358)	Giraud et al. 2001
Kv1.4	Voltage-gated potassium channel	Mouse	26331157 (1–1201)	Negulescu et al. 1998
La1	RNA binding protein—more abundant transcript	Human	511006 (240–345, 2329–2340)	Carter and Sarnow 2000
La1′	RNA binding protein—less abundant transcript	Human	511006 (698–886, 2329–2340)	Carter and Sarnow 2000
LEF-1	Lymphoid enhancer factor	Human	22858703 (1523–2703)	Jimenez et al. 2005
L-myc	Lung myc	Human	188906 (224–431, 796–807)	Jopling et al. 2004
MAP2	Cytoskeleton-associated protein	Rat	987493 (1–370)	Pinkstaff et al. 2001
Mnt	MAX binding protein–transcriptional repressor	Human	1841919 (35–215)	Stoneley et al. 2001
MS	Methionine synthase	Human	1763268 (126–397)	Oltean and Banerjee 2005
MTG8a (RUNX1T1)	Transcription factor	Human	940399 (1–411)	Mitchell et al. 2005
MYCHEX1	Upstream open reading frame on c-Myc transcript	Human	11493193 (2223–2306)	Nanbru et al. 2001
Myt2	Myelin transcription factor 2	Rat	2246660 (997–1158)	Kim et al. 1998
Nap1L1	Nucleosome assembly protein 1–like 1	Human	461207 (16–142)	Qin and Sarnow 2004
NBS1	Nijmegen breakage syndrome allele	Human	Undefined	Maser et al. 2001
Neurogranin (RC3)	Neural-specific regulator of CaMKII activity	Rat	924645 (4217–4478)	Pinkstaff et al. 2001
Nkx6.1	Homeodomain transcription factor	Mouse	11118686 (2988–3959)	Watada et al. 2000
N-myc	Neuronal myc–transcription factor	Human	11692795 (1–324)	Jopling and Willis 2001
Notch2	Intercellular signaling receptor	Fly	1622786 (1–238)	Lauring and Overbaugh 2000
NPM1	Nucleophosmin	Human	2745708 (1222–1320)	Qin and Sarnow 2004
NRF	NF-κB repressing factor–transcription factor	Human	7406601 (1–656)	Oumard et al. 2000
ODC	Ornithine decarboxylase	Rat	205803 (1–426)	Pyronnet et al. 2000
P150(TIF4631)	Translation initiation factor homolog of eIF4G	Yeast	1323279 (14130–14641)	Zhou et al. 2001
P27(Kip1)	Cyclin-dependent kinase inhibitor	Mouse	532771 (1–221)	Miskimins et al. 2001
PKCδ	Protein kinase C delta	Rat	206180 (7–365)	Morrish and Rumsby 2002
PITSLRE	Cyclin-dependent kinase	Human	507159 (946–1128)	Cornelis et al. 2000; Tinton et al. 2005
PP2Cβ	Protein phosphatase 2Cβ	Rat	12666526 (1–400)	Seroussi et al. 2001
Reaper	Pro-apoptotic protein	Fly (Dm)	476009 (1–174)	Hernandez et al. 2004
Runx2 Type I	Runt-related transcription factor 2–UTR2	Mouse	391766 (1–1018)	Xiao et al. 2003
Runx2 Type II	Runt-related transcription factor 2–UTR1	Mouse	3901257 (1–207)	Xiao et al. 2003
Scamper	Calcium channel	Dog	21553346 (268–368)	De Pietri Tonelli et al. 2003
Smad5	Mediator of bone morphogenetic protein signaling	Human	4433529 (259–360)	Shiroki et al. 2002
SNM1	Homolog of yeast "sensitivity to nitrogen mustard" gene	Human	577302 (1–921)	Zhang et al. 2002
TIE2	Tyrosine kinase with immunoglobulin-like and EGF-like domains 1	Human	28411198 (28326–27857)	Park et al. 2005
TFIID	Transcriptional activator	Yeast	172898 (86–275)	Iizuka et al. 1994
TRKB	Neurotrophin receptor–tropomyosin-related tyrosine kinase	Human	18369868 (3761–4040)	Dobson et al. 2005
Ubx	Ultrabithorax–homeotic gene	Fly	8794 (3518–4115)	Hart and Bienz 1996
Unr	Upstream of N-*ras*	Human	52220548 (1–468)	Cornelis et al. 2005
Utr	Utrophin	Mouse	74144053 (195–704)	Miura et al. 2005
V1br	Vasopressin V1b receptor	Rat	945040 (35–544)	Rabadan-Diehl et al. 2003
VEGF-A*iresA*	Vascular endothelial growth factor–A	Human(mouse)	4154290 (2864–3403), 1134964 (1218–2234)	Stein et al. 1998; Huez et al. 2001
VEGF-A*iresB*	Vascular endothelial growth factor–A	Human	4154290 (2363–2863)	Stein et al. 1998; Huez et al. 2001
Vimentin	Structural protein	Human	2437834 (1758–1902)	Qin and Sarnow 2004
XIAP	Apoptosis inhibitor	Human	28290426 (306–409)	Holcik et al. 1999
YAP1	Yes-associated Protein 1 transcriptional activator	Yeast	4797 (207–333)	Zhou et al. 2001

Sequences are either the minimal sequence of the fully functioning IRES or the beginning of the known 5′-UTR. The sequences' 3′-end includes the start codon, position +3. Some errors in the published positions have been corrected upon communications with the authors where possible.

Tab. A3: Cellular IRES elements (Baird et al., 2006)

REFERENCES

1. ICTVdB - The Universal Virus Database, version 4. 2002b.
Ref Type: Generic

2. ICTVdB - The Universal Virus Database, version 4. 2002a.
Ref Type: Generic

3. Abraham,G. and Banerjee,A.K. (1976). Sequential transcription of the genes of vesicular stomatitis virus. Proc Natl Acad Sci U S A *73*, 1504-1508.

4. Albertini,A.A., Schoehn,G., Weissenhorn,W., and Ruigrok,R.W. (2008). Structural aspects of rabies virus replication. Cell Mol. Life Sci *65*, 282-294.

5. Albertini,A.A., Wernimont,A.K., Muziol,T., Ravelli,R.B., Clapier,C.R., Schoehn,G., Weissenhorn,W., and Ruigrok,R.W. (2006). Crystal structure of the rabies virus nucleoprotein-RNA complex. Science *313*, 360-363.

6. Ali,I.K., McKendrick,L., Morley,S.J., and Jackson,R.J. (2001). Activity of the hepatitis A virus IRES requires association between the cap-binding translation initiation factor (eIF4E) and eIF4G. J Virol *75*, 7854-7863.

7. Ali,N., Pruijn,G.J., Kenan,D.J., Keene,J.D., and Siddiqui,A. (2000). Human La antigen is required for the hepatitis C virus internal ribosome entry site-mediated translation. J Biol. Chem. *275*, 27531-27540.

8. Andino,R., Rieckhof,G.E., and Baltimore,D. (1990). A functional ribonucleoprotein complex forms around the 5' end of poliovirus RNA. Cell *63*, 369-380.

9. Andreev,D.E., Fernandez-Miragall,O., Ramajo,J., Dmitriev,S.E., Terenin,I.M., Martinez-Salas,E., and Shatsky,I.N. (2007). Differential factor requirement to assemble translation initiation complexes at the alternative start codons of foot-and-mouth disease virus RNA. RNA *13*, 1366-1374.

10. Auweter,S.D. and Allain,F.H. (2008). Structure-function relationships of the polypyrimidine tract binding protein. Cell Mol. Life Sci *65*, 516-527.

11. Baird,S.D., Turcotte,M., Korneluk,R.G., and Holcik,M. (2006). Searching for IRES. RNA *12*, 1755-1785.

12. Bakhshesh,M., Groppelli,E., Willcocks,M.M., Royall,E., Belsham,G.J., and Roberts,L.O. (2008). The picornavirus avian encephalomyelitis virus possesses a hepatitis C virus-like internal ribosome entry site element. J Virol *82*, 1993-2003.

13. Ball,L.A. and White,C.N. (1976). Order of transcription of genes of vesicular stomatitis virus. Proc Natl Acad Sci U S A *73*, 442-446.

14. Baloul,L., Camelo,S., and Lafon,M. (2004). Up-regulation of Fas ligand (FasL) in the central nervous system: a mechanism of immune evasion by rabies virus. J Neurovirol. *10*, 372-382.

15. Banerjee,A.K. (2008). Response to "Non-segmented negative-strand RNA virus RNA synthesis in vivo". Virology *371*, 231-233.

16. Barreau,C., Dutertre,S., Paillard,L., and Osborne,H.B. (2006). Liposome-mediated RNA transfection should be used with caution. RNA *12*, 1790-1793.

17. Bedard,K.M., Daijogo,S., and Semler,B.L. (2007). A nucleo-cytoplasmic SR protein functions in viral IRES-mediated translation initiation. EMBO J *26*, 459-467.

18. Bedard,K.M. and Semler,B.L. (2004). Regulation of picornavirus gene expression. Microbes Infect *6*, 702-713.

19. Bedard,K.M., Walter,B.L., and Semler,B.L. (2004). Multimerization of poly(rC) binding protein 2 is required for translation initiation mediated by a viral IRES. RNA *10*, 1266-1276.

20. Belsham,G.J. (1992). Dual initiation sites of protein synthesis on foot-and-mouth disease virus RNA are selected following internal entry and scanning of ribosomes in vivo. EMBO J *11*, 1105-1110.

21. Belsham,G.J. (2009). Divergent picornavirus IRES elements. Virus Res. *139*, 183-192.

22. Belsham,G.J. and Brangwyn,J.K. (1990). A region of the 5' noncoding region of foot-and-mouth disease virus RNA directs efficient internal initiation of protein synthesis within cells: involvement with the role of L protease in translational control. J Virol *64*, 5389-5395.

23. Belsham,G.J. and Jackson,R. (2000). Translation Initiation on Picornavirus RNA. In Translational Control of Gene Expression, N.Sonenberg, J.Hershey, and M.B.Mathews, eds. (New York: Cold Spring Harbor Laboratory Press), pp. 869-900.

24. Belsham,G.J. and Sonenberg,N. (2000). Picornavirus RNA translation: roles for cellular proteins. Trends Microbiol. *8*, 330-335.

25. Bert,A.G., Grepin,R., Vadas,M.A., and Goodall,G.J. (2006). Assessing IRES activity in the HIF-1alpha and other cellular 5' UTRs. RNA *12*, 1074-1083.

26. Bieleski,L. and Talbot,S.J. (2001). Kaposi's sarcoma-associated herpesvirus vCyclin open reading frame contains an internal ribosome entry site. J Virol *75*, 1864-1869.

27. Blondel,D., Regad,T., Poisson,N., Pavie,B., Harper,F., Pandolfi,P.P., De The,H., and Chelbi-Alix,M.K. (2002). Rabies virus P and small P products interact directly with PML and reorganize PML nuclear bodies. Oncogene *21*, 7957-7970.

28. Bonnal,S., Pileur,F., Orsini,C., Parker,F., Pujol,F., Prats,A.C., and Vagner,S. (2005). Heterogeneous nuclear ribonucleoprotein A1 is a novel internal ribosome entry site trans-acting factor that modulates alternative initiation of translation of the fibroblast growth factor 2 mRNA. J Biol. Chem. *280*, 4144-4153.

29. Borman,A. and Jackson,R.J. (1992). Initiation of translation of human rhinovirus RNA: mapping the internal ribosome entry site. Virology *188*, 685-696.

30. Both,G.W., Banerjee,A.K., and Shatkin,A.J. (1975). Methylation-dependent translation of viral messenger RNAs in vitro. Proc Natl Acad Sci U S A *72*, 1189-1193.

31. Brinks,H., Conrad,S., Vogt,J., Oldekamp,J., Sierra,A., Deitinghoff,L., Bechmann,I., Alvarez-Bolado,G., Heimrich,B., Monnier,P.P., Mueller,B.K., and Skutella,T. (2004). The repulsive guidance molecule RGMa is involved in the formation of afferent connections in the dentate gyrus. J Neurosci. *24*, 3862-3869.

32. Brown,D.M., Kauder,S.E., Cornell,C.T., Jang,G.M., Racaniello,V.R., and Semler,B.L. (2004). Cell-dependent role for the poliovirus 3' noncoding region in positive-strand RNA synthesis. J Virol *78*, 1344-1351.

33. Brown,E.A., Day,S.P., Jansen,R.W., and Lemon,S.M. (1991). The 5' nontranslated region of hepatitis A virus RNA: secondary structure and elements required for translation in vitro. J Virol *65*, 5828-5838.

34. Brown,E.A., Zajac,A.J., and Lemon,S.M. (1994). In vitro characterization of an internal ribosomal entry site (IRES) present within the 5' nontranslated region of hepatitis A virus RNA: comparison with the IRES of encephalomyocarditis virus. J Virol *68*, 1066-1074.

35. Brown,F., Cartwright,B., Crick,J., and Smale,C.J. (1967). Infective virus substructure from vesicular stomatitis virus. J Virol *1*, 368-373.

36. Brzozka,K., Finke,S., and Conzelmann,K.K. (2005). Identification of the rabies virus alpha/beta interferon antagonist: phosphoprotein P interferes with phosphorylation of interferon regulatory factor 3. J Virol *79*, 7673-7681.

37. Brzozka,K., Finke,S., and Conzelmann,K.K. (2006). Inhibition of interferon signaling by rabies virus phosphoprotein P: activation-dependent binding of STAT1 and STAT2. J Virol *80*, 2675-2683.

38. Brzozka,K., Pfaller,C., and Conzelmann,K.K. (2007). Signal transduction in the type I interferon system and viral countermeasures. Signal Transduction *7*, 5-19.

39. Buck,C.B., Shen,X., Egan,M.A., Pierson,T.C., Walker,C.M., and Siliciano,R.F. (2001). The human immunodeficiency virus type 1 gag gene encodes an internal ribosome entry site. J Virol *75*, 181-191.

40. Buonocore,L., Blight,K.J., Rice,C.M., and Rose,J.K. (2002). Characterization of vesicular stomatitis virus recombinants that express and incorporate high levels of hepatitis C virus glycoproteins. J Virol *76*, 6865-6872.

41. Bushell,M., Stoneley,M., Kong,Y.W., Hamilton,T.L., Spriggs,K.A., Dobbyn,H.C., Qin,X., Sarnow,P., and Willis,A.E. (2006). Polypyrimidine tract binding protein regulates IRES-mediated gene expression during apoptosis. Mol. Cell *23*, 401-412.

42. Campbell,S.A., Lin,J., Dobrikova,E.Y., and Gromeier,M. (2005). Genetic determinants of cell type-specific poliovirus propagation in HEK 293 cells. J Virol *79*, 6281-6290.

43. Campbell,S.A., Mulvey,M., Mohr,I., and Gromeier,M. (2007). Attenuation of herpes simplex virus neurovirulence with picornavirus cis-acting genetic elements. J Virol *81*, 791-799.

44. Cenna,J., Tan,G.S., Papaneri,A.B., Dietzschold,B., Schnell,M.J., and McGettigan,J.P. (2008). Immune modulating effect by a phosphoprotein-deleted rabies virus vaccine vector expressing two copies of the rabies virus glycoprotein gene. Vaccine.

45. Cevallos,R.C. and Sarnow,P. (2005). Factor-independent assembly of elongation-competent ribosomes by an internal ribosome entry site located in an RNA virus that infects penaeid shrimp. J Virol *79*, 677-683.

46. Charlton,K.M. (1994). The pathogenesis of rabies and other lyssaviral infections: recent studies. Curr. Top. Microbiol. Immunol. *187*, 95-119.

47. Chen,M., Ogino,T., and Banerjee,A.K. (2007). Interaction of vesicular stomatitis virus P and N proteins: identification of two overlapping domains at the N terminus of P that are involved in N0-P complex formation and encapsidation of viral genome RNA. J Virol *81*, 13478-13485.

48. Chenik,M., Chebli,K., Gaudin,Y., and Blondel,D. (1994). In vivo interaction of rabies virus phosphoprotein (P) and nucleoprotein (N): existence of two N-binding sites on P protein. J Gen Virol *75 (Pt 11)*, 2889-2896.

49. Chenik,M., Schnell,M., Conzelmann,K.K., and Blondel,D. (1998). Mapping the interacting domains between the rabies virus polymerase and phosphoprotein. J Virol *72*, 1925-1930.

50. Childs,K., Stock,N., Ross,C., Andrejeva,J., Hilton,L., Skinner,M., Randall,R., and Goodbourn,S. (2007). mda-5, but not RIG-I, is a common target for paramyxovirus V proteins. Virology *359*, 190-200.

51. Cho,S., Kim,J.H., Back,S.H., and Jang,S.K. (2005). Polypyrimidine tract-binding protein enhances the internal ribosomal entry site-dependent translation of p27Kip1 mRNA and modulates transition from G1 to S phase. Mol. Cell Biol. *25*, 1283-1297.

52. Colonno,R.J. and Banerjee,A.K. (1976). A unique RNA species involved in initiation of vesicular stomatitis virus RNA transcription in vitro. Cell *8*, 197-204.

53. Conzelmann,K.K. (2004). Reverse genetics of mononegavirales. Curr Top Microbiol. Immunol *283*, 1-41.

54. Conzelmann,K.K. and Schnell,M. (1994). Rescue of synthetic genomic RNA analogs of rabies virus by plasmid-encoded proteins. J Virol *68*, 713-719.

55. Creancier,L., Morello,D., Mercier,P., and Prats,A.C. (2000). Fibroblast growth factor 2 internal ribosome entry site (IRES) activity ex vivo and in transgenic mice reveals a stringent tissue-specific regulation. J Cell Biol *150*, 275-281.

56. Curran,J. and Kolakofsky,D. (2008). Nonsegmented negative-strand RNA virus RNA synthesis in vivo. Virology *371*, 227-230.

57. Curran,J., Marq,J.B., and Kolakofsky,D. (1995). An N-terminal domain of the Sendai paramyxovirus P protein acts as a chaperone for the NP protein during the nascent chain assembly step of genome replication. J Virol *69*, 849-855.

58. Dakic,A., Shao,Q.X., D'Amico,A., O'Keeffe,M., Chen,W.F., Shortman,K., and Wu,L. (2004). Development of the dendritic cell system during mouse ontogeny. J Immunol *172*, 1018-1027.

59. de Breyne,S., Yu,Y., Pestova,T.V., and Hellen,C.U. (2008). Factor requirements for translation initiation on the Simian picornavirus internal ribosomal entry site. RNA *14*, 367-380.

60. Deffaud,C. and Darlix,J.L. (2000). Rous sarcoma virus translation revisited: characterization of an internal ribosome entry segment in the 5' leader of the genomic RNA. J Virol *74*, 11581-11588.

61. Devaney,M.A., Vakharia,V.N., Lloyd,R.E., Ehrenfeld,E., and Grubman,M.J. (1988). Leader protein of foot-and-mouth disease virus is required for cleavage of the p220 component of the cap-binding protein complex. J Virol *62*, 4407-4409.

62. Dietzschold,B., Schnell,M., and Koprowski,H. (2005). Pathogenesis of rabies. Curr Top Microbiol. Immunol *292*, 45-56.

63. Dietzschold,B., Wunner,W.H., Wiktor,T.J., Lopes,A.D., Lafon,M., Smith,C.L., and Koprowski,H. (1983). Characterization of an antigenic determinant of the glycoprotein that correlates with pathogenicity of rabies virus. Proc Natl Acad Sci U S A *80*, 70-74.

64. Ding,H., Green,T.J., Lu,S., and Luo,M. (2006). Crystal structure of the oligomerization domain of the phosphoprotein of vesicular stomatitis virus. J Virol *80*, 2808-2814.

65. Dobrikova,E., Florez,P., Bradrick,S., and Gromeier,M. (2003a). Activity of a type 1 picornavirus internal ribosomal entry site is determined by sequences within the 3' nontranslated region. Proc Natl Acad Sci U S A *100*, 15125-15130.

66. Dobrikova,E.Y., Florez,P., and Gromeier,M. (2003b). Structural determinants of insert retention of poliovirus expression vectors with recombinant IRES elements. Virology *311*, 241-253.

67. Dobrikova,E.Y., Grisham,R.N., Kaiser,C., Lin,J., and Gromeier,M. (2006). Competitive translation efficiency at the picornavirus type 1 internal ribosome entry site facilitated by viral cis and trans factors. J Virol *80*, 3310-3321.

68. Doerr, H. and Gerlich, W. Medizinische Virologie, 2.Auflage; Grundlagen, Diagnostik und Therapie virologischer Krankheitsbilder. 2009.
Ref Type: Generic

69. Doudna,J.A. and Sarnow,P. (2007). Translation Initiation by Viral Internal Ribosome Entry Sites. In Translational Control in Biology and Medicine, M.B.Mathews, N.Sonenberg, and J.Hershey, eds. (New York: Cold Spring Harbor Laboratory Press), pp. 129-153.

70. Eriguchi,Y., Toriumi,H., and Kawai,A. (2002). Studies on the rabies virus RNA polymerase: 3. Two-dimensional electrophoretic analysis of the multiplicity of non-catalytic subunit (P protein). Microbiol. Immunol *46*, 463-474.

71. Etessami,R., Conzelmann,K.K., Fadai-Ghotbi,B., Natelson,B., Tsiang,H., and Ceccaldi,P.E. (2000). Spread and pathogenic characteristics of a G-deficient rabies virus recombinant: an in vitro and in vivo study. J Gen Virol *81*, 2147-2153.

72. Evans,J.R., Mitchell,S.A., Spriggs,K.A., Ostrowski,J., Bomsztyk,K., Ostarek,D., and Willis,A.E. (2003). Members of the poly (rC) binding protein family stimulate the activity of the c-myc internal ribosome entry segment in vitro and in vivo. Oncogene *22*, 8012-8020.

73. Faber,M., Pulmanausahakul,R., Hodawadekar,S.S., Spitsin,S., McGettigan,J.P., Schnell,M.J., and Dietzschold,B. (2002). Overexpression of the rabies virus glycoprotein results in enhancement of apoptosis and antiviral immune response. J Virol *76*, 3374-3381.

74. Faber,M., Pulmanausahakul,R., Nagao,K., Prosniak,M., Rice,A.B., Koprowski,H., Schnell,M.J., and Dietzschold,B. (2004). Identification of viral genomic elements responsible for rabies virus neuroinvasiveness. Proc Natl Acad Sci U S A *101*, 16328-16332.

75. Fan,H. and Penman,S. (1970). Regulation of protein synthesis in mammalian cells. II. Inhibition of protein synthesis at the level of initiation during mitosis. J Mol. Biol. *50*, 655-670.

76. Fekete,C.A., Mitchell,S.F., Cherkasova,V.A., Applefield,D., Algire,M.A., Maag,D., Saini,A.K., Lorsch,J.R., and Hinnebusch,A.G. (2007). N- and C-terminal residues of eIF1A have opposing effects on the fidelity of start codon selection. EMBO J *26*, 1602-1614.

77. Filbin,M.E. and Kieft,J.S. (2009). Toward a structural understanding of IRES RNA function. Curr. Opin. Struct. Biol.

78. Finke,S., Brzozka,K., and Conzelmann,K.K. (2004). Tracking fluorescence-labeled rabies virus: enhanced green fluorescent protein-tagged phosphoprotein P supports virus gene expression and formation of infectious particles. J Virol *78*, 12333-12343.

79. Finke,S. and Conzelmann,K.K. (1997). Ambisense gene expression from recombinant rabies virus: random packaging of positive- and negative-strand ribonucleoprotein complexes into rabies virions. J Virol *71*, 7281-7288.

80. Finke,S. and Conzelmann,K.K. (1999). Virus promoters determine interference by defective RNAs: selective amplification of mini-RNA vectors and rescue from cDNA by a 3' copy-back ambisense rabies virus. J Virol *73*, 3818-3825.

81. Finke,S. and Conzelmann,K.K. (2003). Dissociation of rabies virus matrix protein functions in regulation of viral RNA synthesis and virus assembly. J Virol *77*, 12074-12082.

82. Finke,S. and Conzelmann,K.K. (2005a). Recombinant rhabdoviruses: vectors for vaccine development and gene therapy. Curr Top Microbiol. Immunol *292*, 165-200.

83. Finke,S. and Conzelmann,K.K. (2005b). Replication strategies of rabies virus. Virus Res *111*, 120-131.

84. Finke,S., Cox,J.H., and Conzelmann,K.K. (2000). Differential transcription attenuation of rabies virus genes by intergenic regions: generation of recombinant viruses overexpressing the polymerase gene. J Virol *74*, 7261-7269.

85. Finke,S., Mueller-Waldeck,R., and Conzelmann,K.K. (2003). Rabies virus matrix protein regulates the balance of virus transcription and replication. J Gen Virol *84*, 1613-1621.

86. Flanagan,E.B., Ball,L.A., and Wertz,G.W. (2000). Moving the glycoprotein gene of vesicular stomatitis virus to promoter-proximal positions accelerates and enhances the protective immune response. J Virol *74*, 7895-7902.

87. Fraser,C.S. and Doudna,J.A. (2007). Structural and mechanistic insights into hepatitis C viral translation initiation. Nat. Rev. Microbiol. *5*, 29-38.

88. Fu,Z.F. (2005). Genetic comparison of the rhabdoviruses from animals and plants. Curr Top Microbiol. Immunol *292*, 1-24.

89. Gallie,D.R., Ling,J., Niepel,M., Morley,S.J., and Pain,V.M. (2000). The role of 5'-leader length, secondary structure and PABP concentration on cap and poly(A) tail function during translation in Xenopus oocytes. Nucleic Acids Res. *28*, 2943-2953.

90. Gaudin,Y. (2000). Rabies virus-induced membrane fusion pathway. J Cell Biol. *150*, 601-612.

91. Georgel,P., Jiang,Z., Kunz,S., Janssen,E., Mols,J., Hoebe,K., Bahram,S., Oldstone,M.B., and Beutler,B. (2007). Vesicular stomatitis virus glycoprotein G activates a specific antiviral Toll-like receptor 4-dependent pathway. Virology *362*, 304-313.

92. Gerard,F.C., Ribeiro,E.A., Jr., Albertini,A.A., Gutsche,I., Zaccai,G., Ruigrok,R.W., and Jamin,M. (2007). Unphosphorylated rhabdoviridae phosphoproteins form elongated dimers in solution. Biochemistry *46*, 10328-10338.

93. Gerard,F.C., Ribeiro,E.A., Jr., Leyrat,C., Ivanov,I., Blondel,D., Longhi,S., Ruigrok,R.W., and Jamin,M. (2009). Modular organization of rabies virus phosphoprotein. J Mol. Biol. *388*, 978-996.

94. Gigant,B., Iseni,F., Gaudin,Y., Knossow,M., and Blondel,D. (2000). Neither phosphorylation nor the amino-terminal part of rabies virus phosphoprotein is required for its oligomerization. J Gen Virol *81*, 1757-1761.

95. Gingras,A.C., Svitkin,Y., Belsham,G.J., Pause,A., and Sonenberg,N. (1996). Activation of the translational suppressor 4E-BP1 following infection with encephalomyocarditis virus and poliovirus. Proc Natl Acad Sci U S A *93*, 5578-5583.

96. Gitlin,L., Barchet,W., Gilfillan,S., Cella,M., Beutler,B., Flavell,R.A., Diamond,M.S., and Colonna,M. (2006). Essential role of mda-5 in type I IFN responses to polyriboinosinic:polyribocytidylic acid and encephalomyocarditis picornavirus. Proc Natl Acad Sci U S A *103*, 8459-8464.

97. Glass,M.J., Jia,X.Y., and Summers,D.F. (1993). Identification of the hepatitis A virus internal ribosome entry site: in vivo and in vitro analysis of bicistronic RNAs containing the HAV 5' noncoding region. Virology *193*, 842-852.

98. Greber,U.F. and Way,M. (2006). A superhighway to virus infection. Cell *124*, 741-754.

99. Griffiths,A. and Coen,D.M. (2005). An unusual internal ribosome entry site in the herpes simplex virus thymidine kinase gene. Proc Natl Acad Sci U S A *102*, 9667-9672.

100. Gromeier,M., Alexander,L., and Wimmer,E. (1996). Internal ribosomal entry site substitution eliminates neurovirulence in intergeneric poliovirus recombinants. Proc Natl Acad Sci U S A *93*, 2370-2375.

101. Groppo,R. and Palmenberg,A.C. (2007). Cardiovirus 2A protein associates with 40S but not 80S ribosome subunits during infection. J Virol *81*, 13067-13074.

102. Gupta,A.K., Blondel,D., Choudhary,S., and Banerjee,A.K. (2000). The phosphoprotein of rabies virus is phosphorylated by a unique cellular protein kinase and specific isomers of protein kinase C. J Virol *74*, 91-98.

103. Haglund,K., Forman,J., Krausslich,H.G., and Rose,J.K. (2000). Expression of human immunodeficiency virus type 1 Gag protein precursor and envelope proteins from a vesicular stomatitis virus recombinant: high-level production of virus-like particles containing HIV envelope. Virology *268*, 112-121.

104. Hahm,B., Kim,Y.K., Kim,J.H., Kim,T.Y., and Jang,S.K. (1998). Heterogeneous nuclear ribonucleoprotein L interacts with the 3' border of the internal ribosomal entry site of hepatitis C virus. J Virol *72*, 8782-8788.

105. Haller,O., Kochs,G., and Weber,F. (2007). Interferon, Mx, and viral countermeasures. Cytokine Growth Factor Rev *18*, 425-433.

106. Hennecke,M., Kwissa,M., Metzger,K., Oumard,A., Kroger,A., Schirmbeck,R., Reimann,J., and Hauser,H. (2001). Composition and arrangement of genes define the strength of IRES-driven translation in bicistronic mRNAs. Nucleic Acids Res. *29*, 3327-3334.

107. Herbreteau,C.H., Weill,L., Decimo,D., Prevot,D., Darlix,J.L., Sargueil,B., and Ohlmann,T. (2005). HIV-2 genomic RNA contains a novel type of IRES located downstream of its initiation codon. Nat. Struct. Mol. Biol. *12*, 1001-1007.

108. Hinnebusch,A.G., Dever,T.E., and Asano,K. (2007). Mechanism of Translation Initiation in Saccharomyces cerevisiae. In Translational Control in Biology and Medicine, M.B.Mathews, N.Sonenberg, and J.Hershey, eds. (New York: Cold Spring Harbor Laboratory Press), pp. 225-268.

109. Holcik,M. and Pestova,T.V. (2007). Translation mechanism and regulation: old players, new concepts. Meeting on Translational Control and Non-Coding RNA. EMBO Rep.

110. Hooper,D.C., Morimoto,K., Bette,M., Weihe,E., Koprowski,H., and Dietzschold,B. (1998). Collaboration of antibody and inflammation in clearance of rabies virus from the central nervous system. J Virol *72*, 3711-3719.

111. Horikami,S.M., Curran,J., Kolakofsky,D., and Moyer,S.A. (1992). Complexes of Sendai virus NP-P and P-L proteins are required for defective interfering particle genome replication in vitro. J Virol *66*, 4901-4908.

112. Hornung,V., Ellegast,J., Kim,S., Brzozka,K., Jung,A., Kato,H., Poeck,H., Akira,S., Conzelmann,K.K., Schlee,M., Endres,S., and Hartmann,G. (2006). 5'-Triphosphate RNA is the ligand for RIG-I. Science *314*, 994-997.

113. Humphreys,D.T., Westman,B.J., Martin,D.I., and Preiss,T. (2005). MicroRNAs control translation initiation by inhibiting eukaryotic initiation factor 4E/cap and poly(A) tail function. Proc Natl Acad Sci U S A *102*, 16961-16966.

114. Hunziker,I.P., Cornell,C.T., and Whitton,J.L. (2007). Deletions within the 5'UTR of coxsackievirus B3: consequences for virus translation and replication. Virology *360*, 120-128.

115. Iverson,L.E. and Rose,J.K. (1981). Localized attenuation and discontinuous synthesis during vesicular stomatitis virus transcription. Cell *23*, 477-484.

116. Izumi,R.E., Das,S., Barat,B., Raychaudhuri,S., and Dasgupta,A. (2004). A peptide from autoantigen La blocks poliovirus and hepatitis C virus cap-independent translation and reveals a single tyrosine critical for La RNA binding and translation stimulation. J Virol *78*, 3763-3776.

117. Jackson,R.J., Hunt,S.L., Gibbs,C.L., and Kaminski,A. (1994). Internal initiation of translation of picornavirus RNAs. Mol. Biol. Rep. *19*, 147-159.

118. Jacob,Y., Badrane,H., Ceccaldi,P.E., and Tordo,N. (2000). Cytoplasmic dynein LC8 interacts with lyssavirus phosphoprotein. J Virol *74*, 10217-10222.

119. Jacob,Y., Real,E., and Tordo,N. (2001). Functional interaction map of lyssavirus phosphoprotein: identification of the minimal transcription domains. J Virol *75*, 9613-9622.

120. Jan,E. and Sarnow,P. (2002). Factorless ribosome assembly on the internal ribosome entry site of cricket paralysis virus. J Mol. Biol. *324*, 889-902.

121. Jang,S.K. (2006). Internal initiation: IRES elements of picornaviruses and hepatitis c virus. Virus Res. *119*, 2-15.

122. Jang,S.K., Krausslich,H.G., Nicklin,M.J., Duke,G.M., Palmenberg,A.C., and Wimmer,E. (1988). A segment of the 5' nontranslated region of encephalomyocarditis virus RNA directs internal entry of ribosomes during in vitro translation. J Virol *62*, 2636-2643.

123. Jang,S.K., Pestova,T.V., Hellen,C.U., Witherell,G.W., and Wimmer,E. (1990). Cap-independent translation of picornavirus RNAs: structure and function of the internal ribosomal entry site. Enzyme *44*, 292-309.

124. Johansen,L.K. and Morrow,C.D. (2000). The RNA encompassing the internal ribosome entry site in the poliovirus 5' nontranslated region enhances the encapsidation of genomic RNA. Virology *273*, 391-399.

125. Junemann,C., Song,Y., Bassili,G., Goergen,D., Henke,J., and Niepmann,M. (2007). Picornavirus internal ribosome entry site elements can stimulate translation of upstream genes. J Biol. Chem. *282*, 132-141.

126. Kaku,Y., Chard,L.S., Inoue,T., and Belsham,G.J. (2002). Unique characteristics of a picornavirus internal ribosome entry site from the porcine teschovirus-1 talfan. J Virol *76*, 11721-11728.

127. Kaminski,A., Belsham,G.J., and Jackson,R.J. (1994). Translation of encephalomyocarditis virus RNA: parameters influencing the selection of the internal initiation site. EMBO J *13*, 1673-1681.

128. Kamrud,K.I., Custer,M., Dudek,J.M., Owens,G., Alterson,K.D., Lee,J.S., Groebner,J.L., and Smith,J.F. (2007). Alphavirus replicon approach to promoterless analysis of IRES elements. Virology *360*, 376-387.

129. Kato,H., Sato,S., Yoneyama,M., Yamamoto,M., Uematsu,S., Matsui,K., Tsujimura,T., Takeda,K., Fujita,T., Takeuchi,O., and Akira,S. (2005). Cell type-specific involvement of RIG-I in antiviral response. Immunity *23*, 19-28.

130. Kato,H., Takeuchi,O., Sato,S., Yoneyama,M., Yamamoto,M., Matsui,K., Uematsu,S., Jung,A., Kawai,T., Ishii,K.J., Yamaguchi,O., Otsu,K., Tsujimura,T., Koh,C.S., Reis e Sousa, Matsuura,Y., Fujita,T., and Akira,S. (2006). Differential roles of MDA5 and RIG-I helicases in the recognition of RNA viruses. Nature *441*, 101-105.

131. Kauder,S., Kan,S., and Racaniello,V.R. (2006). Age-dependent poliovirus replication in the mouse central nervous system is determined by internal ribosome entry site-mediated translation. J Virol *80*, 2589-2595.

132. Kauder,S.E. and Racaniello,V.R. (2004). Poliovirus tropism and attenuation are determined after internal ribosome entry. J Clin Invest *113*, 1743-1753.

133. Kim,J.H., Paek,K.Y., Ha,S.H., Cho,S., Choi,K., Kim,C.S., Ryu,S.H., and Jang,S.K. (2004). A cellular RNA-binding protein enhances internal ribosomal entry site-dependent translation through an interaction downstream of the hepatitis C virus polyprotein initiation codon. Mol. Cell Biol. *24*, 7878-7890.

134. Klingen,Y., Conzelmann,K.K., and Finke,S. (2008). Double-labeled rabies virus: live tracking of enveloped virus transport. J Virol *82*, 237-245.

135. Kolupaeva,V.G., Lomakin,I.B., Pestova,T.V., and Hellen,C.U. (2003). Eukaryotic initiation factors 4G and 4A mediate conformational changes downstream of the initiation codon of the encephalomyocarditis virus internal ribosomal entry site. Mol. Cell Biol. *23*, 687-698.

136. Kozak,M. (1987). At least six nucleotides preceding the AUG initiator codon enhance translation in mammalian cells. J Mol. Biol. *196*, 947-950.

137. Kozak,M. (2003). Alternative ways to think about mRNA sequences and proteins that appear to promote internal initiation of translation. Gene *318*, 1-23.

138. Kozak,M. (2005). A second look at cellular mRNA sequences said to function as internal ribosome entry sites. Nucleic Acids Res. *33*, 6593-6602.

139. Kozak,M. (2007). Lessons (not) learned from mistakes about translation. Gene *403*, 194-203.

140. Krausslich,H.G., Nicklin,M.J., Toyoda,H., Etchison,D., and Wimmer,E. (1987). Poliovirus proteinase 2A induces cleavage of eucaryotic initiation factor 4F polypeptide p220. J Virol *61*, 2711-2718.

141. Krumbholz,A., Dauber,M., Henke,A., Birch-Hirschfeld,E., Knowles,N.J., Stelzner,A., and Zell,R. (2002). Sequencing of porcine enterovirus groups II and III reveals unique features of both virus groups. J Virol *76*, 5813-5821.

142. Kullmann,M., Gopfert,U., Siewe,B., and Hengst,L. (2002). ELAV/Hu proteins inhibit p27 translation via an IRES element in the p27 5'UTR. Genes Dev. *16*, 3087-3099.

143. Lafon,M. (2005a). Modulation of the immune response in the nervous system by rabies virus. Curr Top Microbiol. Immunol *289*, 239-258.

144. Lafon,M. (2005b). Rabies virus receptors. J Neurovirol. *11*, 82-87.

145. Lamphear,B.J., Kirchweger,R., Skern,T., and Rhoads,R.E. (1995). Mapping of functional domains in eukaryotic protein synthesis initiation factor 4G (eIF4G) with picornaviral proteases. Implications for cap-dependent and cap-independent translational initiation. J Biol. Chem. *270*, 21975-21983.

146. Lamphear,B.J., Yan,R., Yang,F., Waters,D., Liebig,H.D., Klump,H., Kuechler,E., Skern,T., and Rhoads,R.E. (1993). Mapping the cleavage site in protein synthesis initiation factor eIF-4 gamma of the 2A proteases from human Coxsackievirus and rhinovirus. J Biol. Chem. *268*, 19200-19203.

147. Le,S.Y. and Maizel,J.V., Jr. (1997). A common RNA structural motif involved in the internal initiation of translation of cellular mRNAs. Nucleic Acids Res. *25*, 362-369.

148. Lee,H.K., Lund,J.M., Ramanathan,B., Mizushima,N., and Iwasaki,A. (2007). Autophagy-dependent viral recognition by plasmacytoid dendritic cells. Science *315*, 1398-1401.

149. Lentz,T.L., Burrage,T.G., Smith,A.L., Crick,J., and Tignor,G.H. (1982). Is the acetylcholine receptor a rabies virus receptor? Science *215*, 182-184.

150. Lewis,S.M., Veyrier,A., Hosszu,U.N., Bonnal,S., Vagner,S., and Holcik,M. (2007). Subcellular relocalization of a trans-acting factor regulates XIAP IRES-dependent translation. Mol. Biol. Cell *18*, 1302-1311.

151. Li,J., Wang,J.T., and Whelan,S.P. (2006). A unique strategy for mRNA cap methylation used by vesicular stomatitis virus. Proc Natl Acad Sci U S A *103*, 8493-8498.

152. Lin,J.C., Hsu,M., and Tarn,W.Y. (2007). Cell stress modulates the function of splicing regulatory protein RBM4 in translation control. Proc Natl Acad Sci U S A *104*, 2235-2240.

153. Liu,Z., Dong,Z., Han,B., Yang,Y., Liu,Y., and Zhang,J.T. (2005). Regulation of expression by promoters versus internal ribosome entry site in the 5'-untranslated sequence of the human cyclin-dependent kinase inhibitor p27kip1. Nucleic Acids Res. *33*, 3763-3771.

154. Lomakin,I.B., Hellen,C.U., and Pestova,T.V. (2000). Physical association of eukaryotic initiation factor 4G (eIF4G) with eIF4A strongly enhances binding of eIF4G to the internal ribosomal entry site of encephalomyocarditis virus and is required for internal initiation of translation. Mol. Cell Biol. *20*, 6019-6029.

155. Lopez,d.Q. and Martinez-Salas,E. (1999). Involvement of the aphthovirus RNA region located between the two functional AUGs in start codon selection. Virology *255*, 324-336.

156. Luo,M., Green,T.J., Zhang,X., Tsao,J., and Qiu,S. (2007). Conserved characteristics of the rhabdovirus nucleoprotein. Virus Res.

157. Macejak,D.G. and Sarnow,P. (1991). Internal initiation of translation mediated by the 5' leader of a cellular mRNA. Nature *353*, 90-94.

158. Majumdar,R. and Maitra,U. (2005). Regulation of GTP hydrolysis prior to ribosomal AUG selection during eukaryotic translation initiation. EMBO J *24*, 3737-3746.

159. Maraia,R.J. and Bayfield,M.A. (2006). The La protein-RNA complex surfaces. Mol. Cell *21*, 149-152.

160. Marintchev,A., Edmonds,K.A., Marintcheva,B., Hendrickson,E., Oberer,M., Suzuki,C., Herdy,B., Sonenberg,N., and Wagner,G. (2009). Topology and regulation of the human eIF4A/4G/4H helicase complex in translation initiation. Cell *136*, 447-460.

161. Martinez-Salas,E., Pacheco,A., Serrano,P., and Fernandez,N. (2008). New insights into internal ribosome entry site elements relevant for viral gene expression. J Gen Virol *89*, 611-626.

162. Martinez-Salas,E., Ramos,R., Lafuente,E., and Lopez,d.Q. (2001). Functional interactions in internal translation initiation directed by viral and cellular IRES elements. J Gen Virol *82*, 973-984.

163. Mavrakis,M., Iseni,F., Mazza,C., Schoehn,G., Ebel,C., Gentzel,M., Franz,T., and Ruigrok,R.W. (2003). Isolation and characterisation of the rabies virus N degrees-P complex produced in insect cells. Virology *305*, 406-414.

164. Mavrakis,M., McCarthy,A.A., Roche,S., Blondel,D., and Ruigrok,R.W. (2004). Structure and function of the C-terminal domain of the polymerase cofactor of rabies virus. J Mol. Biol. *343*, 819-831.

165. Mavrakis,M., Mehouas,S., Real,E., Iseni,F., Blondel,D., Tordo,N., and Ruigrok,R.W. (2006). Rabies virus chaperone: identification of the phosphoprotein peptide that keeps nucleoprotein soluble and free from non-specific RNA. Virology *349*, 422-429.

166. Mayer,D., Fischer,H., Schneider,U., Heimrich,B., and Schwemmle,M. (2005). Borna disease virus replication in organotypic hippocampal slice cultures from rats results in selective damage of dentate granule cells. J Virol *79*, 11716-11723.

167. McGettigan,J.P., Pomerantz,R.J., Siler,C.A., McKenna,P.M., Foley,H.D., Dietzschold,B., and Schnell,M.J. (2003). Second-generation rabies virus-based vaccine vectors expressing human immunodeficiency virus type 1 gag have greatly reduced pathogenicity but are highly immunogenic. J Virol *77*, 237-244.

168. Mebatsion,T. (2001). Extensive attenuation of rabies virus by simultaneously modifying the dynein light chain binding site in the P protein and replacing Arg333 in the G protein. J Virol *75*, 11496-11502.

169. Mebatsion,T., Konig,M., and Conzelmann,K.K. (1996a). Budding of rabies virus particles in the absence of the spike glycoprotein. Cell *84*, 941-951.

170. Mebatsion,T., Schnell,M.J., Cox,J.H., Finke,S., and Conzelmann,K.K. (1996b). Highly stable expression of a foreign gene from rabies virus vectors. Proc Natl Acad Sci U S A *93*, 7310-7314.

171. Mebatsion,T., Weiland,F., and Conzelmann,K.K. (1999). Matrix protein of rabies virus is responsible for the assembly and budding of bullet-shaped particles and interacts with the transmembrane spike glycoprotein G. J Virol *73*, 242-250.

172. Merrill,M.K., Dobrikova,E.Y., and Gromeier,M. (2006). Cell-type-specific repression of internal ribosome entry site activity by double-stranded RNA-binding protein 76. J Virol *80*, 3147-3156.

173. Merrill,M.K. and Gromeier,M. (2006). The double-stranded RNA binding protein 76:NF45 heterodimer inhibits translation initiation at the rhinovirus type 2 internal ribosome entry site. J Virol *80*, 6936-6942.

174. Millard,S.S., Yan,J.S., Nguyen,H., Pagano,M., Kiyokawa,H., and Koff,A. (1997). Enhanced ribosomal association of p27(Kip1) mRNA is a mechanism contributing to accumulation during growth arrest. J Biol. Chem. *272*, 7093-7098.

175. Mitchell,S.A., Spriggs,K.A., Coldwell,M.J., Jackson,R.J., and Willis,A.E. (2003). The Apaf-1 internal ribosome entry segment attains the correct structural conformation for function via interactions with PTB and unr. Mol. Cell *11*, 757-771.

176. Mitchell,S.F. and Lorsch,J.R. (2008). Should I stay or should I go? Eukaryotic translation initiation factors 1 and 1A control start codon recognition. J Biol. Chem. *283*, 27345-27349.

177. Monie,T.P., Perrin,A.J., Birtley,J.R., Sweeney,T.R., Karakasiliotis,I., Chaudhry,Y., Roberts,L.O., Matthews,S., Goodfellow,I.G., and Curry,S. (2007). Structural insights into the transcriptional and translational roles of Ebp1. EMBO J *26*, 3936-3944.

178. Morimoto,K., Foley,H.D., McGettigan,J.P., Schnell,M.J., and Dietzschold,B. (2000). Reinvestigation of the role of the rabies virus glycoprotein in viral pathogenesis using a reverse genetics approach. J Neurovirol. *6*, 373-381.

179. Morimoto,K., Hooper,D.C., Spitsin,S., Koprowski,H., and Dietzschold,B. (1999). Pathogenicity of different rabies virus variants inversely correlates with apoptosis and rabies virus glycoprotein expression in infected primary neuron cultures. J Virol *73*, 510-518.

180. Morimoto,K., Shoji,Y., and Inoue,S. (2005). Characterization of P gene-deficient rabies virus: propagation, pathogenicity and antigenicity. Virus Res *111*, 61-67.

181. Moseley,G.W., Filmer,R.P., Dejesus,M.A., and Jans,D.A. (2007). Nucleocytoplasmic Distribution of Rabies Virus P-Protein Is Regulated by Phosphorylation Adjacent to C-Terminal Nuclear Import and Export Signals. Biochemistry.

182. Muller,U., Steinhoff,U., Reis,L.F., Hemmi,S., Pavlovic,J., Zinkernagel,R.M., and Aguet,M. (1994). Functional role of type I and type II interferons in antiviral defense. Science *264*, 1918-1921.

183. Naeve,C.W., Kolakofsky,C.M., and Summers,D.F. (1980). Comparison o;f vesicular stomatitis virus intracellular and virion ribonucleoproteins. J Virol *33*, 856-865.

184. Nakamichi,K., Inoue,S., Takasaki,T., Morimoto,K., and Kurane,I. (2004). Rabies virus stimulates nitric oxide production and CXC chemokine ligand 10 expression in macrophages through activation of extracellular signal-regulated kinases 1 and 2. J Virol *78*, 9376-9388.

185. Nevins,T.A., Harder,Z.M., Korneluk,R.G., and Holcik,M. (2003). Distinct regulation of internal ribosome entry site-mediated translation following cellular stress is mediated by apoptotic fragments of eIF4G translation initiation factor family members eIF4GI and p97/DAP5/NAT1. J Biol. Chem. *278*, 3572-3579.

186. Niepmann,M. (2009). Internal translation initiation of picornaviruses and hepatitis C virus. Biochim. Biophys. Acta.

187. Novella,I.S., Ball,L.A., and Wertz,G.W. (2004). Fitness analyses of vesicular stomatitis strains with rearranged genomes reveal replicative disadvantages. J Virol *78*, 9837-9841.

188. Ochs,K., Rust,R.C., and Niepmann,M. (1999). Translation initiation factor eIF4B interacts with a picornavirus internal ribosome entry site in both 48S and 80S initiation complexes independently of initiator AUG location. J Virol *73*, 7505-7514.

189. Ogino,T. and Banerjee,A.K. (2007). Unconventional mechanism of mRNA capping by the RNA-dependent RNA polymerase of vesicular stomatitis virus. Mol. Cell *25*, 85-97.

190. Ogino,T. and Banerjee,A.K. (2008). Formation of guanosine(5')tetraphospho(5')adenosine cap structure by an unconventional mRNA capping enzyme of vesicular stomatitis virus. J Virol *82*, 7729-7734.

191. Ohlmann,T. and Jackson,R.J. (1999). The properties of chimeric picornavirus IRESes show that discrimination between internal translation initiation sites is influenced by the identity of the IRES and not just the context of the AUG codon. RNA *5*, 764-778.

192. Onoguchi,K., Yoneyama,M., Takemura,A., Akira,S., Taniguchi,T., Namiki,H., and Fujita,T. (2007). Viral infections activate types I and III interferon genes through a common mechanism. J Biol Chem. *282*, 7576-7581.

193. Orlinger,K.K., Kofler,R.M., Heinz,F.X., Hoenninger,V.M., and Mandl,C.W. (2007). Selection and analysis of mutations in an encephalomyocarditis virus internal ribosome entry site that improve the efficiency of a bicistronic flavivirus construct. J Virol *81*, 12619-12629.

194. Otto,G.A. and Puglisi,J.D. (2004). The pathway of HCV IRES-mediated translation initiation. Cell *119*, 369-380.

195. Parsley,T.B., Towner,J.S., Blyn,L.B., Ehrenfeld,E., and Semler,B.L. (1997). Poly (rC) binding protein 2 forms a ternary complex with the 5'-terminal sequences of poliovirus RNA and the viral 3CD proteinase. RNA *3*, 1124-1134.

196. Pasdeloup,D., Poisson,N., Raux,H., Gaudin,Y., Ruigrok,R.W., and Blondel,D. (2005). Nucleocytoplasmic shuttling of the rabies virus P protein requires a nuclear localization signal and a CRM1-dependent nuclear export signal. Virology *334*, 284-293.

197. Passmore,L.A., Schmeing,T.M., Maag,D., Applefield,D.J., Acker,M.G., Algire,M.A., Lorsch,J.R., and Ramakrishnan,V. (2007). The eukaryotic translation initiation factors eIF1 and eIF1A induce an open conformation of the 40S ribosome. Mol. Cell *26*, 41-50.

198. Patton,J.T., Davis,N.L., and Wertz,G.W. (1984). N protein alone satisfies the requirement for protein synthesis during RNA replication of vesicular stomatitis virus. J Virol *49*, 303-309.

199. Pelletier,J., Kaplan,G., Racaniello,V.R., and Sonenberg,N. (1988). Cap-independent translation of poliovirus mRNA is conferred by sequence elements within the 5' noncoding region. Mol. Cell Biol. *8*, 1103-1112.

200. Pelletier,J. and Sonenberg,N. (1988). Internal initiation of translation of eukaryotic mRNA directed by a sequence derived from poliovirus RNA. Nature *334*, 320-325.

201. Perry,L.L. and Lodmell,D.L. (1991). Role of CD4+ and CD8+ T cells in murine resistance to street rabies virus. J Virol *65*, 3429-3434.

202. Pestova,T.V., Borukhov,S.I., and Hellen,C.U. (1998a). Eukaryotic ribosomes require initiation factors 1 and 1A to locate initiation codons. Nature *394*, 854-859.

203. Pestova,T.V., Hellen,C.U., and Shatsky,I.N. (1996a). Canonical eukaryotic initiation factors determine initiation of translation by internal ribosomal entry. Mol. Cell Biol. *16*, 6859-6869.

204. Pestova,T.V., Lorsch,J.R., and Hellen,C.U. (2007). The Mechanism of Translation Initiation in Eukaryotes. In Translational Control in Biology and Medicine,

M.B.Mathews, N.Sonenberg, and J.Hershey, eds. (New York: Cold Spring Harbor Laboratory Press), pp. 87-128.

205. Pestova,T.V., Shatsky,I.N., Fletcher,S.P., Jackson,R.J., and Hellen,C.U. (1998b). A prokaryotic-like mode of cytoplasmic eukaryotic ribosome binding to the initiation codon during internal translation initiation of hepatitis C and classical swine fever virus RNAs. Genes Dev. *12*, 67-83.

206. Pestova,T.V., Shatsky,I.N., and Hellen,C.U. (1996b). Functional dissection of eukaryotic initiation factor 4F: the 4A subunit and the central domain of the 4G subunit are sufficient to mediate internal entry of 43S preinitiation complexes. Mol. Cell Biol. *16*, 6870-6878.

207. Pichlmair,A. and Reis e Sousa (2007). Innate recognition of viruses. Immunity *27*, 370-383.

208. Pichlmair,A., Schulz,O., Tan,C.P., Naslund,T.I., Liljestrom,P., Weber,F., and Reis e Sousa (2006). RIG-I-mediated antiviral responses to single-stranded RNA bearing 5'-phosphates. Science *314*, 997-1001.

209. Pilipenko,E.V., Blinov,V.M., Chernov,B.K., Dmitrieva,T.M., and Agol,V.I. (1989a). Conservation of the secondary structure elements of the 5'-untranslated region of cardio- and aphthovirus RNAs. Nucleic Acids Res *17*, 5701-5711.

210. Pilipenko,E.V., Blinov,V.M., Romanova,L.I., Sinyakov,A.N., Maslova,S.V., and Agol,V.I. (1989b). Conserved structural domains in the 5'-untranslated region of picornaviral genomes: an analysis of the segment controlling translation and neurovirulence. Virology *168*, 201-209.

211. Pilipenko,E.V., Gmyl,A.P., Maslova,S.V., Belov,G.A., Sinyakov,A.N., Huang,M., Brown,T.D., and Agol,V.I. (1994). Starting window, a distinct element in the cap-independent internal initiation of translation on picornaviral RNA. J Mol. Biol. *241*, 398-414.

212. Pisarev,A.V., Kolupaeva,V.G., Yusupov,M.M., Hellen,C.U., and Pestova,T.V. (2008). Ribosomal position and contacts of mRNA in eukaryotic translation initiation complexes. EMBO J *27*, 1609-1621.

213. Platanias,L.C. (2005). Mechanisms of type-I- and type-II-interferon-mediated signalling. Nat Rev Immunol *5*, 375-386.

214. Poole,T.L., Wang,C., Popp,R.A., Potgieter,L.N., Siddiqui,A., and Collett,M.S. (1995). Pestivirus translation initiation occurs by internal ribosome entry. Virology *206*, 750-754.

215. Poyry,T.A., Hentze,M.W., and Jackson,R.J. (2001). Construction of regulatable picornavirus IRESes as a test of current models of the mechanism of internal translation initiation. RNA *7*, 647-660.

216. Prehaud,C., Lay,S., Dietzschold,B., and Lafon,M. (2003). Glycoprotein of nonpathogenic rabies viruses is a key determinant of human cell apoptosis. J Virol *77*, 10537-10547.

217. Racaniello,V.R. (2006). One hundred years of poliovirus pathogenesis. Virology *344*, 9-16.

218. Randall,R.E. and Goodbourn,S. (2008). Interferons and viruses: an interplay between induction, signalling, antiviral responses and virus countermeasures. J Gen Virol *89*, 1-47.

219. Raux,H., Flamand,A., and Blondel,D. (2000). Interaction of the rabies virus P protein with the LC8 dynein light chain. J Virol *74*, 10212-10216.

220. Reagan,K.J. and Wunner,W.H. (1985). Rabies virus interaction with various cell lines is independent of the acetylcholine receptor. Arch. Virol *84*, 277-282.

221. Rieder, M. and Conzelmann, K. Rhabdovirus Evasion of the Interferon System. JICR . 2009.
Ref Type: In Press

222. Rijnbrand,R., van der,S.T., van Rijn,P.A., Spaan,W.J., and Bredenbeek,P.J. (1997). Internal entry of ribosomes is directed by the 5' noncoding region of classical swine fever virus and is dependent on the presence of an RNA pseudoknot upstream of the initiation codon. J Virol *71*, 451-457.

223. Roche,S. and Gaudin,Y. (2004). Evidence that rabies virus forms different kinds of fusion machines with different pH thresholds for fusion. J Virol *78*, 8746-8752.

224. Rupprecht,C.E., Hanlon,C.A., and Hemachudha,T. (2002). Rabies re-examined. Lancet Infect Dis *2*, 327-343.

225. Saito,T., Hirai,R., Loo,Y.M., Owen,D., Johnson,C.L., Sinha,S.C., Akira,S., Fujita,T., and Gale,M., Jr. (2007). Regulation of innate antiviral defenses through a shared repressor domain in RIG-I and LGP2. Proc Natl Acad Sci U S A *104*, 582-587.

226. Sarmento,L., Li,X.Q., Howerth,E., Jackson,A.C., and Fu,Z.F. (2005). Glycoprotein-mediated induction of apoptosis limits the spread of attenuated rabies viruses in the central nervous system of mice. J Neurovirol. *11*, 571-581.

227. Sarnow,P., Cevallos,R.C., and Jan,E. (2005). Takeover of host ribosomes by divergent IRES elements. Biochem. Soc. Trans. *33*, 1479-1482.

228. Sasaki,J. and Nakashima,N. (2000). Methionine-independent initiation of translation in the capsid protein of an insect RNA virus. Proc Natl Acad Sci U S A *97*, 1512-1515.

229. Sawicka,K., Bushell,M., Spriggs,K.A., and Willis,A.E. (2008). Polypyrimidine-tract-binding protein: a multifunctional RNA-binding protein. Biochem. Soc. Trans. *36*, 641-647.

230. Schlender,J., Hornung,V., Finke,S., Gunthner-Biller,M., Marozin,S., Brzozka,K., Moghim,S., Endres,S., Hartmann,G., and Conzelmann,K.K. (2005). Inhibition of toll-like receptor 7- and 9-mediated alpha/beta interferon production in human plasmacytoid dendritic cells by respiratory syncytial virus and measles virus. J Virol *79*, 5507-5515.

231. Schnell,M.J., Mebatsion,T., and Conzelmann,K.K. (1994). Infectious rabies viruses from cloned cDNA. EMBO J *13*, 4195-4203.

232. Seif,I., Coulon,P., Rollin,P.E., and Flamand,A. (1985). Rabies virulence: effect on pathogenicity and sequence characterization of rabies virus mutations affecting antigenic site III of the glycoprotein. J Virol *53*, 926-934.

233. Semler,B.L. (2004). Poliovirus proves IRES-istible in vivo. J Clin Invest *113*, 1678-1681.

234. Semler,B.L. and Waterman,M.L. (2008). IRES-mediated pathways to polysomes: nuclear versus cytoplasmic routes. Trends Microbiol. *16*, 1-5.

235. Shatkin,A.J. and Manley,J.L. (2000). The ends of the affair: capping and polyadenylation. Nat Struct. Biol *7*, 838-842.

236. Shaw,G., Morse,S., Ararat,M., and Graham,F.L. (2002). Preferential transformation of human neuronal cells by human adenoviruses and the origin of HEK 293 cells. FASEB J *16*, 869-871.

237. Shaw-Jackson,C. and Michiels,T. (1999). Absence of internal ribosome entry site-mediated tissue specificity in the translation of a bicistronic transgene. J Virol *73*, 2729-2738.

238. Siler,C.A., McGettigan,J.P., Dietzschold,B., Herrine,S.K., Dubuisson,J., Pomerantz,R.J., and Schnell,M.J. (2002). Live and killed rhabdovirus-based vectors as potential hepatitis C vaccines. Virology *292*, 24-34.

239. Skinner,M.A., Racaniello,V.R., Dunn,G., Cooper,J., Minor,P.D., and Almond,J.W. (1989). New model for the secondary structure of the 5' non-coding RNA of poliovirus is supported by biochemical and genetic data that also show that RNA secondary structure is important in neurovirulence. J Mol. Biol *207*, 379-392.

240. Sonenberg,N. and Hinnebusch,A.G. (2009). Regulation of translation initiation in eukaryotes: mechanisms and biological targets. Cell *136*, 731-745.

241. Sonenberg,N., Rupprecht,K.M., Hecht,S.M., and Shatkin,A.J. (1979). Eukaryotic mRNA cap binding protein: purification by affinity chromatography on sepharose-coupled m7GDP. Proc Natl Acad Sci U S A *76*, 4345-4349.

242. Spriggs,K.A., Stoneley,M., Bushell,M., and Willis,A.E. (2008). Re-programming of translation following cell stress allows IRES-mediated translation to predominate. Biol. Cell *100*, 27-38.

243. Sprinzl,M., Hartmann,T., Weber,J., Blank,J., and Zeidler,R. (1989). Compilation of tRNA sequences and sequences of tRNA genes. Nucleic Acids Res. *17 Suppl*, r1-172.

244. Stewart,S.R. and Semler,B.L. (1998). RNA structure adjacent to the attenuation determinant in the 5'-non-coding region influences poliovirus viability. Nucleic Acids Res *26*, 5318-5326.

245. Strahle,L., Garcin,D., and Kolakofsky,D. (2006). Sendai virus defective-interfering genomes and the activation of interferon-beta. Virology *351*, 101-111.

246. Tan,G.S., Preuss,M.A., Williams,J.C., and Schnell,M.J. (2007). The dynein light chain 8 binding motif of rabies virus phosphoprotein promotes efficient viral transcription. Proc Natl Acad Sci U S A *104*, 7229-7234.

247. Tarun,S.Z., Jr., Wells,S.E., Deardorff,J.A., and Sachs,A.B. (1997). Translation initiation factor eIF4G mediates in vitro poly(A) tail-dependent translation. Proc Natl Acad Sci U S A *94*, 9046-9051.

248. Thoulouze,M.I., Lafage,M., Schachner,M., Hartmann,U., Cremer,H., and Lafon,M. (1998). The neural cell adhesion molecule is a receptor for rabies virus. J Virol *72*, 7181-7190.

249. Tinton,S.A., Schepens,B., Bruynooghe,Y., Beyaert,R., and Cornelis,S. (2005). Regulation of the cell-cycle-dependent internal ribosome entry site of the PITSLRE protein kinase: roles of Unr (upstream of N-ras) protein and phosphorylated translation initiation factor eIF-2alpha. Biochem. J *385*, 155-163.

250. Triqueneaux,G., Velten,M., Franzon,P., Dautry,F., and Jacquemin-Sablon,H. (1999). RNA binding specificity of Unr, a protein with five cold shock domains. Nucleic Acids Res. *27*, 1926-1934.

251. Tsukiyama-Kohara,K., Iizuka,N., Kohara,M., and Nomoto,A. (1992). Internal ribosome entry site within hepatitis C virus RNA. J Virol *66*, 1476-1483.

252. Tuffereau,C., Benejean,J., Blondel,D., Kieffer,B., and Flamand,A. (1998). Low-affinity nerve-growth factor receptor (P75NTR) can serve as a receptor for rabies virus. EMBO J *17*, 7250-7259.

253. Tuffereau,C., Desmezieres,E., Benejean,J., Jallet,C., Flamand,A., Tordo,N., and Perrin,P. (2001). Interaction of lyssaviruses with the low-affinity nerve-growth factor receptor p75NTR. J Gen Virol *82*, 2861-2867.

254. Tuffereau,C., Leblois,H., Benejean,J., Coulon,P., Lafay,F., and Flamand,A. (1989). Arginine or lysine in position 333 of ERA and CVS glycoprotein is necessary for rabies virulence in adult mice. Virology *172*, 206-212.

255. Uematsu,S. and Akira,S. (2007). Toll-like receptors and Type I interferons. J Biol Chem. *282*, 15319-15323.

256. Ugolini,G. (2008). Use of rabies virus as a transneuronal tracer of neuronal connections: implications for the understanding of rabies pathogenesis. Dev. Biol. (Basel) *131*, 493-506.

257. Van Eden,M.E., Byrd,M.P., Sherrill,K.W., and Lloyd,R.E. (2004a). Demonstrating internal ribosome entry sites in eukaryotic mRNAs using stringent RNA test procedures. RNA *10*, 720-730.

258. Van Eden,M.E., Byrd,M.P., Sherrill,K.W., and Lloyd,R.E. (2004b). Translation of cellular inhibitor of apoptosis protein 1 (c-IAP1) mRNA is IRES mediated and regulated during cell stress. RNA *10*, 469-481.

259. Vidy,A., Chelbi-Alix,M., and Blondel,D. (2005). Rabies virus P protein interacts with STAT1 and inhibits interferon signal transduction pathways. J Virol *79*, 14411-14420.

260. Vidy,A., El Bougrini,J., Chelbi-Alix,M.K., and Blondel,D. (2007). The nucleocytoplasmic rabies virus P protein counteracts interferon signaling by inhibiting both nuclear accumulation and DNA binding of STAT1. J Virol *81*, 4255-4263.

261. Volkova,E., Frolova,E., Darwin,J.R., Forrester,N.L., Weaver,S.C., and Frolov,I. (2008). IRES-dependent replication of Venezuelan equine encephalitis virus makes it highly attenuated and incapable of replicating in mosquito cells. Virology *377*, 160-169.

262. Wang,J.T., McElvain,L.E., and Whelan,S.P. (2007). Vesicular Stomatitis Virus mRNA Capping Machinery Requires Specific cis-Acting Signals in the RNA. J Virol *81*, 11499-11506.

263. Wang,Z., Weaver,M., and Magnuson,N.S. (2005a). Cryptic promoter activity in the DNA sequence corresponding to the pim-1 5'-UTR. Nucleic Acids Res. *33*, 2248-2258.

264. Wang,Z.W., Sarmento,L., Wang,Y., Li,X.Q., Dhingra,V., Tseggai,T., Jiang,B., and Fu,Z.F. (2005b). Attenuated Rabies Virus Activates, while Pathogenic Rabies Virus Evades, the Host Innate Immune Responses in the Central Nervous System. J Virol *79*, 12554-12565.

265. Wertz,G.W., Moudy,R., and Ball,L.A. (2002). Adding genes to the RNA genome of vesicular stomatitis virus: positional effects on stability of expression. J Virol *76*, 7642-7650.

266. Whelan,S.P., Barr,J.N., and Wertz,G.W. (2004). Transcription and replication of nonsegmented negative-strand RNA viruses. Curr Top Microbiol. Immunol *283*, 61-119.

267. Wickersham,I.R., Finke,S., Conzelmann,K.K., and Callaway,E.M. (2007a). Retrograde neuronal tracing with a deletion-mutant rabies virus. Nat Methods *4*, 47-49.

268. Wickersham,I.R., Lyon,D.C., Barnard,R.J., Mori,T., Finke,S., Conzelmann,K.K., Young,J.A., and Callaway,E.M. (2007b). Monosynaptic restriction of transsynaptic tracing from single, genetically targeted neurons. Neuron *53*, 639-647.

269. Wilson,J.E., Pestova,T.V., Hellen,C.U., and Sarnow,P. (2000a). Initiation of protein synthesis from the A site of the ribosome. Cell *102*, 511-520.

270. Wilson,J.E., Powell,M.J., Hoover,S.E., and Sarnow,P. (2000b). Naturally occurring dicistronic cricket paralysis virus RNA is regulated by two internal ribosome entry sites. Mol. Cell Biol. *20*, 4990-4999.

271. Yoneyama,M. and Fujita,T. (2007). Function of RIG-I-like receptors in antiviral innate immunity. J Biol Chem. *282*, 15315-15318.

272. Yoneyama,M., Kikuchi,M., Matsumoto,K., Imaizumi,T., Miyagishi,M., Taira,K., Foy,E., Loo,Y.M., Gale,M., Jr., Akira,S., Yonehara,S., Kato,A., and Fujita,T. (2005). Shared and unique functions of the DExD/H-box helicases RIG-I, MDA5, and LGP2 in antiviral innate immunity. J Immunol *175*, 2851-2858.

273. Yoneyama,M., Kikuchi,M., Natsukawa,T., Shinobu,N., Imaizumi,T., Miyagishi,M., Taira,K., Akira,S., and Fujita,T. (2004). The RNA helicase RIG-I has an essential function in double-stranded RNA-induced innate antiviral responses. Nat Immunol *5*, 730-737.

274. Yoneyama,M., Suhara,W., Fukuhara,Y., Sato,M., Ozato,K., and Fujita,T. (1996). Autocrine amplification of type I interferon gene expression mediated by interferon stimulated gene factor 3 (ISGF3). J Biochem. *120*, 160-169.

CURRICULUM VITAE

Adriane Marschalek
* 30.10.1979 in Giessen

Working Experience

since 10/2009	Clinical Research Associate (Freelance) on behalf of Novartis Pharma GmbH BU Oncology

Education

02/2005 – 09/2009	Ludwig-Maximilians-University Munich, Germany Max-von-Pettenkofer Institute; Dept. Virology PhD thesis: IRES elements – a new tool for regulation of gene expression of Rabies virus
10/2001 – 12/2004	Albert-Ludwigs-University Freiburg, Germany Studies in biology (advanced study period) Diploma thesis: Establishment of a new „reverse-genetics-system“ for Thogotovirus
10/1999 – 09/2001	University of Ulm, Germany Studies in biology (basic study period)
09/1990 – 06/1999	Secondary School Neuenbürg, Germany

Publications and Presentations

Publication

Marschalek A, Finke S, Schwemmle M, Mayer D, Heimrich B, Conzelmann KK. Attenuation of rabies virus replication and virulence by picornavirus internal ribosome entry site elements. J Virol. 2009 Feb;83(4):1911-9

Presentations (poster)

03/2006	Annual meeting of the “Deutsche Gesellschaft für Virologie” (GfV) in Munich, Germany
09/2007	„Third European Congress of Virology“ in Nürnberg, Germany

Presentations (oral)

10/2006	SFB455-Retreat Wildbad-Kreuth
09/2007	„Third European Congress of Virology“ in Nürnberg, Germany
03/2008	Annual meeting of the “Deutsche Gesellschaft für Virologie” (GfV) in Heidelberg, Germany
08/2008	„XIV. International Congress of Virology“ in Istanbul, Turkey

DANKSAGUNG

Besonders bedanken möchte ich mich bei Frau Prof. Dr. Brack-Werner, dass sie sich dazu bereit erklärt hat mich als Fachvertreterin und Erstgutachterin dieser Arbeit zu betreuen. Vielen Dank für ihre wertvollen Anregungen und ihre Diskussionsbereitschaft.

Für die Übernahme des Zweitgutachtens danke ich Prof. Dr. Grothe.

Allen voran gilt mein ganz besonderer Dank Prof. Dr. Conzelmann, der es mir ermöglicht hat diese interessante und spannende Arbeit in seinem Labor durchzuführen. Des Weiteren danke ich ihm für die ausgezeichnete Betreuung, für seine Ideen und seine Hilfsbereitschaft und dafür, dass er immer viel Geduld und Mühe aufgebracht hat, um meine Arbeit zum Gelingen zu bringen.

Vielen Dank an Prof. Dr. Schwemmle, für seine Kooperationsbereitschaft und die Durchführung der „brain slice“ Experimente.

Weiterhin möchte ich auch Prof. Dr. Stütz für die Zusammenarbeit und die Durchführung der in vivo Versuche danken.

Herzlichen Dank auch allen derzeitigen und ehemaligen Mitgliedern der Arbeitsgruppe Conzelmann, die immer für gute Stimmung und eine großartige Arbeitsatmosphäre gesorgt haben, wodurch mir die Arbeit viel Freude bereitet hat. Durch ihre Hilfs- und Diskussionsbereitschaft haben sie zum Gelingen dieser Arbeit beigetragen.

Ein sehr herzlicher Dank gilt meinen Eltern und meinen Geschwistern für ihre Unterstützung und ihr Interesse an meiner Arbeit.

Meinem Freund Daniel Gräf danke ich von ganzem Herzen für seine unermüdliche Unterstützung, seine Liebe und Motivation.